Synthesis and Evaluation of Chromo-Fluorescent Properties of a New Class of Aza/ Substituted Acenes

Thesis submitted in

fulfillment and requirement of the degree of

Doctor of Philosophy

Submitted by

Ruhi

(Regd. No. 901409014)

Under the supervision of

Dr. Vijay Luxami

(Associate Professor)

School of Chemistry and Biochemistry

Thapar Institute of Engineering and Technology

Patiala-147004

Punjab, India

June 2021

Candidate's Declaration

It is certified that the thesis entitled "**Synthesis and Evaluation of Chromo-Fluorescent Properties of a New Class of Aza/ Substituted Acenes**" being submitted by Mrs. Ruhi in fulfilment for requirement of the Degree of Doctor of Philosophy in the School of Chemistry and Biochemistry, Thapar Institute of Engineering and Technology, Patiala is an authentic record of candidate's own original and independent research work carried out by her under my supervision and guidance. The material embodied in this thesis has not been submitted in part or full to any other Institute or University for the award of any degree.

Vijay Luxami

(Supervisor)

Dr. Vijay Luxami

Associate Professor

School of Chemistry and Biochemistry

Thapar Institute of Engineering and Technology,

Patiala-147004, Punjab.

Susheel Mittal 19.7.21

(Head)

Dr. Susheel Mittal

Senior Professor

School of Chemistry and Biochemistry

Thapar Institute of Engineering and Technology,

Patiala-147004, Punjab.

Candidate's Declaration

I, hereby declare that the presented work in the thesis entitled "**Synthesis and Evaluation of Chromo-Fluorescent Properties of a New Class of Aza/ Substituted Acenes**" in fulfilment of degree of Doctor of Philosophy is an outcome of research work carried out by me under the supervision of Dr. Vijay Luxami, Associate Professor, School of Chemistry and Biochemistry, Thapar Institute of Engineering and Technology, Patiala, Punjab (India). In keeping with general practice of reporting scientific observations, due acknowledgements have been made wherever work described here has been based on findings of other invigilator. This work has not been submitted in part or full to any other Institute or University for the award of any degree within India or abroad.

Ruhi

Reg. No. 901409014

School of Chemistry and Biochemistry,

Thapar Institute of Engineering and Technology,

Patiala-147001, Punjab (India).

Dr. Vijay Luxami

Associate Professor

School of Chemistry and Biochemistry,

Thapar Institute of Engineering and Technology,

Patiala-147001, Punjab (India)

Primarily, I would thank the Almighty for providing me the potency, vision and power to complete this interesting research and persist on the path to success.

A statement of thanks is not enough to inculcate my deep sense of gratitude to all those who helped me in one way or the other to complete my research work. I would take this opportunity to thank all those people who supported and motivated me all these years.

No words of thanks can be summed up to express my gratitude to my research supervisor Dr. Vijay Luxami, Associate Professor, School of Chemistry and Biochemistry, Thapar Institute of Engineering and Technology, Patiala, for her support, wise counsel, the inputs she made to encourage me and for having faith in me by giving me this opportunity to pursue my research under her guidance. Her consistent motivation at my rough times surely helped me in completing my research work.

I express my gratitude to Director, Thapar Institute of Engineering and Technology, Patiala, Dr. Susheel Mittal, Senior Professor and Head, School of Chemistry and Biochemistry, for providing all the facilities which were helpful for completing my work as well as for providing me with teaching associateship which was helpful for me to bear the expenditure of characterization as well as my general life.

I would like to thank Dr. Kamaldeep Paul, Associate Professor, Thapar Institute of Engineering and Technology, Patiala, for supporting and giving guidance during my work. Special thanks to Dr. Diptiman and Ms. Pawandeep Kaur for their collaboration with me to carry out my sample application studies.

I am highly obliged to my doctoral committee members: Dr. Manmohan Chhibber, Dr. Davinder Kumar, Dr. N. Tejoprakash for their fruitful discussions and valuable suggestions.

Besides thanking my advisor and other faculty members, I would like to thank the non-teaching staff of School of Chemistry and Biochemistry, Thapar institute of Engineering and Technology, Patiala, as well for their support and guidance during the whole course of my research. I am thankful to Mr. Chandar Thakur and Mr. Mayank, School of Chemistry and Biochemistry, for their timely official help and for their cooperation.

I would like to thank my seniors Dr. Richa Rani, Dr. Akul Sen Gupta, Dr. Rashmi and Dr. Rohini Verma who have always helped me at time of need and have also supported me in every possible way. I have gained a lot from their research experiences, their suggestions and comments, which was the most important part for carrying out my work.

I am also thankful to my friends and labmates Dr. Manisha, Ms. Richa Bansal, Ms. Sudesh, Mr. Gulshan Sharma, Mr. Iqubal, Ms. Rekha, Ms. Shivali Gupta, Ms. Shagun Kainth, Ms. Aastha Palta, Ms. Geetika, Ms. Rohini Gupta and Mr. Saurabh Gupta for always standing by my side, motivating me and sharing a great relationship as friends. I will always remember and cherish the time I have spent with them.

I would like to extend my thanks to SAI, Labs Patiala, IIT, Ropar, Punjab University, Chandigarh and Mulatni Mal Modi College, Patiala for providing all the facilities for carrying out the sample analysis and characterizations.

Last but not the least, I would like to thank my both the families, my parents (Father, Mr. Ashok Kumar and Mother, Mrs. Neeraj Bahia) and in-laws (Father In-law, Mr. Suresh Mehta and mother In-law, Mrs. Lalita Mehta), my brother (Mr. Rahul) for supporting me spiritually since initial years of research till writing of my thesis and my life in general. A special thanks to my husband Mr. Rohin Mehta who has been by my side through thick and thin. The immense support and encouragement that he provided me all these years gave me mental strength without which I wouldn't have been able to carry out my research.

Besides this, I am thankful to all those people who have knowingly/ unknowingly helped me in successfully completing my work.

Ruhi

List of Abbreviations

HEPES	(4-hydroxyethyl)-1-piperazineethanesulfonic acid
Phenalenedicarbonitrile	1-oxo-1*H*-phenalene-2,3-dicarbonitrile
NMR	Nuclear Magnetic Resonance
EDTA	Ethylene Diamine Tetra Acetic Acid
Tris	tris(hydroxymethyl)aminomethane
COSY	Correlated SpectroscopY
CHEF	Chelation Enhanced Fluorescence
FRET	Fluorescence Resonance Energy Transfer
PET	Photo-induced Energy Transfer
TBET	Through Bond Energy Transfer
ICT	Intramolecular Charge Transfer
BODIPY	boron-dipyrromethene
THF	Tetrahydrofuran
DMSO	Dimethyl sulfoxide
TEA	Triethylamine
TLC	Thin Layer Chromatography
IR	Infra-red
IMP	Implication
IMP-INH	Implication-Inhibit
Cy	Cystein
Hcy	Homo-cystein
Ppi	Pyrophosphate
ppm	Parts per million
M.Pt.	Melting Point
RSD	Relative Standard Deviation

Symbols

K_a	Association constant
K_r	Rate constant for radiative pathway
K_{nr}	Rate constant for non-radiative pathway
Φ	Quantum efficiency
μM	Micro Molar
nM	Nano Molar
ns	Nano second
λ_{abs}	Absorption maximum
λ_{em}	Emission maximum
χ	Chi
τ_{avg}	Average life-time

LIST OF CONTENTS

CHAPTER 1

General Introduction:

Over the past several decades, selective and sensitive recognition of ions has attracted attention in the field of supramolecular chemistry because of the increasing ion pollution in the environment. For this purpose numerous chemosensors have been developed which are capable of sensing specific ions and have proven to be useful in fluorescence based cell imaging, molecular catalysis etc. [1-5]. Earlier, the techniques employed for sensing of heavy metal ions were not only costly but also required large sample quantities. Thus, efforts have been made to develop simple, adequate, inexpensive and reliable methods for detection of a specific ion without the interference of other analytes and could be used for sensing of ion in living systems. One such tool is the formulation of chemosensors [6-10]. Different chromogenic and fluorogenic sensors have been deployed and were proved to be unorthodox to the conventional methods as they are selective and have the potential to detect the analytes at very low concentrations. In chromogenic sensors, color change is induced on binding with ion, which is advantageous due to its appearance with naked eyes and expensive instrumentation is avoided. Whereas in fluorogenic chemosensors, on interaction with specific ion, changes in fluorescence pattern occur. A fluorescent chemosensor is constituted of two parts: i) fluorophore ii) guest receptor, both the parts are connected *via*.spacer [11]. The binding of the guest species to the receptor site induces a change in the fluorescence. Sensors based on these changes have attracted attention that led to advancements in the field of supramolecular chemistry due to their sensitivity, simplicity, rapidity, real-time fluorescence monitoring and inexpensiveness. The radiative pathway where a molecule excited by absorbing photons comes back to its ground state by reemission of the absorbed photons is called fluorescence. This phenomenon can be explained by the Jablonski diagram for fluorescence (**Figure 1**) where the molecule absorbs energy and jumps from its ground state (S_0) to higher energy state and while coming back to its ground state it undergoes vibrational relaxations that induce shift in absorption and emission maxima which is known as stroke shifts [12]. During the relaxation process, photon of longer wavelength is emitted by the molecule. The two essential conditions that allow fluorescence in molecules is

conjugation as π-bonds induce excitation at longer wavelengths in comparison to σ-bonds and structure rigidity which prohibits fully non-radiative process while coming back to ground state.

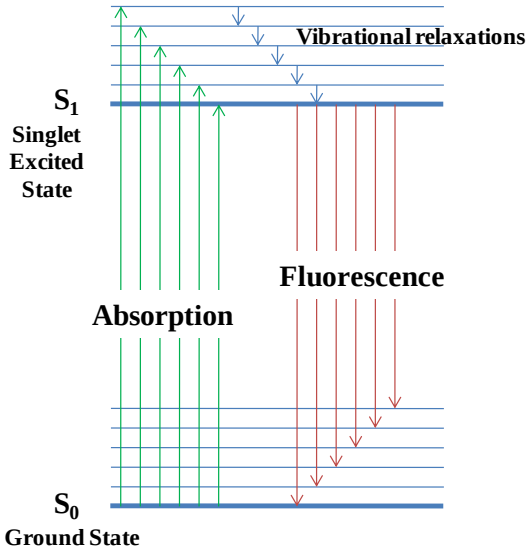

Figure 1: Jablonski diagram for fluorescence

Numerous ion sensing fluorescent compounds have been fabricated by using small molecules like BODIPY, coumarin, naphthalimide, fluorescein, rhodamine etc. [13-21]. All these molecules have worked as excellent fluorophore for the preparation of fluorescent chemosensors because of π-conjugated skeletons and rigid structure. A fluorochrome (fluorophore as well as chromophore), rhodamine has always been the interest of the researchers for formulating ion sensors.

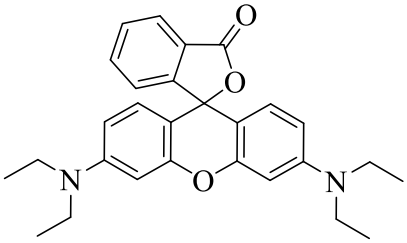

Rhodamine B

I

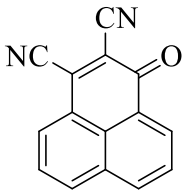

1-oxo-1H-phenalene-2,3-dicarbonitrile

II

Rhodamine(**I**) is a xanthenes moiety having tertiary amines attached to it. Rhodamine has excellent photophysical properties such as strokes shifts, quantum yields and absorption coefficients, which makes it a better organic scaffold for designing of chemosensors than rest of the molecules. The unique mechanism of the spirolactam ring opening and closing of rhodamine

has been useful in colorimetric detection of particular ion(s) [22]. The spirolactam ring closed form of rhodamine is non-fluorescent and colorless, whereas, in the presence of lewis acid, the spirolactam ring opens and this 'ring open' form leads to change in color and make the moiety fluorescent. In neutral medium, both the forms i.e. 'ring closed' and 'ring open' form exist in equilibrium.

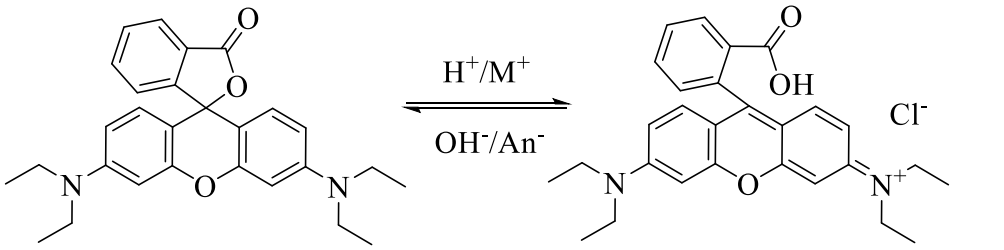

Spirolactam ring close form
Non-fluorescent and colorless

Spirolactam ring open form
Fluorescent and pink/red in color

Scheme 1

Apart from, the well known precursors like rhodamine, BODIPY, naphthalimide etc., smaller and novel molecules can also be used for designing fluorescent chemosensors due to their excellent spectral properties, structural rigidity and easy synthetic pathways for their preparation.

One such molecule which has been explored less for its sensing purpose is1-oxo-1*H*-phenalene-2,3-dicarbonitrile (phenalenedicarbonitrile) (**II**). Compound **II** is a planar, rigid and is highly electron deficient moiety due to the presence of electron withdrawing cyano groups. The amino derivatives of **II** are strongly fluorescent and ICT (intramolecular charge transfer) active due to the presence of electron-withdrawing and donating groups [23,24].

1.1. Literature Review:

The preparation of rhodamine was first reported in 1905 by Noelting and Dziewonsky[25]. Till 1997, various colorimetric rhodamine sensors were prepared by various research groups but it was in 1997 when the unique spirolactam ring-opening and closing mechanism of rhodamine was given attention [26]. Since then various rhodamine based chemosensors have been formulated for different metal ions *viz.* Hg^{2+}, Cu^{2+}, Pb^{2+} etc. and anions such as OCl^-, OAc^-, F^-, CN^- etc. [20, 27-39] but the sensing of trivalent metal ions such as Al^{3+}, Cr^{3+} and Fe^{3+} has always been a challenging task. These trivalent metal ions are biologically and environmentally important.

The sensing of all these three trivalent metal ions has always faced challenges. For instance, even though Al^{3+} being diamagnetic in nature and its chelation with the sensor leads to fluorescence enhancement, still the sensing of Al^{3+} has always been problematic due to its strong hydration and poor co-ordination ability. Different analytical techniques such as voltametric and colorimetric and ion sensitive electrodes have been deployed for Al^{3+} sensing. Furthermore, Cr^{3+} and Fe^{3+} being paramagnetic, lead to fluorescence quenching. In sensing of ions, the sensors which display fluorescence 'turn-on' response are generally preferred over the sensors which display 'turn-*off*' response. Due to this, very few sensors for Cr^{3+} and Fe^{3+} have been reported which show fluorescence 'turn-on' response. For sensing of all these metal ions, new compounds having multiple chelating sites have been put into use such as rhodamine which has N and O as the co-ordinating sites. Different rhodamine based fluorescent compounds have been formulated for sensing of trivalent metal ions by various research groups.

On the other hand, in 2005, Qian's research group first described the synthesis and strong fluorescence properties of small conjugated polycyclic molecule 8-oxo-8*H*-acenaphtho[1,2-*b*]pyrrol-9-carbonitrile and its derivatives [23]. Since then, these structures have also appeared in other major publications, which described their great optical properties for fluorescent chemosensor devices. Regarding their biological activity, these structures were reported for their promising effect as potent inhibitors of Bcl-2 (B-cell lymphoma 2) and Mcl-1 (Myeloid cell leukemia 1) proteins as well as for selective FGFR-1 (fibroblast growth factor receptor 1) inhibition but their ion sensing capabilities have been less explored.

Synthesis of the originally proposed 8-oxo-8*H*-acenaphtho[1,2-*b*]pyrrol-9-carbonitrile led to a structural revision in 2014 [39], and the product has now been identified as 1-oxo-1*H*-phenalene-2,3-dicarbonitrile. The structural assignment was corroborated by detailed NMR studies and unambiguously confirmed by X-ray diffraction.

Based upon the design and preparation of various chemosensors, the literature review has been divided into two sections:

1.1.1 Rhodamine based sensors

1.1.2 Phenalenedicarbonitrile based sensors

1.1.1. Rhodamine based sensors:

1.1.1.1. Rhodamine based Cr^{3+} and Fe^{3+} sensors

Xiang *et al.* in 2006 [40] synthesized a novel fluorescent compound **1** based on the rhodamine spirolactam (ring closed and non-fluorescent) and amide form (ring open and fluorescent) having completely opposite fluorescence properties. In the absence of metal ions fluorescence spectrum gave a weak emission band at 550 nm of **1** (10 μM). But in the presence of Fe^{3+} ions, elevation of 114-fold in the emission intensity along with red shift of 25 nm in C_2H_5OH and 48-fold enhancement in tris-HCl buffer having *p*H = 7.15 was observed. Interference by background metal ions such as Cr^{3+}, Fe^{2+}, Zn^{2+}, Ag^{+}, Pb^{2+}, Ba^{2+}etc was observed in ethanol whereas in tris-HCl aqueous buffered solution, compound **1** (10 μM) was selective towards detection of Fe^{3+} even in the presence of other metal ions. Even though in aqueous media, compound **1** (10 μM) wasn't able to show strong binding towards Fe^{3+} and hence couldn't be used in biological systems; however, it could selectively detect Fe^{3+} at a low concentration of 10^{-5} M.

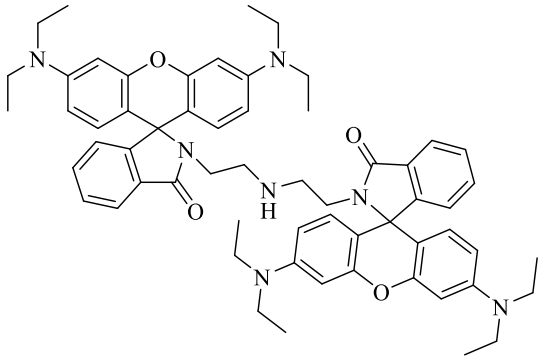

1

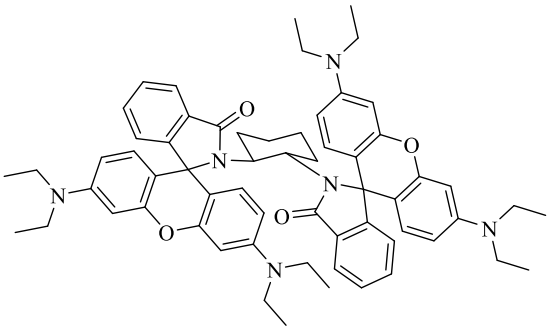

2

Linking of two rhodamine hydrazide units by *trans*-1,2-diamino cyclohexane moiety gave the fluorescence '*off-on*' chemosensor **2** [41] for selective estimation of Cr^{3+} in CH_3CN:H_2O (4:1 (v/v) HEPES buffer *pH* = 7). On binding with Cr^{3+}, compound **2** (10μM) gave a visible color change with red shift in absorption band and formation of new characteristic band of rhodamine spirolactam ring-open form at 556 nm. When excited at 520 nm, emission enhancement of more than 100-fold at 580 nm was observed. The job's plot experiment indicated the formation of complex in 1:1 stoichiometry having a binding constant of 3.4×10^4 M^{-1}. For proposing its binding mechanism, ^{1}H-NMR and ^{13}C-NMR titrations were performed in presence of Cr^{3+}. ^{1}H-NMR titration proved the participation of N in binding with Cr^{3+}whereas, ^{13}C-NMR showed the absence of peak between 67.0-69.0 ppm (which is the characteristic peak of spirocyclic C of ring closed form), thus confirming the ring-opening of rhodamine in presence of Cr^{3+}. The reversibility in color as well as spectral changes was attained in the presence of EDTA. The *p*H-titrations revealed that compound **2** was resistant towards *pH* change within a range of 4.0-10.0 and its stability at physiological *pH* was further used to test its capability of monitoring Cr^{3+} in living cancer cells (HeLa).

By changing the linker between two rhodamine units, Kumar and co-workers [42] designed compound **3** and characterized it by exploring its spectroscopic, optical and analytical properties. It has been revealed that compound **3** showed selectivity towards the recognition of Fe^{3+} in THF at a very low detection limit of 1.1×10^{-9} M. Compound **3** (5μM) did not give any absorption or emission band above 500 nm owing to existence of spirolactam ring-closed form but on the introduction of Fe^{3+}, characteristic absorption band at 555 nm and emission band enhancement by 684-fold at 582 nm was observed that clearly pointing towards metal-chelate formation

leading to ring-opening of rhodamine. Competitive experiments showed that metal ions like Fe^{2+}, Cu^{2+} and Ni^{2+} also gave absorption band at 555 nm but no interference by these ions was observed in fluorescence spectra. Further, Li *et al.* [43] prepared another colorimetric and fluorescence '*off-on*' compound **4** by linking two rhodamine moieties *via* cyst-amine unit. Compound **4** (10μM) was originally colorless and non-emissive but on incubation with Fe^{3+}, a colorimetric change to pink as well as red emission under UV-Vis was observed. The spectral changes were also in accordance with the visible changes i.e. absorbance band in the visible region was attained at 552 nm and emission band at 576 nm with 60-fold enhancement in (tris-HNO_3 buffer *pH* = 7.0) H_2O-C_2H_5OH (99:1 (v/v)). All the colorimetric and spectral changes were the result of metal induced ring opening of rhodamine. It was found that compound **4** can selectively sense Fe^{3+} within a *pH* range of 6.0-8.0 and its stability at neutral *pH* suggested its use for Fe^{3+} monitoring in living HeLa cells.

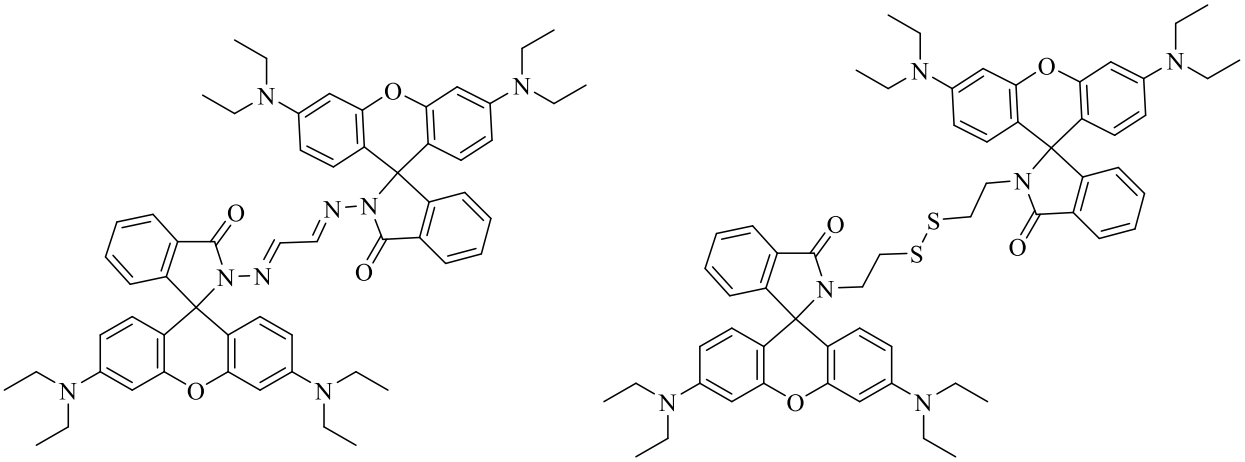

3 **4**

By altering the chelation cavity size, number and nature of chelation, Mandal and his co-workers [44] designed and synthesized a series of mono-rhodamine and bis-rhodamine Fe^{3+}sensors having interference with Cu^{2+}. The mono-rhodamine compounds **5a** and **5b** (10 μM) formed complex with Fe^{3+} and Cu^{2+} in 2:1 stoichiometries and the bis-rhodamine compounds **5c-f** (10 μM) formed 1:1 complexes with Fe^{3+} and Cu^{2+} in 0.01 M tris-HCl-CH_3CN (1:1 (v/v) *pH* = 7.4). All the compounds (mono and bis-rhodamine) originally gave colorless solution due to existence of spirolactam ring closed form with no absorption band above 500 nm but when incubated with Fe^{3+} or Cu^{2+}, the metal chelate caused ring opening and color turned to pink with formation of absorption band centered at 555 nm with shoulder at 520 nm. Similarly, no emission band was

observed in the absence of metal ions (Fe^{3+} or Cu^{2+}) but when these metal ions were injected into solution of compounds (**5a-f**), emission band appeared above 500 nm. Among all the bis-rhodamine compounds, compound **5e** (10 μM) displayed excellent fluorescence enhancement of 443-fold at ~576 nm, in the presence of Fe^{3+} whereas the emission enhancement for Cu^{2+} was just 23-fold, clearly indicating its selectivity and sensitivity towards Fe^{3+}. The detection limits for **5e** to selectively sense Fe^{3+} was calculated to be 4×10^{-7} M. The *pH* titration showed the stability of spirolactam ring of compound **5e** above *pH* = 4 which suggested that it could be used for live cell imaging of fibroblast cells.

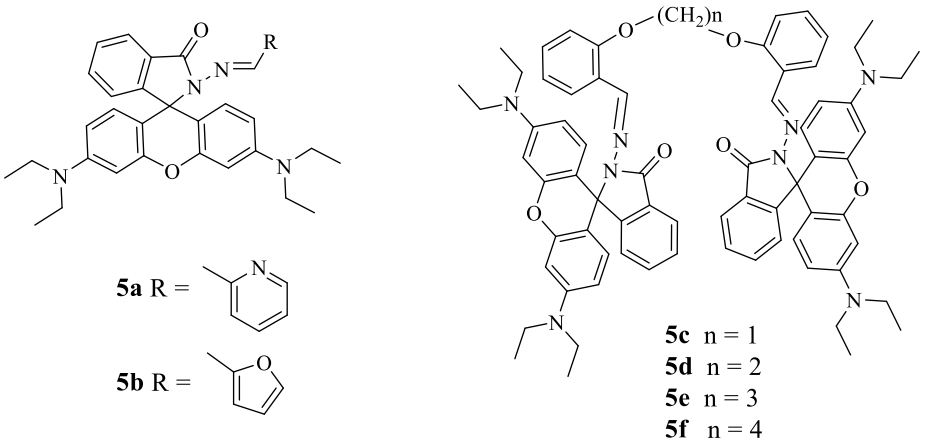

In 2008, Li. *et al*. [45] reported another rhodamine-quinoline based Cr^{3+} sensor **6** by linking rhodamine derivative with ferrocene, forming a multi-signal sensor which showed a prominent enhancement in the emission band at 530 nm on incubating with Cr^{3+} in aqueous ethanolic medium (1:1 (v/v). *pH* = 7.4). It further proved to have potential application in monitoring of Cr^{3+} in living cells.

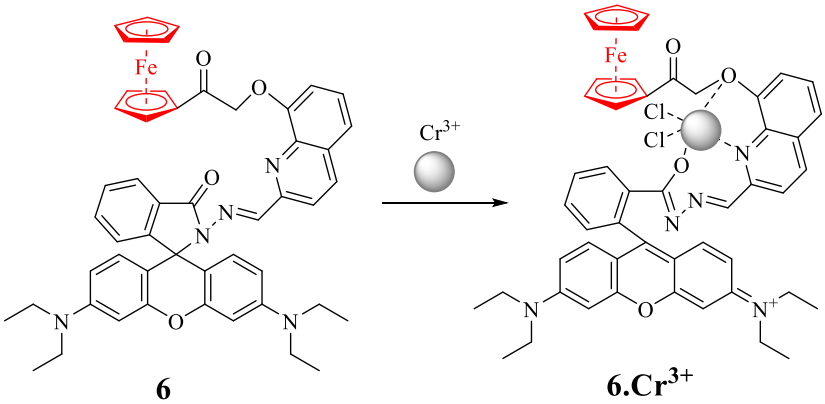

Scheme 2

Li and his co-workers formed a Cr^{3+} sensing multi-chelating FRET-based system by joining rhodamine and 1,8 naphthalimide derivatives [46]. Compound **7** displayed its absorption band at 380 nm and emission band at 544 nm in H_2O-C_2H_5OH medium (2:1 (v/v)). On addition of Cr^{3+}, a new absorption band centered at 568 nm was observed and the change in color from yellow to red orange was noticeable. The emission response of compound **7** towards Cr^{3+} was observed with a 15-fold enhancement in the band at 590 nm. Compound **7** was also tested for monitoring Cr^{3+} in living cells and was the first example where a fluorescent compound was used for sensing of Cr^{3+} in living cells.

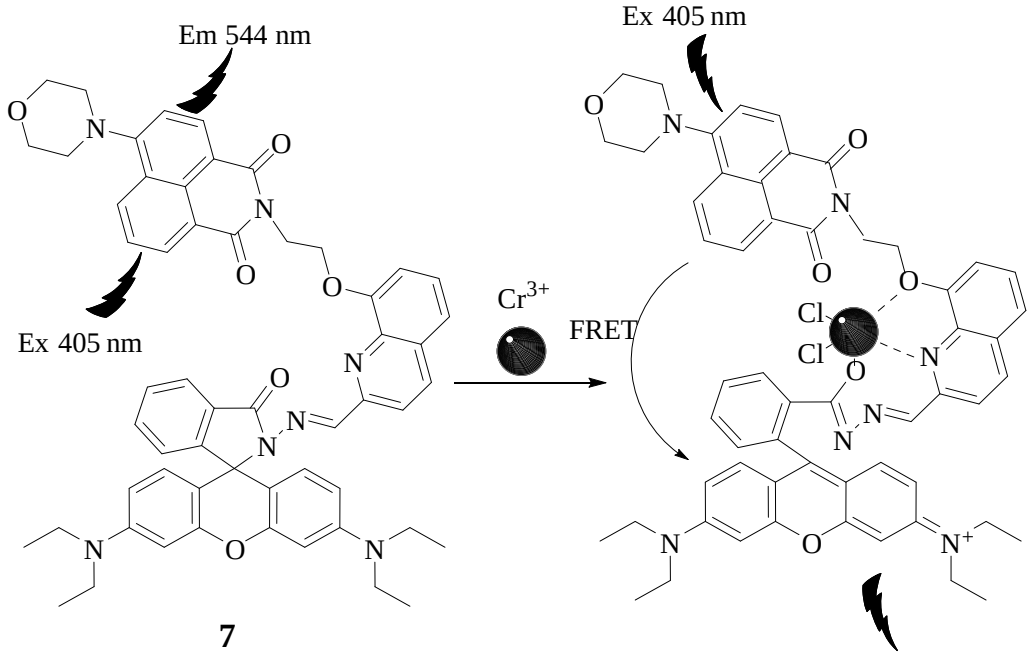

7

Scheme 3

Quinoline derivatives have been useful in preparation of Ni^{2+} sensors. Therefore, rhodamine-quinoline derivatives have been developed for effective detection of Cr^{3+} ions wherein Cr^{3+} binds with four donor atoms and the octahedron is completed with the binding of two anions [45,46]. Following this, Sinn *et al.* [47] synthesized two rhodamine-quinoline based sensors which proved to be better sensors for Cr^{3+} and Ni^{2+} in CH_3CN than earlier reported rhodamine-quinoline based sensors. Compound **8** was prepared by linking rhodamine-B and quinoline derivative *via* amide unit. Due to presence of –OH group on the quinoline ring, compound **8** (20 μM) showed remarkable enhancement in absorption intensity at 560 nm in presence of Ni^{2+} ions (183-fold) as compared to Cr^{3+} (55-fold) and Co^{2+} (56-fold). On contrary, when excited at 510

nm, fluorescence band was attained at 580 nm in presence of Cr^{3+} and the enhancement of 1100-fold was observed whereas, no fluorescence change was observed in the presence of Ni^{2+} and Co^{2+}in CH_3CN. On the other hand, compound **9** was found to be selective for Cr^{3+}even though the color change was attained in the presence of Cu^{2+} as well, but the fluorescence change was observed in the presence of Cr^{3+}. The complex **8.Cr^{3+}**(1:1 stoichiometry) was further used to detect CN^-due to metal-displacement which further led to colorimetric as well as spectral reversibility. The detection limit for complex **8.Cr^{3+}** to selectively detection of CN^- was determined to be 5.4 μM.

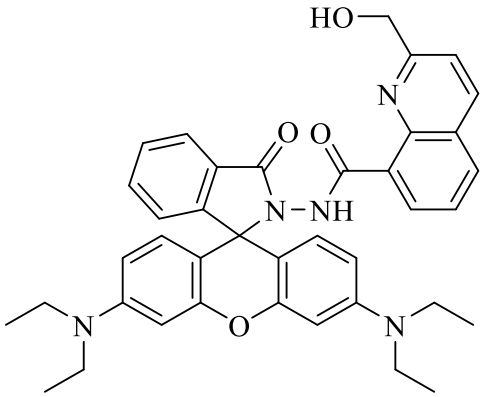

8

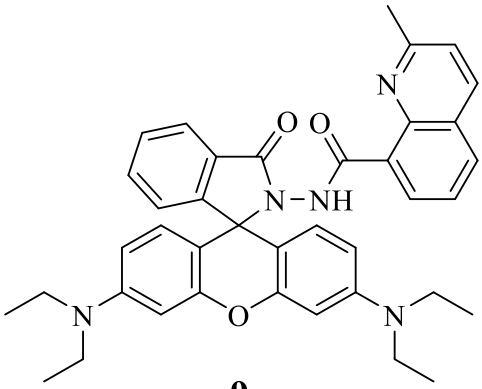

9

Mandal and co-workers [48] synthesized rhodamine-quinoline based colorimetric and fluorescence '*off-on*' sensor **10** having 'O-N-N-O-N' combination, which is preferable for Fe^{3+} sensing. Compound **10** (10 μM) was found to be selective and sensitive towards Fe^{3+} without interference from other background metal ions in aqueous buffer. Compound **10** was originally colorless and did not have absorption or emission band above 500 nm. The incubation of Fe^{3+} led to change in color to pink due to metal induced rhodamine spirocyclic ring open form. In the presence of Fe^{3+} the absorption band at 530 nm intensified by 744-folds and the emission band at 552 nm increased by 427-fold. These spectral changes revealed the high sensitivity of compound **10** towards Fe^{3+} ions over other analytes. The detection limit for compound **10** to selectively sense Fe^{3+} was 5 $\times 10^{-8}$ M. The stability of compound **10** in the *pH* range of 6.0-10.0 formed the basis for Fe^{3+} imaging in living fibroblast cells and also useful for the formation of a polymeric thin film for Fe^{3+} sensing.

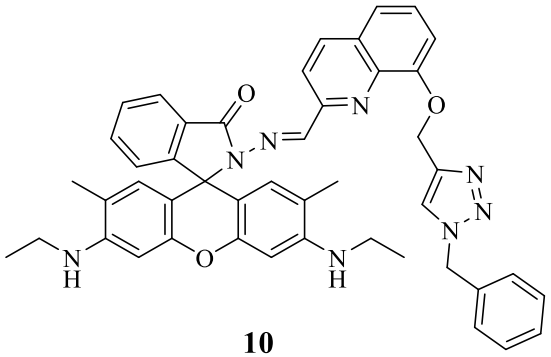

10

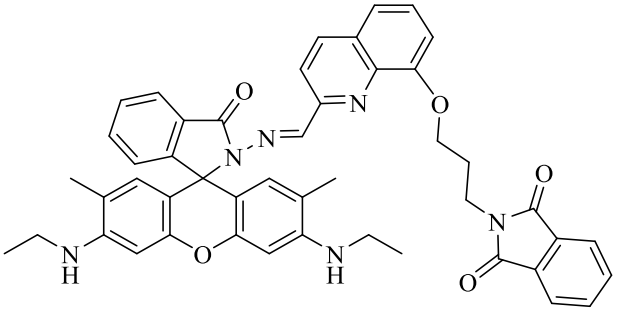

11

With a slight modification in substitution at quinoline part of compound **10,** Zeng and his co-workers [49] prepared another rhodamine based colorimetric and fluorescence '*off-on*' compound **11** which could efficiently sense Fe^{3+}. The spectral properties of compound **11** were explored in C_2H_5OH-H_2O (3:7 (v/v)). Originally the solution of compound **11** (5 μM) was colorless due to the existence of rhodamine in the spirolactam ring close form which was further confirmed by the presence of peak at 67.56 ppm in ^{13}C-NMR spectrum which represents the spirocyclic carbon. The absorption spectra showed a weak band at above 500 nm ascribed to the presence of ring open form. The compound has the preferred combination for chelating with Fe^{3+} and on binding with other metal ions, the visible colorimetric change (pink) was observed along with formation of absorption band at 532 nm which is ascribed to the ring opening mechanism triggered by metal ion binding. The 1:1 stoichiometric binding of Fe^{3+} with compound **11** was established through job's plot analysis and the association constant was calculated to be 1.1×10^6 M^{-1} in C_2H_5OH-H_2O (3:7 (v/v)). Further, the *pH* titrations showed the stability of compound **11** at physiological *pH* which was considered for testing its applicability in biological systems and hence, compound **11** proved to be excellent fluorescence turn-on sensors for Fe^{3+} in living cells.

By employing quinoline, a simple and novel rhodamine-8-aminoquinoline compound **12** liked *via* ethylene diamine was also developed by Zhang *et al.* [50] to offer solvent dependent detection of ions. It gave a fluorescence turn-on response on binding with Cr^{3+} in CH_3CN and for Cu^{2+} in ethanolic solution. The complex formation with both the ions gave 1:2 stoichiometry in Job's plot analysis. The fluorescence titrations were carried out in CH_3CN-H_2O (99:1 (v/v) *pH* = 7) for Cr^{3+} and in CH_3OH-H_2O (99:1 (v/v) *p*H=7) for Cu^{2+} ions. Both the ions formed 1:2 complexes with compound **10**. The association constants and detection limits were calculated from the fluorescence titration profiles wherein the association constants were calculated to be

$2.9 \times 10^8\ M^{-2}$ for Cr^{3+} and $6.0 \times 10^8\ M^{-2}$ for Cu^{2+} and detection limits were 0.047 and 0.076 μM for Cr^{3+} and Cu^{2+}, respectively.

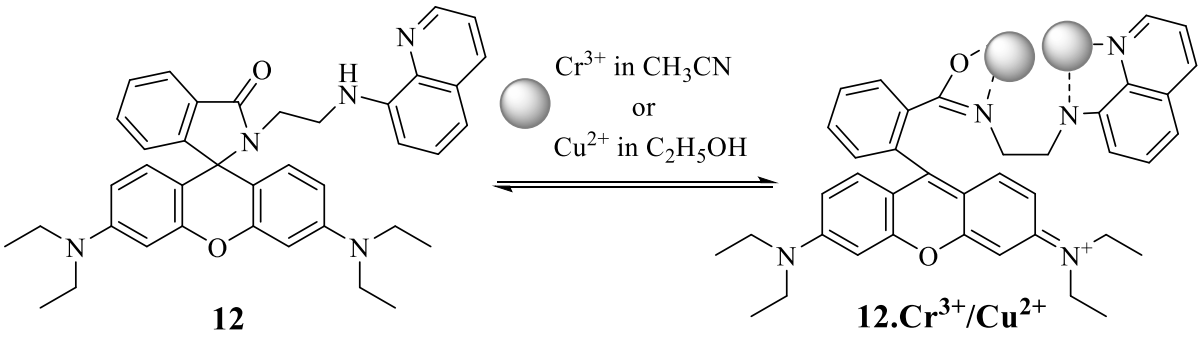

Scheme 4

Das *et al.* [51] formulated a rhodamine 6G derivative with another fluorophore quinoline **13** which showed preference towards binding with Hg^{2+} and Cr^{3+} in CH_3CN-HEPES buffer (3:2 (v/v) *pH* = 7.3). Compound **13** was characterized by different spectroscopic techniques like ^{1}H-NMR, ^{13}C-NMR, mass spectrometry, and single crystal X-ray. It could be used as a dual chemosensor for sensing of two ions by considering its optical and spectral changes. From the UV-Vis and fluorescence studies for compound **13** (7.05 μM), it was concluded that in the presence of Hg^{2+}, a new absorption band at 527 nm was attained. While in the presence of Cr^{3+}, the band was centered at 531 nm wherein the absorption band intensity was prominent for Hg^{2+}. On the other hand, when compound **13** was excited at 500 nm, an emission band at 556 nm was observed in the presence of the metal ions. Furthermore, the studies suggested that the colorimetric as well as spectral reversibility of the complexes **13.Hg^{2+}** and **13.Cr^{3+}** could be achieved in the presence of I^- or EDTA. Introduction of EDTA into the solution of these complexes caused demetalation giving back the original compound. Investigation of *pH* studies inferred that the spirocyclic closed form was resistant to *pH* change within 5.0-11.0 and its stability at biological *pH* allowed monitoring of Hg^{2+} and Cr^{3+} in MCF-7 cells.

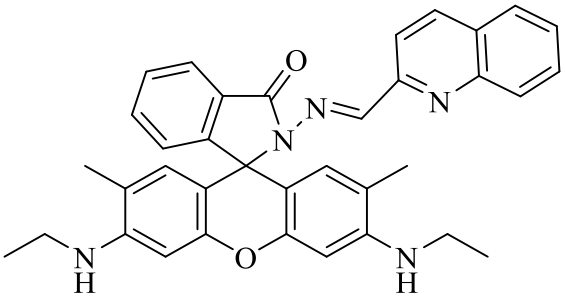

13

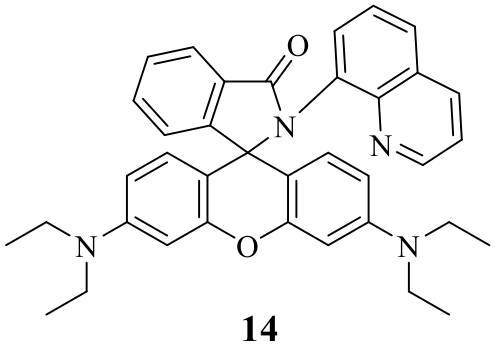

14

By directly linking rhodamine and quinoline, Qian *et al.* [52] reported compound **14** as a selective and sensitive sensor for recognition of Fe^{3+} in 50% CH_3CN-HEPES buffer (20 mM, *pH* = 6.95). The presence of Fe^{3+} led to dual changes i.e. colorimetric as well as spectral. Presence of Fe^{3+} in compound **14** (10 μM) led to color change from colorless to purple and the absorption band at 530 nm was formed. The fluorescence was turned-on showing a 50-fold intense band at 590 nm. These changes clearly suggested that ring opening process occurred on binding of compound **14** with metal ion. Slight interferences of 18-fold by Cr^{3+} and Cu^{2+} were observed whereas no other metal ion interfered in the sensing of Fe^{3+}. The detection limit of compound **14** (10 μM) for sensing Fe^{3+} was calculated to be 3.5 μM. The binding stoichiometry of 2:1 was analyzed by 1D ^{1}H-NMR and 2D ^{1}H-^{1}H-COSY. The insensitivity of compound **14** towards change in *pH* within 6.0-12.0 was useful in the live cell imaging.

The linking of diarylethene having 1,8-naphthalimide derivative and rhodamine unit gave the novel compound **15** which effectively responded to the presence of Cr^{3+} in CH_3CN [53]. The binding of Cr^{3+} to the compound triggered the fluorescence enhancement at 603 nm due to metal induced spirolactam ring-opening of rhodamine which was accompanied by change in the color of the colorless solution to purple. The reversibility of complex **15.Cr^{3+}** was achieved by the addition of EDTA which causes decomplexation and gives back the original compound, accompanied by color change to colorless as well as decrease in the fluorescence intensity. This was further used to construct a 4-input and 1-output logic circuit.

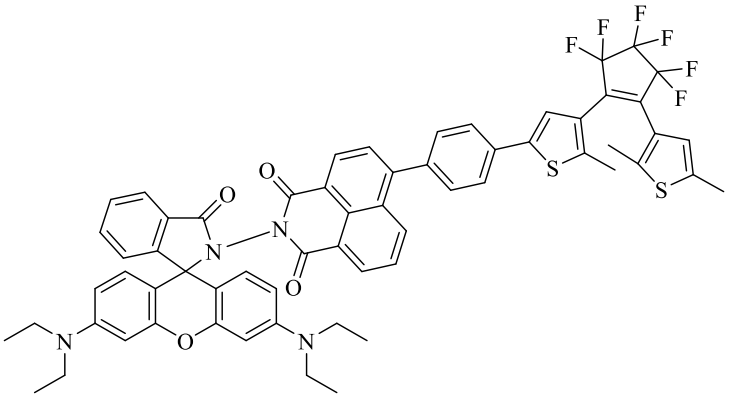

15

Adhikari and co-workers [54] designed and synthesized a CHEF-FRET based system **16**, by using rhodamine and naphthalimide derivatives for sensing of Cr^{3+} in aqueous buffered CH_3CN (*pH* = 7.4). Compound **16** gave an emission band at 382 nm and in presence of Cr^{3+}, the intensity of band at 382 nm was increased due to inhibition of PET and initiation of CHEF process and a new band at 575 nm was formed (characteristic band of rhodamine amide form). As the emission band at 385 nm and absorption band of rhodamine B (~550 nm) could not show effective overlap, hence, compound **16** could not be represented as FRET based compound. On contrary, compound **17** gave a large spectral overlap between the emission band of compound **17** centered at 529 nm and absorption band of rhodamine B (~550 nm), proved to be an efficient FRET based compound and had high selectivity and sensitivity towards Cr^{3+} ions. It had the capability of detecting Cr^{3+} at a very low limit of 1.81×10^{-6} M and was used for Cr^{3+} imaging in various cells like MCF-7, HeLA, Hep3B, HEK and SiHA.

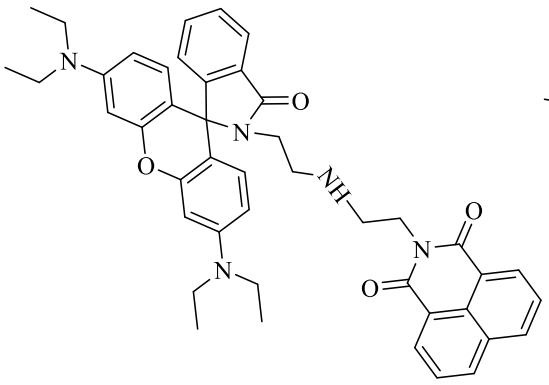

16

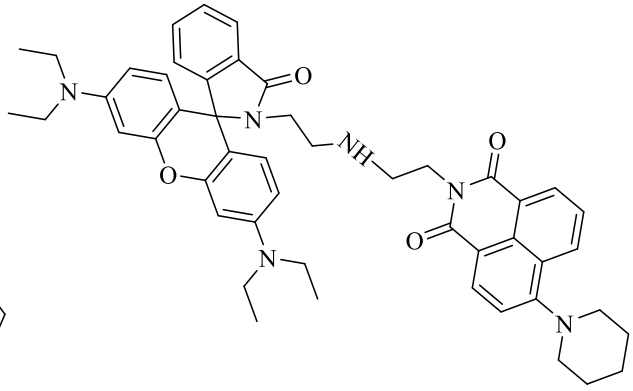

17

Another rhodamine-naphthalimide sensor **18** based on FRET mechanism was synthesized by Das *et al.* [55] for the ratiometric sensing of Cr^{3+} and Hg^{2+} wherein naphthalimide part acted as a donor and rhodamine part was the acceptor. This probe could detect the Cr^{3+} and Hg^{2+} uptake by the cells when used on epithelial A431 cells.

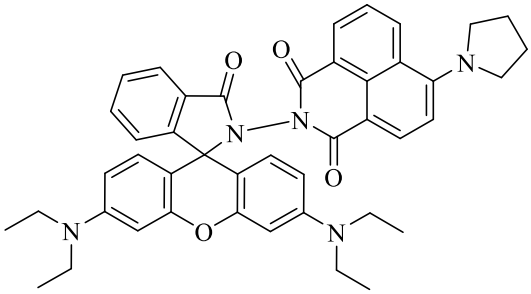

18

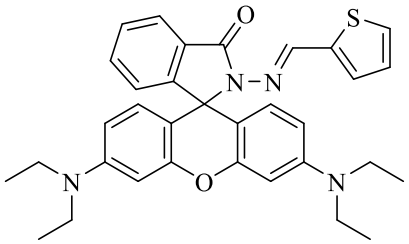

19

A novel fluorescence 'turn-on' compound**19** was designed and fabricated by reacting rhodamine B derivative (rhodamine B hydrazide) with thiophene-2-furanaldehyde [56]. The compound **19** was found to be highly sensitive towards Cr^{3+} with slight interference from Hg^{2+}, Zn^{2+} and Pb^{2+}. On binding with Cr^{3+} in 1:1 stoichiometry, the spirolactam ring opening of rhodamine occurs leading to the delocalizating within xanthenes part of rhodamine and enhancement of emission band at 583 nm was observed. The association constant was calculated to be 2.0×10^4 M^{-1}. Furthermore, its reversibility was achieved by the addition of EDTA which causes decomplexation.

In 2010, Tang *et al*. [57] reacted rhodamine B derivative (rhodamine B ethylenediamine) with thiophene-2-furanaldehyde. The difference between compound **19** and compound **20** is the linker that joins rhodamine B to thiophene-2-furanaldehyde. In the linker was hydrazide whereas in compound **20** the linker was ethylenediamine. The change in the linker has changed the sensing properties of the compound. This compound was found sensitive towards Fe^{3+} with slight interference from Cr^{3+} ions in CH_3OH-HEPES buffer (10mM, *pH* = 7.4). Compound **20** formed a 1:1 complex with Fe^{3+} which led to metal induced spirolactam ring-opening of rhodamine B moiety and gave an intense emission band at 580 nm.

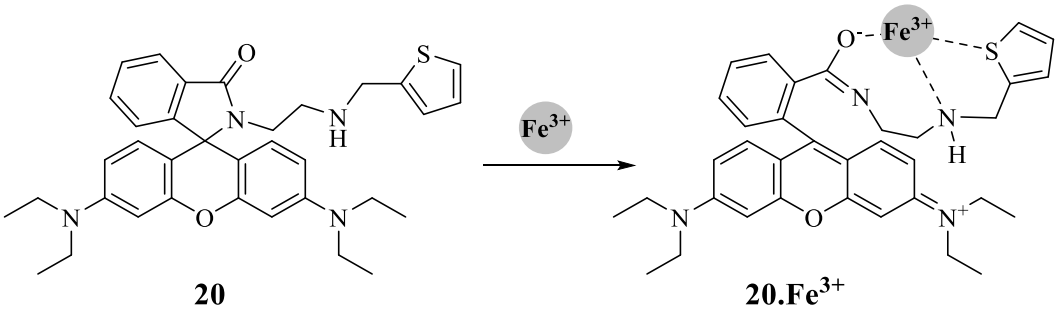

20 **20.Fe^{3+}**

Scheme 5

Xie and co-workers [58] formulated a rhodamine based chromo-fluorescent 'turn-on' sensor **21** for Cr^{3+} in aqueous medium. Cr^{3+} induces rhodamine spirolactam ring opening which leads to formation of absorption band at 581 nm and enhancement of fluorescence band at 600 nm. It forms a strong 1:1 complex with Cr^{3+} with association constant of 5.75×10^4 M^{-1} and lowest detection limit of 3.75×10^{-9} M. Compound **21** was further used for monitoring Cr^{3+} in live Hela cell.

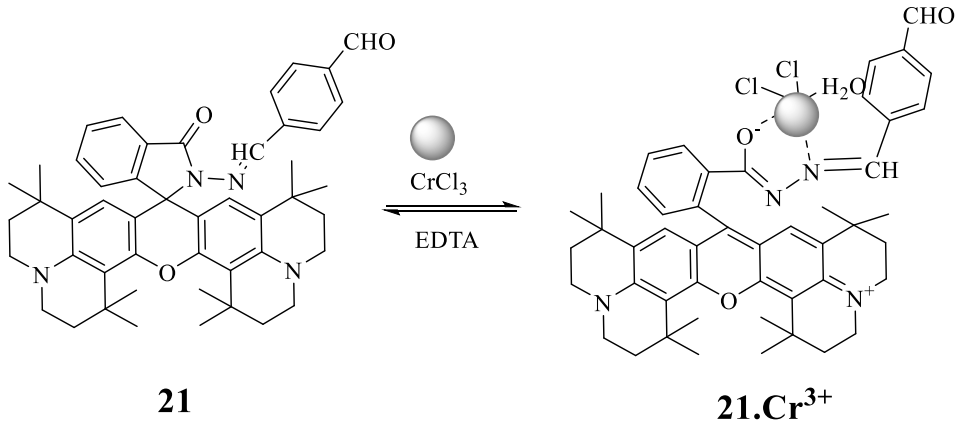

21 **21.Cr^{3+}**

Scheme 6

Two novel fluorescent compounds **22** and **23,** having rhodamine derivative linked with different salicylaldehydes through ethylene diamine were prepared by Gupta and his co-workers [59]. Both these compounds formed a 1:1 complex with Cr^{3+} and gave a visible color change to pink. The fluorescence was also enhanced at ~575 nm. The stability constants for both the compounds were calculated by Benesi-Hieldebrand equation and were found to be 2.7×10^4 M^{-1} for compound **22** and 4.5×10^3 M^{-1} for compound **23**. The detection limits were calculated on the

basis of fluorescence titration and was found that the compound **22** (4.9×10^{-8} M) could detect Cr^{3+} more effectively as compared to compound **23** (2.4×10^{-7} M).

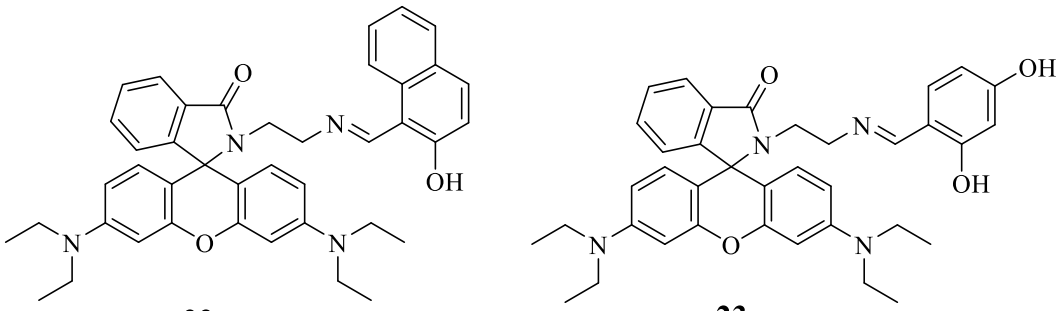

22 **23**

Lie *et al.* [60] developed a novel rhodamine B based poly(amidoamine) dendrimer having rhodamine B in core and 1-phenyl-3-methyl-5-pyrazolone in the periphery. This dendrimer **24**, on binding with Cr^{3+}in 1:10 stoichiometry, showed a drastic enhancement in the emission band at 571 nm along with the visible change in color. Compound **24** proved to be better sensor than only rhodamine B for Cr^{3+}.

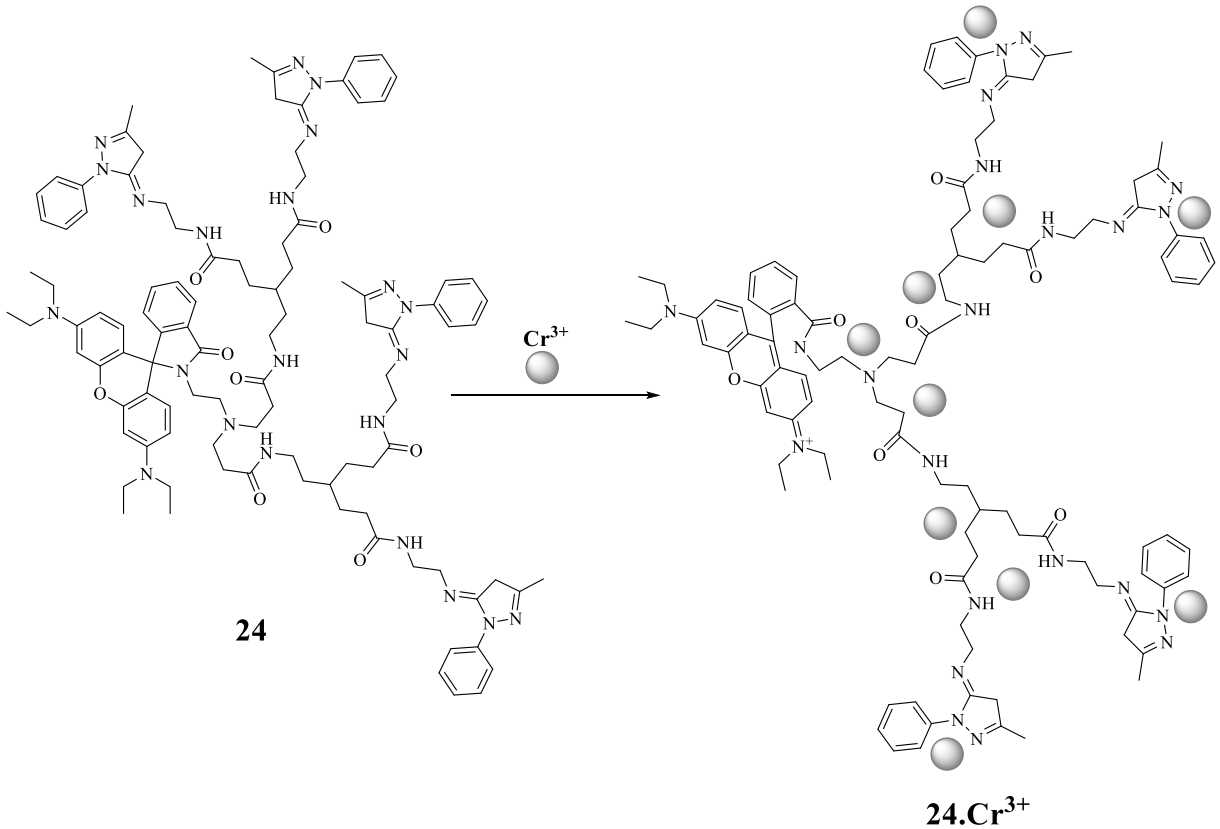

24 **24.Cr^{3+}**

Scheme 7

Sunnapu and co-workers [61] prepared a novel rhodamine hydrazide-3,4-dimethoxybenzaldehyde based fluorescence '*off-on*' chemosensor. Compound **25** was highly selective and sensitive towards Cr^{3+} ions in CH_3CN-H_2O (2:8 (v/v)) without significant interference from other metal ions. It formed a 1:1 complex with Cr^{3+} ions and the association constant was calculated to be 2.582×10^4 mol L^{-1} that could detect Cr^{3+} at a low concentration of 17.8 nM. The biological applicability of compound **25** was further tested for monitoring Cr^{3+} in HeLa cells.

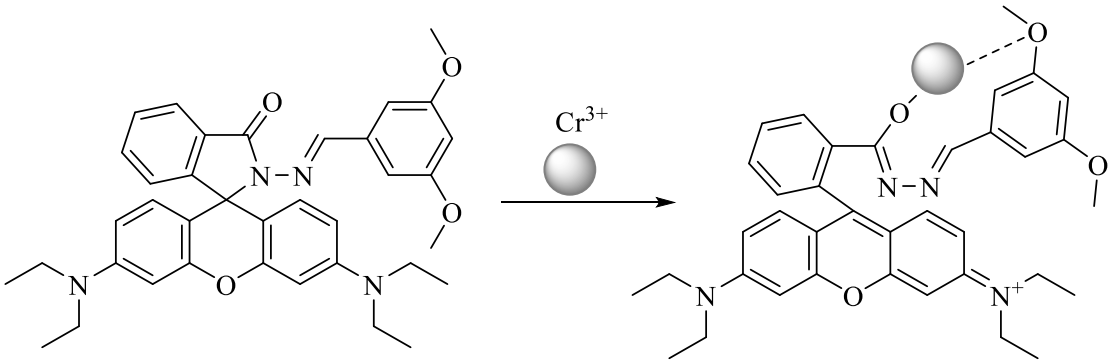

25 **25.Cr^{3+}**

Scheme 8

A novel cascade fluorescence '*off-on-off*' rhodamine-urea methacrylate based chemosensor was reported by Liu *et al.* [62]. Compound **26** was found to selectively detect Cr^{3+}over other background metal ions in aqueous organic medium (CH_3CN-H_2O (90/10 (v/v), *pH* = 7.0). On binding with Cr^{3+} in 1:1 stoichiometry, the fluorescence was turned-on and emission was observed at the range of 540-700 nm. Further, the complex **26.Cr^{3+}** was used for detection of F^- ions. Soon after $F^-$was injected into the complex **26.Cr^{3+},** a sudden decrease in the emission band was observed leading to fluorescence turn-*off*. The detection limits were calculated and found to be 5.5×10^{-8} M for Cr^{3+} and 1.2×10^{-7} M for F^-.

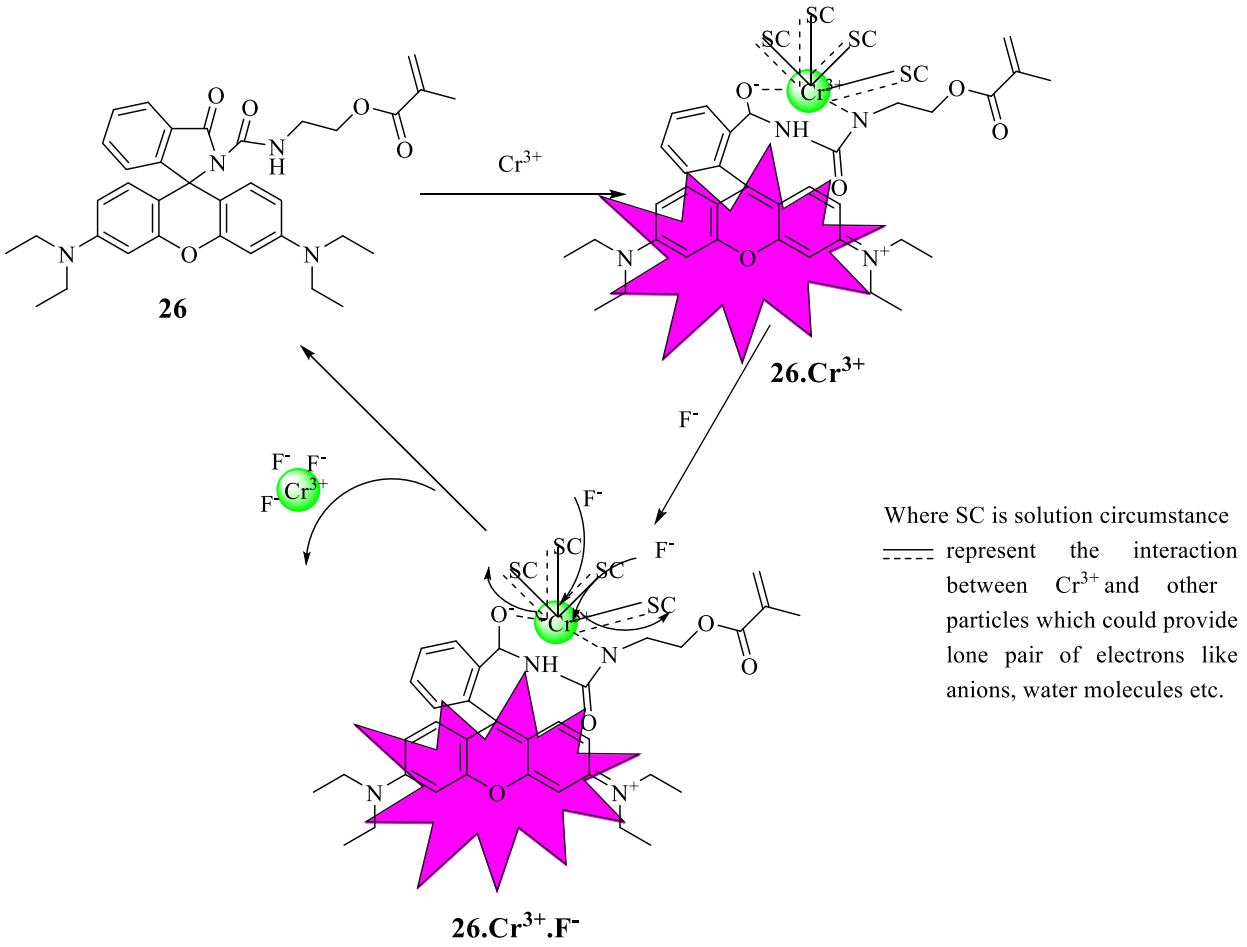

Scheme 9

Luo*et al.* [63] developed a rhodamine-coumarin dyad having 1,2,3-triazole as linker. Compound **27** was capable of detecting multiple ions such as Cu^{2+}, Fe^{3+} and Cr^{3+} in different medium, exhibiting visible color changes. Compound **27** (5μM) gave its absorption band at 415 nm in CH_3CN, CH_3OH and THF. The addition of Fe^{3+}, Cu^{2+} and Cr^{3+}in methanolic solution of compound **27** (5μM) caused colorimetric change from yellow to pink and the absorption band got red shifted. The characteristic band of spirolactam ring open form was observed at 550 nm. On contrary, although presence of Cu^{2+}led to spirolactam ring opening of rhodamine but it did not lead to formation of emission band above 500 nm (emission of spirolactam ring open form of rhodamine B) rather it led to fluorescence quenching at 470 nm (emission band due coumarin), ascribed to its heavy metal effect. Whereas, presence of Fe^{3+} and Cr^{3+} gave emission band at 579 nm along with decrease in intensity of band at 470 nm, clearly showing the transfer of energy from coumarin to rhodamine due to FRET.

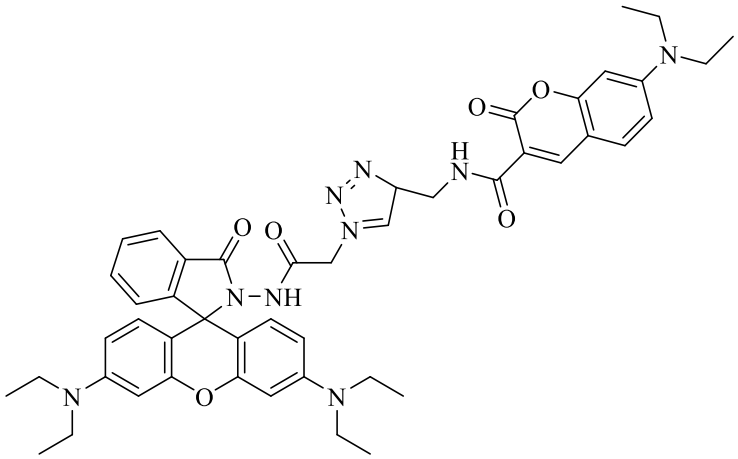

27

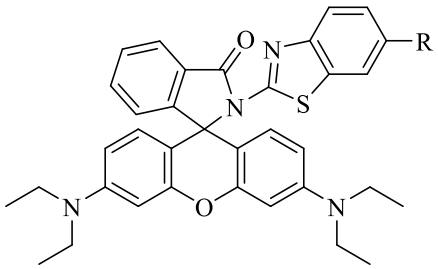

28 **R = Br**
29 **R = NO_2**
30 **R = OCH_3**

A series of rhodamine-aminobenzothiazole fluorescent compounds **28-30** for sensing of Fe^{3+} were prepared by Li and co-workers [64]. In the absence of Fe^{3+}, no emission and absorption changes were observed because of the ring-closed spirocyclic form of rhodamine which is colorless and non-fluorescent. But, on the addition of Fe^{3+} into the solutions of these compounds, absorption band at 558 nm and emission band at 580 nm were observed, which was attributed to metal-induced spirolactam ring opening of rhodamine. The biological applicability of these compounds was proven as they responded to Fe^{3+} concentration changes in the living cells.

Wang and co-workers [65] also designed a rhodamine-coumarin based FRET-system **31** which showed Fe^{3+} ion induced PET '*on-off*' and FRET '*off-on*'. It showed visible color change from yellow to pink due to ring opening of spirolactam ring of rhodamine in presence of Fe^{3+} ions. Along with visible color change, red shift from 420 nm to 555 nm was also observed. Overlap between the emission band of coumarin and absorption band of complex **31.Fe^{3+}** suggests energy transfer from coumarin to rhodamine thus enabling FRET-mechanism. When compared with coumarin, the intensity of fluorescence of compound **31** was strongly quenched which indicated the PET phenomenon from amide to coumarin. Compound **31** was found to bind with Fe^{3+} in 1:1 stoichiometry and the association constant was found out to be $0.99 \times 10^{-4}\ M^{-1}$.

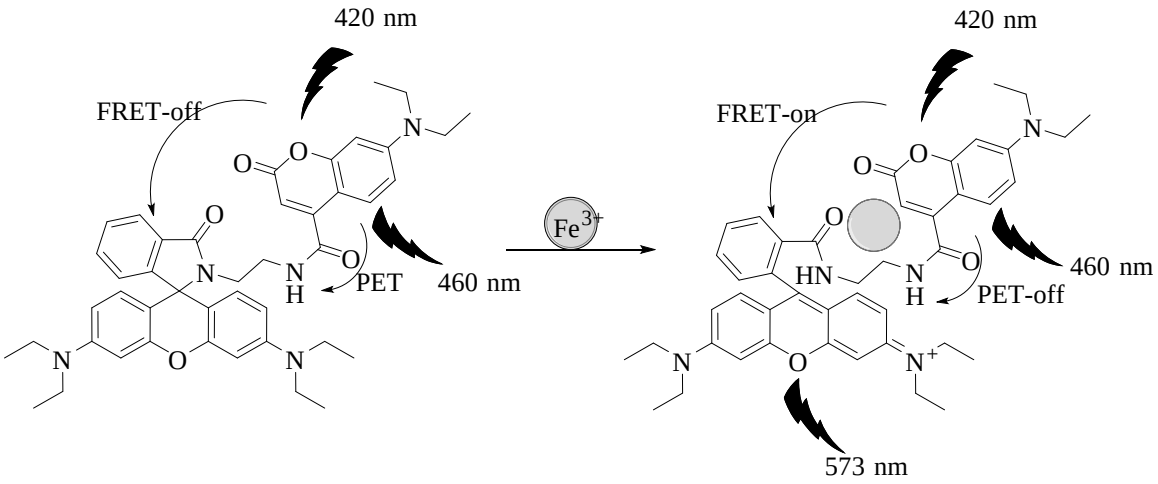

31 **31.Fe^{3+}**

Scheme10

Another rhodamine-coumarin FRET-based ratiometric sensor **32** was synthesized by Yang *et al*. [66] which was also found to be selective and sensitive towards Fe^{3+} ions in aqueous medium at *pH* = 7.4. The compound **32**, itself showed an emission band at 475 nm but in presence of Fe^{3+} ions, the band shifted to longer wavelength i.e. at 550 nm. This shift occurs because of the fluorescence energy transfer from coumarin to rhodamine in the presence of Fe^{3+}. The detection limit was found out to be 10^{-6} M.

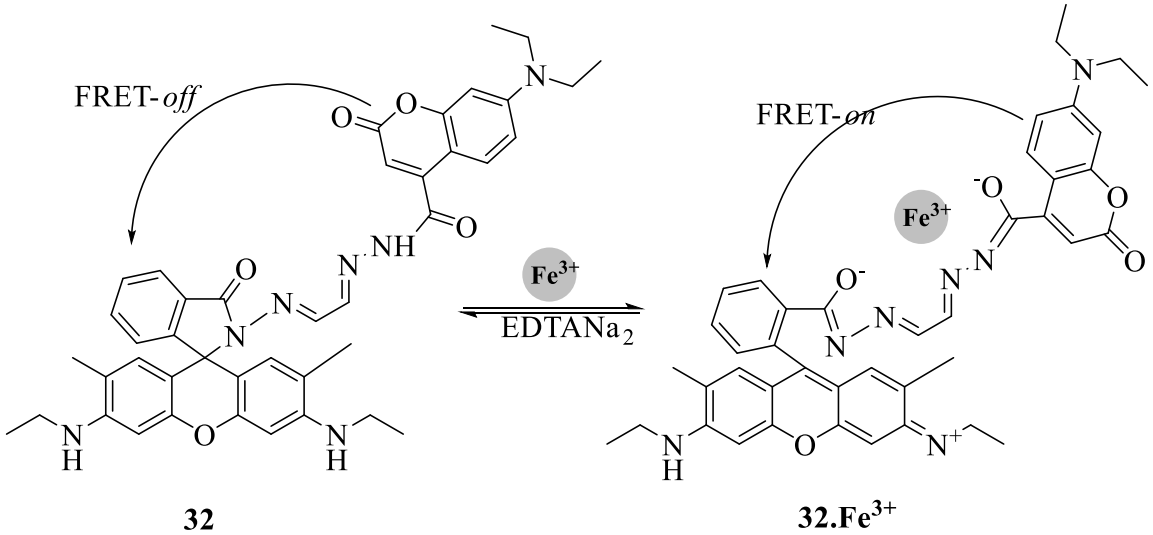

32 **32.Fe^{3+}**

Scheme 11

1.3.1.2. Rhodamine based Al^{3+} and other metal ions sensors:

Xin *et al.* [67] formulated a novel chromo-fluorescent chemosensor for Al^{3+} by linking two rhodamine units *via* diphenyl thiourea moieties. The presence of Al^{3+} into solution of compound **33** in CH_3OH gave an intense fluorescent band at 579 nm and absorption band at 557 nm, accompanied by visible color change from colorless to pink. The lowest detection limit of compound **33** for detecting Al^{3+} was calculated from the fluorescence titration profile and was found to be 2.0×10^{-6} M. Formation of 1:1 complex between compound **33** and Al^{3+} was revealed by performing job's plot experiment with an equilibrium association constant of 4.4. The complex **33.Al^{3+}** was further found to be capable of detecting argenine in aqueous medium with visible color change from pink to colorless. The presence of argenine into the solution of complex **33.Al^{3+}** led to the fluorescence 'turn-*off*' which is attributed to the spirolactam ring closure which occurred due to the decomplexation caused in the presence of argenine. The detection range for complex **33.Al^{3+}** to successfully detect argenine was found to be 2.3×10^{-6} mol L^{-1}.

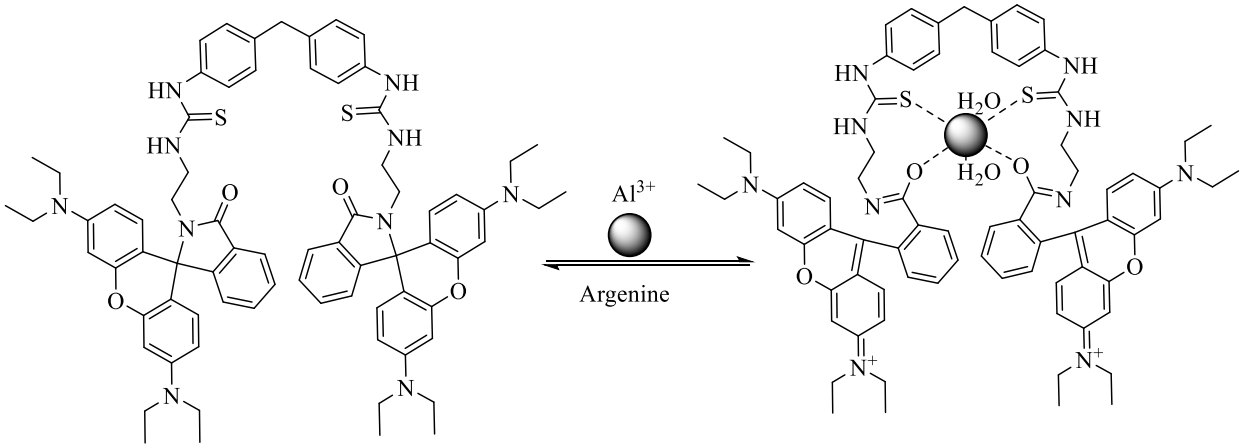

33 **33.Al^{3+}**

Scheme 12

Another rhodamine B based complex **34.Al^{3+}** was prepared by Lee and his co-workers [68] which was used as an ensemble for detection of pyrophosphate in 100% aqueous medium. The presence of pyrophosphate in the ensemble **34.Al^{3+}** led to the quenching of the fluorescence band at 585 nm and absorption band at 560 nm along with visible color change from pink to colorless.

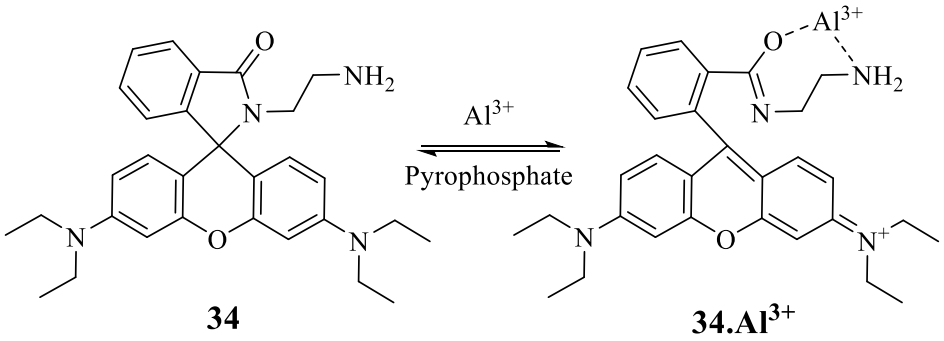

34 **34.Al^{3+}**

Scheme 13

Goswami *et al.* [69] reported similar sensing process by synthesizing compound **35** which was found to be highly selective for detection of Al^{3+}. Further, the ensemble **35.Al^{3+}** was used for sensing of pyrophosphate in HEPES buffer (20 mM, *pH* = 7.1). This dual sensing was accompanied by colorimetric as well as fluorescence emission changes. On binding with Al^{3+} in 1:1 stoichiometry, the color of compound **35** was changed from colorless to reddish orange. The absorption band at approx. 528 nm and the emission band at 552 nm has been attained which was attributed to Al^{3+} induced spirolactam ring opening of rhodamine. The spectral as well as colorimetric changes were reversed on adding pyrophosphate and the detection limit was found to be 2.19 μM. The binding constant of compound **35** for Al^{3+} was calculated to be $2.51 \times 10^4\ M^{-1}$ from UV-Vis titration profile and $8 \times 10^4\ M^{-1}$ by fluorescence titration profile. The fluorescence signal changes were considered for mimicking INHIBIT logic gate having two inputs i.e. Al^{3+} and pyrophosphate.

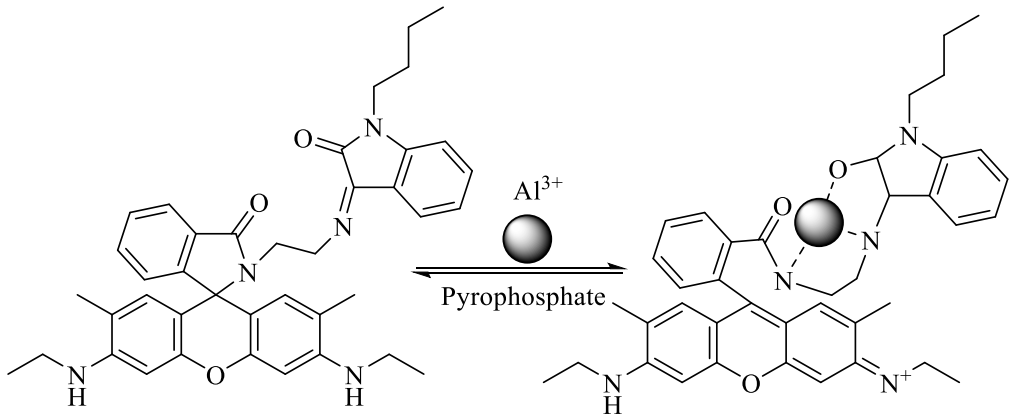

35 **35.Al^{3+}**

Scheme 14

In 2013, Li and his co-workers [70] designed and synthesized two rhodamine based compounds **36** and **37**, which had the capability of detecting Al^{3+} and Cu^{2+} ions. Compound **36** had 1,8-naphthyridine unit attached to rhodamine moiety which could detect Al^{3+} in C_2H_5OH medium accompanied by a fluorescence 'turn-*on*' response that could detect Cu^{2+}colorimetrically in aqueous medium. Whereas, compound **37** had 8-hydroxyquinoline derivative attached to rhodamine unit and was selective towards sensing of Al^{3+} in C_2H_5OH, accompanied by color change as well as fluorescence 'turn-on' response. Both the sensors formed 1:1 complex with each of the metal ions and the detection limits of Al^{3+} by compound **36** and **37** in C_2H_5OH were calculated to be 4.34×10^5 L/mol and 5.23×10^5 L/mol, respectively. The reversibility of the Al^{3+}/Cu^{2+} complexes of each of the sensors was tested and achieved in the presence of F^-/EDTA solution.

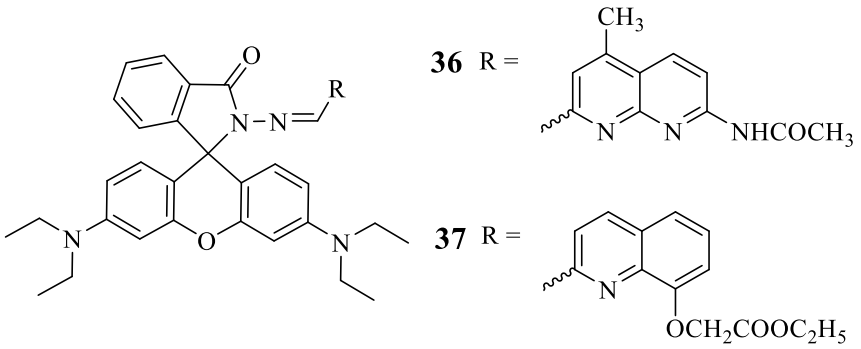

Yan and co-workers [71] fabricated three rhodamine based sensors **38-40** for sensing of Al^{3+} and Hg^{2+}. All the three sensors proved to be colorimetric as well as fluorescent sensors for Hg^{2+}/Al^{3+}. Compounds **38** and **39** were found to be selective towards Hg^{2+} ions in CH_3OH-H_2O (4:6 (v/v) HEPES *pH* = 7.0), accompanied by visible color change from colorless to pink with bright orange emission. The detection limits were calculated to be 2.5×10^{-8} M for compound **38** and 4.2×10^{-8} M for compound **39**. Whereas compound **40** had a benzyl group due to which it was observed to be selective towards Al^{3+}. All the compounds formed 1:1 complex with metal ions and on complexation enhancement in the emission band was observed. The color change to pink was attained due to metal induced spirolactam ring opening of rhodamine. For investigating the biological importance of these compounds, live images were done and satisfying results were obtained.

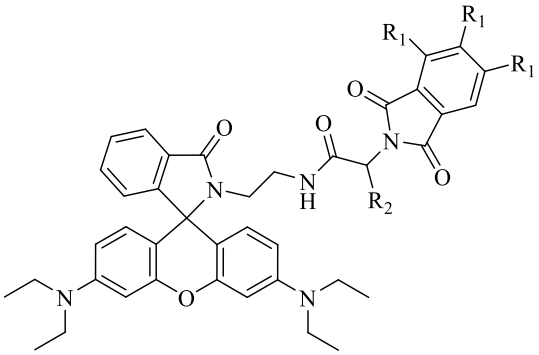

38: R_1 = H, R_2 = CH_3
39: R_1 = Cl, R_2 = CH_3
40: R_1 = H, R_2 = $CH_2C_6H_5$

Zhu *et al.* [72] synthesized compound **41** by joining rhodamine and imidazole moieties which proved to be highly sensitive and selective towards binding with Al^{3+} ions without any significant interference from other metal ions in C_2H_5OH. The job's plot analysis revealed the formation of 1:1 complex between compound **41** and Al^{3+} ions with significant enhancement in fluorescence band at 578 nm and visible color change to pink. The binding constant was found to be 1.8×10^2 M^{-1} and detection limit for sensing Al^{3+} by compound **41** was calculated to 2.02×10^{-9}mol L^{-1}.

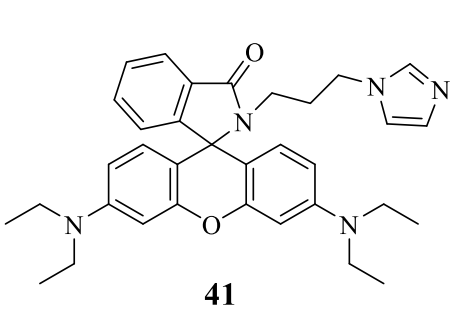

41

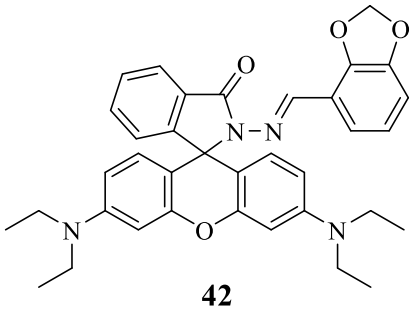

42

Compound **42** based on dual-channel changes i.e. fluorescence and UV-Vis changes, was synthesized by Guchhait and his co-workers [73] which was found to be selective towards Al^{3+} and Cr^{3+}ions with slight interference from Fe^{3+} and Cu^{2+}. The color change from colorless to magenta and spectral changes (in the UV-Vis i.e. formation of new characteristic band ~558 nm and fluorescence band at 580 nm) were attained due to the spirolactam ring opening of rhodamine on formation of metal chelate in 1:1 stoichiometry. The detection limits were calculated to be 2 ppb for Al^{3+} and 100 ppb for Cr^{3+} in buffered CH_3OH-H_2O ((3:7 (v/v) HEPES

buffer *pH* = 7.2). The biological applicability of compound **42** was investigated by live imaging technique by detecting Al^{3+} in HeLa cells.

For a first time, a FRET based Al^{3+} sensor **43** was developed by Das *et al.* [73] by linking two rhodamine units with diformyl *p*-cresol moiety. Compound **43** was found to be selective and sensitive towards binding with Al^{3+}*via* PET-CHEF and FRET mechanisms which were illustrated with time-resolved fluorescence, ^{1}H-NMR and live cell imaging studies. The detection limit was found to be 5×10^{-9} M in C_2H_5OH:H_2O (0.1 M, 4:1 (v/v), *pH* = 7.4). The *pH* studies showed that in acidic condition intense emission band at 585 nm (red emission) was observed and in basic conditions intense green emission was observed at 535 nm and hence, this sensor could be used as *pH* sensor.

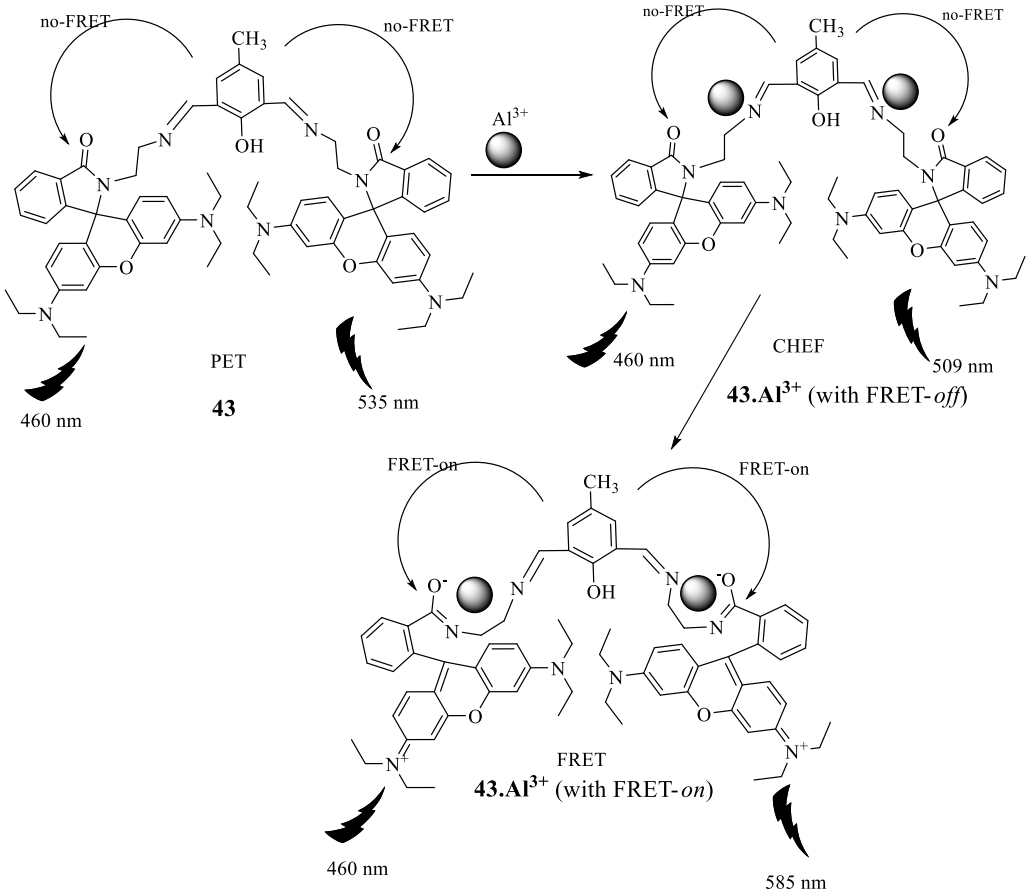

Scheme 15

By linking naphthalimide moiety to rhodamine *via* a quinolinol linker gave FRET '*off-on*' based fluorescent sensor **44** where naphthalimide acted as the energy donor and 8-hydroxyquinilone

attached to rhodamine behaved as the acceptor [75]. This was considered to be the first report where FRET based compound **44** could be used for detection of Fe^{3+}, Al^{3+} and Cr^{3+}. Amongst various metal ions, compound **44** was found to be selective for sensing of trivalent metal ions i.e. Al^{3+}, Cr^{3+} and Fe^{3+}in H_2O-CH_3CN (1:1 (v/v), 0.01 M Tris HCl-CH_3CN, *pH* = 7.4). On adding either of the trivalent metal ions, the compound **44** led to the spirolactam ring opening of rhodamine and hence, the absorption band at 562 nm and emission band at 583 nm were attained. The intensity of absorption and emission bands was high in the presence of Fe^{3+} as compared to Al^{3+} and Cr^{3+}. The formation of complexes of compound **44** and each of the metal ions was found to be in 1:1 stoichiometry in job's plot experiments. Its stability at physiological *pH* proved its biological applicability as it could monitor trivalent metal ions in the W138 cells.

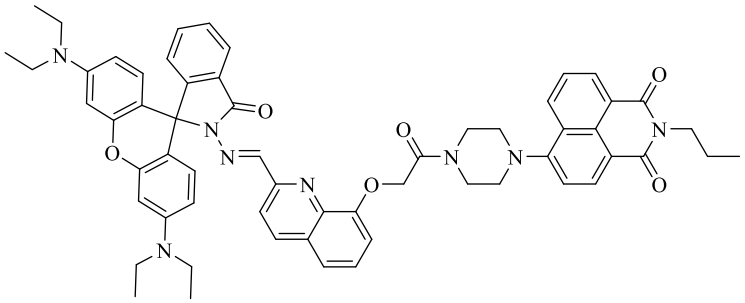

44

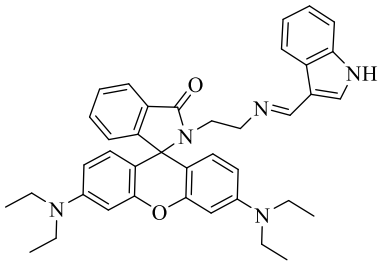

45

Another sensor for sensing of trivalent metal ions was synthesized by Das and his co-workers [76] wherein they linked indole with rhodamine. Compound **45** displayed colorimetric as well as spectral changes in presence of trivalent metal ions such as Al^{3+}, Cr^{3+} and Fe^{3+} in CH_3OH-H_2O (1:1 (v/v)) without interferences due to other monovalent or diavalent metal ions. The binding of metal ions with compound **45** initiated H^+ production in aqueous medium which initiated spirolactam ring opening of rhodamine that in-turn led to fluorescence 'turn-on' *via* FRET mechanism. The quantum yield of compound **45** was very low initially ($\varphi = 0.014$) but in the presence of metal ions the quantum yields increased to $\varphi = 0.024$ in presence of Fe^{3+}, $\varphi = 0.034$ due to Al^{3+} and $\varphi = 0.49$ due to Cr^{3+}. The detection limits for sensing of Cr^{3+}, Al^{3+} and Fe^{3+} were calculated to be 15 μM, 12 μM and 20 μM, respectively.

BODIPY-rhodamine TBET based compound **46** was synthesized by Rao and co-workers[77] that proved to be another trivalent metal ion sensor wherein BODIPY acted as energy donor and rhodamine as acceptor and conjugated thiophene-acetylene acted as the linker. On addition of

Al^{3+} or Fe^{3+} or Cr^{3+}into compound **46** in aqueous-CH_3CN (1:1 CH_3CN/0.01 M Tris-HCl buffer (*pH* = 7.4)) led to ratiometric change in fluorescence i.e. decrease in the emission band at 517 nm and increase in the intensity of band at 585 nm with isobestic point at 563 nm. The increase in the emission intensity was 13-fold in Al^{3+}, 9-fold in Fe^{3+} and 12-fold in Cr^{3+}. Live cell imaging was performed to investigate the biological applicability of compound **46** and the results obtained were satisfactory.

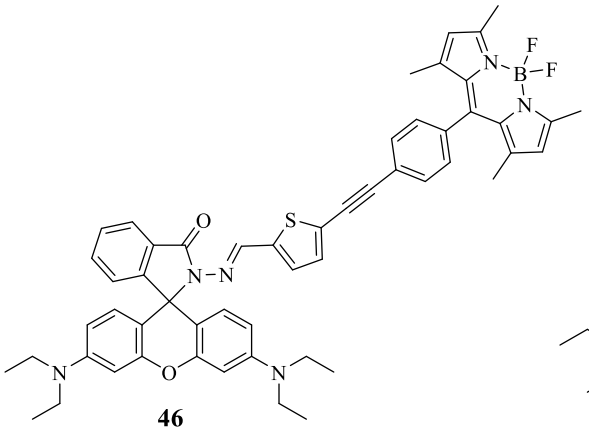

46

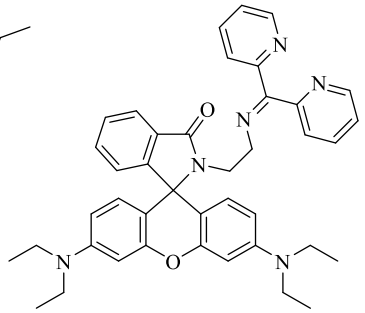

47

Another rhodamine based sensor **47** for trivalent metal ion sensing was prepared by Kilic and Bozkurt [78]. The formation of metal chelate in 1:2 stoichiometry gave absorption peak at 560 nm alongwith visible color change and intense emission band at 583 nm. By using the fluorescence titration profile, the binding constants were calculated to be $1.42 \times 10^3\ M^{-1}$ for Fe^{3+}, $3.88 \times 10^3\ M^{-1}$ for Al^{3+} and $9.16 \times 10^3\ M^{-1}$ for Cr^{3+} whereas the of compound **47** to sense Fe^{3+}, Al^{3+} and $Cr^{3+}$was 2.50 μM, 1.17 μM and 3.16 μM

Another trivalent metal ion sensor **48** was prepared by Ali and co-workers [79] by linking rhodamine 6G and methyl benzaldehyde. Compound **48** was capable of sensing Al^{3+}, Cr^{3+} and Fe^{3+} through CHEF mechanism; no other mono-valent or di-valent metal ions interfered in the sensing. The metal induced spirolactam ring opening of rhodamine caused color change and enhancement in the fluorescence emission band at 555 nm with 21-fold enhancement in presence of Fe^{3+} ions, 14-fold in presence of Al^{3+} and 10-fold due to Cr^{3+} ions in CH_3OH-H_2O at *pH* = 7.2. The fluorescence titration profile of compound **48** with each metal ion was used for calculating binding constants and were found out to be $6.7 \times 10^4\ M^{-1}$, $8.2\times 10^4\ M^{-1}$ and $6.0\times 10^4\ M^{-1}$ for Fe^{3+}, Al^{3+} and Cr^{3+}, respectively. The lowest detection limit of compound **48** for

detecting Fe^{3+} was 0.29 μM, 0.34 μM for Al^{3+} and 0.31 μM for Cr^{3+}. Reversibility of the complex **48.Al^{3+}** was achieved in the presence of arsenate ion. The fluorescence switch '*on-off*' signal formed the basis for constructing molecular logic devices and memory devices.

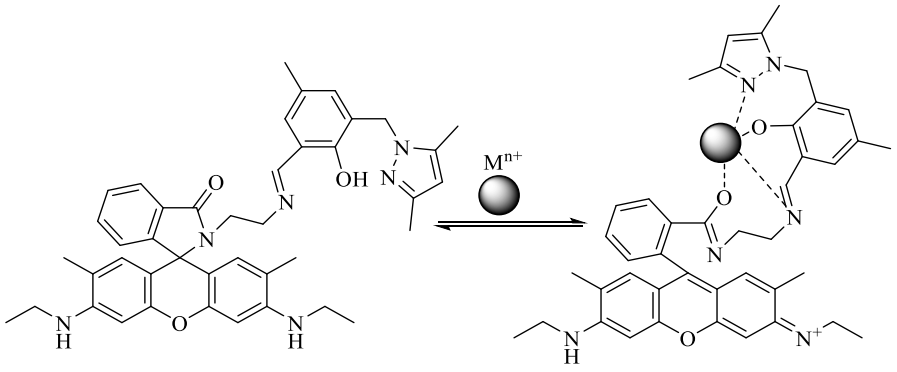

48 **48.M^{n+}**

Scheme 16

Compound **49** was designed and prepared by Roy *et al.* [80] for sensing of trivalent metal ions (Fe^{3+}, Al^{3+} and Cr^{3+}) without significant interference by monovalent or divalent metal ions. The binding of these metal ions with compound **49** (40 μM, 10 mM HEPES buffer at *pH* 7.2 inH_2O/methanol = 3:7 (v/v)) led to visible color change from colorless to pink due to the metal induced spirolactam ring opening of rhodamine moiety alongwith red-shift in absorption spectra and formation of new absorption band at 528 nm whereas, enhancement in the emission band at 552 nm was observed with 98-fold increase in presence of Al^{3+}, 50-fold in presence of Cr^{3+} and 38-fold due to Fe^{3+}. The detection limit for compound **49** to selectively sense Al^{3+}, Fe^{3+} and Cr^{3+} were determined to be 1.18, 4.04 and 1.80 nM, respectively. The spectral as well as colorimetric reversal for complex **49.Al^{3+}** was attained in the presence of AsO_4^-. The '*on-off*' spectral changes helped in constructing 3-input and 5-input logic gates, memory devices and keypad lock.

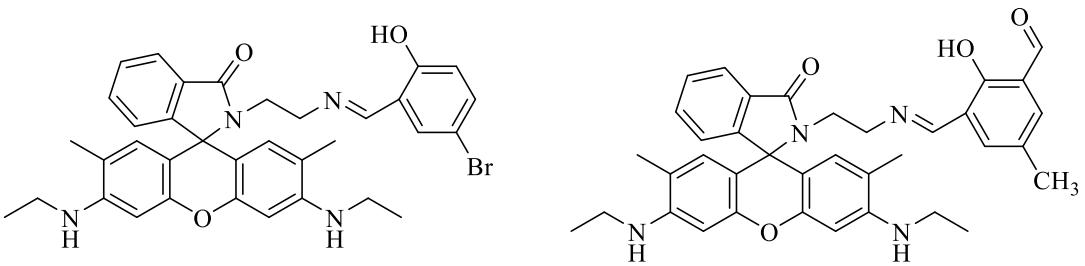

49 **50**

Roy *et al.* [81] prepared another dual signal fluorescent compound **50** by linking rhodamine and methylbenzaldehyde moieties. The optical as well as the colorimetric changes revealed its high sensitivity and selectively towards trivalent metal ions i.e. Al^{3+}, Cr^{3+} and Fe^{3+} in CH_3OH-H_2O (9:1 (v/v) *pH* = 7.4). Compound **50** on chelating in 1:1 stoichiometry, with trivalent metal ions, visible color change from colorless to pink was observed along with a large red-shift of absorption band to 528 nm whereas, the emission band increased at 550 nm by 1465-fold in presence of Al^{3+}, 588-fold in presence of Cr^{3+} and 800-fold in presence of Fe^{3+}. The association constants suggested the strong binding of **50** with Al^{3+} ions (K_a=1.47 × 10^5M) than the other two metal ions (K_a=6.24 × 10^4 M for Cr^{3+} and K_a=8.74 × 10^4 M for Fe^{3+}) and the detection limits of compound **50** for sensing Al^{3+}, Cr^{3+} and Fe^{3+} were determined to be 6.97, 15.80 and 14.00 nM, respectively.

A rhodamine based Schiff base was fabricated by Gupta and his co-workers [82]. Compound **51** (50 μM) in CH_3OH−DMSO (99:1 v/v) has shown fluorescence '*off-on-off*' response in the presence of ions. On the addition of Al^{3+}, the spirolactam ring of rhodamine opened up due to which the emission enhancement at 587 nm and new absorption band formation at 555 nm with shoulder at 517 nm were attained. A slight interference from Cr^{3+} and Cu^{2+} was also observed in sensing of Al^{3+} by compound **51**. Whereas, on adding CH_3COO^-/F^- ions, the emission and absorption changes were reversed leading to fluorescence 'turn-*off*'. All these spectral changes were accompanied by visible color changes as well i.e. in presence of Al^{3+}, the color changed from colorless to pink but on adding CH_3COO^-/ F^- into complex **51.Al^{3+}** the color was changed to colorless. Compound **51** could detect Al^{3+} at 14μM whereas, the complex **51.Al^{3+}** could detect CH_3COO^-/F^- at lowest concentration of 0.4 μM.

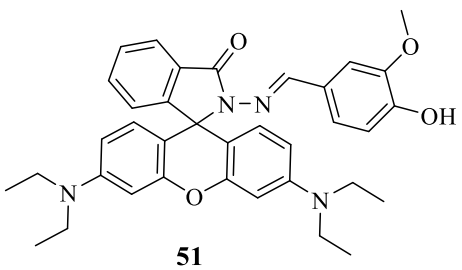

51

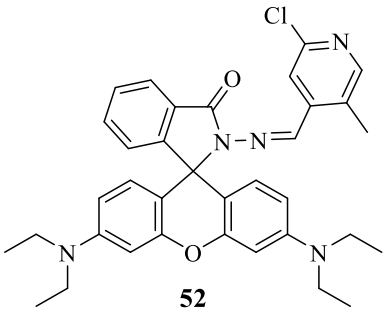

52

Another rhodamine based fluorescence '*off-on*' sensor **52** for Al^{3+} was synthesized by Son *et al.*[83] The metal-chelate formed in 1:1 stoichiometry that led to the spirolactam ring opening of

rhodamine which caused enhancement of emission band at 584 nm and formation of new absorption band centered at 560 nm. Compound **52** (10μM, CH_3CN) showed high binding affinity towards Al^{3+} with binding constant of 2.96×10^{-5} M^{-1}, calculated from UV-Vis titration profile and could detect Al^{3+} as low as 2.96×10^{-8} M in CH_3CN. Furthermore, the complex **52.Al^{3+}** was investigated for its reversibility and it was observed that in presence of azide (N_3^-), the spectral changes were reversed and it is the first example where Al^{3+} complex of the sensor was used for sensing of azide.

Compound **53** was synthesized by Zhang *et al.* [84] for the recognition of three metal ions i.e. Hg^{2+}, Cr^{3+} and Al^{3+} through FRET mechanism in H_2O-CH_3OH (1:4 (v/v) medium. It was formed by linking rhodamine and benzothiazole moieties by a non-conjugated linker (phenol compound). The metal ions formed complexes with compound **53** in different stoichiometries, e.g. Hg^{2+} and Al^{3+} formed complexes in 1:1 mode whereas Cr^{3+} formed complex with 2:1 mode. The binding of metal ion with compound **53** led to spirolactam ring opening of rhodamine and the color turned from colorless to pink. The *pH* studies revealed that compound **53** showed strong absorption behavior within *pH* range of 5-9 in the presence of Hg^{2+} or Cr^{3+} whereas, when Al^{3+} was added the absorbance, response remained stable within *pH* 5-7. The stability of compound **53** at biological *pH* range i.e. 6-7.6 indicate that it can be used in live cell imaging.

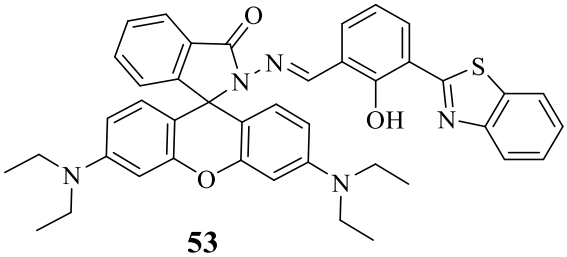

53

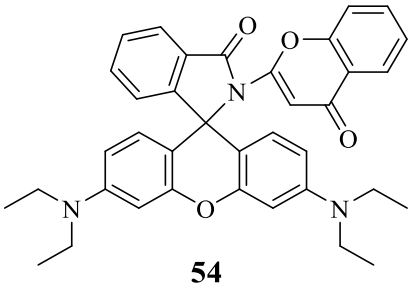

54

Ghosh and co-workers [85] designed and synthesized a rhodamine-chromenone based sensor **54**, which was capable of recognizing Al^{3+} and Hg^{2+}in CH_3CN-H_2O (3:1 (v/v) HEPES buffer, *pH* = 6.85) *via* weak FRET mechanism where donor is the chormenone moiety and acceptor is rhodamine part. Binding of either of the metal ions with compound **54** in 1:1 stoichiometry, induced spirolactam ring opening of rhodamine leading to enhancement of emission band at 586 nm and absorption band at 560 nm alongwith visible color change to pink from colorless. The reversibility of color as well as spectral changes for the complex **54.Hg^{2+}** was achieved by

adding either TBAF i.e. tetrabutylammonium fluoride or TBAI i.e. tetrabutylammonium iodide. Compound **54** had the capability of detecting Hg^{2+} to the lowest limit of 1.26×10^{-7} M and for Al^{3+}, it was 1.90×10^{-7} M.

A new rhodamine based compound **55** was synthesized for the recognition of Al^{3+} and Zn^{2+}, even in the presence of background metal ions [86]. The sensing of both the metal ions was accompanied by different spectral changes. On binding with Al^{3+}, compound **55** (10 mM HEPES buffer in H_2O/CH_3OH (1:9 (v/v), *pH* 7.4)) gave absorption band at 528 nm with a visible color change whereas, emission band at 550 nm was observed due to the spirolactam ring opening of rhodamine. However, no color change was observed in the presence of Zn^{2+} with attainment of absorption band at 375 nm and emission band at 457 as no ring opening occurred on Zn^{2+} chelate formation with compound **55**. The detection limits for both the metal ions, Al^{3+} and Zn^{2+} were calculated to be 10.98 nM and 76.92 nM, respectively. Compound **55** was further investigated for its applicability in live cell imaging and the results were satisfactory.

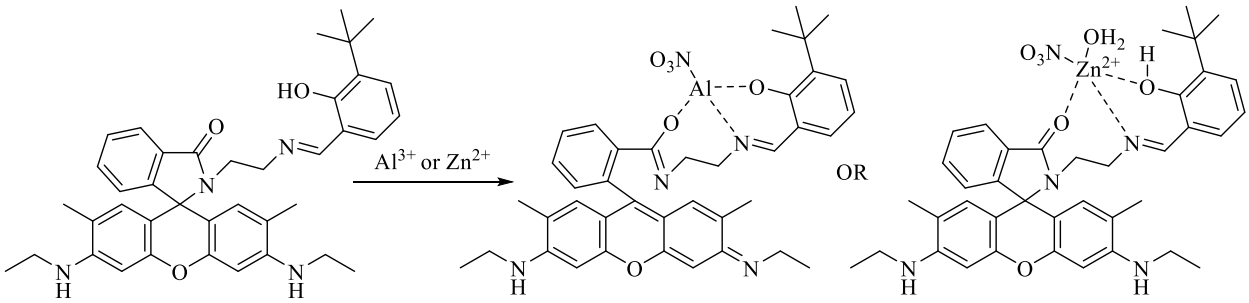

Scheme 17

A new rhodamine-azobenzene based multiple ion sensor **56** was prepared by Jana and co-workers [87]. Compound **56** was capable of sensing Al^{3+}, Cr^{3+} and Cu^{2+} *via* PET i.e. photoinduced electron transfer and CHEF i.e. chelation-enhanced fluorescence mechanisms. The absorption studies revealed the sensitivity of compound **56** towards Al^{3+}, Cu^{2+} and Cr^{3+} in buffer of CH_3OH-H_2O alongwith colorimetric change whereas fluorescence studies showed 21-fold enhancement in emission band on addition of Al^{3+} and Cr^{3+}that showed 16-fold increase. The 1:1 complex formation led to PET inhibition with simultaneous spirolactam ring opening of rhodamine which caused the fluorescence 'turn-on'. The binding constants for Al^{3+} and Cr^{3+} were calculated to be 6.7×10^3 M^{-1} and 3.8×10^3 M^{-1} and the limits of detection of compound **56**

for Al^{3+} was 1×10^{-6} and for Cr^{3+} was 2×10^{-6} M. The addition of EDTA caused decomplexation of 1:1 complexes of **56.Al^{3+}** and **56.Cr^{3+}**. The dual metal ion sensing along with reversible signal '*off-on*' response was useful in construction of 2-input-1-output INHIBIT logic gate. Compound **56** was further applicable in live cell imaging.

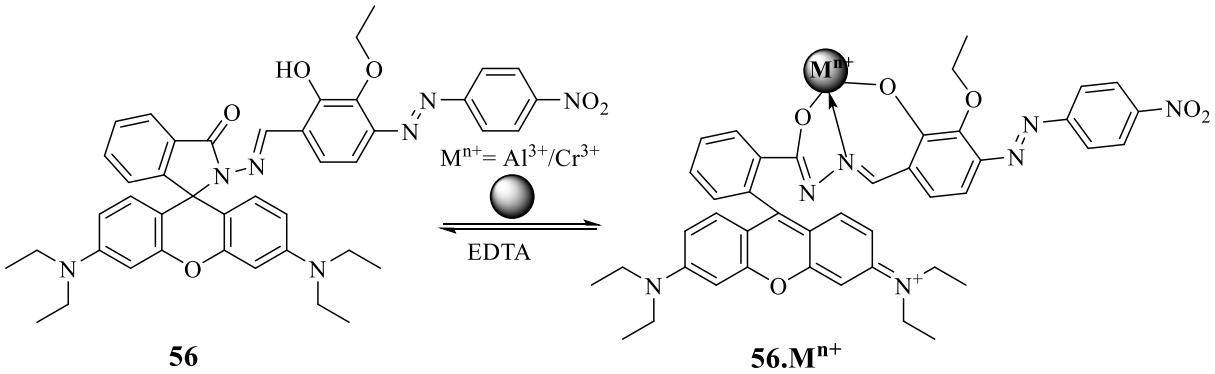

56 **56.M^{n+}**

Scheme 18

1.1.2. Phenalenediacrbonitrile based sensors:

Qian and his co-workers [88] prepared a series of esters and derivatives of 8-oxo-8H-acenaphthol[1,2-*b*]pyrrole-9-carboxylic acid **57** and evaluated their cytotoxicity against cancer cell lines P388 and A549. The biological studies revealed that the methyl esters were more cytotoxic against cancer cell lines, whereas, the 3-amino derivatives having bromine had the highest activity against the cell lines.

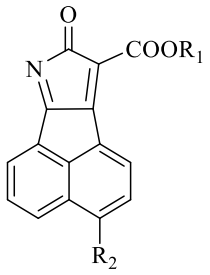

57

57a: R_1= CH_3, R_2= 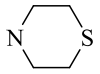

57b: R_1= CH_3, R_2= 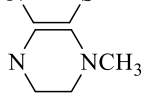

57c: R_1= CH_3, R_2= 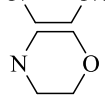

57d: R_1= CH_3, R_2= 

57e: R_1= CH_3, R_2=$NH(CH_2)_2N(CH_3)_2$
57f: R_1= CH_3, R_2=$NH(CH_2)_3N(CH_3)_2$
57g: R_1= CH_3, R_2=$NH(CH_2)_2SC_2H_5$
57h: R_1= CH_3, R_2=$NH(CH_2)_2NHPh$

Another phenalenedicarbonitrile based compound **58** was synthesized by Qian *et al.* [89]. The compound **58** proved to be excellent sensor for Cys and Hcy in CH_3OH. This was the first example where a sensor for Cys/Hcy having fluorescence 'turn-on' emission and excitation in

visible region was prepared. It was further used for evaluating the effects of Cys and Hcy in living HeLa cells.

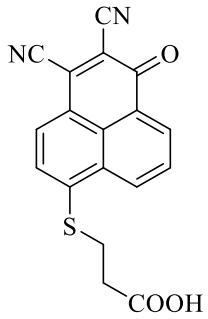

58

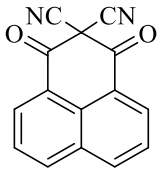

59

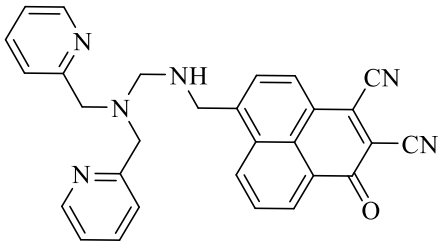

60

Wang *et al.* [90] synthesized a fluorescent chemodosimeter from compound **59** for live-cell monitoring of aqueous sulfides and the compound was further explored for the fluorescence imaging sensing of aqueous sulfide in HeLa cells.

Compound **60,** an acenaphthopyrrolone-dipicolylamine derivative, has been found as a selective and sensitive chemosensor for group IIB cations (Zn^{2+}, Cd^{2+}, Hg^{2+}) [91]. In the presence of Zn(II), the emission band at 588 nm was enhanced by 7-fold. The binding constants were calculated from the fluorescence titration profile and by applying Benesi-Hieldebrand equation, and were found to be 5.4×10^5 M^{-1} for Cd(II), 2.3×10^6 M^{-1} for Zn(II) and 2.9×10^6 M^{-1} for Hg(II).

Li *et al.* [92] fabricated a compound **61** from 6-thiol phenalenedicarbonitrile (fluorophore) and cyclic peptide (targeting unit). This compound exhibited low cytotoxicity and high solubility due to which it can be used in various biological systems.

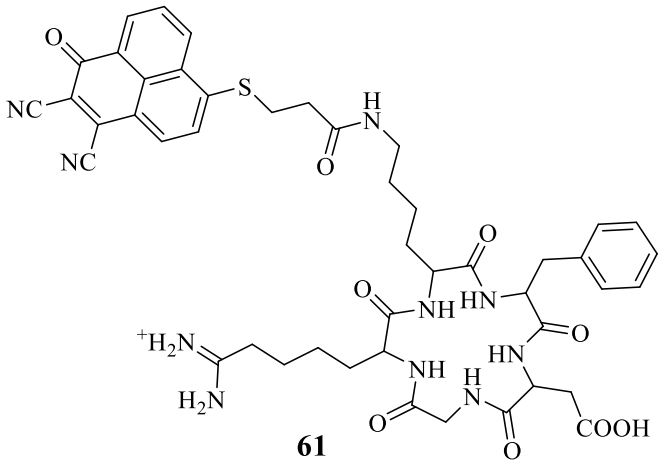

61

Compounds **62-64** were identified as very promising antitumor drugs with high activities having submicromolar IC_{50} values [93]. They also found that compound **62** could inset and occupy the BH3 groove (hydrophobic). Moreover, even the nanomolar amount of compound **62** could efficiently induce apoptosis of tumor cells. Compound **63** showed activities against P388 and A549 cell lines with IC_{50} values of 0.80 μM and 0.45 μM, respectively. Compound **64** showed activity against A549 cancer cell lines having IC_{50} value 0.14 μM and against P388 having IC_{50} value of 0.019 μM towards Mcl-1.

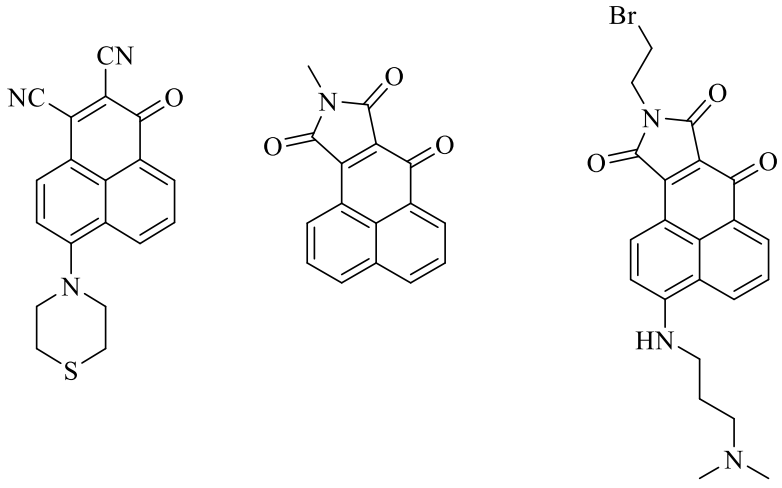

62 **63** **64**

1.2. Research Gap and Objectives

1.2.1. Research Gaps:

- Selective sensing of Al^{3+} without interference from of other metal ions in aqueous medium.
- The reports for use of CN^- sensors in construction of logic gates are rare.
- To-date numerous reports are based on use of rhodamine B and its derivatives as a turn-*on* sensor for sensing of ions but construction of turn-*off* sensor for an anion are rare.
- The sensing capabilities of small polycyclic phenalenedicarbonitrile has been explored less
- Formation of molecular memory devices, encoders, decoders and keypad locks have been less explored

1.2.2. Objectives:

- Synthesis and characterization of substituted/azaacenes
- Study of photophysical properties of aza /substituted acenes and their behavior towards various metals, anions and biological ions.

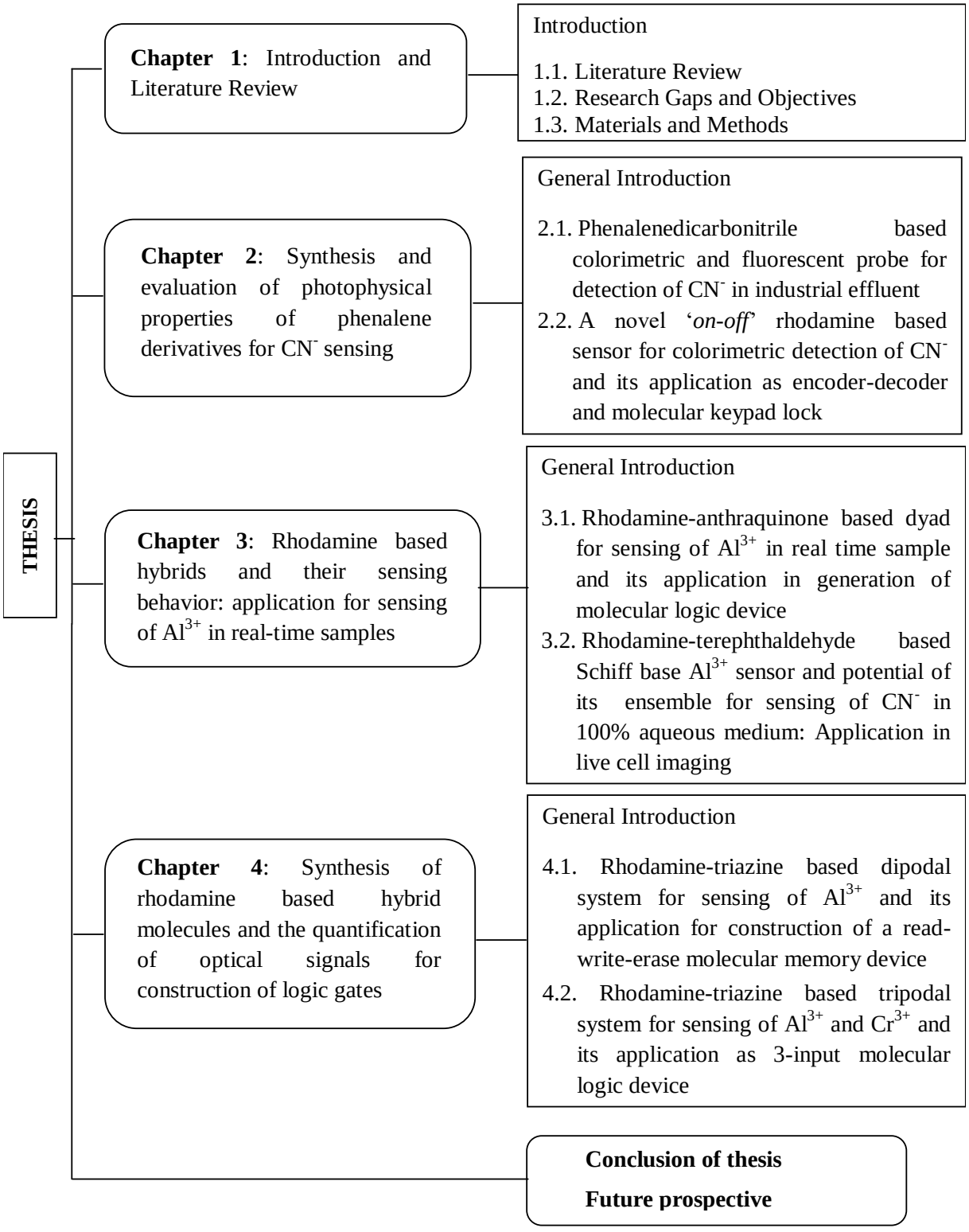

Flowchart 1: Brief outlook of thesis

1.3. Methods and Materials:

- **Chemicals and instrumentation for synthesis:**

All the chemicals used in synthesis were purchased from Loba-chemie and Sigma Aldrich, depending upon their availability. Silica gel GF 254 was used for making Thin Layer Chromatographic plates which were adopted for monitoring the progress and completion of the reaction by observing it under visible or UV light. Hexane-ethylacetate or $CHCl_3$-CH_3OHsolvent mixtures were chosen to be the mobile phase for carrying out TLC as well as column chromatography, depending upon the polarity of the probes.

- **Characterization of the probes:**

The characterization of the synthesised probes was done by recording their $^1H/^{13}C$-NMR and mass spectra. ^1H-NMR and ^{13}C-NMR were recorded on JEOL ECX-400 MHz and TMS (tetramethylsilane) was used as an internal reference. Mass spectra of the synthesized moieties were taken in Waters Micromass Q-TOF Micro or in XEVO G2-XS QTOF.For ^1H-NMR titrations, stock solution of probes at 5×10^{-3} M were prepared in deuterated solvents and were taken in NMR tube. Addition of analytes into the solution was done with micropipettes in 3.0-6.0 μL of amount and the spectra was recorded within few minutes of addition.

- **Techniques for UV-Vis and fluorescence studies:**

The solvents used for carrying out the spectral studies of all the probes were of HPLC or analytical grade. The perchlorates/nitrates of metal ions (Na^+, K^+, Mg^{2+}, Al^{3+}, Ca^{2+}, Ag^+, Cr^{3+}, Fe^{3+}, Co^{2+}, Ni^{2+}, Cu^{2+}, Zn^{2+}, Pb^{2+}, Hg^{2+}, Ga^{3+}) and tetrabutylammonium salts of different anions (SCN^-, CN^-, F^-, Cl^-, Br^-, I^-, HSO_4^- , $H_2PO_4^-$, OAc^- and NO_3^-) were purchased from Sigma Aldrich and Spectrochem Pvt. Ltd. for carrying out the UV-Vis and fluorescence studies. The UV-Vis spectra were recorded in Shimadzu UV-2600 using quartz cuvettes and fluorescence studies were carried out in Cary Eclipse Fluorescence Spectrophotometer.0.1 M stock solutions of all the anions/metal ions were prepared in either CH_3CN or H_2O depending upon their solubilities and 10^{-3} M solutions of all the probes were prepared in CH_3CN or mixture of CH_3CN-THF.For carrying out the optical studies the stock solutions of the probes were diluted to 20 μMin the different solvent systems used for carrying out the studies. This solution was taken in quartz cuvettesfor recording the UV-Vis or emission spectrum having 1 cm path length and different

concentrations of the metal ions/anions were added during titration in 1.5-3.0 μL aliquots. The contents in the cuvette were allowed to rest for atleast 3 min. and then the spectra were recorded.

- **Calculation of binding constants, detection limits and pKa values:**

Benesi-Hieldebrand equation **(1)** was used for calculating binding constants.

$$\frac{1}{Ex-Ex_0} = \frac{1}{Ex_{max}-Ex_0} + 1/(K(Ex_{max} - Ex_0)[Ion]^n) \quad (1)$$

Where, $\mathbf{Ex_0}$is the emission in absence of analyte,

Ex is the emission at an intermediate

And, $\mathbf{Ex_{max}}$ is the emission at saturation

K is the binding/association constant and **[Ion]** is the concentration of ion at **n** stoichiometric ratio

For calculating the lowest detection limit the linear plot of $[M^{n+}]$ versus fluorescence intensity was formed and the following equation was applied

$$\text{Detection Limit} = 3\sigma/S \quad (2)$$

Where, σis the standard deviation of blank, S is the slope (intensity vs. concentration of sample)

For calculating the pKa values Henderson-Hasselbalch-type mass equation**(3)**was used [94]**:**

$$\text{pKa} = pH - \log[(E_{max}\text{-}E)/(E\text{-}E_{min})] \quad (3)$$

Where, E is the experimentally observed emission intensity at a fixed wavelength, E_{max} is the maximum intensity observed at particular wavelength and E_{min} is the minimum value of fluorescence intensity at particular wavelength respectively.

- **Job's plot analysis:**

The stoichiometry of the complex formation was revealed by carrying out job's plot analysis. Solutions with different ratio of probe and ions were prepared and the absorption spectra were recorded and a plot between $\Delta In.X_p$ vs X_p (where, ΔIn = absorption intensity changes during titration, X_p = mole fraction of probe). X i.e. the mole fraction of probe varies from 0.1 to 1.

- **Methodology for *pH* titrations:**

Equiptronics *pH* meter was used for determine and adjusting the *pH* from 2-13 and then the spectra were recorded. Effect of change in *pH* on the UV-Vis and fluorescence spectra of probes and their complexes with the ions were investigated. To study the effect of varying *pH* on the probes as well as their complexes, *p*H titrations were performed where, 20 μM solutions of the probes/complexes were prepared in different solutions. The initial *pH* of both the solutions was recorded on *pH* meter thereafter, 3 ml of the solution was drawn out by using 1000 μl pipette and was taken in quartz cuvette for recording its absorption and emission spectra. For carrying out the studies at basic *pH* 0.1M NaOH solution was added with the help of capillary to ensure minimum addition. After each addition the mixture was stirred to maintain homogeneity and was kept undisturbed for 2-3 min. After this, the *p*H of the solutions was recorded and again the UV-Vis and emission spectra were recorded.

Similarly, the studies at acidic *pH* were carried out by adding 0.1M HCl with capillary into 20 μM solutions of the probes/ complexes prepared in their respective solutions in which selectivity was attained, without maintaining the *pH* of the solutions. After each addition the solutions were stirred and left undisturbed for 2-3 min and after change of 0.2-0.3 in *p*H, the UV-Vis and fluorescence spectrum of the solutions were recorded by taking 3 ml of the solution into cuvettes.

The absorption and emission data was converted and saved in Microsoft excel. A plot between changing *pH* and intensity changes of absorption maximum and emission maximum at particular wavelength were considered to find out the effect of changing *pH* on probes/ complexes.

- **Calculation of quantum yield of probes:**

The quantum yield of probes was calculated by using equation **(4)**. The emission and absorption of probes in respective solvents were recorded. The integrated areas of the emission peaks were calculated by using maximal wavelength (excitation). The quantum yield of the standard in particular solvent used for calculating the quantum efficient of probe [95]:

$$\Phi_{probe} = \Phi_{std} \times (IA_{probe}/IA_{std}) \times (A_{std}/A_{probe}) \times (\eta_{sol}/\eta_{std.sol}) \quad \textbf{(4)}$$

Where, IA represents the integrated area under the emission spectra of probe or complexes and standard, A is the absorbance of probe and standard and η_{sol} is the refractive index of the solvent used for recording the spectra of probe and $\eta_{std.sol}$ is the refractive index of standard solvent [95c].

- **Detection of analytes in real time samples:**

The applicability of probe for sensing of analytes in real sample was carried out by collecting the sample water and spiking the sample with different concentration of analytes and the AAS (Atomic Absorption Spectroscopy) of the samples was recorded. Further, these samples were added into probe of particular concentration and the actual concentration was found by carrying out the UV-Vis and fluorescence studies. The UV-Vis spectra of the spiked samples was then compared with the AAS (Atomic Absorption Spectroscopy) as well as the spectra of probe attained by adding same concentration of standard analyte. The concentration of the spiked samples was calculated from the difference in the absorption/ emission intensities graph at particular wavelength levels.

- ***In vitro* determination of detection limits of Al^{3+} sensitivity**

For cell imaging, A549 cells were seeded on the sterile cover slips and allowed it to grow in 70-75% confluence. Thereafter cultured cells were incubated with 20 μM of Al^{3+} for 6 h and then cells were incubated with different concentrations of probe (10, 1, 0.1 and 0.01 μM) for 1 h. After that, cells were processed for imaging. For each set 3 independent experiments were carried out.

Futhermore, experiments were conducted by using different concentration of Al^{3+} ions and keeping the concentration of probe constant. Cells were seeded similarly as before. Thereafter cultured cells were incubated with various concentrations of Al^{3+} (2, 0.5, 0.1, 0.01, 0.001 and 0 μM) for 6h. After incubation 1 μM of probe was added on each well and incubated further for 1 h. Subsequently, cells were processed for imaging. For each set 3 independent experiments were carried out.

- **Cell Imaging**

The treated cells were washed thrice with 1X PBS *pH*7.4 (10 mins each) to remove excess Al^{3+} and probe **4**. Further, the cells were incubated with 2% formaldehyde and were kept for 20 minutes, after this the cells were again washed with 1X PBS *pH*7.4. Cells were transferred

on the glass slides and the images were captured with Dewinter fluorescence inverted microscope, using excitation in green light and 20X objective.

- **Construction of logic devices:**
    - **2-to-1 encoder and 1-to-2 decoder:**

For the formation of 2-to-1 encoder, two inputs (ion(s) which cause spectral changes) for probes were taken and fluorescence band(s) or absorption band(s) at particular wavelength(s) were considered as outputs. For constructing 1-to-2 decoder, only one input (responsible for the spectral change) was considered and two outputs at absorption or emission wavelengths were observed. The threshold values were set according to the absorption or fluorescence band intensity changes on particular wavelength and if the intensity is lower than the threshold value then the output was considered to be 0 i.e. "*off*" state and if the intensity is more than the threshold value then the output value was considered to be 1 i.e. "*on*" state.

CHAPTER 2

Synthesis and evaluation of photophysical properties of phenalene derivatives for CN^- sensing

General Introduction: Phenalenedicarbonitrile is a class of fluorophores having smaller, planar and rigid π-conjugated structure. The introduction of cyano groups into the system and restricting their out-of-plane movement, favoured the emission properties of the fluorophore. The presence of two electron withdrawing –CN groups and carbonyl group on this precursor made it highly electron deficient and hence nucleophilic substitution reactions could be carried out with ease and under mild conditions. Moreover, the nucleophilic substitution reactions where the aromatic hydrogen atoms are involved and not any other leaving group, are classified under green chemistry. Such reactions are rare and are termed as oxidative nucleophilic substitution reaction of aromatic hydrogen i.e. S_NAr^H. According to reports, phenalenedicarbonitrile could easily undergo nucleophilic reactions with N, O and S. Its amino derivatives had emissions at longer wavelengths, high quantum yields and low stroke shifts. The excellent properties of these fluorophores could be ascribed to their rigid structures and the ICT (intramolecular charge transfer) nature. Even though phenalenedicarbonitrile and its derivatives have been widely explored for their anti-cancer and other biological activities, still they have been explored less in the field of ion sensing. With all these factors we designed two probes having phenalenedicarbonitrile as the parent fluorophore.

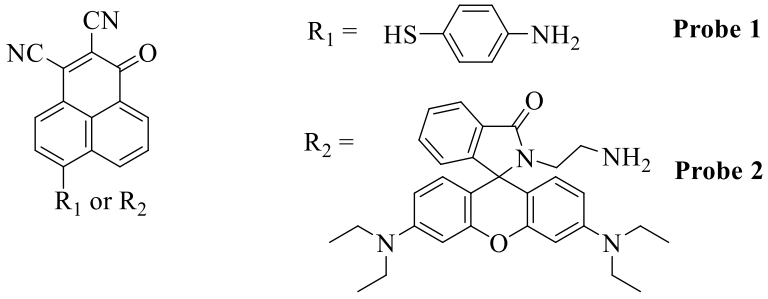

So, to explore the photophysical properties of phenalenedicarbonitriledue to the presence of different substituent's, we have categorized this chapter into two parts:

2.1. Phenalenedicarbonitrile based colorimetric and fluorescent probe for detection of CN^- in industrial effluent

2.2. A novel '*on-off*' rhodamine based sensor for colorimetric detection of CN^- and its application as encoder-decoder and molecular keypad lock

2.1. Phenalenedicarbonitrile based colorimetric and fluorescent probe for detection of CN^- in industrial effluent

2.1.1. Abstract

Probe **1** has been synthesized by linking 4-aminothiophenol to electron deficient phenalenedicarbonitrile unit which can selectively detection of CN^- ions. Probe **1** showed a pink color with absorption maxima centered at 527 nm and weak emission at 567 nm but, the presence of CN^- led to decrease in the intensity of absorption band at 527 nm and a new band of low intensity at 454 nm was formed. Whereas, the emission intensity increased in the presence of CN^- at 567 nm alongwith glowing yellow emission under UV light. Probe **1** showed strong binding for CN^- ions and binding constant was calculated to be 1.1 x 10^4 M^{-1} through fluorescence titration and could detect CN^- as low as 5.5×10^{-8} M. Binding mechanism of CN^- with probe **1** was analyzed through IR spectroscopy and NMR titration which revealed that CN^- ions attack chemodosimetrically on the -C=O of probe **1** to form cyanohydrins compound. Probe **1** was also used for detection of CN^- in industrial waste. The spectral changes of probe **1** in presence of a specific ion, was used to design a 1-to-2 decoder.

2.1.2. Synthesis of probe 1:

To a methanolic solution of phenalenedicarbonitrile (1 g, 4.34 mmol), *p*-aminothiophenol (0.54 g, 4.32 mmol) and 10 equiv. of TEA (triethylamine) were added and the contents were stirred at 0-5^{o}C for 3 hours (**Scheme 19**). The progress of the reaction was monitored by TLC. On reaction completion, the mixture was filtered and then washed with methanol to obtain deep wine colored solid. M.pt. >300 ˚C, Percentage yield = 75% (1.14 g). The ^{1}H NMR spectrum displayed a multiplet for 2H at 8.87 ppm, doublet for 1H at δ 8.01 ppm, multiplet for 1H at δ 7.95 ppm, doublet for 2H, 1H and 2H at δ 7.4 ppm, δ 7.06 ppm and δ 6.81 ppm, respectively.^{13}C NMR spectrum displayed peaks at δ 175.2 for -C=O, 149.1 for -C-NH_2, 137.3, 133.9, 133.5, 132.4, 130.9, 129.1, 128.3, 123.0, 122.8, 116.7, 115.3, 114.8, 113.1, 112.7 for aromatic C. The mass spectrum of probe **1** showed MS(ESI): m/z at 354.07 (M^++1). The ^{1}H and ^{13}C NMR data corroborated the structure of 6-((4-aminophenyl)thio)-1-oxo-1H-phenalene-2,3-dicarbonitrile (probe **1**).

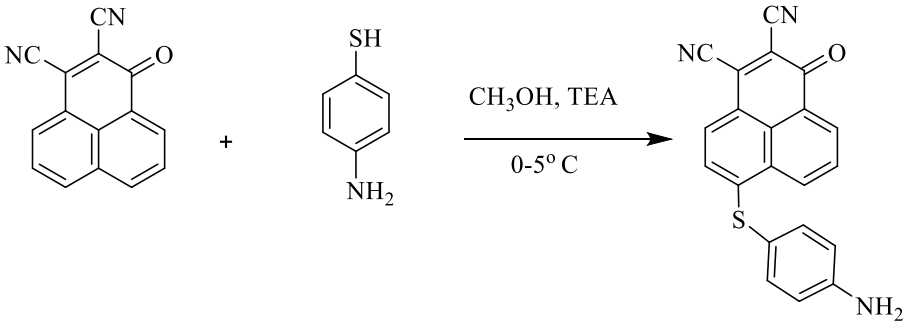

Probe 1

Scheme 19: Synthesis of probe **1**

2.1.3. Results and discussion

2.1.3.1. Absorption behavior of probe 1 towards various anions

The chromogenic response of probe **1** (20 μM, H_2O-CH_3CN (1:9, v/v)) towards different anions was recorded by adding 50 equiv. of different anions *viz*. CN^-, F^-, Cl^-, Br^-, AcO^-, I^-, HSO_4^-, OH^-, NO_3^-, $SCN^-$and $H_2PO_4^-$ as their tetrabutyl ammonium salts. Visible color change from pink to colorless was observed in the presence of CN^- ions, however, no color change was observed in the presence of rest of the anions (**Figure 2a**). These visible color changes prompted us to carry out the UV-Vis studies of probe **1**.

The absorption maximum band of probe **1** (20μM, H_2O-CH_3CN (1:9, v/v)) was obtained in visible region centered at 527 nm. No change or shifting in the absorption maxima of probe **1** was observed in presence of F^-, Cl^-, Br^-, AcO^-, I^-, OH^-, HSO_4^-, NO_3^-, SCN^-, $H_2PO_4^-$, however, in presence of CN^- ions a dramatic decrease in the absorption intensity (i.e. hypochromic shift) at 527 nm was observed and led to formation of low intensity absorption bands at 454 nm and 597 nm with two isobestic points at 468 nm and 570 nm **(Figure 2b)**.

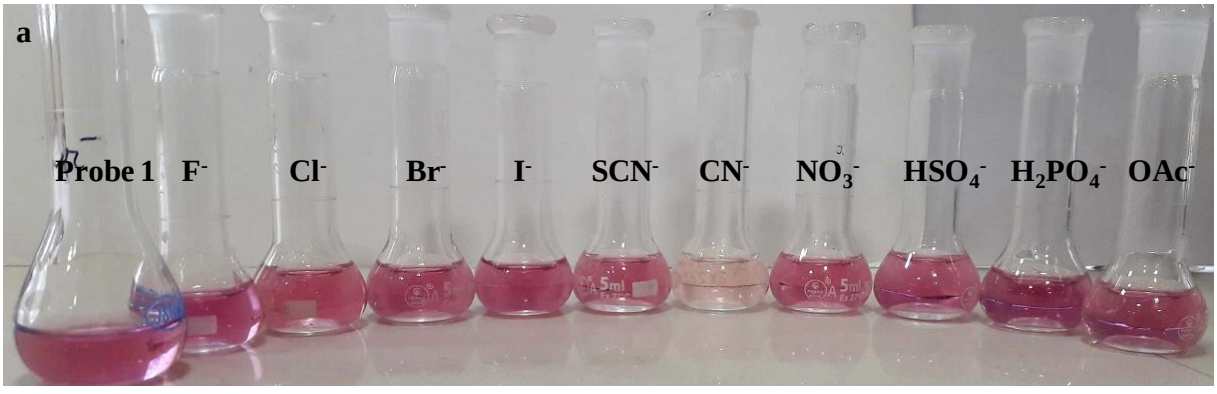

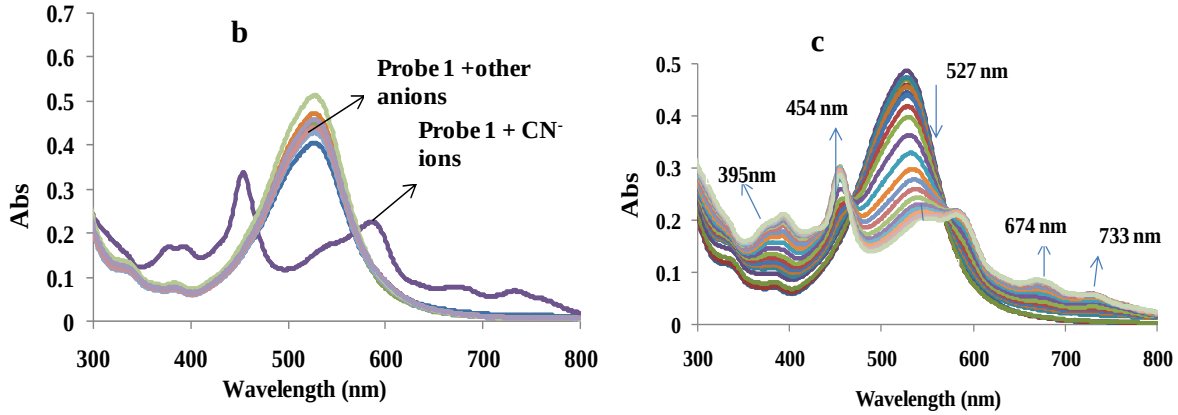

Figure 2: (a) Color changes of probe **1**(20μM, H_2O-CH_3CN (1:9, v/v)), in presence of different anions; (b) Absorption spectra of probe **1** in presence of different anions in H_2O-CH_3CN (1:9, v/v); (c) Effect of incremental addition of CN^-ions from 0-126 µM to probe**1**(20μM, H_2O-CH_3CN (1:9, v/v)) on absorption spectra.

To test the sensitivity of probe **1** towards CN^- ions, gradual addition of CN^- was done into probe **1** (20 μM, H_2O-CH_3CN (1:9, v/v). With the increasing concentration of CN^- from 0-126 µM into probe **1** the decrease in the intensity of absorption band at 527 nm and simultaneous enhancement of band at 454 nm was observed **(Figure 2c).** This decrease in absorption intensity at 527 nm and formation of new band at 454 nm helped in determining CN^-ions ratiometrically **(Figure 3)**. The variation of absorption ratio from 0.34 to 1.56, showed 4.59 fold ratiometric changes. Thus, probe **1** could be used to detect CN^- from 0 to 126 µM ratiometrically without interference of any other analyte.

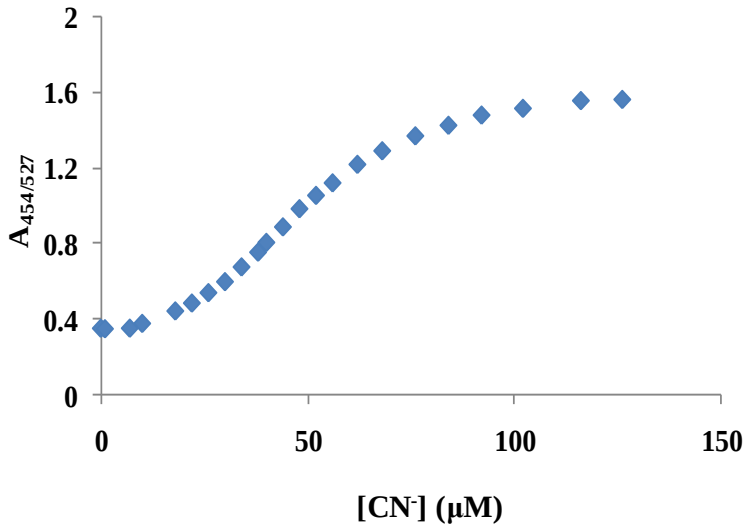

Figure 3: Ratiometric change at 454 nm and 527 nm (A_{454}/A_{527}) vs. [CN^-] ions of probe **1.**

2.1.3.2. Emission behavior of probe 1 towards various anions

The emission response of probe **1** towards 50 equiv. of different anions like F^-, Cl^-, Br^-, CN^-, AcO^-, I^-, HSO_4^-, OH^-, NO_3^-, SCN^-, $H_2PO_4^-$was recorded under UV-light. Probe **1**displayed a yellow emission in presence of CN^- ions **(Figure 4)** whereas; other anions did not show any significant change.

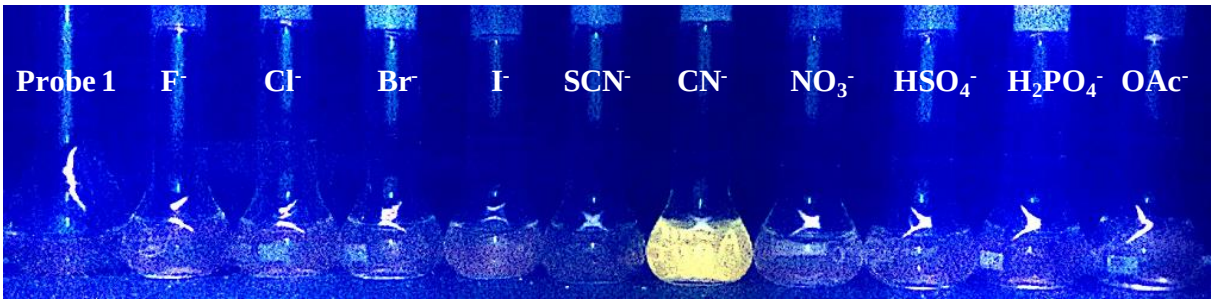

Figure 4: Emission color changes of probe **1** (20 μM, H_2O-CH_3CN (1:9, v/v)) in the presence of various anions under UV light.

The probe **1** (20 μM, H_2O-CH_3CN (1:9, v/v)) upon excitation at 480 nm, displayed a weak emission band at 567 nm. To test its selectivity, the emission spectra of probe **1** (20 μM, H_2O-CH_3CN (1:9, v/v)) was also recorded in presence of 50 equiv. of different anions viz., F^-, Cl^-, Br^-, CN^-, AcO^-, I^-, HSO_4^-, OH^-, NO_3^-, SCN^- and $H_2PO_4^-$. Interestingly, increase in the emission intensity was observed only in the presence of CN^- ions at 567 nm and the emission spectra remained unaffected in presence of all the other anions **(Figure 5a).**

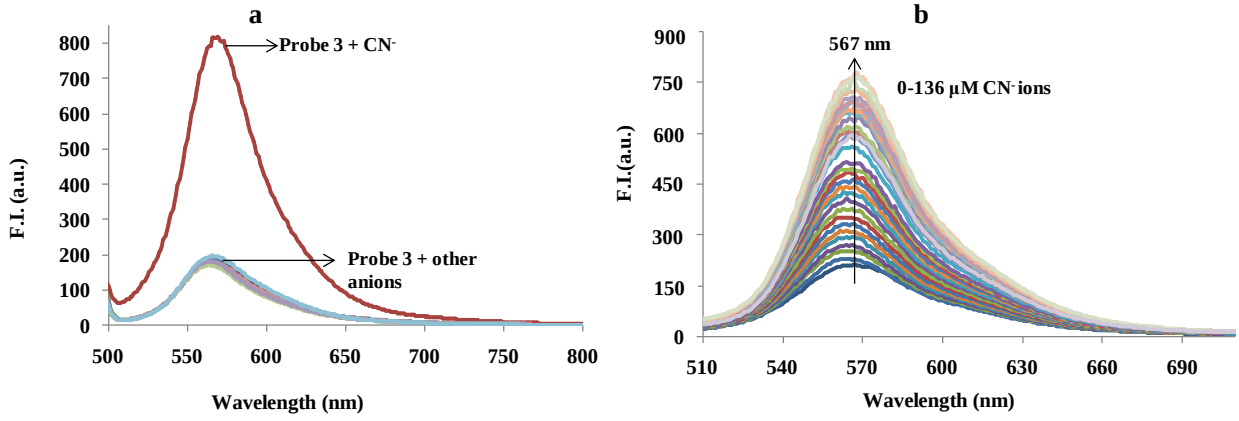

Figure 5: (a) Emission spectra of probe **1** (20 μM, H_2O-CH_3CN (1:9, v/v)) in presence of various anions; (b) Emission spectra of probe **1** (20 μM, H_2O-CH_3CN (1:9, v/v)) upon incremental addition of cyanide ions from 0-136 µM.

Upon incremental addition of CN^- to the solution of probe **1**, gradual increase in emission intensity at 567 nm was observed **(Figure 5b).** A linear plot between the emission intensity and [CN^-] ions, the lowest detection limit was determined and was found out to be 5.5×10^{-8} M. The binding constant was determined by Benesi-Hilderband equation, probe **1** showed a strong affinity towards binding with CN^- ions with $K_a = 1.1 \times 10^4\ M^{-1}$.

2.1.3.3. Effect of *pH* change on probe 1 and its CN^- complex

To find out the stability of probe **1** (20 μM, H_2O-CH_3CN (1:9, v/v)) and its complex **1.CN$^-$**, the absorption and emission spectra are recorded with varying pH. The change in *pH* of probe **1** did not show any change in the absorption (at 527 nm) and emission spectra (at 567 nm) (**Figure 6a, 6b**) in a wide *pH* range of 3-10.

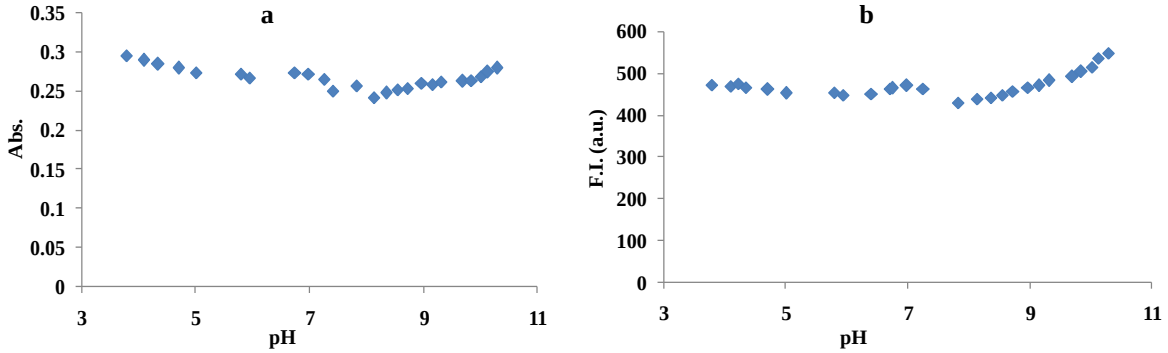

Figure 6 (a) Absorption response of probe **1** towards changing *pH* conditions at λ_{ab}= 527 nm (b)Emission response of probe **1** towards changing *pH* conditions at λ_{em}= 567 nm

The effect of varying *pH* on complex **1.CN$^-$** was also studied. The absorption at 527 nm and emission spectra at 567 nm, of the complex **1.CN$^-$** did not show any significant change within *pH* range of 6-10. On decreasing the *pH* below 6, the absorption spectra showed an increase intensity (**Figure 7a**) whereas, the emission intensity showed a drastic decrease (**Figure 7b**) which can be attributed to the breaking of the complex due to protonation. These changes in absorption and emission spectra showed that the complex **1.CN$^-$** was stable within *pH* 6-10 hence; probe **1** could be used for detection of CN^- within a wide *pH* range of 6-10.

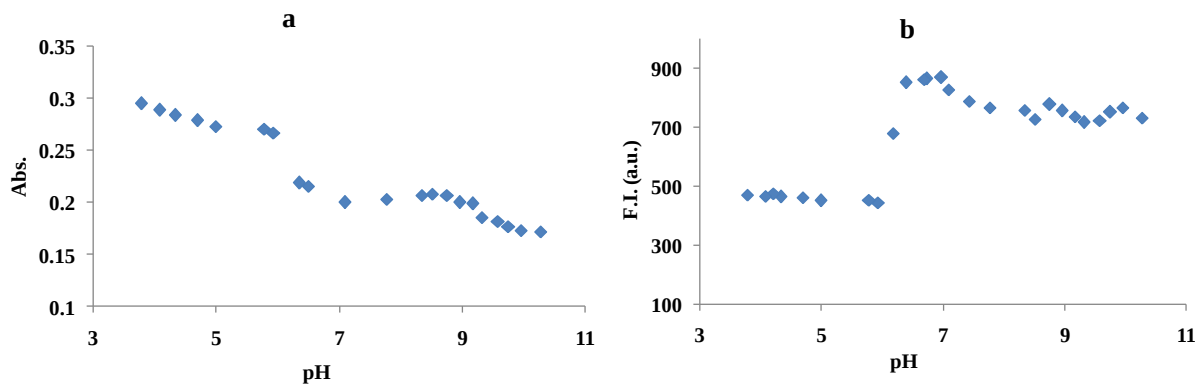

Figure 7 (a) Absorption response of complex of probe **1** with CN^- ions towards changing *pH* conditions (b) Emission response of complex of probe **1** with CN^- ions towards changing *pH* conditions.

2.1.3.4. Interferences

To get an insight into the selectivity of probe **1** for binding with CN^- ions over other anions, emission response of probe **1** (20 μM, H_2O-CH_3CN (1:9, v/v)) in presence of different anions as well as the emission response of the probe **1.CN**$^-$ complex in presence of different anions was measured. It was observed that the emission response induced by CN^- was unaffected even in presence of 50 equiv. of other anions like F^-, Cl^-, Br^-, AcO^-, I^-, HSO_4^-, OH^-, NO_3^-, SCN^-, $H_2PO_4^-$. Therefore, the binding of probe **1** with CN^- ions over the wide *pH* range can take place in coexistence of other anions. **(Figure 8)**

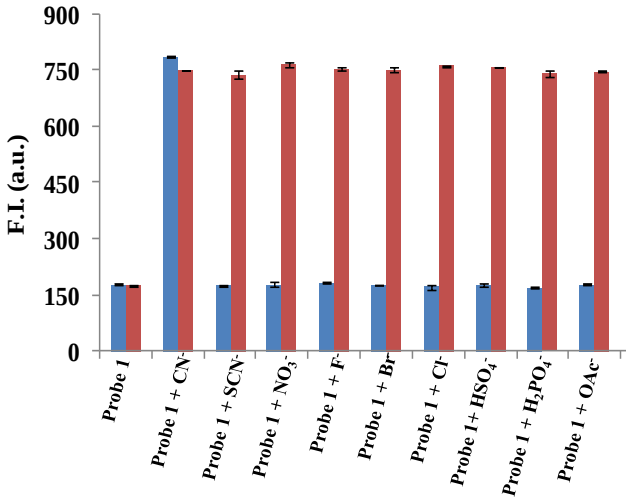

Figure 8: Fluorescence selective profile of probe **1** (20 μM, H_2O-CH_3CN (1:9, v/v)), towards CN^- ions in presence of 50 equiv. of other anions. Red bars represent the emission intensities of probe**1** in presence of 50 equiv. of CN^- ions and 50 equiv. of different anions. Blue bars represent the emission intensity of probe **1** in presence of 50 equiv. of different anions.

2.1.3.5. Binding mechanism of CN^- binding with probe 1:

In order to explore the binding mechanism of probe **1** towards CN^- ions, ^1H NMR and IR studies were performed upon additions of TBACN to probe **1** (DMSO-d_6). Probe **1** displayed peaks of aromatic protons within δ 6.5 to δ 9.0 ppm range and a characteristic –NH peak at δ 5.0 ppm but in presence of TBACN a new signal near δ 4.75 ppm appeared whose intensity increased with the increasing addition of CN^- ions suggesting nucleophillic addition of cyanide ions to carbonyl group (-C=O) and formation of new adduct and the formation of new singlet at δ 4.75 ppm suggests the formation of -OH. The emergence of new signal at δ 4.75 indicate that CN^-ions chemodosimetrically attack at carbonyl carbon and leads to the breaking of the conjugation resulting in the shifting of the peaks at aromatic region to aliphatic region to for cyanohydrins **(Scheme 20)**.In order to confirm -OH formation, D_2O exchange was performed and the signals at 4.75 ppm (due to -OH) and 5.0 ppm (due to $-NH_2$), suppressed (**Figure 9**).To further support the binding mechanism the IR (infra-red) spectra of probe **1** (CH_3CN) (**Figure 10**) and the IR spectra of probe **1** in presence of CN^- ions was recorded (**Figure 11**). Probe **1** showed peak of –CN at 2222 cm^{-1}, –NH peak at 3365-3458 cm^{-1} and –C=O peak at 1737 cm^{-1}(**Figure 10**). With the addition of CN^- ions broad peak at 3454-3558 cm^{-1} was observed showing the formation of -OH, the peak of –CN at 2256 cm^{-1} intensified and the sharp peak of –C=O at 1737 cm^{-1} diminished and an intense peak at 1640.6cm^{-1} corresponding to –C-O stretching was attained (**Figure 11**). The inference drawn out from the ^1H-NMR titration and IR suggests the chemodosimetric attack of CN^- on carbonyl carbon and formation of cyanohydrin and the plausible mechanism is shown in **Scheme 20**.

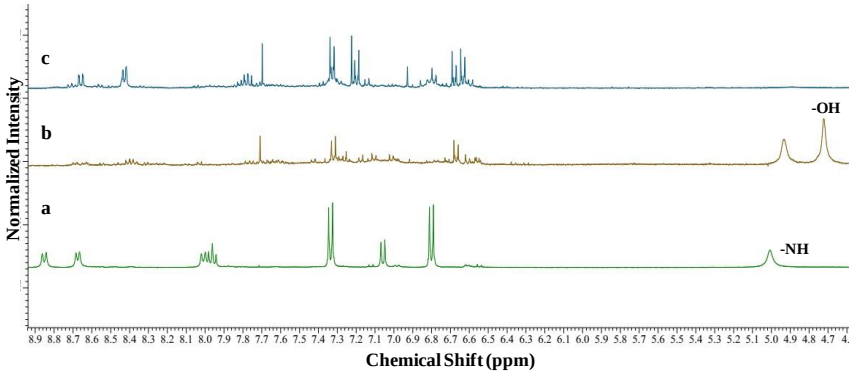

Figure 9:^1H NMR spectra of probe **1** upon addition of CN^- ions in DMSO-d_6; Where, **a** is the ^1H-NMR of probe **1** (DMSO-d_6); **b** is the ^1H-NMR spectra of probe **1** in presence of 2 equiv. of CN^- ions and **c** is the ^1H-NMR spectra of probe **1.CN**$^-$ complex in presence of D_2O in probe **1** in DMSO-d_6.

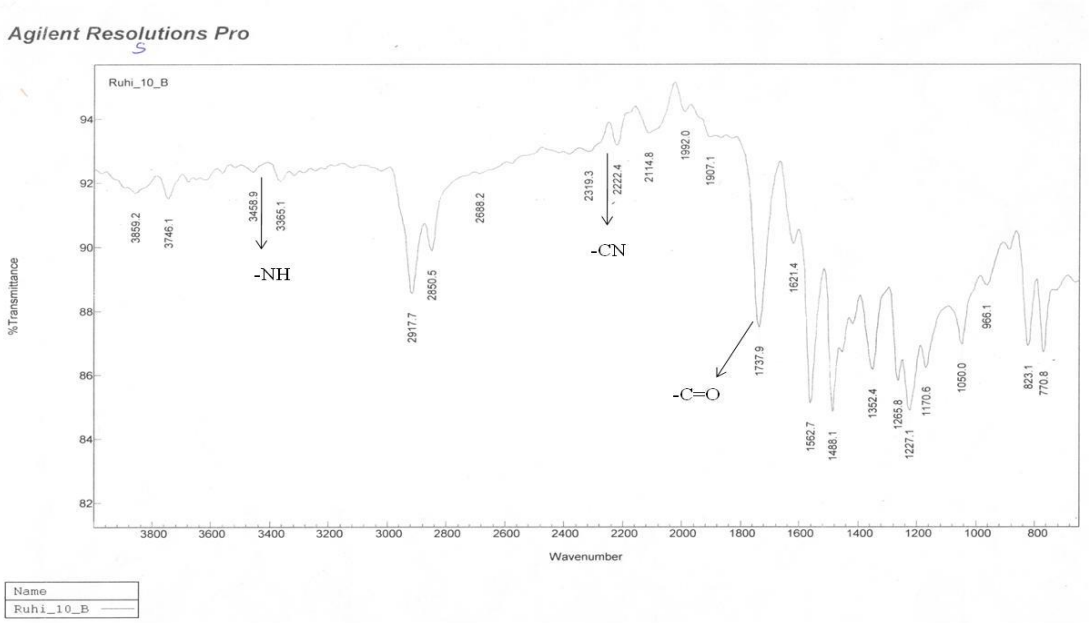

Figure 10: IR spectra of probe**1**

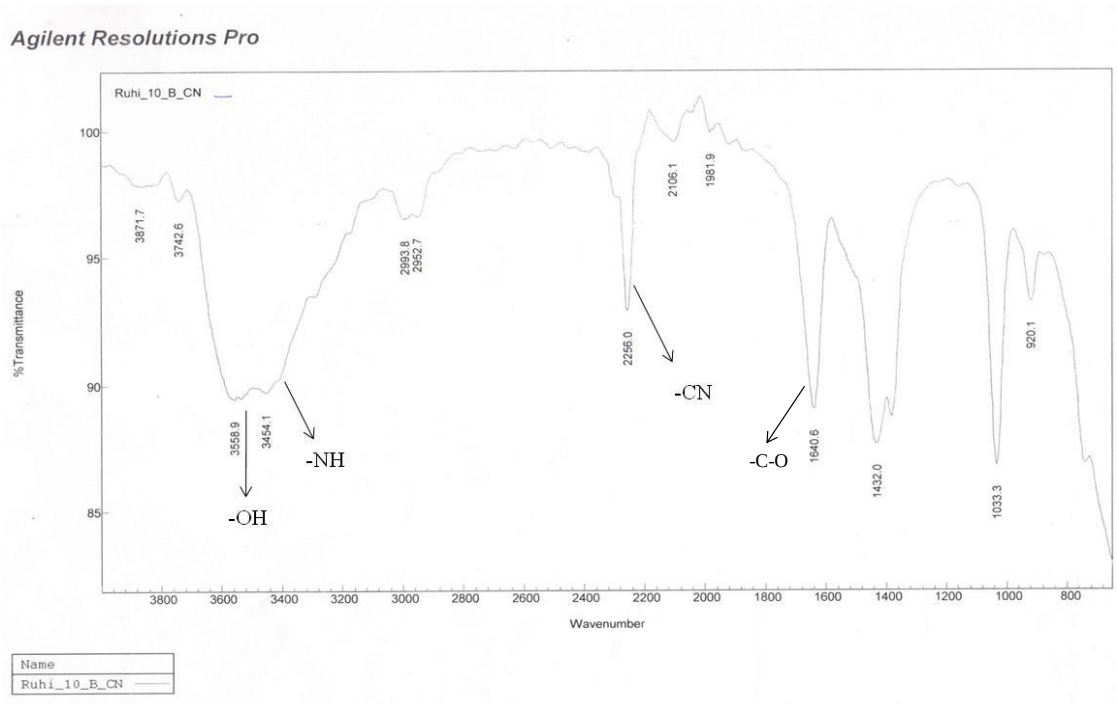

Figure 11: IR spectra of probe **1** in presence of 2 equiv. of CN^- ions in CH_3CN.

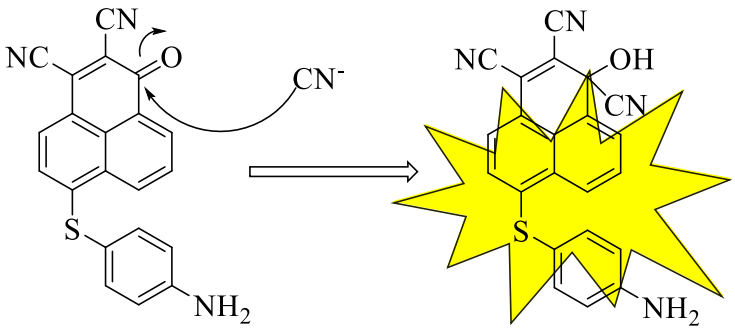

Scheme 20: Plausible mechanism of binding of CN^- with probe **1**

2.1.3.6. Practical Applicability:

2.1.3.6.1. Detection of CN^- in industrial effluent:

To demonstrate the applicability of probe **1** as CN^- sensor in real samples, industrial effluent from a printing ink manufacturing industry was collected. The pigments used in the printing inks involve various cyanide complexes such as, potash blue which has ferro and ferricyanide complexes. These cyano-complexes liberate free cyanide under acidic condition which can lead to CN^- toxicity in nearby areas where the waste is discarded if untreated [96]. To test the presence of free cyanide in the industrial waste, we spiked the industrial waste with different concentration of CN^- (20 μM and 40 μM). This spiked solution was added into the solution of probe **1** (20 μM H_2O-CH_3CN (1:9, v/v)) and its absorption and emission spectra were recorded. The absorption spectra showed the decrease in the band at 527 nm which is the characteristic band of the probe **1** accompanied by the formation of a new band at 454 nm (**Figure 12a**) and enhancement at 567 nm was also observed in the emission band (**Figure 12b**), from the spectral change the actual concentration and % recovery was calculated as shown in **Table 1.** This suggests that probe **1** could be used for detecting CN^- in real samples.

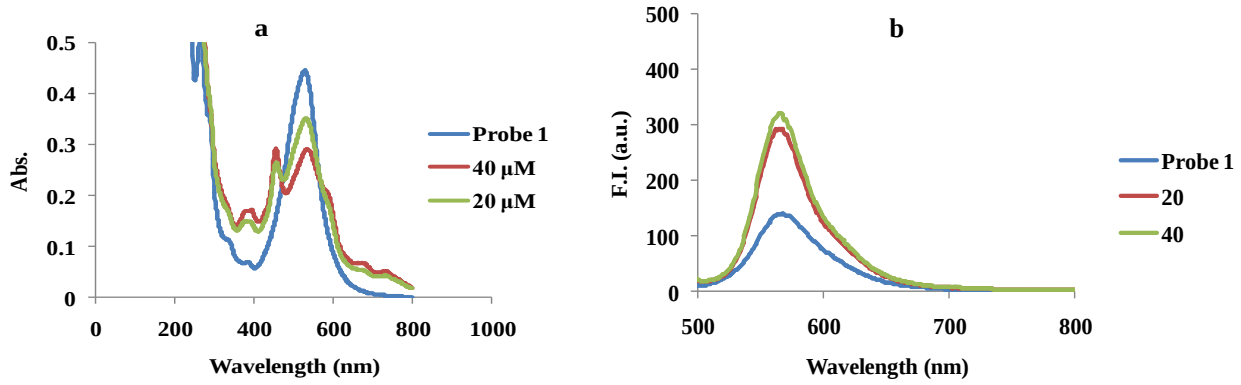

Figure12: (a) Absorption and (b) Emission spectra of probe **1**(20 μM, H_2O-CH_3CN (1:9, v/v)) in presence of different concentration of CN^- in industrial waste water samples

S. No.	Spiked (μM)	Found (μM)	Recovery (%)
1	20 µM	20.45±0.04	102.25
2	40 µM	40.75±0.03	101.87

Table 1: The percentage recovery of CN^- in industrial effluent.

2.1.3.6.2. Construction of 1-to-2 decoder:

The absorption spectral change of probe **1** in presence of CN^- ions, prompted us for using probe **1** in miniaturizing logic gates. A 1-to-2 decoder was designed by using CN^- as input and absorbance values at 527 nm and 454 nm, as the OUT_1 and OUT_2 respectively. For the $OUT_1$and OUT_2 the threshold values were taken as 0.2 and 0.16 respectively. While constructing the decoder a NOT gate was placed at OUT_1. In the presence of CN^- the intensity of absorption band at 527 nm decreased thus, OUT_1 was below the threshold value and was considered to be in '*off*' state i.e. 0 whereas, the absorption intensity at 454 increased and hence, OUT_2 was in '*on*' state i.e. 1. But in the absence of CN^- the OUT_1 (i.e. absorption at 527) was in "'*on*' state represented by 1 and OUT_2 (i.e. absorption at 454 nm) was below the threshold value and hence it was in '*off*' state represented by 0. Based on these input and outputs the decoder and truth table was formed. (**Figure 13**)

a

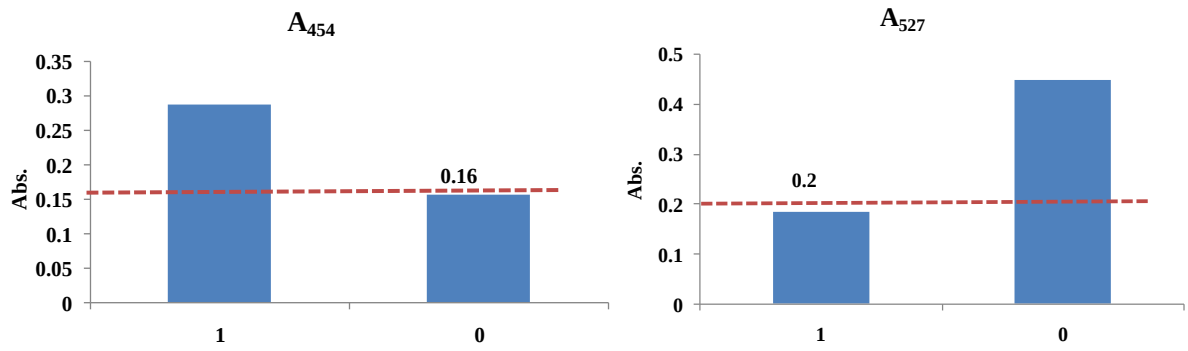

b

c Truth Table

In_1 (CN^-)	OUT_1 (λ_{abs}= 527 nm)	OUT_2 (λ_{abs}= 454 nm)
1	0	1
0	1	0

Figure 13: a) Absorption response of probe **1** at 527 nm and 454 nm in presence/absence of CN^- (the dashed line represents the threshold values); b) 1-to-2 decoder representation; c) Truth table for 1-to-2 decoder.

2.1.4. Conclusion:

Herein, we have synthesized a chromo-fluorescent sensor **1**. The optical and fluorescence studies of probe **1** revealed its selectivity to detect CN^- ions over other anions. Probe **1** was originally pink in color, displayed its absorption band at 527 nm and a weak emission band at 567 nm. In the presence of CN^- ions the pink color was bleached out, the absorption band at 527 nm diminished and band at 454 nm was formed. Whereas, the emission band showed an enhancement at 567 nm in the presence of CN^- ions, with a bright yellow emission under UV light. From the fluorescence titration profile of probe **1** the binding constant and detection limit was calculated to be K_{em}= 1.1 x 10^4 M^{-1} and 5.5×10^{-8} M respectively. Probe **1** was further used for detecting CN^- in real sample and for mimicking 1-to-2 decoder.

2.1.5. Experimental section:

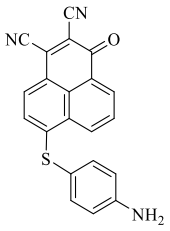

Probe 1

To a methanolic solution of phenalenedicarbonitrile (0.52 g, 4.2 mmol), 1 equiv. of *p*-aminothiophenol (0.54 g, 4.32 mmol) and 1.0 equiv. of TEA (triethylamine) (0.61 g) were added and the contents were stirred at 0-5^{o}Cfor 3 hours. The progress of the reaction was monitored by TLC. On reaction completion, the mixture was filtered and then washed with methanol to obtain deep wine solid. M.pt. >300 ˚C, yield = 75% (1.14g); **^{1}H NMR** (400 MHz, $CDCl_3$): δ 8.87 (m, 2H), 8.01 (d, 1H), 7.95 (m, 1H),7.4 (d, 2H), 7.06 (d, 1H), 6.81 (d, 2H); **^{13}C NMR** (100 MHz, $CDCl_3$): δ 175.2, 149.1, 137.3, 133.9, 133.5, 132.4, 130.9, 129.1, 128.3, 123.0, 122.8, 116.7, 115.3, 114.8, 113.1, 112.7.**MS (ESI):** m/z calcd. = 353.06, found = 354.07 (M^{+}+1).

2.2. A novel '*on-off*' rhodamine based sensor for colorimetric detection of CN^- and its application as encoder-decoder and molecular keypad lock

2.2.1. Abstract:

A novel rhodamine-phenalenedicarbonitrile ICT "*on-off*" sensor has been synthesized and characterized by ^1H NMR, ^{13}C NMR and mass spectrometric techniques. The photophysical studies of the probe suggest its existence in spirolactam ring open form of rhodamine. The ICT active sensor displayed an absorption band at 577 nm with shoulder at 520 nm and fluorescence band at 593 nm. The treatment of probe **2** with different anions showed its sensitivity and selectivity towards CN^- ions in aqueous methanolic solution with a lowest detection limit of 0.2 μM. The presence of CN^- ions hindered the ICT process of probe **2** and showed a blue shift in absorption band of probe **2** with formation of new band at 488 nm and decrease in emission intensity was also observed. The reversibility of **2.CN**$^-$ complex has been achieved with Fe^{3+} ions which formed the basis for the construction of multiple molecular logic circuits.

2.2.2. Synthesis of probe 2:

The solution of N-(rhodamine-B) lactam-ethylenediamine prepared in CH_3CN was added to the solution of phenalenedicarbonitrile in CH_3CN, $TBAHSO_4$ was added as phase transfer catalyst and the reaction was carried out in basic condition using K_2CO_3 (**Scheme 21**). The reaction mixture was stirred for 6 hours at room temperature. Thin layer chromatography technique was used for monitoring the progress of the reaction. On the completion of the reaction the contents were filtered and the obtained precipitates were further purified by column chromatography. Purple coloured precipitates were obtained in 60% (0.88 g) yield. M.pt >300^{o}C. ^1H NMR (400 MHz, $CDCl_3$) displayed a triplet for –NH at δ 8.99-8.98 ppm, two double doublets for 1H each at δ 8.86-8.83 and δ 8.73-8.70 ppm, multiplets for 3H, 2H and 5H at δ 8.01-7.92, δ 7.53-7.49, δ 6.44-6.38 respectively, doublets representing 1H each at δ 6.27-6.26, δ 6.19-6.18 and δ 6.17-6.16, three multiplets for 2H of ethylene protons, 8H representing $–CH_2$- of N,N diethylamine part and 2H of ethylene protons at δ 3.73-3.70, δ 3.37-3.31 and δ 3.1-3.05 respectively, a triplet for 12H representing $–CH_3$ N,N diethylamine part attached to xanthenes part of rhodamine at δ 1.19-1.15. The^{13}C NMR (100 MHz, DMSO- d_6) displayed peaks at δ 178.0 due to -C=O, 177.0 due to phenalene -C=O, 168.1, 155.2, 153.8, 153.2, 148.0, 138.5, 133.5, 133.3, 131.6, 130.2,

129.8, 129.2, 128.6, 127.1, 126.2, 123.8, 122.9, 116.2, 114.7, 111.5, 108.2, 107.2, 104.9, 104.9, 104.7, 97.3, 79.0, 78.9, 78.8, 43.6, 41.4, 31.3, 29.1, 14.0, 12.2. The mass spectrum of probe **2** showed MS (ESI); m/z = 714.13 (M^++1). The structure of the synthesized probe was corroborated as probe **2** (**Scheme 21**)

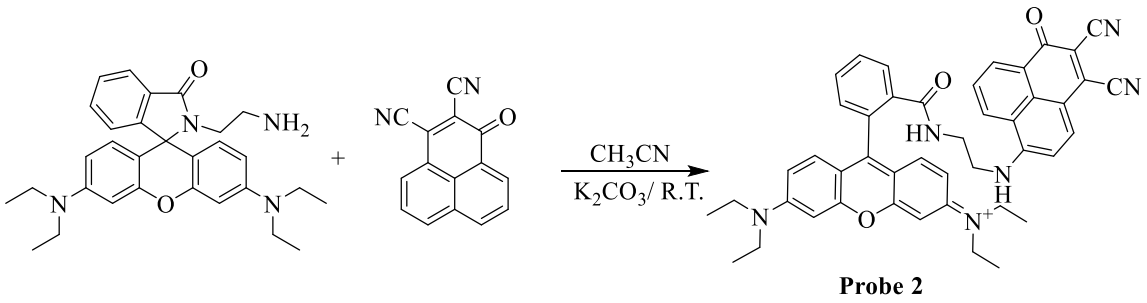

Scheme 21: Synthesis of probe **2**.

2.2.3. Results and discussion

2.2.3.1. Absorption changes of probe 2 in presence of different metal ions and anions:

The visible color changes for probe **2** (20 μM, CH_3OH-H_2O (4:1 v/v) *pH* 7.04) were captured in presence of 1000 µM of different inorganic anions. Probe **2** (20 μM, CH_3OH-H_2O (4:1 v/v) *pH* 7.04) showed a purple color initially (**Figure 14**) but in the presence of CN^- ions the purple color bleached out whereas, no colorimetric changes were observed in presence of rest of the ions.

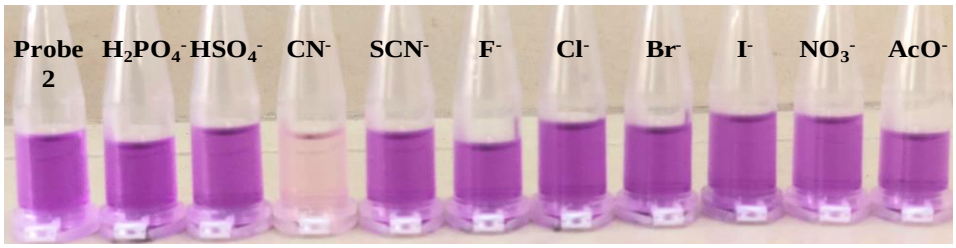

Figure 14: Visible color changes of probe **2**(20 μM, CH_3OH -H_2O (4:1, v/v) *pH* 7.04) in presence of different inorganic anions

The absorption response of probe **2** towards different metal ions and anions was determined under physiological conditions. Probe **2** (20 μM, CH_3OH-H_2O (4:1 v/v) *pH* 7.04) displayed a characteristic band of ring opened form of rhodamine at 577 nm with a shoulder at 520 nm. The UV-Vis spectra of probe **2** was also recorded in aprotic solvent i.e. CH_3CN (**Figure 15a**) which gave similar band as was attained in protic solvent (CH_3OH). This confirmed the presence of

probe **2**remain in spirolactam-ring-open form irrespective of the nature of solvent. The polar solvents favour the intramolecular charge separation on ring open-rhodamine derivative thus stabilized the structure. The spirolactam ring open form leads to the charge transfer to the acceptor moiety i.e. phenalenedicarbonitrile and the absorption occur at higher wavelength. No change was observed in the presence of metal ions Na^{+}, K^{+}, Mg^{2+}, Ca^{2+}, Al^{3+}, Pb^{2+}, Cr^{3+}, Fe^{2+}, Co^{2+}, Ni^{2+}, Cu^{2+}, Zn^{2+}, Hg^{2+} and Pd^{2+} (**Figure 15b**).

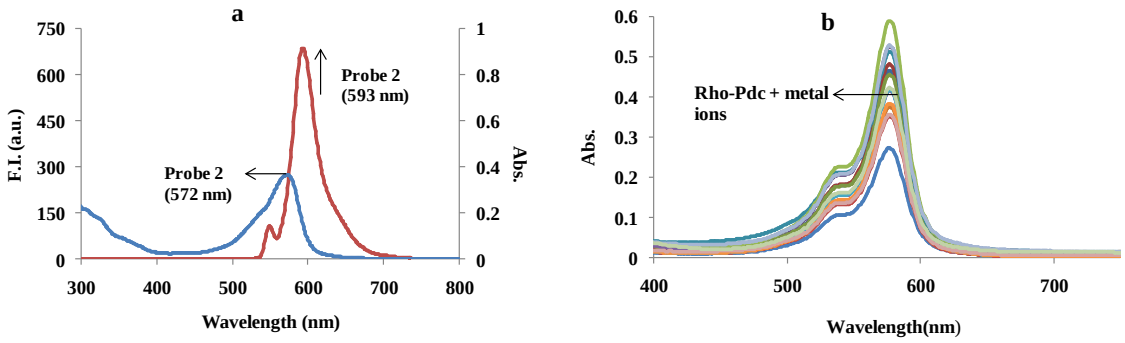

Figure 15: a) Absorption and Emission band of probe **2** in CH_3CN; b) Absorption spectra of probe **2** (20 μM, CH_3OH/HEPES-H_2O (4:1, v/v) *pH* 7.04) in presence of 50 equiv. of different metal ions

Furthermore, absorption spectra of probe **2**was recorded in presence of different anions like $H_2PO_4^-$, HSO_4^-, CN^-, SCN^-, F^-, Cl^-, Br^-, I^-, NO_3^- and OAc^- (**Figure 16a**). The addition 1000 µM of $H_2PO_4^-$, HSO_4^-, SCN^-, F^-, Cl^-, Br^-, I^-, NO_3^- and OAc^- did not show any change in the absorption band of probe **2** but, when incubated with CN^- the ICT is ceased and blue shift of 89 nm was observed and the strong absorption peak at 577 nm decreased and new absorption peak of low intensity was formed at 488 nm showing a clear isobestic point at 525 nm.

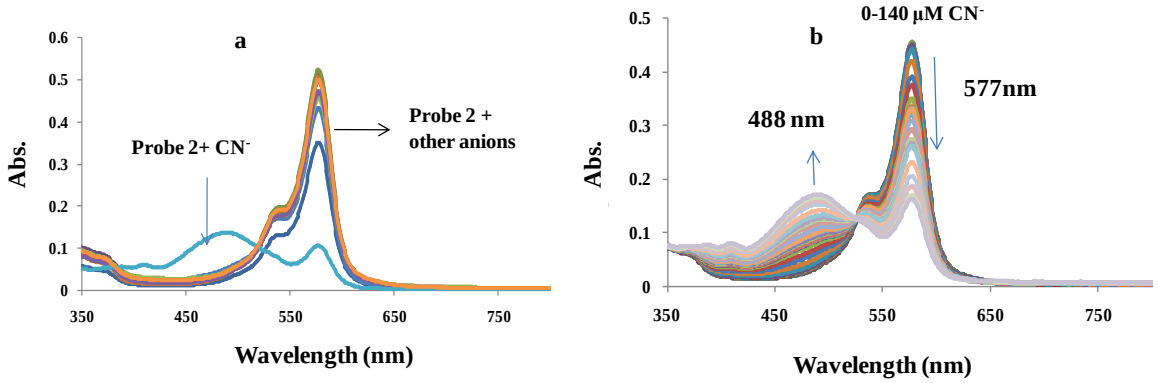

Figure **16**: a) Absorption spectra of probe **2** (20 μM, CH_3OH-H_2O (4:1, v/v) *pH* 7.04) in presence of 50 equiv. of different anions; b) Spectral titration of probe **2** with different amounts of CN^-.

Further, gradual addition of CN^- was done to test the sensitivity of probe **2** (20 μM, CH_3OH-H_2O (4:1 v/v) *pH* 7.04) towards CN^- ions. The increasing concentration of CN^- led to the gradual decrease in absorption band at 577 nm and simultaneous increase in absorption intensity at 488 nm with isobestic point at 525 nm. With the addition of 140 μM of CN^- the absorption intensity achieved plateau at 488 nm (**Figure 16b**) associated with discharge of purple color to light brown color. This change in color depicted the CN^- induced spirolactam ring closure of rhodamine moiety. The plot of $A_{488/577}$ versus varying [CN^-] showed a ratiometric change of 3.75 fold.

2.2.3.2. Emission response of probe 2 towards different anions:

The visual fluorescence effect of different biologically important inorganic anions on probe **2** was observed under UV lamp (**Figure 17**). Probe **2** displayed a bright pink emission which was discharged in presence of only CN^- ions.

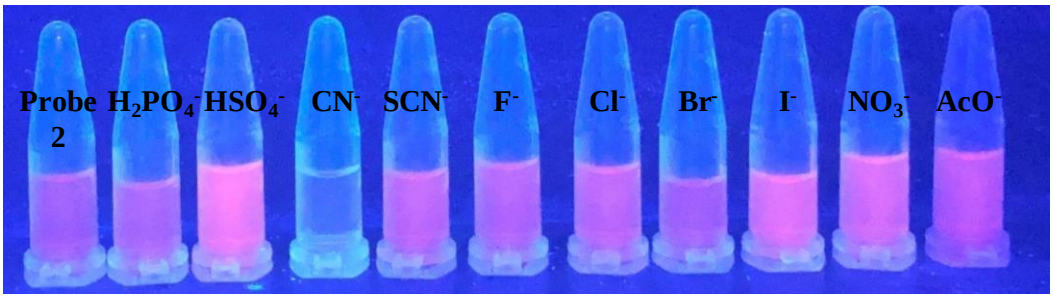

Figure 17: Visible fluorescence changes of probe **2** (20 μM, CH_3OH -H_2O (4:1, v/v) *pH* 7.04) in presence of different anions under UV lamp.

Further, the emission response of probe **2** was investigated. Probe **2** (20 μM, CH_3OH-H_2O (4:1 v/v) *pH* 7.04) when excited at 550 nm, gave its emission peak at 593 nm which is characteristic peak of ring open form of rhodamine which is in compliance with the bright pink fluorescence observed under UV lamp. The fluorescence spectra of probe **2** in CH_3CN also gave an intense emission band at approx. 593 nm which is a characteristic band of ring-open form of rhodamine. The response of probe **2** towards various anions was recorded by adding 1000 µM of anions viz., $H_2PO_4^-$, HSO_4^-, CN^-, SCN^-, F^-, Cl^-, Br^-, I^-, NO_3^- and OAc^- into solution of probe **2**. No change was observed in the presence of $H_2PO_4^-$, HSO_4^-, SCN^-, F^-, Cl^-, Br^-, I^-, NO_3^- and AcO^-. However, when same amount of CN^- was added, a significant decrease in the intensity was observed

(**Figure 18a**). This is attributed to the CN^- induced spirolactam ring closure of rhodamine due to which the ICT (intramolecular charge transfer) was hindered.

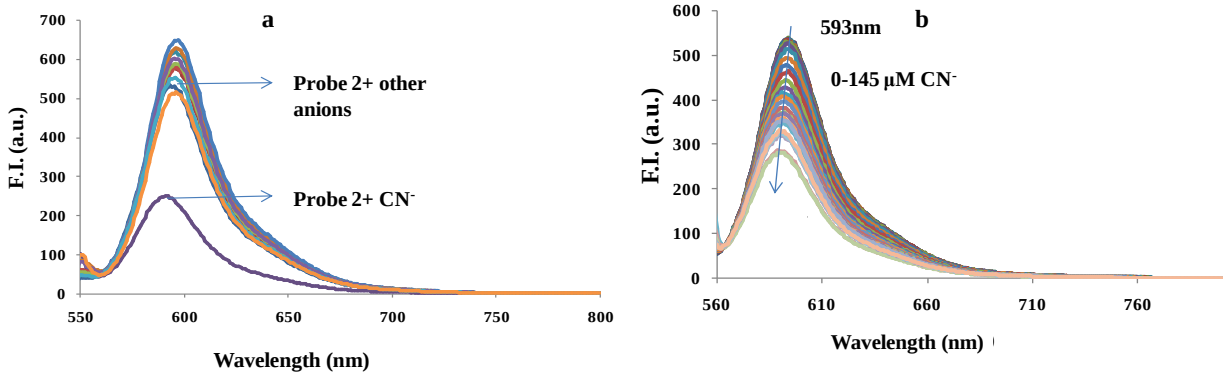

Figure 18: a) Emission spectra of probe **2** (20 μM, CH_3OH-H_2O (4:1, v/v) *pH* 7.04) in presence of 50 equiv. of different anions; b) Spectral titration of probe **2** with different amounts of CN^-.

The sensitivity of probe **2** towards CN^- ions was also tested by adding increasing amount of CN^- ions into solution of probe **2** (20 μM, CH_3OH-H_2O (4:1 v/v) *pH* 7.04). It was observed that with addition of 145 μM of CN^- the intensity of emission peak at 593 nm decreased (**Figure 18b**). From the titration profile the lowest detection limit was calculated to be 0.20 μM and the binding constant $K = 1.17 \times 10^4\ M^{-1}$ was determined by applying Benesi-Hielderband equation.

2.2.3.3. Selectivity profile of probe 2:

To check the selectivity of probe **2** to bind with CN^- over other anions was also checked by performing competitive experiments in the presence of background anions. The absorption spectra (**Figure 19a**) and emission (**Figure 19b**) of probe **2** in presence of CN^- ions did not show any change even in the presence of 50 equiv. of other anions ($H_2PO_4^-$, HSO_4^-, SCN^-, F^-, Cl^-, Br^-, I^-, NO_3^- and OAc^-).

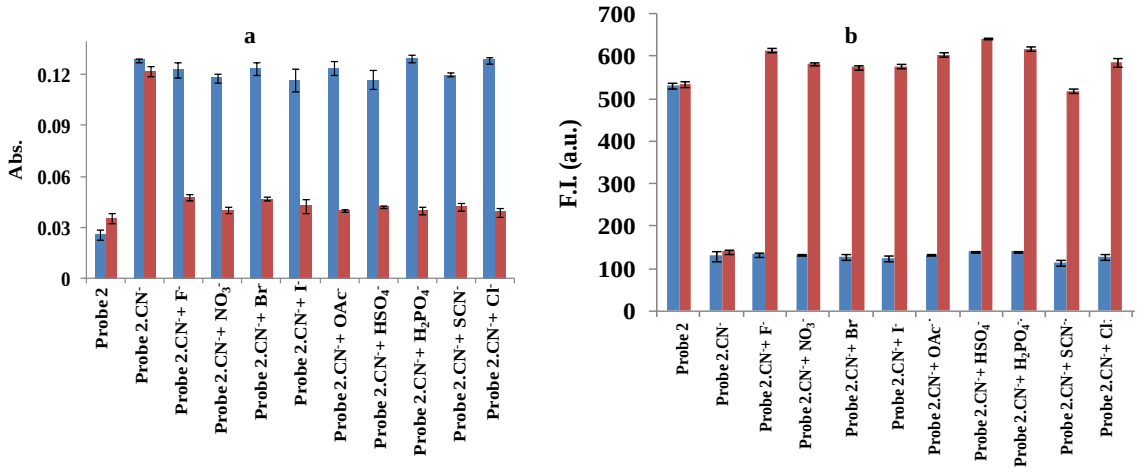

Figure 19: Selectivity profile of probe **2** in presence of different background anions where blue bars represent the absorption/emission intensities in presence of CN^- and various other ions and red bars represent the intensities on addition of 50 equiv. of different anions in probe **2;** a) UV-Vis response at 488 nm, b) Fluorescence response at 593 nm.

2.3.3.4. Effect of *pH* on probe 2 and probe 2.CN^- complex:

Furthermore, the effect of varying *pH* on probe **2** was studied *via* UV-Vis and fluorescence spectroscopy. The increase in *pH* (on adding 0.1M NaOH) of dyad probe **2** showed a slight decrease in absorption intensity at 577 nm (**Figure 20a**) and emission intensity at 593 nm (**Figure 20b**), and then on further increasing the *p*H, the intensities did not show further change between *pH* 8-13. This is due to the base induced ring closure of probe **2** whereas a decrease in *pH* by adding 0.1M HCl led to increase in absorption and emission intensities owing to further protonation of ring-opened form of rhodamine.

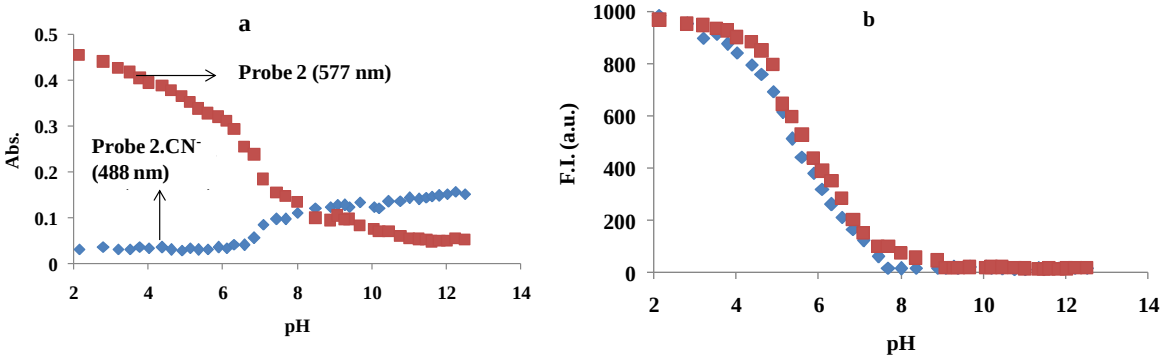

Figure 20: a) Effect of *pH* on absorption spectra of probe **2** in absence of CN^- ions represented by red dots at 577 nm and on complex of probe **2**.**CN^-** ions at 488 nm; b) Effect of *pH* change on emission spectra of probe **2** at 593 nm in absence of CN^- ions represented by blue dots and presence of CN^- represented by red dots.

The effect of *pH* change was also observed on complex of probe **2** at 488 nm (**Figure 20a (blue dots)**). The *pH* of complex was recorded to be 9.56. On adding 0.1M of NaOH into the solution of probe **2**.**CN**$^-$, the absorption and emission intensities did not show significant changes between *pH* 7-13. Whereas, on decreasing the *pH* i.e. on adding acid (0.1M HCl), depletion in intensity at 488 nm was observed suggesting the ring opening of rhodamine due to protonation. Furthermore, the emission intensity was increased gradually on adding 0.1M HCl and below *pH* 4 it remained almost constant whereas an increase in *pH* (adding 0.1M NaOH) did not show any change in fluorescence intensity of the complex probe **2.CN**$^-$ within *pH* range of 8-13 (**Figure 20b (blue dots)**).

2.2.3.5. Mechanistic Pathway:

To deduce the binding mechanism of probe **2** with CN^- ions, ^{1}H-NMR (**Figure 21**) and ^{13}C-NMR (**Figure 22**) titrations were performed in DMSO-d_6. The imine proton (-NH (16)) appeared at δ 9.51 ppm while the protons of phenalenedicarbonitrile appeared at 8.6 ppm and 8.72 ppm corresponding to one proton each. On addition of 1 equiv. of CN^-, shifting in the ^{1}H signals of Phenalenedicarbonitrile at 8.86 ppm and 8.73 ppm were observed. Further, proton shuffling was also observed in the aromatic region. The multiplets at 7.8 ppm (3H), 7.5 ppm (2H) and 7.0 ppm (1H) showed rearrangement of protons amongst themselves on adding CN^- into the solution of probe **2** i.e. the multiplet at 7.8 ppm corresponded to 1H, 7.5 ppm corresponded to 5H and at 7.0 ppm corresponded to 2H. The imine proton at 9.51 ppm also disappeared in presence of CN^- ions clearly showing the spirolactam ring closure. The binding mechanism was further explored by performing ^{13}C-NMR in presence and absence of CN^- ions into solution of probe **2** in DMSO- d_6. The carbonyl carbons C_b and C_a of probe **2** were observed at 168 ppm and 177 ppm but on addition of CN^- ions, the peak at 177 ppm corresponding to the –C=O of phenalenedicarbonitrile disappeared and a peak at 68 ppm (C_c) was observed suggesting that the CN^- attack occurs at carbonyl carbon of phenalenedicarbonitrile part of probe **2.**

From the results of photophysical studies as well as NMR titrations the plausible binding site of CN^- with probe **2** is shown in **scheme 22**. Probe **2** initially existed in spirolactam ring open form owing to the fact that phenalenedicarbonitrile being an electron deficient precursor gets charge/energy transfer from rhodamine B moiety. Whereas, upon exposing probe **2** to CN^-, the nucleophilic addition at –C=O of phenalenedicarbonitrile unit satisfies the charge deficiency of

the phenalenedicarbonitrile unit and the charge/energy transfer from rhodamine unit comes to a halt and thus closes the spirolactam ring.

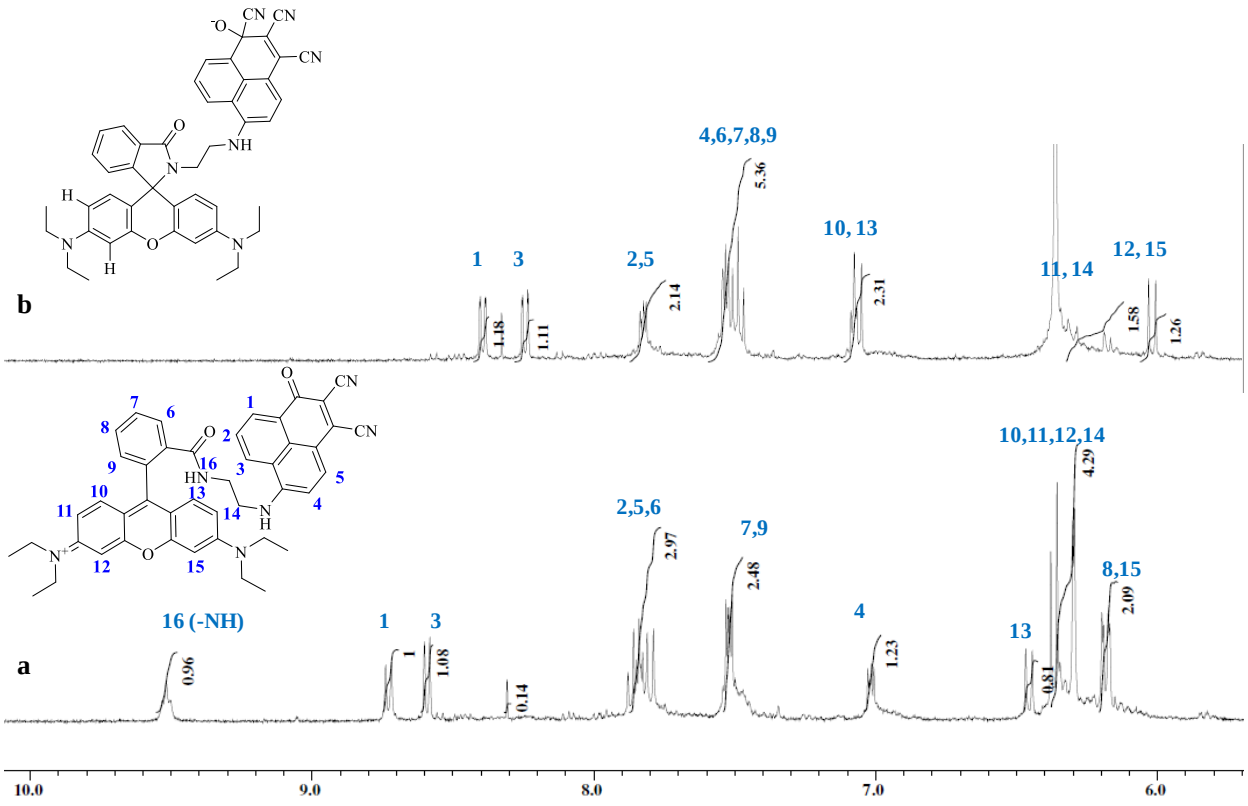

Figure 21:[1]H-NMR of probe **2** in presence of 1 equiv. of CN^- ions.

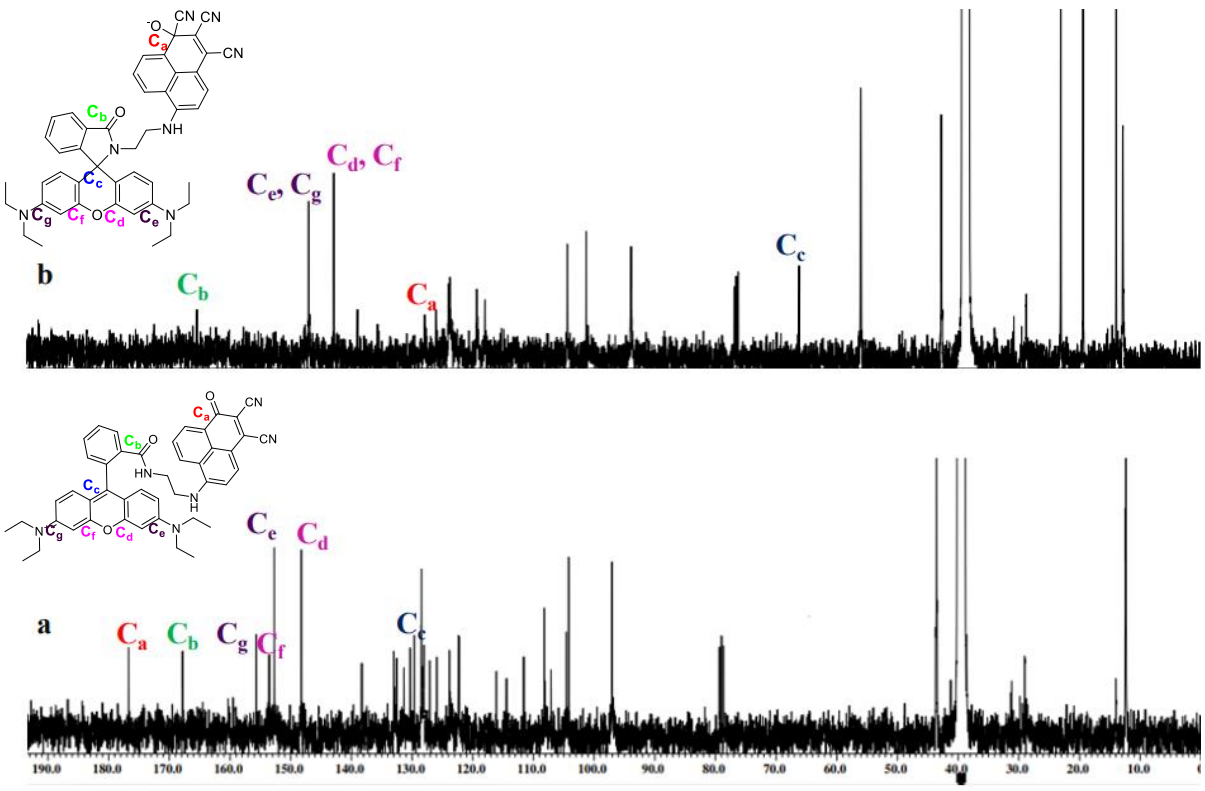

Figure 22: ^{13}C-NMR of probe **2** in presence of 1 equiv. of CN^- ions (as TBACN).

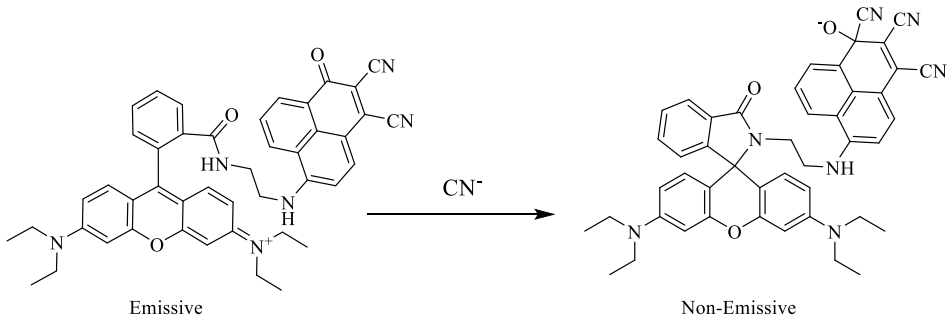

Scheme 22: Plausible binding mechanism of probe **2** and CN^- ions.

2.2.3.6. Practical Applicability:

To test the practical application of probe **2** to selectively detect CN^- ions, silica loaded with probe **2** was prepared. Silica gel of 60-120 mesh was immersed into 5 mL solution of probe **2** (10^{-4} M, CH_3OH) and was left to dry in oven. 5 mL solutions of varying concentration of CN^- ions (10^{-2} M, 10^{-3} M, 2×10^{-4} M, 4×10^{-4} M, 6×10^{-4} M, 10^{-4} M) were prepared and the silica loaded with probe **2** was immersed into each solution. The color changes were from purple to light brown (**Figure 23a**). Each sample was then dried in oven for 15-20 min and the color changes

were clearly visible. The color changes suggest that probe **2** could be used for naked eye detection of CN^- even at low concentrations.

For exploring the analytical application of probe **2** for CN^- ions we dipped cotton swabs into solution of probe **2** (10^{-3} M, CH_3OH-H_2O, 4:1 (v/v)) and were left to dry. Further, the cotton swabs were dipped into the solutions of various anions i.e. $H_2PO_4^-$, HSO_4^-, CN^-, SCN^-, F^-, Cl^-, Br^-, I^-, NO_3^- and AcO^- (10^{-3}M) and were again left to dry. The color change from purple to light brown was observed on the cotton swab which was dipped into CN^- solution (**Figure 23b**).

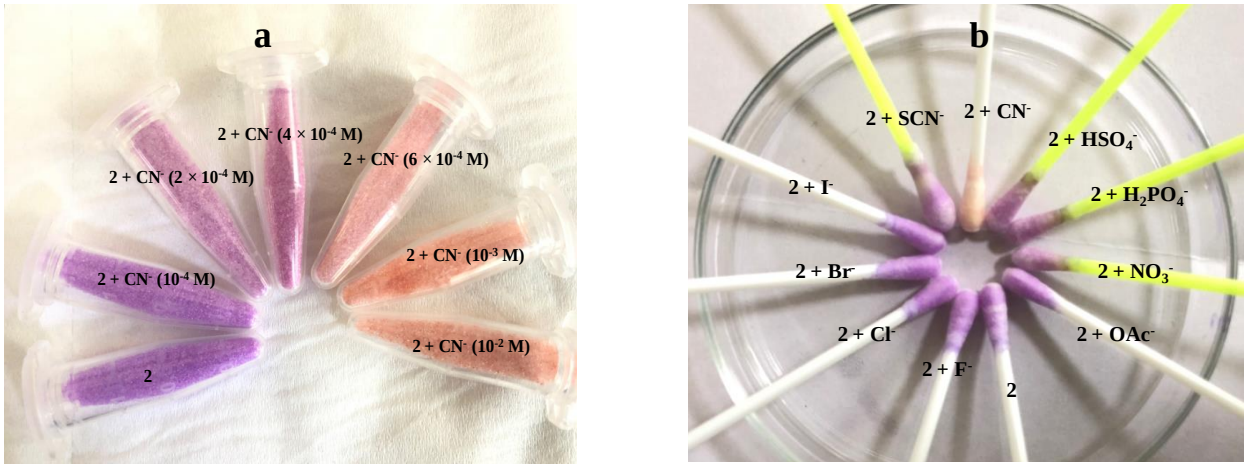

Figure 23: a) Color changes in the solid state of probe **2** in presence of different concentration of CN^- (10^{-2} M, 10^{-3} M, 2×10^{-4} M, 4×10^{-4} M, 6×10^{-4} M, 10^{-4} M) (b) Color changes in the cotton swabs of probe**2** when dipped in various anions.

2.2.3.7. Application in Molecular logic functions

The unique spirolactam ring opening and closing phenomenon of rhodamine prompted us to test if we can establish an '*on-off*' switch which can be used for mimicking logic circuits. Presence of CN^- ions in probe **2** led to deprotonation of –NH which resulted in ring closure of rhodamine. It has already been studied and explored earlier that complexation of rhodamine B with metal ion can result in ring opening phenomenon and hence reverse the optical and fluorescence properties. Following this consideration, we studied the absorption and emission response of probe **2.CN**$^-$ complex towards various metal ions like, Na^+, K^+, Mg^{2+}, Ca^{2+}, Al^{3+}, Pb^{2+}, Cr^{3+}, Fe^{2+}, Co^{2+}, Ni^{2+}, Cu^{2+}, Zn^{2+}, Hg^{2+} and Pd^{2+} was recorded to find out reversibility of complex. It was observed that with addition of 1000 μM of Fe^{3+} ions the absorption band at 488 nm disappeared and the band at 577 nm was regained (**Figure 24a**) whereas, enhancement in the emission band at 593 nm was

observed (**Figure 24b**). This reversible switching process of probe **2.CN$^-$** complex can be used for representing molecular logic gates by building up 2-to-1 encoder, 1-to-2 decoder and two output combination molecular logic circuits.

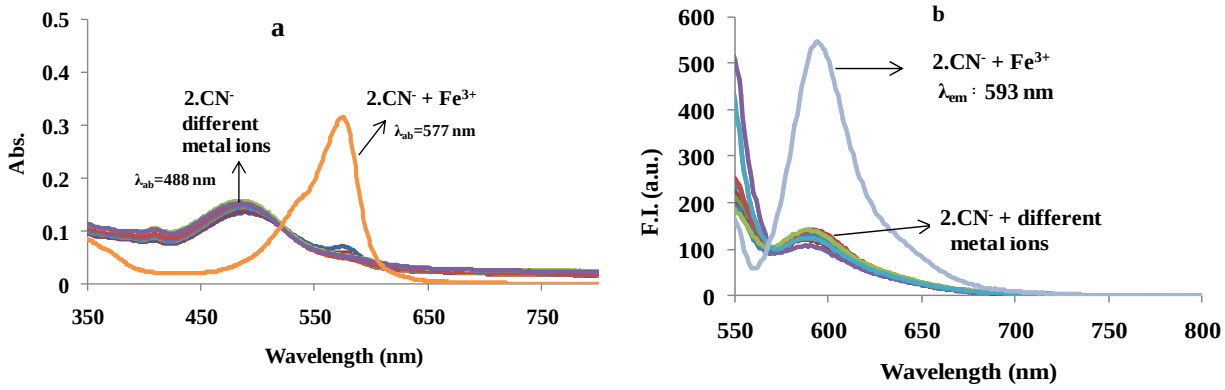

Figure 24: a) Absorption spectra b) Emission spectra of probe **2.CN$^-$**complex in presence of different metal ions

The 2-to-1 combination logic encoder (**Figure 25**) having one output is planned with dual inputs of CN^- (In_1) and Fe^{3+} (In_2) and output with emission value at 593 nm (OUT_1). For lower threshold value of emission intensity (F.I.<150) "0" value has been assigned corresponding to "off" and for higher threshold value (F.I. >150) "1" was assigned corresponding to '*on*' state. The four possible inputs were (0,0), (1,0), (0,1) and (1,1). In the absence of both the ions (In_1 and In_2 = 0), in the presence of only Fe^{3+} i.e. In_1 = 0 and In_2 = 1 and in the presence of both the inputs i.e. In_1 and In_2 = 1 the OUT_1 state is turned "on" with value "1". Whereas, in the presence of only In_1, the OUT_1 is in '*off*' state with value "0". The combination of the data led to the formation of IMPLICATION gate and truth table was formed.

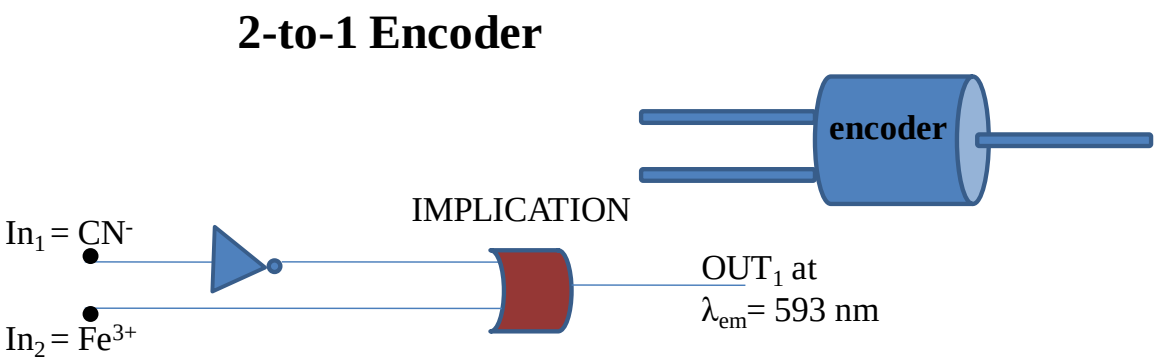

Truth Table:

In_1 (CN^-)	In_2 (Fe^{3+})	OUT_1 (λ_{em} = 593nm)
0	0	1
1	0	0
0	1	1
1	1	1

Figure 25: Emission response on addition of $In_1 = CN^-$ and $In_2 = Fe^{3+}$; Truth table for the addition of anion and cation and its 2-to-1 encoder representation.

A 1-to-2 decoder (**Figure 26**) was also formed having single input $In_1 = CN^-$ and OUT_2 at λ_{abs} = 577 nm and OUT_3 at λ_{abs}= 488 nm (OUT_3). In the presence of In_1 the OUT_3 is in 'on' state and OUT_2 is in 'off' state and in the absence of In_1, the OUT_2 is in 'on' state whereas OUT_3 is in 'off' state. Thus, fulfilling the conditions for the formation of 1-to-2 decoder along with formation of truth table.

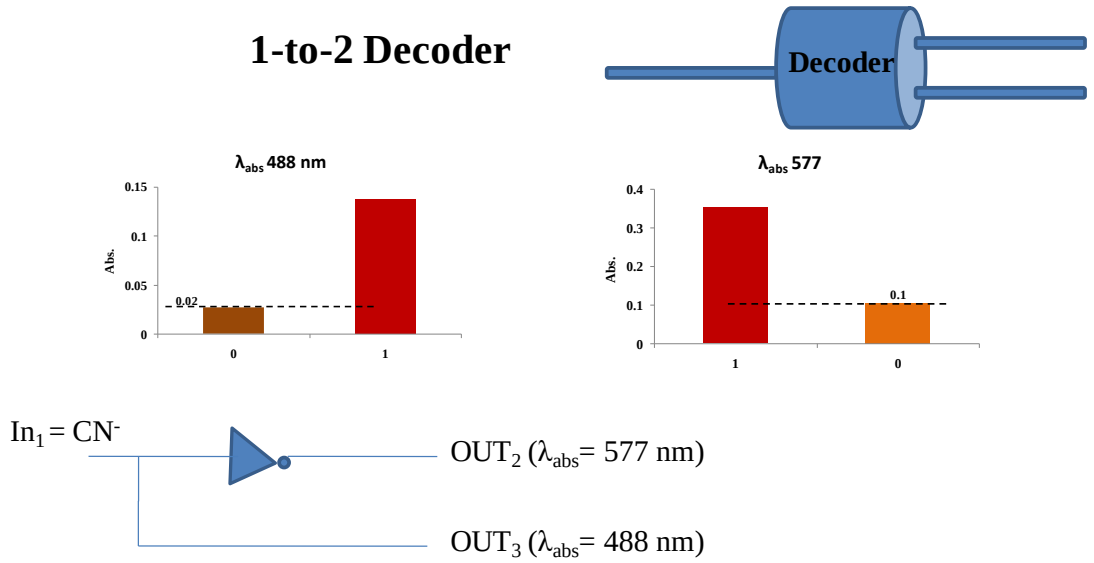

In_1 (CN^-)	OUT_2 (λ_{abs}= 577 nm)	OUT_3 (λ_{abs}= 488 nm)
0	1	0
1	0	1

Figure 26: Absorption response on addition of $In_1 = CN^-$; Truth table for the addition of anion and its 1-to-2 decoder representation.

Further, fascinated by the *on-off* switching behavior of UV-Vis and fluorescence spectra, a logic circuit with two inputs (i.e. $In_1 = CN^-$ and $In_2 = Fe^{3+}$) and two outputs (signals of absorbance at λ_{abs} = 488 nm (OUT_4) and λ_{abs}= 577 nm/ λ_{em} = 593 nm (OUT_5)) was composed having IMPLICATION and INHIBIT logic gates and the truth table is represented in table (**Figure 27**). When both the inputs were absent (In_1=In_2=0), present (In_1=In_2=1) or only In_2 was present (In_1=0, In_2=1) the OUT_5 at λ_{abs}= 577 nm/ λ_{em} = 593 nm was turned '*on*' with value "1" and when only In_1 was present then the OUT_4 at 488 nm was turned '*on*' with value "1" and OUT_5 at λ_{abs}= 560 nm/ λ_{em} = 593 nm was turned '*off*' with value "0". Hence, truth table was obtained.

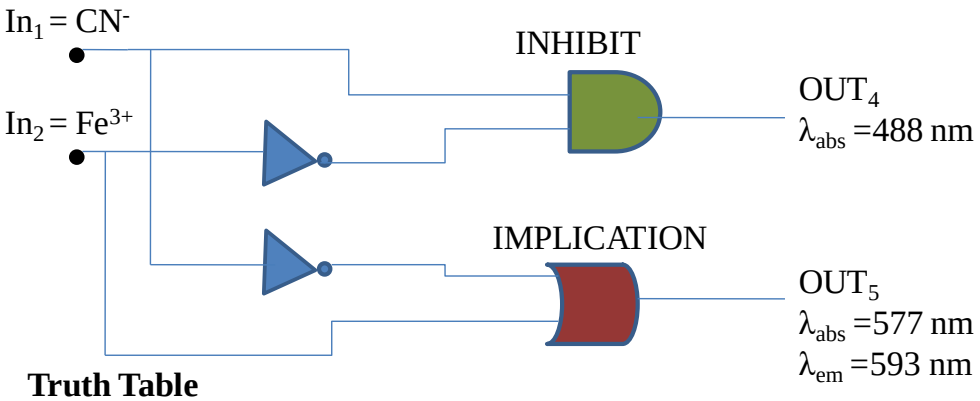

Truth Table

In_1 (CN^-)	In_2 (Fe^{3+})	OUT_4 (λ_{abs} = 488 nm)	OUT_5 (λ_{abs} = 577 nm/λ_{em} =593 nm)
0	0	0	1
1	0	1	0
0	1	0	1
1	1	0	1

Figure 27: Emission and absorption response on addition of $In_1 = CN^-$ and $In_2 = Fe^{3+}$; Truth table for the addition and its representation as molecular logic device.

Depending on the sequential addition of probe **2** (denoted by 'R'), CN^- (denoted by 'T') and Fe^{3+} (denoted by 'M') as inputs we have constructed a molecular keypad lock. This sequential addition gave six possible combinations i.e. RTM, RMT, MRT, MTR, TRM and TMR. For performing this experiment the concentration of the first component was fixed to 20 μM and rest of the two components were added accordingly (**Figure 28**). The output at λ_{em} = 593 nm was considered. It was observed that the fluorescence intensity was maximum (more than the threshold value) when T followed by M is added into 20μM solution of R. The emission intensity remained less than threshold value (200) in rest of the combinations. Hence, the correct password to open the molecular keypad lock is RTM.

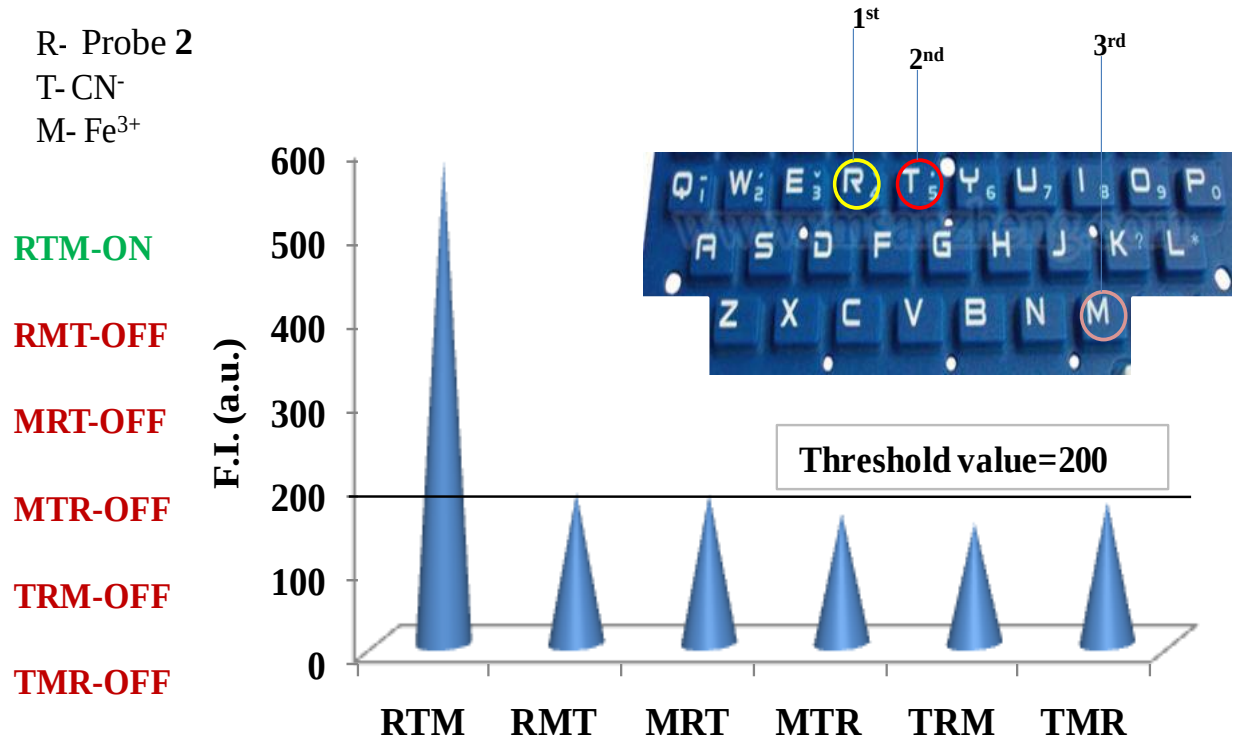

Figure 28: Emission response of probe **2** corresponding to sequential addition of three components. The inset shows a molecular keypad lock generating emission of maximum intensity when the password is entered correct. The keys R, T and M correspond to probe **2**, CN^- and Fe^{3+}.

2.2.4. Conclusion:

A novel rhodamine-phenalenedicarbonitrile fluorescence '*on-off*' based probe was designed and synthesized, which was found out to be excellent CN^- sensor. The absorption band of probe **2** gave the characteristic absorption and emission band of spirolactam ring open form at 577 nm and 593 nm respectively. On injecting CN^- into the solution of probe **2** the intensity of absorption and emission bands decreased and a new band in absorption spectra was obtained at 488 nm. Further, the reversibility of complex **2.CN**$^-$ were investigated and attained in the presence of Fe^{3+}. These changes in the absorption and emission responses were considered for mimicking the logic gates and a molecular keypad lock was formed.

2.2.5. Experimental Section:

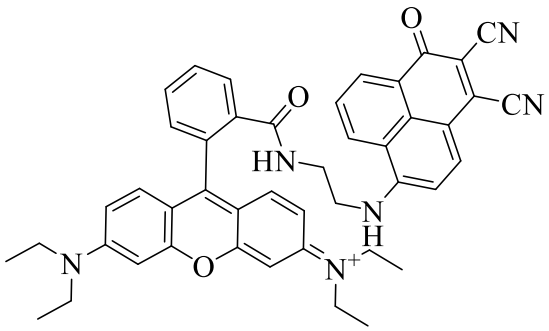

probe 2

The solution of N-(rhodamine-B)lactam-ethylenediamine (1g, 2.07 mmol) prepared in CH_3CN was added to the solution of phenalenedicarbonitrile (0.5g, 2.06 mmol) in CH_3CN, $TBAHSO_4$ was added as phase transfer catalyst and 1 equiv. of K_2CO_3 (0.28g, 2.03 mmol) was added as base. The reaction mixture was stirred for 6 hours at room temperature. TLC (Thin Layer Chromatography) the progress of the reaction. On the completion of the reaction the contents were filtered and the obtained precipitates were further purified by column chromatography. Purple coloured precipitates were obtained in 60% (0.88 g) yield. M.pt > 300^oC,**^{1}H NMR** (400 MHz, $CDCl_3$): δ 8.99-8.98 (t, *J* = 6.4 Hz, 1H, -NH), 8.86-8.83 (dd, ^2J = 6.4 Hz, ^3J = 0.92 Hz, 1H, ArH), 8.73-8.70 (dd, ^2J = 6.88 Hz, ^3J = 1.36, 1H, ArH), 8.01-7.92 (m, 3H, ArH), 7.53-7.49 (m, 2H, ArH), 6.44-6.38 (m, 5H, ArH), 6.27-6.24 (d,*J* = 8.72 Hz, 1H, ArH), 6.19-6.18 (d, J = 2.72 Hz, 1H, ArH), 6.17-6.16 (d, *J* = 2.72 Hz, 1H, ArH), 3.73-3.70 (m, 2H), 3.37-3.31 (m, 8H), 3.1-3.05 (m, 2H), 1.19-1.15 (t, *J* = 14.2 Hz, 12H); **^{13}C NMR** (100 MHz, DMSO- d_6) displayed peaks at δ 178.0 due to -C=O, 177.0 due to phenalene -C=O, 168.1, 155.2, 153.8, 153.2, 148.0, 138.5, 133.5, 133.3, 131.6, 130.2, 129.8, 129.2, 128.6, 127.1, 126.2, 123.8, 122.9, 116.2, 114.7, 111.5, 108.2, 107.2, 104.9, 104.9, 104.7, 97.3, 79.0, 78.9, 78.8, 43.6, 41.4, 31.3, 29.1, 14.0, 12.2; **MS(ESI):** m/z calcd. = 713.32, found = 714.13 (M^++1).

Chapter 2: Conclusion

In this chapter we have discussed the ion sensing behavior and changes in the photophysical properties of two phenalenedicarbonitrile based probes having different chromophoric units. Both these probes we found out to be selective and sensitive towards sensing of CN^- ions. Probe **1** gave fluorescence turn-*on* response in presence of CN^- on contrary; probe **2** gave a turn-*off* response. Phenalenedicarbonitrile is a highly electron deficient unit and acts as the charge acceptor and when it is attached to rhodamine B derivative; the spirolactam ring of rhodamine opens and thus making rhodamine B unit as the charge donor. Rhodamine B which generally shows a fluorescence turn-*on* response in presence of metal ions, showed an opposite behavior (optical and spectroscopic) when attached to electron deficient unit as in case of probe **2**.

Probe	**Sensing of ion**	**Medium**	**Association constant**	**Detection limit**
Probe **1**	CN^-	CH_3CN-H_2O (9:1, v/v)	$1.1 \times 10^4\ M^{-1}$	5.5×10^{-8} M
Probe **2**	CN^-	CH_3OH-H_2O (4:1, v/v)	$1.17 \times 10^4\ M^{-1}$	0.20 μM

CHAPTER 3

Rhodamine based hybrids and their sensing behavior: Application for sensing of Al^{3+} in real-time samples

General Introduction: Over the last few decades, rhodamine has been widely used as a precursor for formulation of fluorescent chemosensors, due to its unique spirolactam ring-opening and closing phenomenon which imparts it excellent optical as well as fluorescence properties. For the rational designing of excellent fluorescent chemosensor, presence of certain combination(s) of functional groups is essential. Rhodamine and its derivatives provide hard base donor sites i.e. oxygen and nitrogen, which can bind with specific metal ion/ions. To date, rhodamine based sensors have been effectively and efficiently used for sensing of various heavy and transition metal ions like Cr^{3+}, Fe^{3+}, Cu^{2+}, Hg^{2+} etc. but rhodamine based sensors having easy synthetic pathways and inexpensive reactants for selectively sensing Al^{3+} ions are not as much developed when compared to rest of the ions. The sensing of Al^{3+} in mixed-aqueous/aqueous medium has been considered to be problematic due to poor coordination and strong hydration ability of Al^{3+}. Considering all these facts we have synthesized, characterized and studied the behavior of two rhodamine based sensors which selectively formed chelate with Al^{3+} ions in different media. Probe **3** has one rhodamine unit attached to anthraquinone whereas; probe **4** has two rhodamine units attached to terephthaldehyde unit. Both these probes followed different sensing pathways.

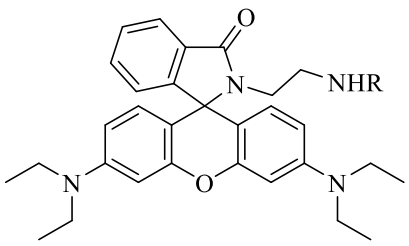

Rhodamine B ethylenediamine

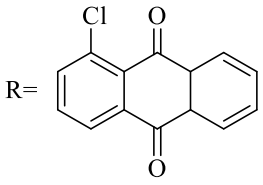

Probe 3

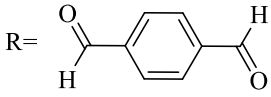

Probe 4

So, we have briefly compiled the results of the probes into following sub-chapters:

3.1. Rhodamine-anthraquinone based dyad for sensing of Al^{3+} in real sample and its application in generation of molecular logic device

3.2. Rhodamine-terephthaldehyde based Schiff base Al^{3+} sensor and potential of its ensemble for sensing of CN^- in 100% aqueous medium: Application in live cell imaging

3.1. Rhodamine-anthraquinone based dyad for sensing of Al^{3+} in real time sample and its application in generation of molecular logic device

3.1.1. Abstract:

A new rhodamine-anthraquinone based '*off-on-off*' colorimetric and fluorimetric sensor was designed, synthesized and characterized by ^{1}H, ^{13}C NMR and Mass spectrometric techniques. It was found out to be sensitive and selective towards Al^{3+} without any interference from other competitive metal ions. Probe **3** did not display any emission but on treating with Al^{3+} fluorescence enhancement at 587 nm was observed. Probe **3** formed a stable 1:1 complex with Al^{3+} ions with a binding constant of 7.07×10^{4} M^{-1} and was able to detect Al^{3+} ions with lowest detection limit of 0.2 μM. The complex **3.Al^{3+}** was further tested for its reversibility by treating it with different anions. The emission of **3.Al^{3+}** was quenched only in the presence of CN^{-} ions. Based on this result, molecular logical circuits were constructed with a combination of AND, OR, NOT, NOR gates. The capability of probe **3** to detect Al^{3+} in real sample was also achieved.

3.1.2. Synthesis of probe 3

Probe **3** was obtained by refluxing N-(rhodamine-B) lactam-ethylenediamine, 1-chloroanthraquinone and K_2CO_3 were added in THF along with catalytic amounts of bis-(triphenylphosphine) palladium (II) dichloride for 24 hrs 110 ℃ as shown in scheme **23**. On completion of reaction the contents were filtered and the filtrate was extracted using water and ethyl acetate mixture. The organic layer was concentrated and was further purified through column chromatography to obtain red colored solid in 80% (1.16 g) yield. M.pt = 220-235^{o}C. The ^{1}H NMR (400 MHz, $CDCl_3$) displayed a triplet for –NH at 9.66, a multiplet for aromatic 2H at δ 8.25 ppm, another multiplet for aromatic 1H at δ 7.97 ppm, multiplet for aromatic 2H at δ 7.76 ppm, doublet for aromatic 1H at δ 7.55 ppm, multiplet for aromatic 4H at δ 7.48 ppm, triplet for aromatic 1H at δ 7.13 ppm, doublet for aromatic 1H at δ 7.0 ppm, doublet for aromatic 2H at δ 6.48 ppm, doublet for aromatic 2H at δ 6.41 ppm, multiplet for aromatic 2H at δ 6.25 ppm, in aliphatic region the multiplet of 12H for two $–N(CH_2)_2-$ protons (attached to the xanthenes ring of rhodamine B part) merged with $–CH_2-$ of ethylenediamine linker at δ 3.39 ppm and triplet for 12H of $-CH_3$ of two N,N diethyl part attached to xanthenes unit at δ 1.17 ppm;^{13}C NMR (100 MHz, $CDCl_3$)δ: 184.82 (C=O), δ 183.89 (C=O), δ 168.51, δ 153.74, δ 153.40, δ 151.52, 148.88,

135.34, 133.96, 132.92, 128.93, 128.25, 126.81, 126.68, 123.98, 122.86, 115.87, 108.16, 105.10, 97.70, 65.03, 44.41, 40.30, 39.05, 29.79, 12.69. MS (ESI): m/z calcd. = 690.32, found = 691.11 (probe **3**+H^+). According to the ^{1}H-NMR, ^{13}C-NMR and Mass spectroscopy we assigned the structure of probe **3** as 1-((2-(3',6'-bis(diethylamino)-3-oxospiro[isoindoline-1,9'-xanthen]-2-yl)ethyl) amino) anthracene-9,10-dione.

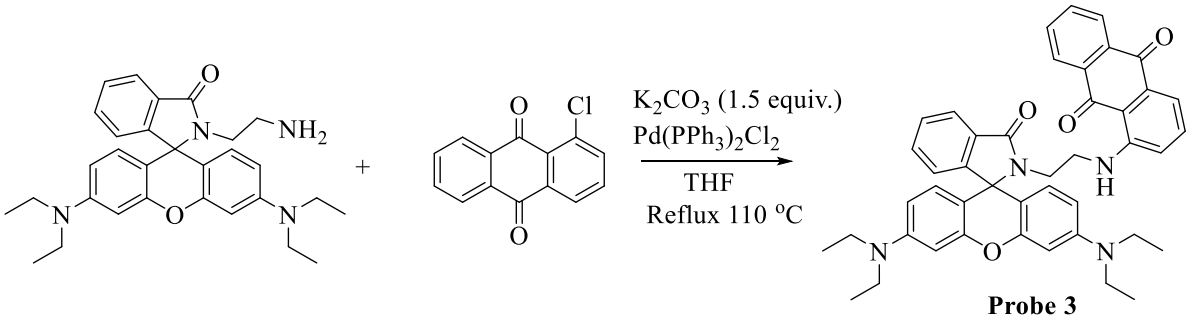

Scheme 23: Synthesis of probe**3**.

3.1.3. Results and Discussion:

3.1.3.1. UV-Vis studies of probe 3 in presence of different metal ions.

In order to investigate the metal ion selection behavior, visual color changes and UV-Vis spectroscopic studies were performed. The solution of probe **3** (20 μM, CH_3OH-H_2O (2:1, v/v) *pH* 7.04) displayed light pink color and its associated absorption maxima at 512 nm. Different metal ions (viz., K^+, Mg^{2+}, Ca^{2+}, Cr^{3+}, Al^{3+}, Fe^{3+}, Co^{2+}, Ni^{2+}, Cu^{2+}, Zn^{2+}, Pb^{2+}, Hg^{2+}, Ag^+ and Ga^{3+}) were treated with probe **3**. Among all the aforesaid metal ions, incubation of Al^{3+} in probe **3** (20 μM, CH_3OH-H_2O (2:1, v/v) *pH* 7.04) showed an immediate color change to intense pink (**Figure 29a**) and a red shift of 50 nm was observed. The absorption maxima observed in the presence of Al^{3+} was formed at 560 nm and shoulder at 520 nm which is the characteristic peak of ring-opened form of rhodamine (**Figure 29b**). However, no change in color as well as no alteration in the nature of absorption spectrum was observed in the presence of rest of the metal ions.

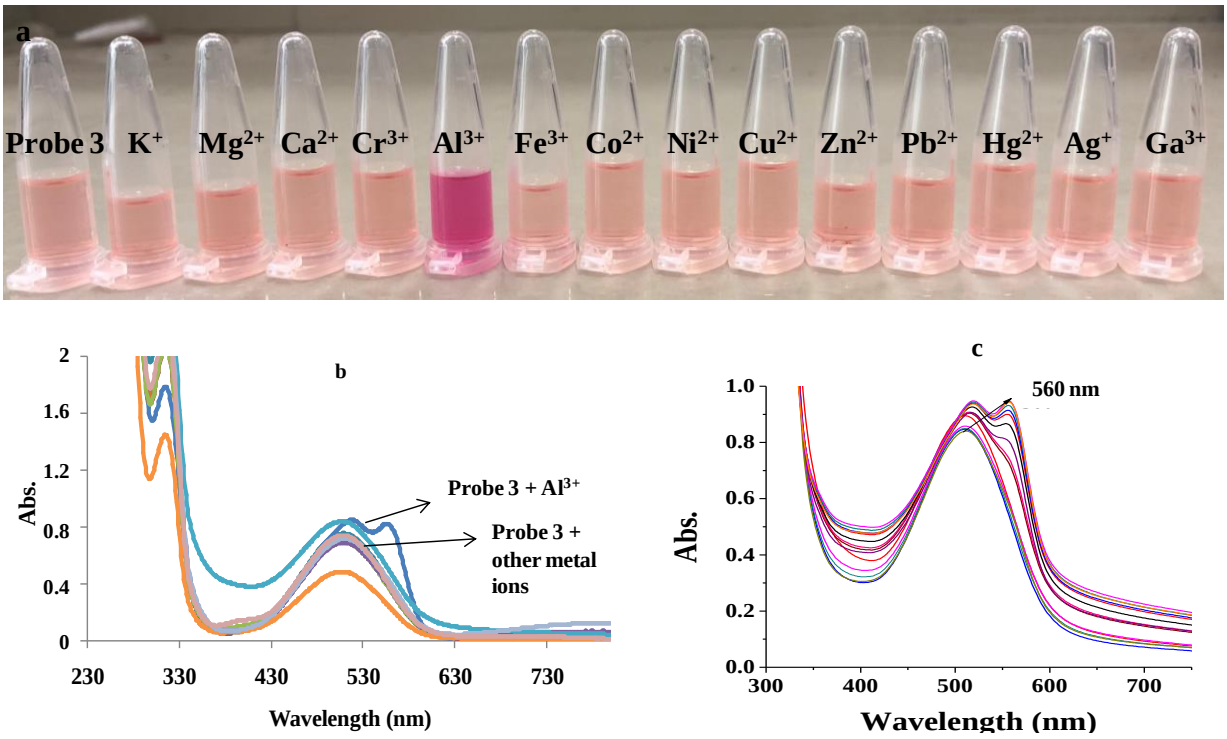

Figure **29**: a) Visible color changes of probe **3** (20 μM, CH_3OH-H_2O (2:1, v/v) *pH* 7.04) in presence of different metal ions; b) Absorption spectra of probe **3** (20 μM, CH_3OH-H_2O (2:1, v/v) *pH* 7.04) in presence of 1000 μM of different metal ions; c) Effect of incremental addition of Al^{3+} ions on absorption spectra probe **3.**

To determine the sensitivity of probe **3** (20 μM, CH_3OH-H_2O (2:1, v/v) *pH* 7.04) towards Al^{3+}, absorption spectra was recorded with incremental addition of Al^{3+} ions (**Figure 29c**). The changes achieved their plateau with addition of 136 μM of Al^{3+}. The binding stoichiometry of 1:1 was established by carrying out the job's plot analysis (**Figure 30**).

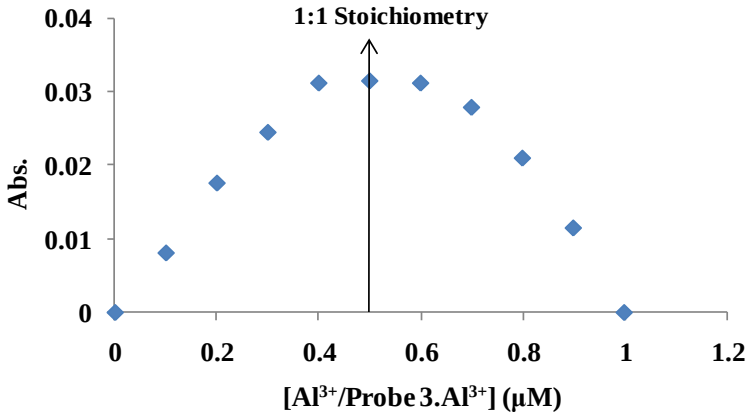

Figure 30: Absorbance at 560 nm of probe **3** and Al^{3+} indicating 1:1 stoichiometry.

3.1.3.2. Fluorescence response of probe 3 towards different metal ions:

The visual fluorescence changes of different metal ions on probe **3** were observed on illumination under UV lamp. Probe **3** did not show any emission under UV lamp (**Figure 31**). Presence of different metal ions did not alter the emission changes however presence of Al^{3+} ions led to the turning 'on' of the pink emission.

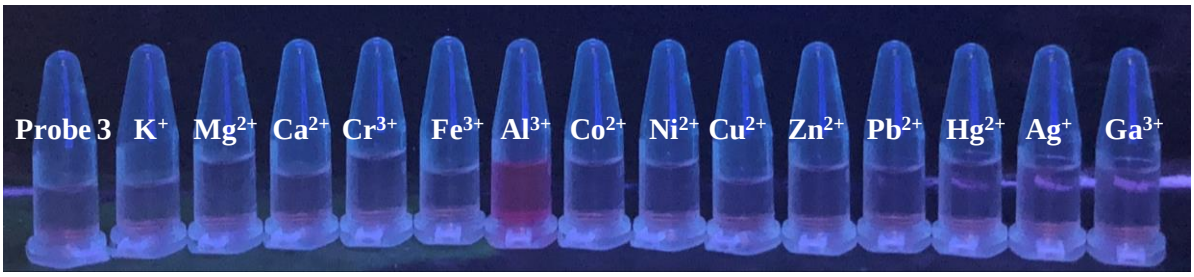

Figure 31: Visible fluorescence changes of probe**3** (20 μM, CH_3OH-H_2O (4:1, v/v) *pH* 7.04) in presence of different metal ions under UV lamp.

Probe **3** (20 μM, CH_3OH-H_2O (2:1, v/v) *pH* 7.04) did not show any characteristic emission band when excited at 480 nm. Furthermore, the fluorescence studies of probe **3** were pursued comprehensively with various metal ions. Interestingly, the fluorescence intensity was amplified at 587 nm only on incubating probe **3** with 1000 μM of Al^{3+}. No enhancement or change was observed in the emission spectrum of probe **3** in the presence same amount of rest of the metal ions like K^+, Mg^{2+}, Ca^{2+}, Cr^{3+}, Fe^{3+}, Co^{2+}, Ni^{2+}, Cu^{2+}, Zn^{2+}, Pb^{2+}, Hg^{2+}, Ag^+ and Ga^{3+}etc. (**Figure 32a**).

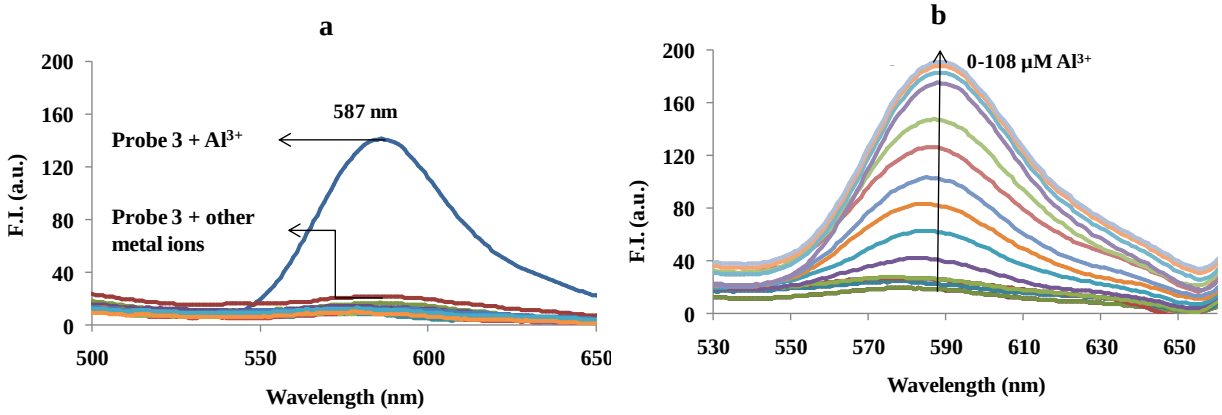

Figure **32**: a) Emission spectra of probe **3** (20 μM, CH_3OH-H_2O (2:1, v/v) *pH* 7.04) in presence of 50 equiv. of different metal ions; b) Spectral titration of probe **3** with different amounts of Al^{3+}**.**

Consequently, the quantitative sensing behavior of probe **3** towards Al^{3+} was explored by performing titration experiments of fixed concentration of probe **3** with varying concentration of Al^{3+}. With progressive addition of Al^{3+} to probe **3** the systematic enhancement of emission intensity at 587 nm was observed. The increase continued till the addition of 100 μM and it remained steady thereafter (**Figure 32b**). From the titration profile, a linear plot between [Al^{3+}] and the emission intensity at 587 nm with R^2 = 0.969, was used for calculating the lowest detection limit of probe **3** for Al^{3+} and was found out to be 0.2 μM (**Figure 33**). The binding constant was determined from the fluorescence titration as a function of [Al^{3+}], by implying Benesi-Hieldebrand equation and was calculated to be $7.07 \times 10^4\ M^{-1}$.

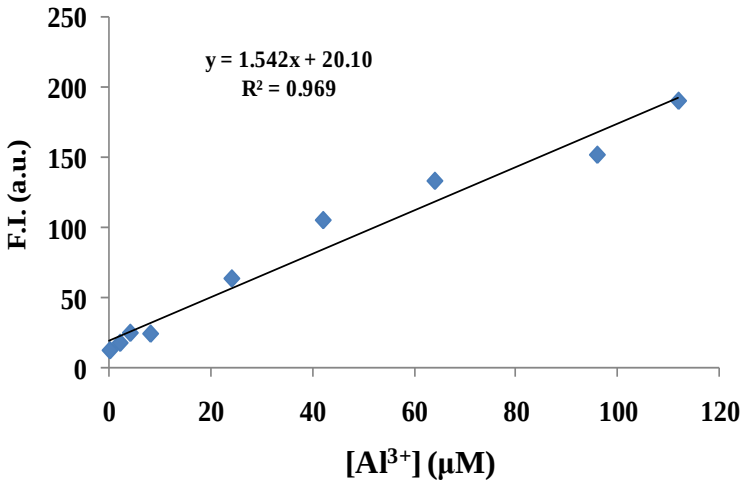

Figure 33: Determination of detection limit of Al^{3+} by probe **3** (20 μM, CH_3OH-H_2O (2:1, v/v) *pH* 7.04)

3.1.3.3. Selectivity profile of probe 3:

Furthermore, the selectivity of probe **3** for Al^{3+} in the presence of background metals was also investigated by adding same amount of other metal ions into probe **3.Al^{3+}** complex. It was observed that the absorption (**Figure 34a**) and fluorescence (**Figure 34b**) intensity of probe **3.Al^{3+}** complex was not affected even in the presence of other metal ions confirming that probe **3** was highly selective towards binding with Al^{3+} ions.

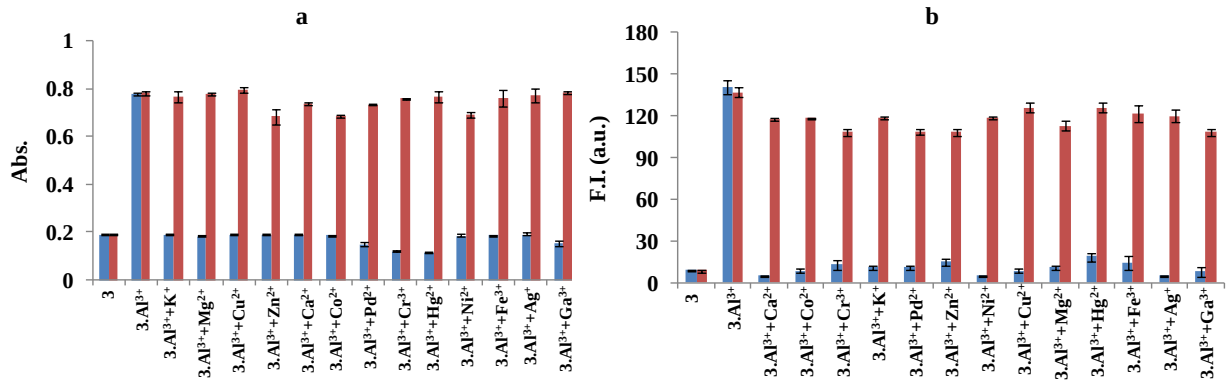

Figure 34: Interference studies of probe **3**. Where, the red bars depict the intensity of probe **3** in presence of 1000 μM of Al^{3+} and 1000 μM of other analytes and the blue bars represent the intensities of probe **3** in presence of different analytes a) absorption intensities b) emission intensities

3.1.3.4. Effect of varying *pH* on probe 3:

In order optimize the workability of probe **3** in wide *pH* range, the emission spectra of probe **3** in presence and absence of Al^{3+} has been explored. The emission intensity at 587 nm increases with decrease in the *pH*. This is attributed to the opening of the spirolactam ring of rhodamine. The emission intensity remains almost constant above *pH* 6 due to the existence of spirolactam ring closed form of rhodamine. The curve obtained by plotting emission intensity ratio versus changing *pH* did not show any change within a wide *pH* range of 6-12 which proved that the spirolactam-ring closed form of rhodamine in probe **3** was not affected by the changing *pH* within this range (**Figure 35a**) whereas, below *pH* 6 the emission intensity increased due to the spirolactam ring opening of rhodamine in probe **3** and the intensity amplifies with gradual addition of acid due to further protonation.

We also investigated the *pH* range in which the complex **3.Al^{3+}** was found out to be stable (**Figure 35b**). With the addition of base into the solution the emission intensity decreased and then remained almost constant within *pH* 7-11, suggesting the removal of metal ion from the complex which led to spirolactam ring-closure. Whereas, with the decrease in the *pH* of the solution of **3.Al^{3+}** the emission intensity increased due to further protonation of the complex. This suggested that with the decrease in the *pH* of probe **3** similar structural and optical changes

occurred as caused by the complexation of probe **3** with Al^{3+}. Hence, probe **3** could be used for detection of Al^{3+} in wide *pH* range of 7-12.

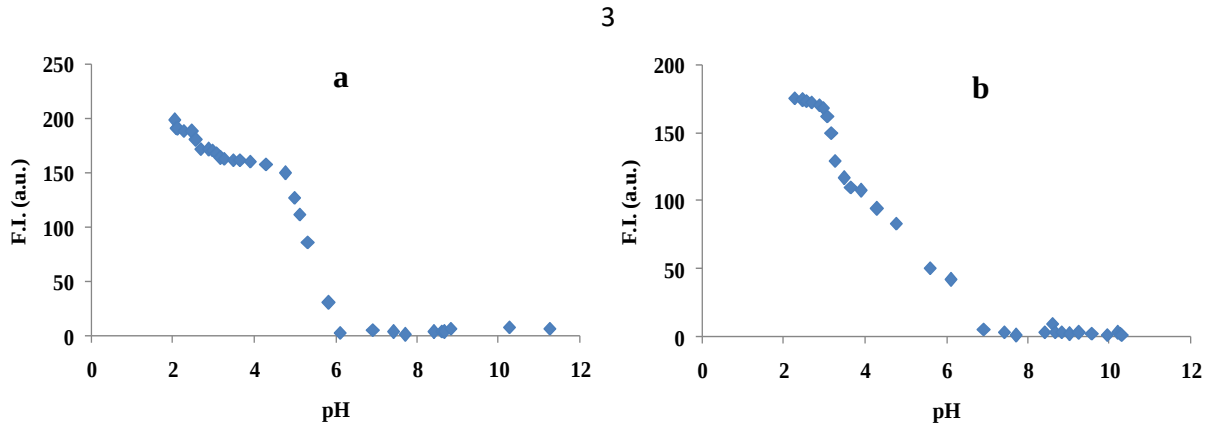

Figure 35: Effect of *pH* on emission spectra of a) probe **3** in absence of Al^{3+} ions; b) complex of probe **3** and Al^{3+} ions at 587 nm.

The change in the *pH* of probe **3** from 4.3 to 7.42 and 3.08 to 6.92 for complex **3.Al^{3+}** showed a sharp change in fluorescence intensity at 587 nm and this can be quantified and fitted well into the Hendersone-Hasselbalch-type mass equation:

$$pKa = pH - \log[(E_{max}-E)/(E-E_{min})]$$

Where, E is the experimentally observed emission intensity at a fixed wavelength (587 nm), E_{max} is 193.48 for probe **3** and 150.23 for complex **3.Al^{3+}** and E_{min} 1.04 for probe **3** and 3.78 for complex **3.Al^{3+}** respectively. On application of this equation, the pKa of probe **3** was calculated to be 5.4 and the pKa for complex **3.Al^{3+}** was calculated to be 1.9. The emission intensity $\log[(E_{max}-E)/(E-E_{min})]$ of probe **3**showed a linear response to the change in *pH* between 4.3 and 7.42 in coherence with the function, $Y = 0.823X-5.459$, $R^2 = 0.943$. Similarily, a linear response between *pH* change between 3.08 to 6.92 and emission intensity ($\log[(E_{max}-E)/(E-E_{min})]$) of complex **3.Al^{3+}** was in coherence with the function, $Y = 0.406X-1.9$, $R^2 = 0.977$. This function of probe **3** can be used to calculate the *pH* of any sample with *pH* ranging from 4.3 to 7.42 based on the emission intensity.

3.1.3.5. Binding mechanism

To deduce the binding mechanism for binding of Al^{3+} ion to probe **3**, ^{1}H-NMR titration was performed. Probe **3** showed characteristic triplet of $–CH_3$ (of *N*, *N*-diethyle part of xanthenes core) at 1.0 ppm represented by H_a and $–CH_2$ multiplet at 3.3 ppm represented by H_b (**Figure 36**). On adding 1 equiv. of Al^{3+} into 5 mM solution of probe **3** in CD_3CN/CD_3OD-d_4 (due to its limited solubility in D_2O/CD_3OD) new peaks were formed i.e. a triplet at 1.3 ppm (H_c) and multiplet at 3.6 ppm (H_d). Shifting in the signals of aromatic region from 6.0-9.0 ppm was also observed. The Effect of Al^{3+} on −OH and −NH peaks could not be monitored, as these peaks disappeared due to presence of D_2O. The electron deficiency on probe **3**, due to complexation with Al^{3+} causes the downfield shift of H_e (ortho to amide O atom of spiro-carbonyl C) protons. The other protons (H_f, H_g, H_h) on the benzene ring which is attached to spiro ring did not show much shifts. However, downfield shift was observed in the protons of xanthenes ring (H_i, H_j, H_k) due to Al^{3+} induced ring opening and formation of quaternary amine salt. The formation of these new peaks suggests the ring opening of rhodamine on addition of Al^{3+} which led to the splitting of the signals of both the *N*, *N*-diethyle parts attached to xanthenes core of rhodamine. Furthermore, new peak was formed at 7.3 ppm due to the splitting up of the doublet at 7.0 ppm and shifting in the signal at 7.0 ppm to 7.2 ppm was also observed this suggest the interaction of the Al^{3+} with the O of anthraquinone part (H_m and H_n). Hence, the titration study indicated that Al^{3+} was attached to the O of spiro-ring and N of ethylamine linker. According to the results the plausible mechanism and the structure of complex is depicted in **scheme 24**. The presence of D_2O led to the suppression of the signals of –OH, -NH therefore, mass of the **3.Al^{3+}** complex (20μM, CH_3OH-H_2O (2:1, v/v)) was also recorded with one peak at m/z = 691.44 corresponding to the mass of the probe **3+H$^+$** and the peak at m/z = 813.47 corresponding to **3.Al^{3+}.3(CH_3OH)** which is further compared to the theoretical isotopic pattern of the complex **3.Al^{3+}**.

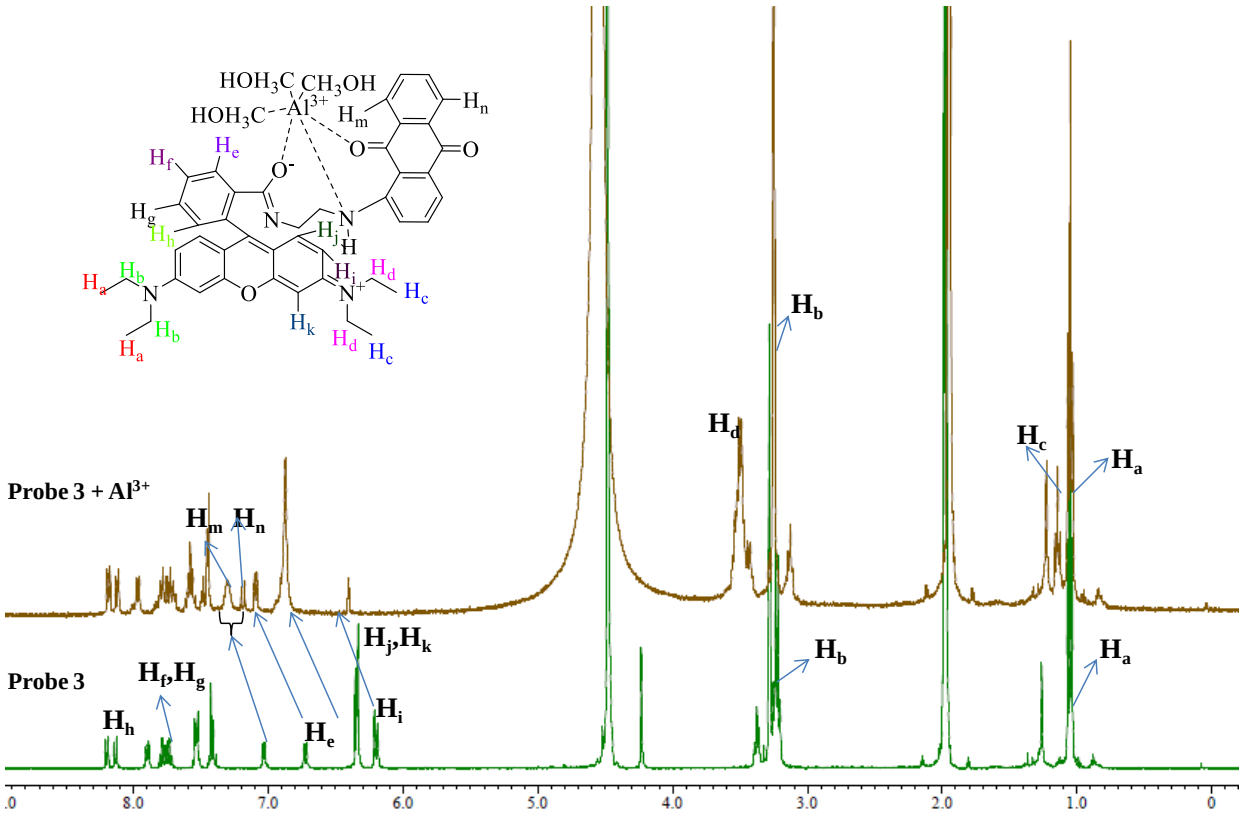

Figure 36: ^{1}H-NMR spectra on addition of 1 equiv. of Al^{3+} ions in probe **3.**

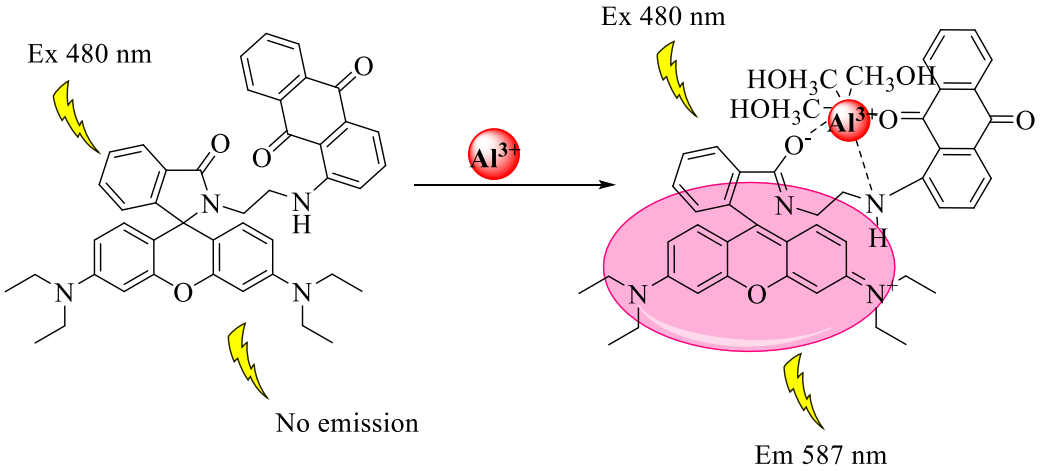

Scheme 24: Plausible mechanism for complexation of Al^{3+} with probe **3**.

3.1.3.6. Practical Application

To test the accuracy and practical applicability of determining Al^{3+} ion in water taken from drain of Thapar Institute and Engineering and Technology campus, certain amount of Al^{3+} was spiked

into the sample (5 ppm and 6 ppm) and were given for AAS (Atomic Absorption Spectroscopy). The amount we have added i.e. 5 ppm and 6 ppm and the amount found out from AAS analysis, were then compared and the results listed in **Table 2**. The RSD% (Relative Standard Deviation) and percentage recovery of 110.4 and 114.5 % were calculated by spiking with different concentrations of Al^{3+} with RSD values of 0.54 and 0.9%. The colorimetric changes as well as the fluorescence spectra of probe **3** in presence of different concentration of Al^{3+} samples (5 ppm and 6 ppm) was recorded (**Figure 37**). Therefore, probe **3** can be used as colorimetric probe for selective and sensitive detection of Al^{3+} ions in environmental samples.

S.No.	Added (ppm)	Found (ppm)	Recovery (%)	RSD (%)
1	5	5.52	110.4	0.54
2	6	6.87	114.5	0.9

Table 2: Probe **3** for analyzing Al^{3+} in real samples.

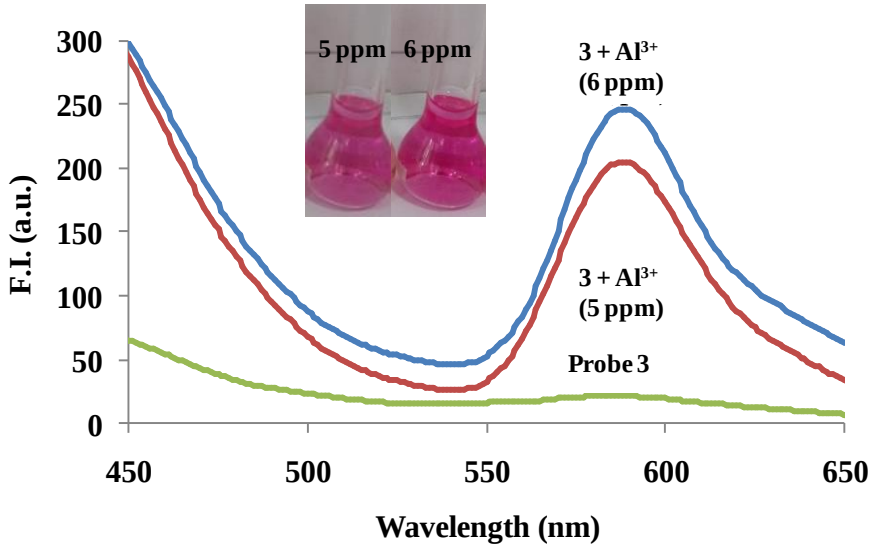

Figure 37: Fluorescence spectra of probe **3** in presence of different concentration of Al^{3+} sample. Inset: colorimetric changes in presence of different concentration of Al^{3+} in probe **3.**

3.1.3.7. Reversibility and Molecular logic function:

To check the reversibility of complex **3.Al^{3+}** it was treated with different anions viz., F^-, Cl^-, Br^-, I^-, SCN^-, CN^-, NO_3^-, HSO_4^-, $H_2PO_4^-$ and OAc^-. The absorption spectrum of complex **3.Al^{3+}** showed reversibility and reemergence of band at 512 nm accompanied with suppression of band at 560 nm, in the presence of CN^- ions and remained unaffected in presence of other anions

(**Figure 38a, 39a**). On the other hand, the fluorescence intensity at 587 nm, decreased on adding CN^- into complex **3.Al^{3+}** and no other anion showed significant change (**Figure 38b**).

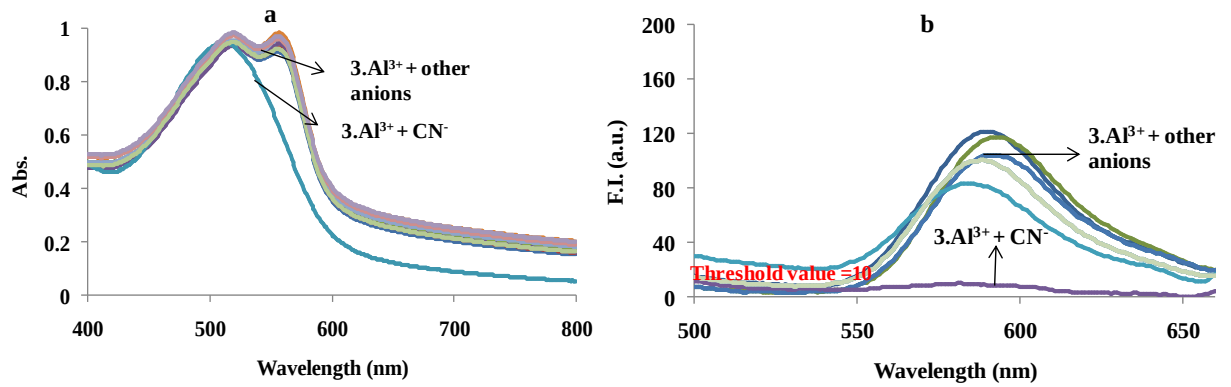

Figure 38: a) Absorption spectra of complex **3.Al^{3+}** (20 μM, CH_3OH-H_2O ((2:1, v/v) *pH* 7.04) in presence of different anions (F^-, Cl^-, Br^-, I^-, SCN^-, CN^-, NO_3^-, HSO_4^-, $H_2PO_4^-$ and OAc^-); b) Emission spectra of complex **3.Al^{3+}** (20 μM, CH_3OH-H_2O ((2:1, v/v) *pH* 7.04) in presence of different anions (F^-, Cl^-, Br^-, I^-, SCN^-, CN^-, NO_3^-, HSO_4^-, $H_2PO_4^-$ and OAc^-)

The molecular logic function was also devised via. UV-Vis and Fluorimetric '*on-off*' switch. Depending on the above UV-Vis and Fluorescence results, the two inputs In_1 and In_2 were considered to be Al^{3+} and CN^- respectively and the outputs were considered to be the UV-Vis spectroscopy data (as OUT_1) at 560 nm (i.e. if the band is formed at 560 nm then the output will be considered to be "1" and if no band is formed at 560 nm then the output is considered to be "0") and Fluorescence data at 587 nm (as OUT_2)by taking threshold value = 10 i.e. if the intensity of fluorescence band at 587 nm is more than 10 then the output is considered to be 1 and if it is below 10 then the output value will be considered as 0 (**Figure 39b**). The molecular logic circuits included combination of various gates like AND, OR, NOR and NOT and based on the spectroscopy data we built the truth table (**Figure 40**). OUT_1 was obtained by using the INHIBIT logic gate (combination of AND and NOT gate) where NOT gate was used at In_2 and then the AND gate was put to combine both the inputs i.e. In_1 and the output of NOT gate, OUT_2 was obtained by using NOT gate at In_1 and NOR gate to combine In_2 and the output of NOT gate. Both the outputs were combined to give single output by using OR gate (as both the outputs were same).

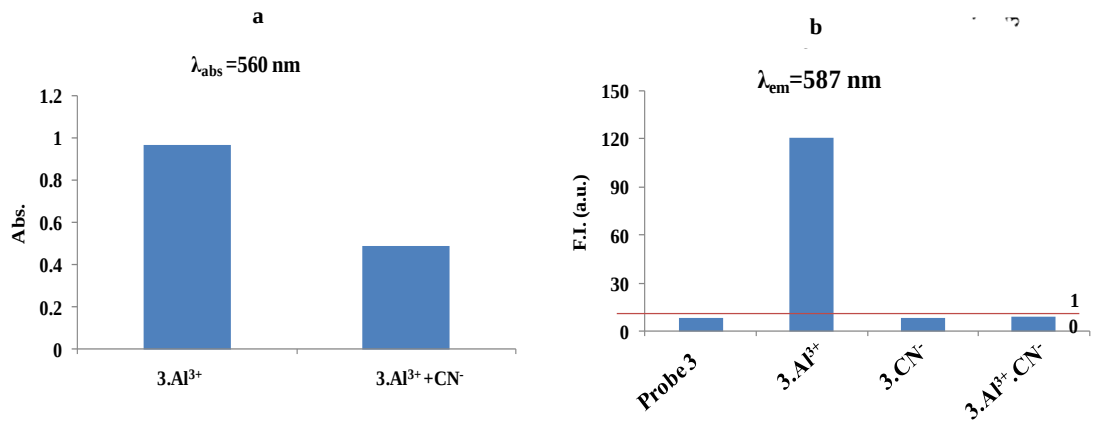

Figure 39: Bar graph representation of a) absorption profile at 560 nm in presence of different inputs; b) emission profile at 587 nm in presence of different inputs.

TRUTH TABLE:

INPUT		OUTPUT	
In_1 (Al^{3+})	**In_2 (CN^-)**	**OUT_1 (λ_{ab} = 560 nm)**	**OUT_2 (λ_{em}= 587 nm)**
0	0	0	0
1	0	1	1
0	1	0	0
1	1	0	0

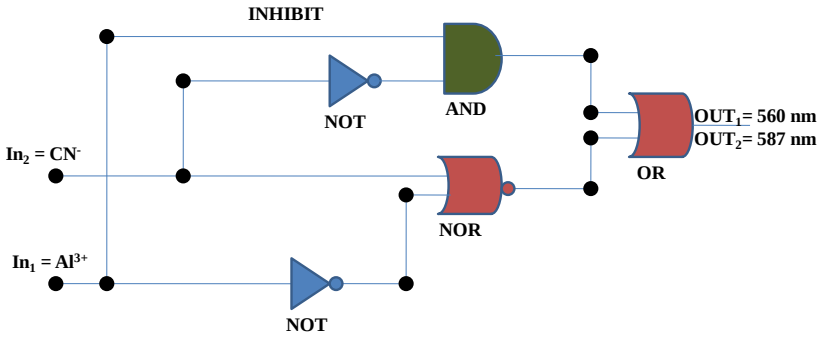

Figure 40: Truth table and Molecular logic circuit of probe**3**.

3.1.4. Conclusion:

Herein, we have designed and synthesized a rhodamine-anthraquinone based probe which was found to rapidly and selectively detect Al^{3+} without any interference of background metal ions.

Probe **3** displayed an '*off-on*' fluorescence signal as it was non-fluorescent initially but in the presence of Al^{3+} enhancement in the emission band at 587 nm was observed. The binding constant and lowest detection limit of probe **3** for Al^{3+} were calculated from the fluorescence titration profile and were found out to be 7.07×10^4 M and 0.2 μM respectively. The reversibility in the absorption and emission spectra of complex **3.A^{3+}** in presence of CN^- formed the basis of building the molecular logic circuits with a combination of AND, OR, NOT, NOR gates. Probe **3** was also found out to be capable of detecting Al^{3+} in samples of tap water.

3.1.5. Experimental Section:

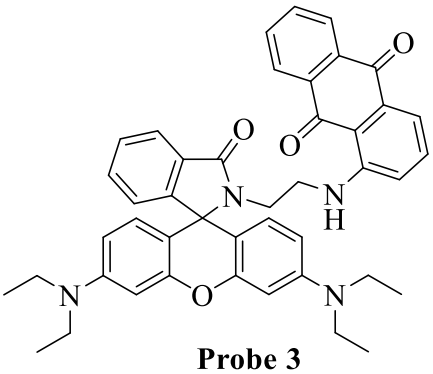

Probe 3

Synthesis: Buchwald-Hartwig cross coupling reaction was followed for synthesis of the probe **3.** In 10 ml of THF, N-(rhodamine-B) lactam-ethylenediamine (1.02 g, 2.11 mmol), 1-chloroanthraquinone (0.5 g, 2.11 mmol) and K_2CO_3(0.29 g, 2.10 mmol) were added along with catalytic amounts of bis-(triphenylphosphine) palladium (II) dichloride. The reaction mixture was refluxed for 24 hours at 110 °C.

The progress of reaction was checked on TLC plate. On completion of reaction the contents were filtered and the filtrate was extracted using water and ethyl acetate mixture. The organic layer was concentrated and was further purified through column chromatography to obtain red colored solid. M.pt = 220-235ºC, yield 80% (1.16 g); **^{1}H NMR** (400 MHz, $CDCl_3$): δ 9.66-9.62 (t, *J* = 12.16 Hz, 1H), 8.25-8.19 (m, 2H), 7.97-7.93 (m, 1H), 7.76-7.65 (m, 2H), 7.55-7.53 (d, *J* = 6.88 Hz, 1H),7.48-7.44 (m, 4H), 7.13-7.09 (t, *J* = 8.68 Hz, 1H), 7.0-6.96 (d, *J* = 8.24 Hz, 1H), 6.48-6.44 (d, *J* = 9.2 Hz, 2H), 6.41-6.37 (d, *J* = 2.72 Hz, 2H), 6.25-6.21 (m, 2H), 3.39-3.25 (m, 12H), 1.17-1.12 (t, *J* = 13.76 Hz,12H); **^{13}C NMR** (100 MHz, $CDCl_3$): δ 184.82, 183.89, 168.51, 153.40, 151.52, 148.88, 135.34, 133.96, 132.92, 128.93, 128.25, 126.81, 126.68, 123. 98, 122.86, 115.87, 108.16, 105.10, 97.70, 65.03, 44.41, 40.30, 39.05, 29.79, 12.69**MS (ESI):** m/z calcd. = 690.32, found = 691.11 (probe **3**+H^+)

3.2. Rhodamine-terephthaldehyde based Schiff base Al^{3+} sensor and potential of its ensemble for sensing of CN^- in 100% aqueous medium: Application in live cell imaging

3.2.1. Abstract

A novel Schiff base having terephthaldehyde appended with two rhodamine units has been synthesized, which exhibited fluorogenic and chromogenic response on binding with Al^{3+} ions in 100% aqueous system at *pH* 7.04. The binding of probe **4** with Al^{3+} ions was not hindered by the presence of background metal ions. The co-ordination mode of probe **4** was established by Job's plot method that has been found to be 1:1 stoichiometry with Al^{3+} ions. The probe **4**could detect Al^{3+} as low as 1.68 μM in a *pH* range of 6-10. NMR and mass spectrometry analysis revealed that the Al^{3+} induced hydrolysis occurs on one side of the Schiff base and led to the formation of free –CHO group. The hydrolysed ensemble (**4.Al^{3+}**) was used for detection of CN^- ions (H_2O-HEPES buffer at *pH* 7.04) accompanied by colorimetric and fluorimetric changes. Probe **4** was used to detect Al^{3+} ions in A549 cells through live cell imaging technique.

3.2.2. Synthesis of probe 4

The synthetic pathway followed for synthesis of the probe **4** has been shown in **Scheme 1**. The ethanolic solution of *N*-(rhodamine-B) lactam-ethylenediamine was slowly added to the ethanolic solution of terephthaldehyde. The reaction mixture was stirred at room temperature for 24 hours. On completion of reaction, the contents were filtered and white colored precipitates were obtained in 80% (2.3 g) yield and the M.pt =240-244^{o}C. The ^{1}H NMR (400 MHz, $CDCl_3$) displayed a singlet peak for 2H of –CH=N- (Schiff base) at δ 8.01 ppm, a multiplet for 2H at δ 7.90-7.88 ppm, another singlet for 4H of the terephthaldehyde phenyl ring at δ 7.56 ppm, multiplet for aromatic 4H at δ 7.44-7.39 ppm, multiplet for 2H at δ 7.09-7.05 ppm, multiplet for 8H at δ 6.43-6.36 ppm, multiplet for 4H at δ 6.24-6.21 ppm, a multiplet for 8H of the ethylenediamine part at δ 3.49-3.48 ppm, a multiplet for 16 H of the $–N(CH_2)_2-$ attached to the xanthenes ring of rhodamine at δ 3.33-3.28 ppm, a multiplet for 24H of $–CH_3$ of to the N,N diethyl part attached to the xanthenes ring at δ 1.17-1.13 ppm. The^{13}C NMR (100 MHz, $CDCl_3$) displayed peaks atδ: 168.3 (-C=O), 162.0 (-CH=N-), 153.8, 153.4, 148.5, 138.0, 132.4, 131.0, 128.9, 128.1, 127.9, 123.8, 122.8, 108.0, 105.4, 97.7, 65.0, 59.1, 44.3, 41.2, 12.5. MS(ESI): m/z calcd.

= 1066.58, found = 1067.24 (M^++1). According to the ^1H, ^{13}C and mass spectroscopy we gave the structure of probe **4** having two rhodamine derivatives attached to one terephthaldehyde unit.

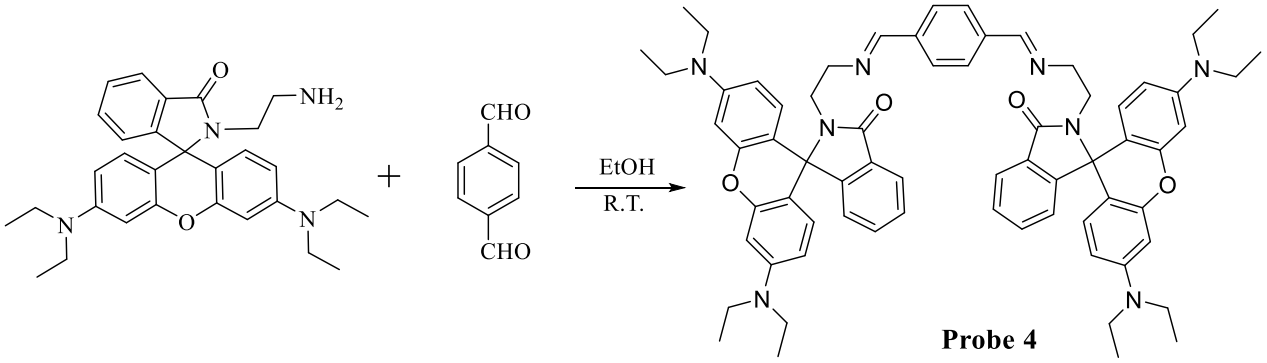

Scheme 25: Synthetic pathway for probe **4**

3.2.3. Results and Discussion:

3.2.3.1. Absorption response of probe 4 towards different metal ions

The sensing properties of probe **4** (20 μM, H_2O-HEPES buffer, *pH* 7.04) towards different metal ions, like K^+, Mg^{2+}, Ca^{2+}, Cr^{3+}, Fe^{3+}, Al^{3+}, Co^{2+}, Ni^{2+}, Cu^{2+}, Zn^{2+}, Cd^{2+}, Pb^{2+}, Hg^{2+}, $Cr^{3+}$and Pd^{2+} were checked through optical spectroscopic studies. The addition of Al^{3+} ions caused the visible color change to pink whereas; no visible color change was observed by other metal ions. These results showed the selectivity of probe **4** towards Al^{3+}(**Figure 41**).

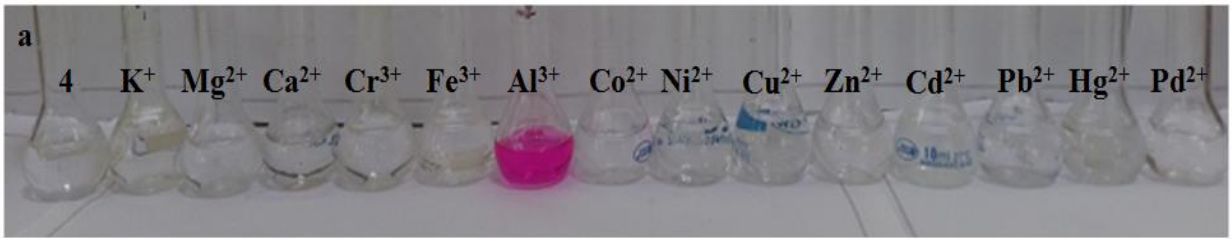

Figure 41: Visual color changes of probe **4** in presence of different metal ions.

The absorption spectra of probe **4** (20 μM, H_2O-HEPES buffer *pH* 7.04) gave two absorption peaks centered at 323 nm and 276 nm. In the presence of different metal ions like K^+, Mg^{2+}, Ca^{2+}, Cr^{3+}, Fe^{3+}, Co^{2+}, Ni^{2+}, Cu^{2+}, Zn^{2+}, Cd^{2+}, Pb^{2+}, Hg^{2+}, $Cr^{3+}$and $Pd^{2+}$to probe **4** (20 μM, H_2O-HEPES buffer *pH* 7.04) no significant change in the absorption spectra was observed. However, in the presence of Al^{3+} ions, a large red-shift (bathochromic shift) was observed and absorption maxima at 562 nm with a shoulder at 520 nm (**Figure 42a**) was formed due to spirolactam ring opening of rhodamine moiety on complexation with Al^{3+} ions.

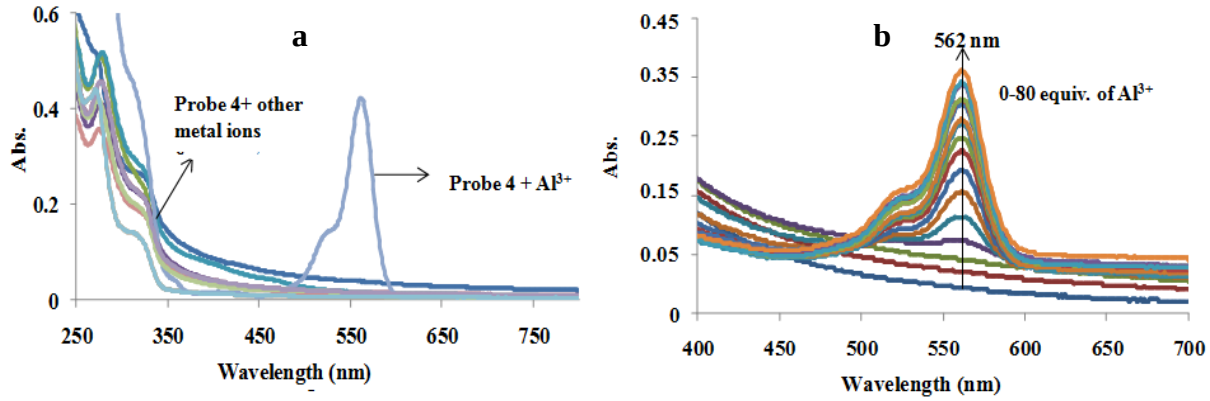

Figure 42: (a) Effect of different metal ions on absorption spectra of probe **4** (20 μM, H_2O-HEPES buffer, *pH* 7.04) (b) Effect of gradual addition of Al^{3+} ions into solution of probe **4** (20 μM, H_2O-HEPES buffer, *pH*7.04).

Upon gradual addition of Al^{3+} ions to probe **4** (20 μM, H_2O-HEPES buffer, *pH* 7.04) an increment in the absorption band centered at 562 nm was obtained which achieved its plateau with addition of 1600μM of Al^{3+} ions (**Figure 42b**). A dramatic increase of 2.56 fold in ratiometric absorption response was observed varying from 0.221 to 0.566 (**Figure 43a**). The job's plot (**Figure 43b**) analysis was carried out for determining the binding stoichiometry of probe **4** with Al^{3+} ions. The plot of $[Al^{3+}]/\{[Al^{3+}]+[\mathbf{4}]\}$ versus the changing molar fraction of Al^{3+} from 0.1 to 1, showed the inclination point at 0.50 which indicated 1:1 binding stoichiometry of Al^{3+} with probe **4**. The binding constant has been obtained by absorption titration as a function of $[Al^{3+}]$ and was calculated to be 3.98 ×

$10^3 M^{-1}$by using Benesi-Heildebrand equation suggesting the strong binding of probe **4** with Al^{3+} ions.

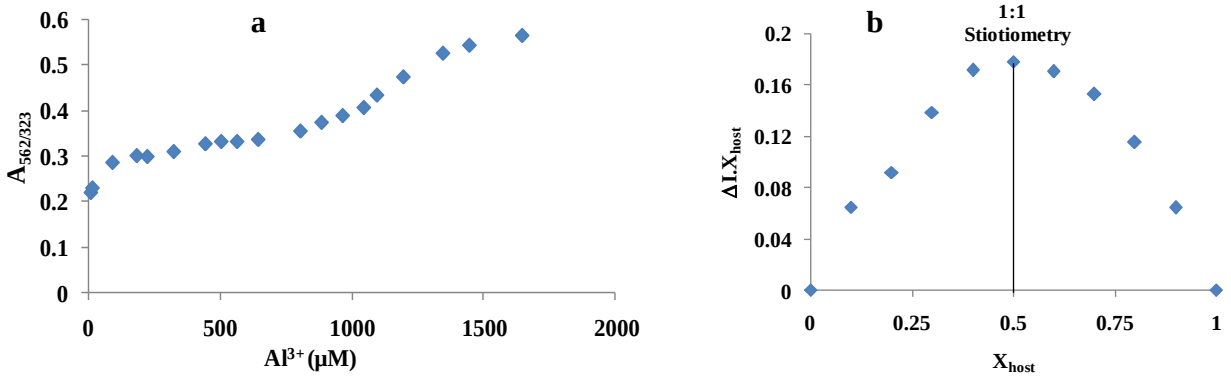

Figure 43: (a) Absorbance at 562 nm of probe **4** and Al^{3+} (20 μM, H_2O-HEPES buffer, pH7.04, indicating 1:1 stoichiometry (b) Ratiometric change at 562 nm and 323 nm (A_{562}/A_{334}) vs. concentration of Al^{3+} ions of probe **4**.

3.2.3.2. Emission response of probe 4 towards various metal ions

The emission response of probe **4** (20 μM, H_2O-HEPES buffer, *pH* 7.04) towards different metal ions like K^+, Mg^{2+}, Ca^{2+}, Cr^{3+}, Fe^{3+}, Al^{3+}, Co^{2+}, Ni^{2+}, Cu^{2+}, Zn^{2+}, Cd^{2+}, Pb^{2+}, Hg^{2+}, $Cr^{3+}$and Pd^{2+} was tested under UV light. No fluorescence was observed in solutions containing K^+, Mg^{2+}, Ca^{2+}, Cr^{3+}, Fe^{3+}, Co^{2+}, Ni^{2+}, Cu^{2+}, Zn^{2+}, Cd^{2+}, Pb^{2+}, Hg^{2+}, $Cr^{3+}$and Pd^{2+} ions but in presence of Al^{3+} ions, bright pink emission was observed (**Figure 44**).

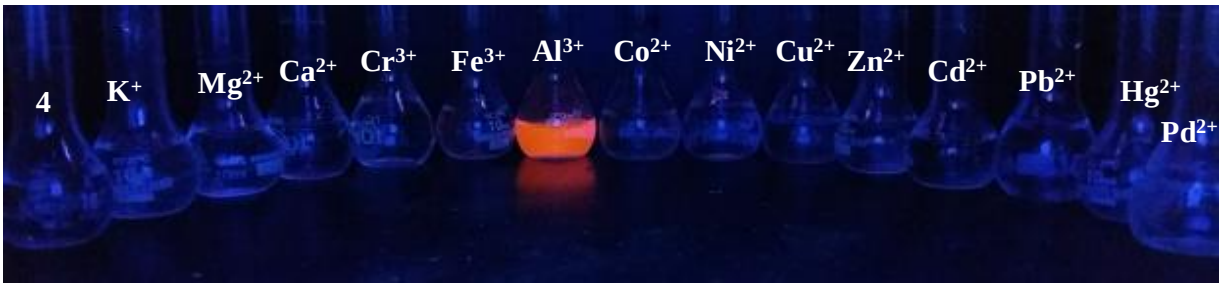

Figure 44: Effect of different metal ions on solution of probe **4** (20 μM, H_2O-HEPES buffer, *pH* 7.04) under UV light.

The probe **4** (20 μM, H_2O-HEPES buffer, *pH* 7.04) on excitation at 350 nm did not show any emission band (**Figure 45a**). On addition of different metal ions K^+, Mg^{2+}, Ca^{2+}, Cr^{3+}, Fe^{3+}, Co^{2+}, Ni^{2+}, Cu^{2+}, Zn^{2+}, Cd^{2+}, Pb^{2+}, Hg^{2+}, $Cr^{3+}$and Pd^{2+}, no change in emission spectra was observed but with the addition of 50 equiv. of Al^{3+} ions, new emission peak at 588 nm was formed. These spectral changes could be ascribed to the Al^{3+} ions induced spirolactam ring opening of rhodamine moiety of the probe **4** that led to the "turn-on" emission.

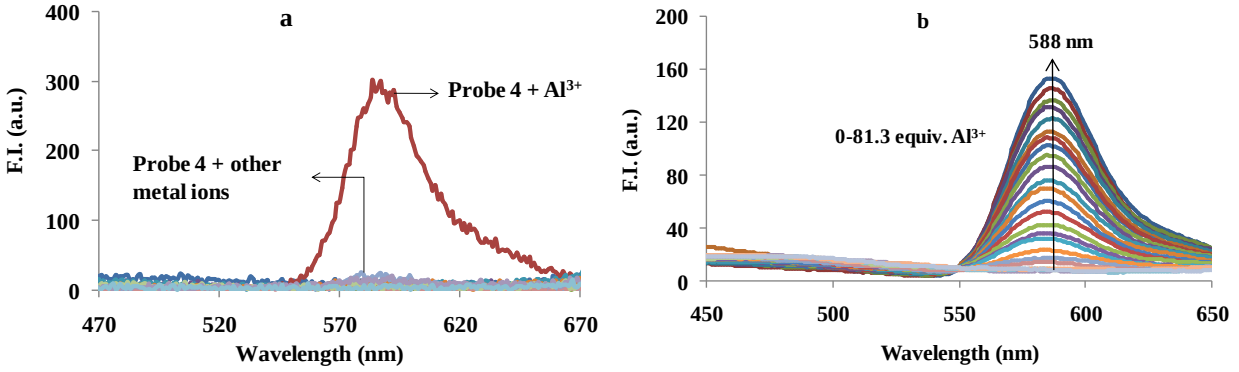

Figure 45: (a) Effect of different metal ions on the emission spectra of probe **4** (20 μM, H_2O-HEPES buffer, *pH* 7.04) (b) Effect of incremental addition of Al^{3+} ions on emission spectra of probe **4** (20 μM, H_2O-HEPES buffer, *pH*7.04)

To investigate the interaction and sensitivity of probe **4** (20 μM, H_2O-HEPES buffer, *pH* 7.04) towards Al^{3+}, the emission spectra were recorded with varying concentration of Al^{3+} (0-1626 μM) (**Figure 45b**). A new emission band centered at 588 nm appeared upon increasing concentration of Al^{3+} ions. The linear plot between the [Al^{3+}] (700-1400 μM) versus fluorescence intensity was used to calculate the detection limit. The detection limit of **4** towards Al^{3+} ions was found through fluorimetric titration profile and was determined to be 1.68 μM.

3.2.3.3. Effect of *pH* on probe 4 and probe 4.Al^{3+} complex.

The effect of change in *pH* on absorption spectra of probe **4** (**Figure 46a**) and its Al^{3+} complex (**Figure 46b**) was also investigated in aqueous medium to find out their stability at different *pH*. The probe **4** remained stable between the *pH* range 6-10. However, upon

decreasing the *pH* of solution of probe **4** from *pH* 6 to 3, the intensity of the absorption peak at 562 nm intensified. This suggested that at lower *pH* the spirolactam ring of rhodamine opened due to protonation.

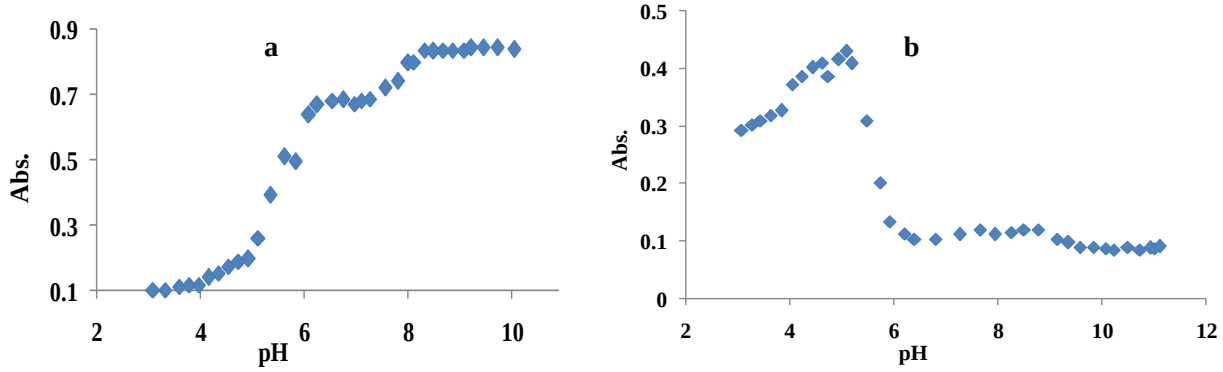

Figure 46: (a) Effect of *pH* on absorption spectra of (a) probe **4** in absence of Al^{3+} ions (at 323 nm) (b) complex of probe **4** and Al^{3+} ions.

Further, effect of *pH* change was also studied on probe **4.Al^{3+}** complex. The probe **4.Al^{3+}** complex did not show any significant absorption between *pH* range of 6-10. However, on decreasing the *pH* from 6 to 3, the decrease in absorption band at 562 nm was observed which suggested that in acidic conditions, the complex has been dissociated and converted into metal free ring open form. Thus, probe **4** can detect Al^{3+} ions in a wide *pH* range of 6-10.

3.2.3.4. Competitive Binding Studies

Experiments were conducted to check the selectivity of probe **4** to bind with Al^{3+} which suggested that no background metal interfered with binding of Al^{3+} ions. The absorption (**Figure 47a**) and emission response (**Figure 47b**) revealed that the probe **4** in presence of Al^{3+} showed no change in its pattern with 50 equiv. of various background metal ions like K^{+}, Mg^{2+}, Ca^{2+}, Cr^{3+}, Fe^{3+}, Co^{2+}, Ni^{2+}, Cu^{2+}, Zn^{2+}, Cd^{2+}, Pb^{2+}, Hg^{2+}, Cr^{3+} and Pd^{2+}. No perturbation in the intense fluorescence band at 588 nm was observed in the presence of other metal ions suggesting the selectivity of probe **4** towards Al^{3+} ions.

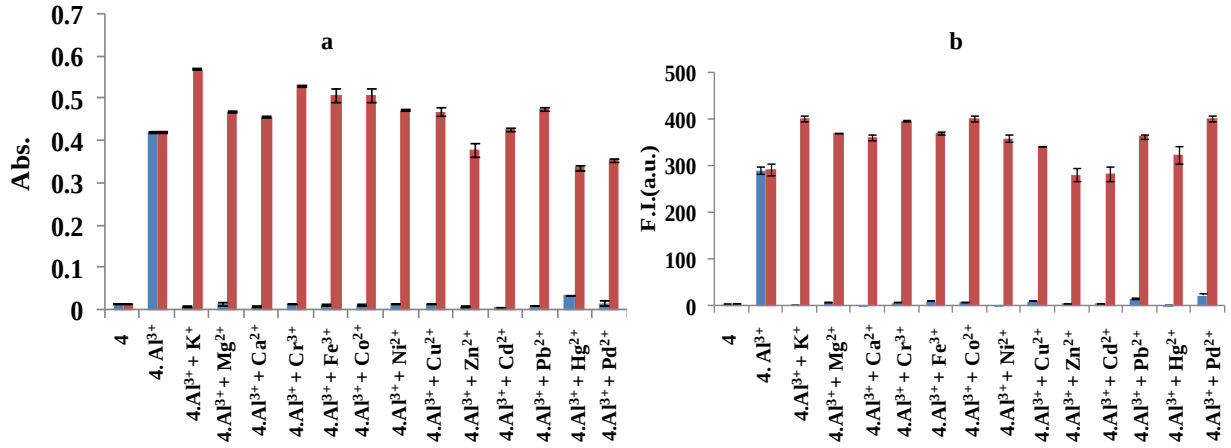

Figure 47: Selectivity profile of probe **4** (20 μM, H_2O-HEPES buffer, *pH* 7.04), towards Al^{3+} ions in presence of 50 equiv. of different metal ions. The blue bars represent the intensity of probe **4** (20 μM, H_2O-HEPES buffer, *pH* 7.04) in presence of 50 equiv. of different metal ions and red bars represent the intensity of probe **4** (20 μM, H_2O-HEPES buffer, *pH* 7.04) in presence of 50 equiv. of Al^{3+} and 50 equiv. of other metal ions a) absorption b) fluorescence.

3.2.3.5. Mechanistic Pathway of Al^{3+} binding to probe 4:

To elucidate the binding mechanism of Al^{3+} ions to probe **4**, ^{1}H-NMR and mass analysis were performed. Probe **4** displayed a characteristic singlet peak of imine =C-H (H_a) at 8.0 ppm corresponding to 2H in ^{1}H-NMR. On addition of 1 equiv. of Al^{3+} ions to the solution of probe **4** (5 mM in CD_3CN), a new singlet at 10.1 ppm (H_b) was observed along with the characteristic peak of imine =C-H (H_a) at 8.0 ppm, corresponding to 1H. Moreover, a slight shift in peaks of aromatic protons was also observed (**Figure 48**). To further support the data, mass spectrum of this mixture was recorded which showed M^++1 peak at 663.46 a.m.u. and 485.0a.m.u. corresponding to hydrolysed probe **4.Al^{3+}** ensemble and the most stable fragment of rhodamine B ethylenediamine**.** From ^{1}H-NMR and mass spectrometric analysis, it can be concluded that probe **4** underwent hydrolysis from one side resulting in the formation of free –CHO group on the other end. Moreover, slight shift in the peaks of the aromatic protons was also observed (**Scheme 26**).

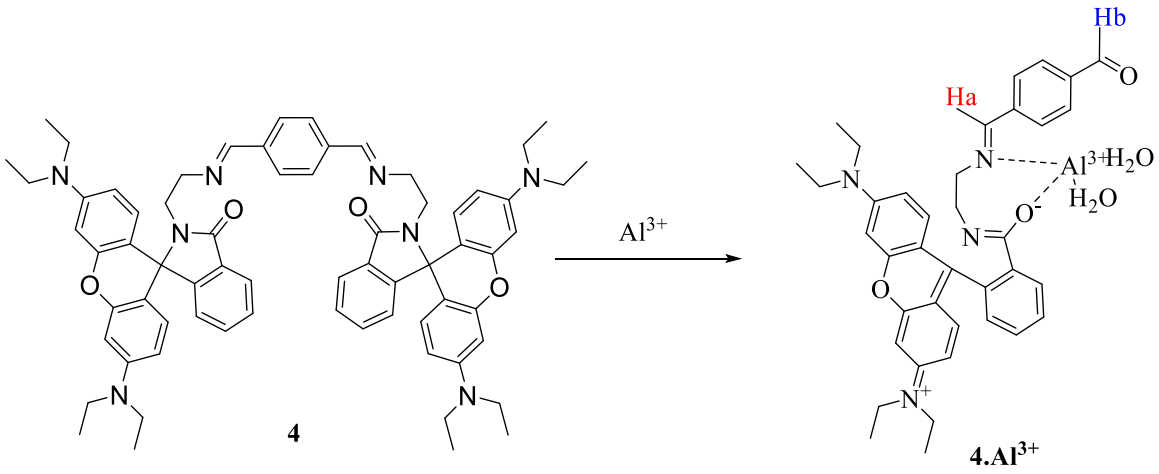

Scheme 26: Plausible mechanism for binding of Al^{3+} ions to probe **4**.

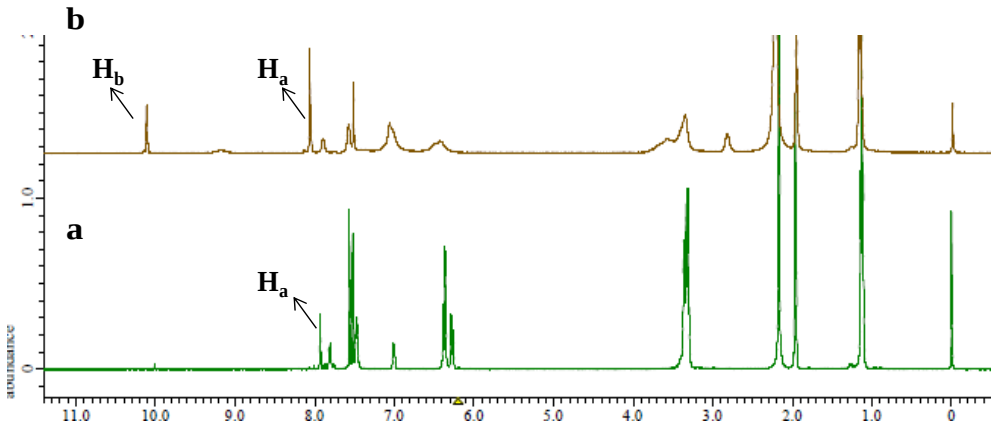

Figure 48: ^{1}H-NMR spectra of (a) probe **4** in CD_3CN where H_a represents the imine proton (b) probe **4.Al^{3+}** complex solution of CD_3CN where H_a represent the imine proton and H_b represents the aldehydic proton.

The free -CHO group formed due to Al^{3+} ions induced hydrolysis of probe **4** prompted us to evaluate the absorption and emission response of ensemble **(4.Al^{3+})** towards various anions. The free –CHO group in ensemble **(4.Al^{3+})** is prone to various nucleophilic additions. To further test the sensing of anions, ensemble **(4.Al^{3+})** (20μM, H_2O-HEPES buffer, *pH* 7.04) was prepared and its spectral changes as well as color changes in presence of different anions like F^-, Cl^-, Br^-, I^-, CN^-, SCN^-, $H_2PO_4^-$, HSO_4^-, NO_3^- and OAc^-, were recorded.

3.2.3.6. Absorption response of ensemble(4.Al^{3+}) towards anions

The ensemble (**4.Al^{3+}**) (20μM, H_2O-HEPES buffer, *pH* 7.04) showed an absorption maximum at 562 nm with a small shoulder peak at 520 nm. The absorption maximum at 562 nm represents Al^{3+} induced spirolactam ring opening of rhodamine B. Upon incubation of ensemble (**4.Al^{3+}**) with different anions like F^-, Cl^-, Br^-, I^-, SCN^-, $H_2PO_4^-$, HSO_4^- , NO_3^- and OAc^-, no change in the absorption band of the ensemble (**4.Al^{3+}**) was observed. However, in presence of 50 equiv. of CN^-ions the color of solution changed from pink to colorless and the absorption band at 562 nm quenched and new bands at 310 nm and 269 nm were formed (**Figure 49a**).

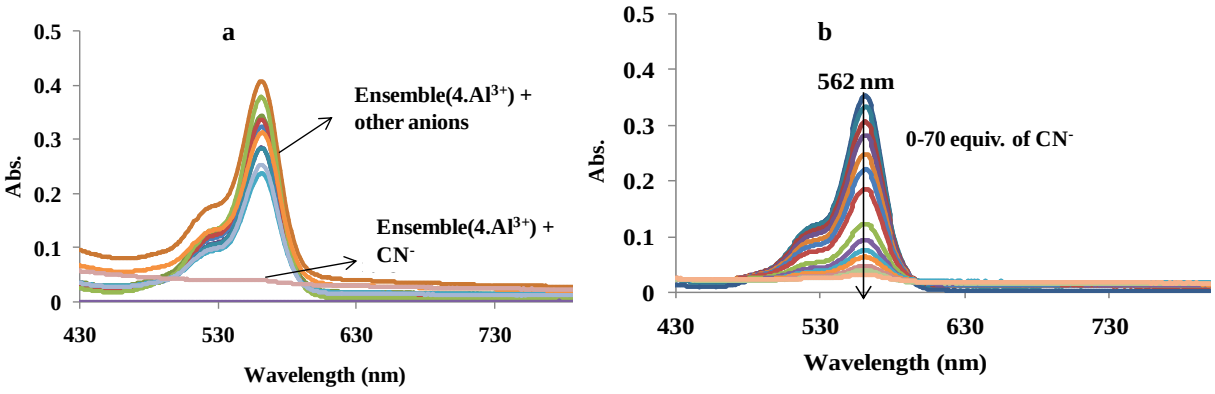

Figure 49: (a) Effect on absorption spectra of the ensemble (**4**.**Al^{3+}**) (20 μM, H_2O-HEPES buffer, *pH* 7.04) in presence of different anions (F^-, Cl^-, Br^-, I^-, SCN^-, $H_2PO_4^-$, HSO_4^- , NO_3^-, OAc^-, CN^-) (b) Effect of incremental addition on of CN^- ions on ensemble (**4**.**Al^{3+}**) (20 μM, H_2O-HEPES buffer, *pH* 7.04).

Upon incremental addition of CN^- ions from 0-1400μM in the solution of ensemble (**4.Al^{3+}**) (20μM, H_2O-HEPES buffer, *pH* 7.04), the absorption band centered at 562 nm gets quenched (**Figure 49b**) and new bands at 310 nm and 269 nm were formed. The quenching of band at 562 nm suggested the closure of spirolactam ring of rhodamine B which is further supported by the color change from pink to colorless. A dramatic change was observed and showed 11.35 folds (varying from 0.352 to 0.031) ratiometric response which clearly predict that ensemble (**4.Al^{3+}**) could be used to detect CN^- without interference of other analytes (**Figure 50a**).

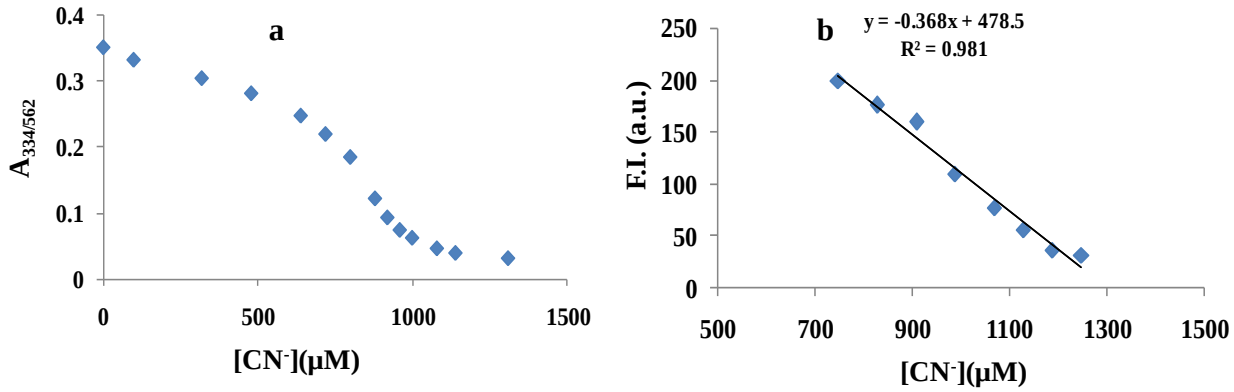

Figure 50: (a) Ratiometric change at 562 nm and 310 nm (A_{310}/A_{562}) vs. concentration of CN^- ions on ensemble (**4.Al^{3+}**) through UV-Vis spectrophotometric titration (b) Determination of detection limit of CN^- by ensemble (**4.Al^{3+}**) (20 μM,H_2O-HEPES buffer, *pH* 7.04) (λ_{ex}= 350nm, λ_{em}= 588 nm through fluorimetric titration.

3.2.3.7. Effect of various anions on emission of ensemble (4.Al^{3+})

The emission band of ensemble (**4.Al^{3+}**) (20μM, H_2O-HEPES buffer, *pH* 7.04) on excitation at 350 nm showed an emission band at 588 nm. In presence of different anions like F^-, Cl^-, Br^-, I^-, SCN^-, $H_2PO_4^-$, HSO_4^- , NO_3^- and OAc^-, no change in the emission was observed whereas, with the addition of CN^- ions the emission band at 588 nm was quenched (**Figure 51a**) and the pink emission of the solution discharged.

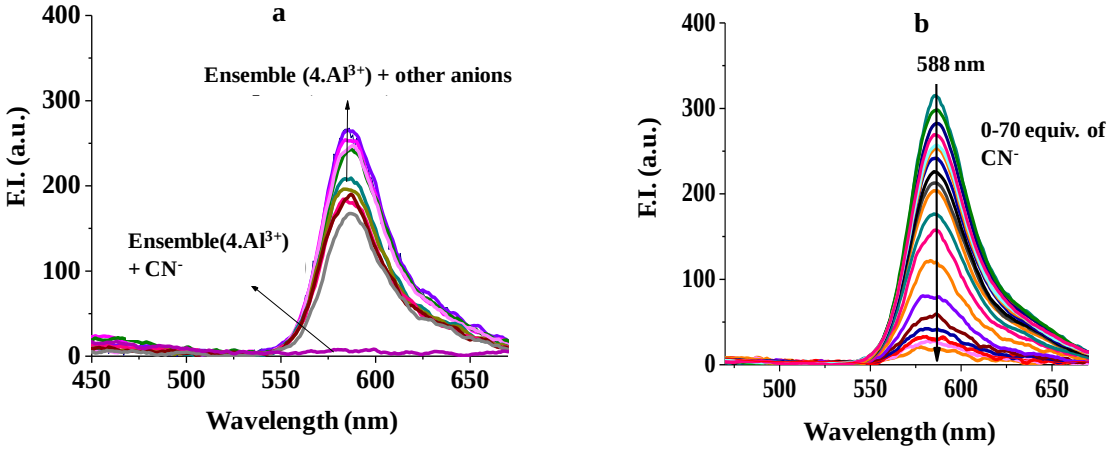

Figure 51: (a) Effect of different anions (F^-, Cl^-, Br^-, I^-, SCN^-, $H_2PO_4^-$, HSO_4^- , NO_3^-, OAc^-, CN^-) on emission spectra of ensemble (**4.Al^{3+}**) (20 μM, H_2O-HEPES buffer, *pH* 7.04), (b) Effect of incremental addition of CN^- ions on emission spectra of ensemble (**4.Al^{3+}**) (20 μM, H_2O-HEPES buffer, *pH*7.04).

On incremental addition of CN^-ions from 0-1400 μM to the solution of probe ensemble (**4.Al^{3+}**) (20μM, H_2O-HEPES buffer, *pH* 7.04), the emission band at 588 nm was quenched (**Figure 51b**). The linear plot of fluorescence intensity versus concentration has been used to calculate the lowest detection limit for sensing of CN^- ions and was found out to be 0.815 μM (**Figure 50b**).

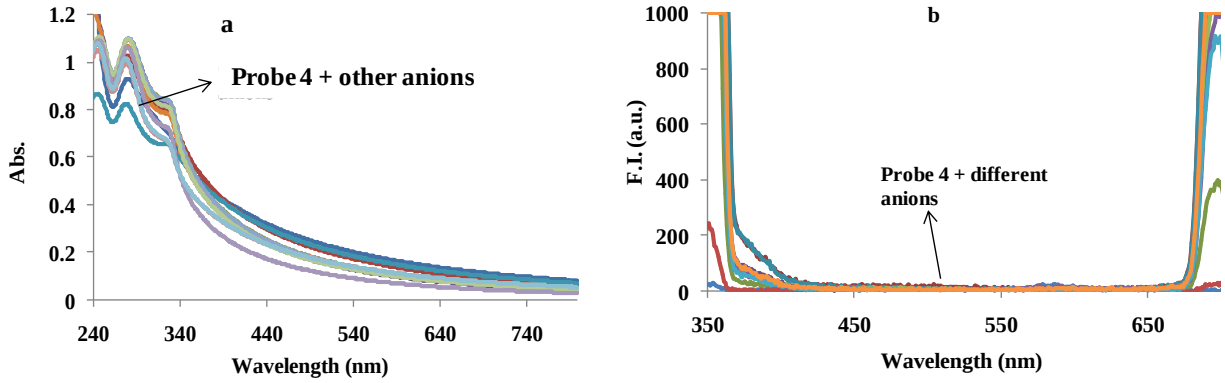

Figure 52: (a) Effect of different anions on probe **4** (20 μM, H_2O-HEPES buffer at *pH* 7.04) (b) Effect of different anions on emission spectra of probe **4** (20 μM, H_2O-HEPES buffer at *pH* 7.04)

The interaction study of probe **4** (20μM, H_2O-HEPES buffer, *pH* 7.04) with different anions was also observed through absorption (**Figure 52a**) and emission (**Figure 52b**) techniques. No change in the spectra was observed when50 equiv. of anions like F^-, Cl^-, Br^-, I^-, SCN^-, CN^-, $H_2PO_4^-$, HSO_4^- , NO_3^-, OAc^- were added. Hence, it made clear that the changes attained in the absorption and emission spectra of ensemble (**4.Al^{3+}**) in presence of CN^- ions was due to the chemodosimetric attack of CN^- on –C=O and not due to any other interaction with probe **4**.

3.2.3.8. Selectivity profile ofensemble (4.Al^{3+})

To study the selectivity of ensemble (**4.Al^{3+}**) (20μM, H_2O-HEPES buffer, *pH* 7.04) towards CN^- ions, competitive binding assay was studied in presence of CN^- ions mixed with other anions like F^-, Cl^-, Br^-, I^-, SCN^-, $H_2PO_4^-$, HSO_4^-, NO_3^- and OAc^- in UV-Vis (**Figure 53a**) and fluorescence (**Figure 53b**). The absorption and emission intensities were not affected by the presence of any background anions into the complex of **4.Al^{3+}.CN$^-$**.

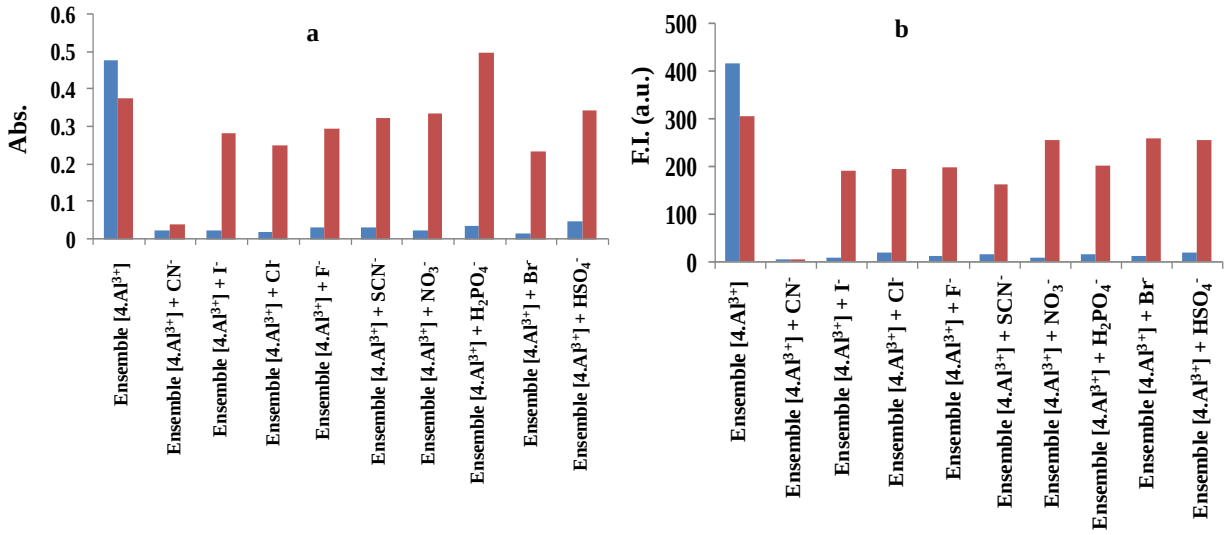

Figure 53: Selectivity profile of ensemble (**4.Al^{3+}**) (20μM, H_2O-HEPES buffer, *pH* 7.04) for CN^- ions in presence of 50 equiv. of different anions. The red bars represent the intensities of ensemble (**4.Al^{3+}**) (20μM, H_2O-HEPES buffer, *pH* 7.04) in presence of different anions and blue bars represent the intensities of ensemble (**4.Al^{3+}**) (20μM, H_2O-HEPES buffer, *pH* 7.04)in presence of 50 equiv. of CN^- and 50 equiv. of other anions a) absorption b) fluorescence.

3.2.3.9. Mechanistic pathway

In order to find out the mechanism for binding of CN^- ions to ensemble (**4.Al^{3+}**), ^{1}H-NMR and mass spectrometric analysis were carried out. In the presence of 1 equiv. of CN^- ions, the characteristic aldehydic peak at δ 10.1 ppm (H_b) was suppressed and new singlet at δ 4.6 ppm (H_c) (**Figure 54**) emerged. The new peak at δ4.6 ppm represents the cyanohydrins formation, suggesting thechemodosimetric attack of CN^- ions on –CHO group of the ensemble (**4.Al^{3+}**).These results were further supported by mass analysis. The M^++1 peak at 628.34 a.m.u. corresponds to the **4.Al^{3+}+CN$^-$** adduct **(Scheme 27).** Due to the chemodosimetric attack of CN^- on the free –CHO the intramolecular charge transfer occurred which is accompanied by the removal of Al^{3+}. The Al^{3+} induced spirolactam ring opening of rhodamine was reversed due to the charge transfer and spirolactam ring regains its original structure.

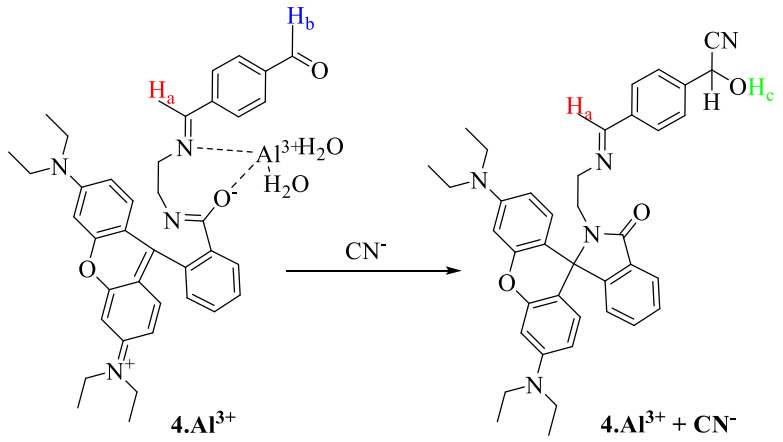

Scheme 27: Plausible mechanism for the binding of CN^- to **4.Al^{3+}**.

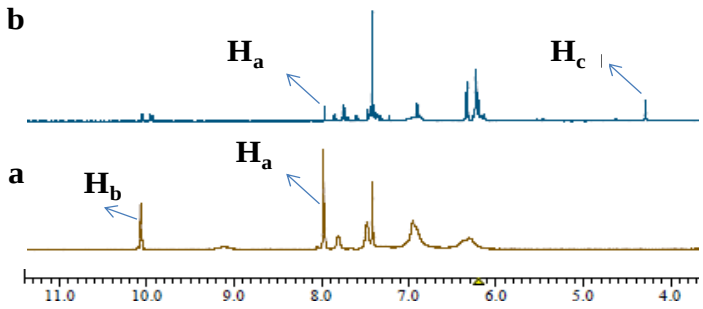

Figure 54: (a) NMR spectra of probe **4**(5×10^{-3}M, CD_3CN) on addition of 1 equiv. of Al^{3+} (10^{-1} M, CD_3CN) (b) NMR spectra of chemosensing ensemble (**4.Al^{3+}**) on addition of 1 equiv. of CN^- (10^{-1} M, CD_3CN).

3.2.3.10. Cancer Cell Viability

Trivalent metal like Al^{3+} is well known for promoting cancer incidents to various organs like lung, stomach, bladder etc, among various factory workers who get exposed to an aerosol containing Al^{3+} ions. We have selected lung cancer cells (A549) for carrying out our studies that has caused highest number of cancer-related deaths.

The results of MTT depends on the mitochondrial activity of cells which are directly proportional to the viability or cell division rate of the cells. Cell viability assay results showed that upon exposure to Al^{3+} in the viability/division, the rate of cells has increased. With 1 μM of Al^{3+}, around 3.7 ± 4.2% increase in cell viability was observed. Here, as in

case of exposure to high Al^{3+}, 26.3 ± 4.7 % an increase in cell growth was observed within 24 h of exposure. *In vitro* data also showed a significant reduction (63.1 ± 4.8 %) of cell viability due to exposure of 10 μM of probe **4**, although no significant reduction of cell viability was observed after exposure of 1 μM probe **4** for 24 h.

A significant loss of cell viability was observed when probe **4** was treated with Al^{3+}ions. Cells exposed to 1 μM of Al^{3+} showed 12.5 ± 2.6 % reduction of cell viability due to treatment with 1 μM of probe **4** which drastically increased 74.2 ± 1.3% in the presence of 10 μM compound (**Figure 55**). The effect drastically increased in the presence of 20 μM of Al^{3+}. 20 μM of Al^{3+} treated lung cancer cells (A549) showed a decrease of 31.6 ± 0.5% cell viability in exposure to 1 μM probe **4**. The number had increased to 84.1 ± 1% in presence of 10 μM probe **4** (**Figure 55**). The results suggested the potential therapeutic use of probe **4** in lung cancer especially when patient get a chronic exposure and bioaccumulation of Al^{3+} in lung tissue.

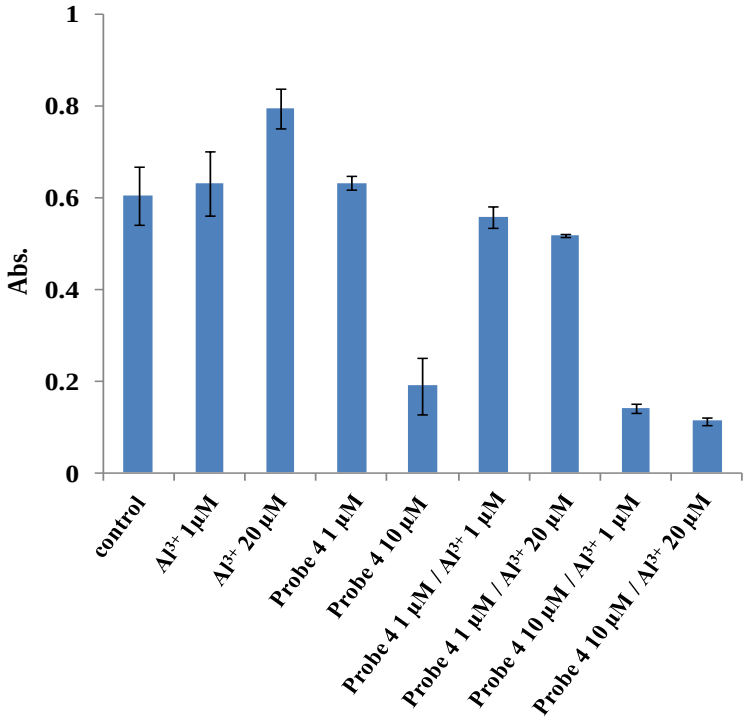

Figure 55: Lung cancer cells viability in presence of probe **4**. Lung cancer cells (A549) exposed to probe **4** (1μM and 20 μM) in absence or presence of Al^{3+} (1μM and 20 μM) for 24 h.

3.2.3.11. *In vitro* determination of detection limits of Al^{3+} sensitivity of the probe 4:

Probe **4** is highly selective for Al^{3+} binding and in presence of Al^{3+}, it shows high fluorescence intensity. Therefore, probe **4** could be used to detect and generate a 3-D map of cancer, especially, where bioaccumulation of Al^{3+} took place. Further, the detection limit in a cell-free system and inside the cells may vary for the contribution of other physiological factors. Therefore, determination of the detection limit inside the cells is essential to explore for further possibility of use of probe **4** as a pre-surgical 3-D cancer map development tool. A gradient of probe **4** concentration was used for 1 h against 20 μM Al^{3+} pre-treated lung cancer cells. **Figure 56** clearly indicates a huge increase of red fluorescence in presence of Al^{3+} in compare with control. The results suggested that probe **4** can differentiate the fluorescence between 20 μM Al^{3+} treated cells even at 0.01 μM concentration. Although the difference between treated and untreated cells are not very prominent. The best difference of fluorescence had been observed at 1 μM and 0.1 μM concentrations where the Al^{3+} treated cells have bright fluorescence but control cells have negligible fluorescence.

Thereafter, 1 μM of probe **4** was used *in vitro* for the determination of limit of Al^{3+} sensitivity. A549 cells were treated with various concentrations of Al^{3+} (2, 0.5, 0.1, 0.01, 0.001 and 0) for 6 h. Thereafter cells were treated with 1 μM of probe **4** and processed for imaging under a fluorescence inverted microscope. The results clearly indicate that probe **4** can detect Al^{3+} in A549 cells up to 0.01 μM (*i.e.* 10 nM). Although better efficiency has been observed in presence of 0.1 μM or more (**Figure 57)**.

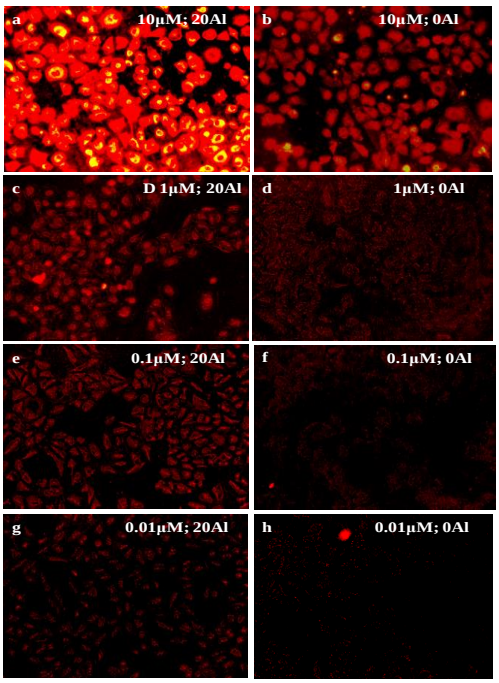

Figure 56: Determination of Al^{3+} sensitivity on A549 cells (*in vitro*) by images captured (a) in presence of 10 μM probe **4** and 20μM Al^{3+} ions; (b) 10 μM probe **4,** in absence of Al^{3+} ions; (c) in presence of 1 μM probe **4** and 20 μM Al^{3+} ions; (d) 1 μM probe **4** in absence of Al^{3+} ions; (e) in presence of 0.1 μM probe **4** and 20μM Al^{3+} ions; (f) 0.1 μM probe **4** in absence of Al^{3+} ions; (g) in presence of 0.01 μM probe **4** and 20μM Al^{3+} ions; (h) 0.01 μM probe **4** in absence of Al^{3+} ions.

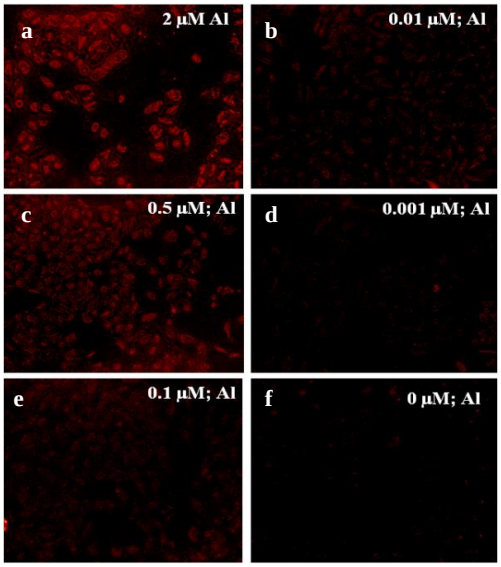

Figure 57: Determination of Al^{3+} sensitivity *in vitro* using concentration gradient of Al^{3+}: Lung cancer cells (A549). Images captured by keeping fixed concentration of probe **4** as 1 μM and concentration of Al^{3+} is (a) 2 μM; (b) 0.01μM; (c) 0.5μM; (d) 0.001μM; (e) 0.1μM; (f) 0μM.

3.2.4. Conclusions

We have designed and synthesised a new rhodamine based dual signal based (chromogenic and fluorogenic change) chemosensor for Al^{3+} ions in HEPES buffer at *pH* 7.04. The binding constant was calculated to be 3.98 × $10^3M^{-1}$and 1:1 binding stoichiometry of the complex of metal and probe **4**was established by UV-Vis spectroscopy. This chemosensor can detect Al^{3+} as low as 1.68 μM in a wide *pH* range of 6-10. The ensemble of probe **4** with Al^{3+}showed high selectivity and sensitivity towards CN^- ions with lowest detection limit of 0.815 μM in HEPES buffer at *pH*7.04 accompanied by colorimetric and fluorimetric changes. Further, the compound has huge potential for use as anticancer therapeutics. In addition to that, upon formation of complex with Al^{3+}; probe **4** showed large increase in fluorescence which gives it the excellent potential to be used as pre-surgical 3-D map detection tool.

3.2.5. Experimental section

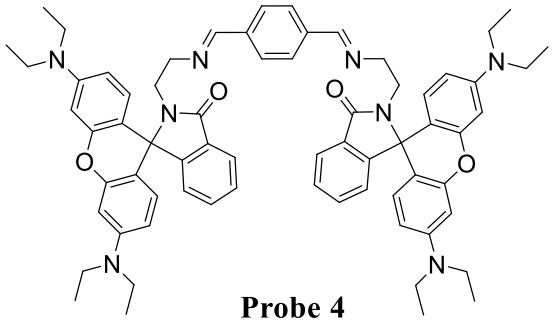

Probe 4

Synthesis: The ethanolic solution of *N*-(rhodamine-B) lactam-ethylenediamine (1.9 g, 4.1 mmol) was slowly added to the solution of terephthaldehyde (0.276 g, 2.22mmol) in 15 ml ethanol. The reaction mixture was stirred at room temperature for 24 hours. The progress of reaction was checked on TLC plate. On completion of reaction, the contents were filtered and white colored precipitates were obtained.M.pt=240-244ºC, yield = (2.3 g) 80%,**^{1}H NMR** (400 MHz, $CDCl_3$): δ8.01 (s, 2H),7.90-7.88 (m, 2H), 7.56 (s, 4H), 7.44-7.39(m, 4H), 7.09-7.05 (m, 2H), 6.43-6.36 (m, 8H), 6.24-6.21 (m, 4H), 3.49-3.48 (m, 8H), 3.33-3.28 (m, 16H), 1.17-1.13 (m, 24H); **^{13}C NMR** (100 MHz, $CDCl_3$): δ 168.3, 162.0, 153.8, 153.4, 148.5,138.0, 132.4, 131.0, 128.9, 128.1, 127.9, 123.8, 122.8, 108.0, 105.4, 97.7, 65.0, 59.1, 44.3,41.2, 12.5; **MS(ESI):** m/z calcd. = 1066.58, found = 1067.24 (M^++1)

Chapter 3: Conclusion

Herein, we have discussed the synthesis, characterization and sensing behavior of two rhodamine based colorimetric and fluorescence "*off-on*" probes. The selectivity of probe **3** was achieved in mixed-aqueous medium and hence was used for detection of Al^{3+} in real samples. Whereas; the ability of probe **4** to sense Al^{3+} ions in 100% aqueous medium and its stability at physiological *pH* made it capable of intracellular sensing of Al^{3+} ions.

Probe	**Sensing of ion**	**Medium**	**Association constant**	**Detection limit**
Probe **3**	Al^{3+}	CH_3OH-H_2O (2:1, v/v)	$7.07 \times 10^4\ M^{-1}$	0.2 μM
Probe **4**	Al^{3+}	100% aqueous medium	$3.98 \times 10^3\ M^{-1}$	1.68 μM

CHAPTER 4

Synthesis of rhodamine based hybrid molecules and the quantification of optical signals for construction of logic gates

General Introduction: Rhodamine B and its mono derivatives have been widely used for designing chemosensors for heavy and transition metal ions but, the di- and tripodal systems have been scarcely investigated. There are reports on aggregation based sensing mechanism of mono rhodamine derivatives but a single probe having multiple binding sites and multi-fluorophores have been reported only by a few scientists[72,97,98]. The dipodal and tripodal systems have numerous binding sites due to which they have the capability of forming strong complexes with metal ions. Hence, we designed probes **5** and **6** keeping in mind a few considerations; 1) rhodamine has suitable binding groups which bind with specific ions 2) presence of more than one rhodamine unit will provide number of chelating sites and the sensor will have high binding affinity towards metal ion 3) the formation of a cavity will ensure selective binding as it will strongly bind to metal ions having smaller ionic radii 4) the rhodamine`s spirolactam ring opening and closing process can generate '*on-off*' colorimetric and fluorimetric switch which can form the basis of constructing molecular logic operations 5) presence of cyanuric chloride can give the probe some therapeutic benefits.

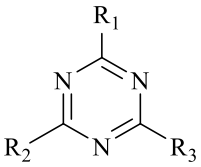

Probe **5**: R_1= Cl and R_2, R_3= rhodamine B ethylenediamine

Probe **6:** R_1, R_2, R_3= rhodamine B ethylenediamine

Hence, considering all the facts we designed two probes having cyanuric chloride as basic unit where rhodamine b ethylenediamine as the appended groups with the variable number. On these basis, we have divided this chapter into two sub sections:

4.1. Rhodamine-triazine based dipodal system for sensing of Al^{3+} and its application for construction of a read-write-erase molecular memory device

4.2. Rhodamine-triazine based tripodal system for sensing of Al^{3+} and Cr^{3+} and its application as 3-input molecular logic device

4.1. Rhodamine-triazine based dipodal system for sensing of Al^{3+} and its application for construction of a read-write-erase molecular memory device

4.1.1 Abstract:

A novel rhodamine B fluorescent probe has been designed for the selective detection of Al^{3+} ions over other metal ions in CH_3OH. The Al^{3+} induced spirolactam ring opening of rhodamine unit of probe **5** was accompanied by colorimetric and '*off-on*' fluorescence changes due to metal-induced spirolactam ring opening of rhodamine. Probe **5** formed a 1:1 complex on binding with Al^{3+} ions and the binding constant was calculated to be 9.3×10^{-4} M^{-1}. The lowest detection limit was calculated from the fluorescence titration profile and was found out to be 2.9×10^{-7} M. Further, probe **5** was utilized for the construction and interpretation of logic gates and memory devices.

4.1.2. Synthesis:

Probe **5** was synthesized by following facile one step reaction as shown in **scheme 28** wherein, cyanuric chloride (0.1 g, 0.54 mmol) and Rhodamine B ethylenediamine (0.52 g, 1.1 mmol) and TEA were dissolved in ethanol and the reaction was stirred for 24 hours at room temperature. The colour of the reaction mixture turned from light brown to light pink. The reaction was monitored through TLC in $CHCl_3$: CH_3OH (9:1). On completion of the reaction the reaction mixture was filtered and the filtrate was concentrated to get light pink colour solid in 70% (0.41 g) yield, M.pt. > 200˚C.^{1}H NMR (400 MHz, $CDCl_3$) showed a multiplet for two aromatic protons at δ 7.89-7.85 ppm, a multiplet for four aromatic protons was attained at δ 7.46-7.42 ppm, multiplet for two aromatic proton at δ 7.09-7.03 ppm, multiplet for twelve aromatic protons at δ 6.45-6.12 ppm, a triplet for –NH was attained at δ 5.46 ppm, a multiplet for 16H of $–CH_2$ of N,N diethyleamine protons attached to xanthenes core merged with 4H of the -NH-CH_2-C*H*$_2$-N (of spirolactam ring) linker's were attained at δ 3.34 ppm, 4H aliphatic protons i.e. -NH-C*H*$_2$-CH_2-N(of spirolactam ring) (ethylenediamine linker) were attained at δ 3.11 and a triplet for 24 H for $–CH_3$ of N,N diethyleamine part attached to xanthenes core was attained at δ 1.15-1.12; ^{13}C NMR (100 MHz, $CDCl_3$) showed the signals at δ 169.9 (-C=O), δ 168.1 (-C-Cl), δ 165.2 (-C=N), δ 153.7 (C-O-C), δ 153.4, 148.5, 137.8, 132.8, 131.2, 129.1, 128.7, other aromatic carbon at 123.7, 123.1, 108.0, 105.6, 97.8, 65.0 (spirocyclic C), 46.4 (-CH_2 of the

diethyleamine attached to N of spirolactam ring), 44.2 (-CH_2 of the N,N diethyleamine attached to xanthenes), 41.1 (-CH_2 of the diethyleamine attached to cyanuric chloride), 12.5 (-CH_3 of the N,N diethyleamine attached to xanthenes). The mass spectrum of probe **5** showed MS (ESI): m/z at 1080.19 (M^++1). Hence, from the ^{1}H-NMR, ^{13}C-NMR and mass spectrum obtained, we corroborated the structure of probe **5** as shown in **scheme 28**.

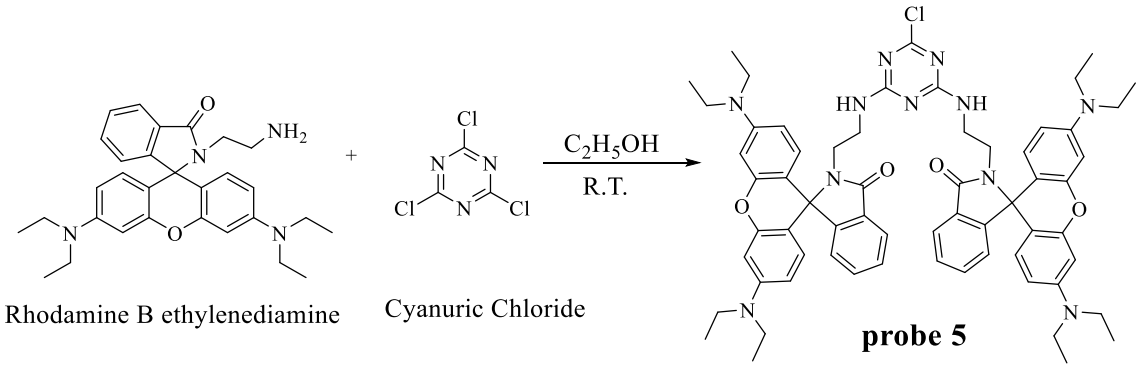

Scheme 28: Synthesis of probe **5**

4.1.3. Results and Discussion

4.1.3.1. UV-Vis Studies for probe 5:

Different solution of probe **5** (20 μM, CH_3OH) were prepared by adding 50 equiv. of different metal ions *viz*, Na^+, K^+, Mg^{2+}, Ca^{2+}, Al^{3+}, Pb^{2+}, Cr^{3+}, Fe^{2+}, Co^{2+}, Ni^{2+}, Cu^{2+}, Zn^{2+}, Cd^{2+}, Hg^{2+} and Pd^{2+} ions. Visible colour change from colorless to pink was observed only in the presence of Al^{3+} whereas the solution remained colorless in presence of all the other metal ions (**Figure 58**).

The absorption spectra of probe **5** (20 μM, CH_3OH), in presence of different metal ions was recorded. Probe **5** (20 μM, CH_3OH) showed a band in UV region at 313 nm (**Figure 59a**). No significant change in the spectra was observed in presence of all the other ions except for $Al^{3+}$and mild changes were observed in case of Cr^{3+} ions. In presence of Al^{3+}, a large red shift was observed accompanied by formation of new band at 557 nm which is attributed to the spirolactam ring opening of rhodamine due to interaction with Al^{3+} ions whereas, the intensity of the band at 313 nm decreased. Whereas, in the presence of Cr^{3+}, no colorimetric change was attained and the slight spectral change can be ascribed to the presence of number of chelating sites.

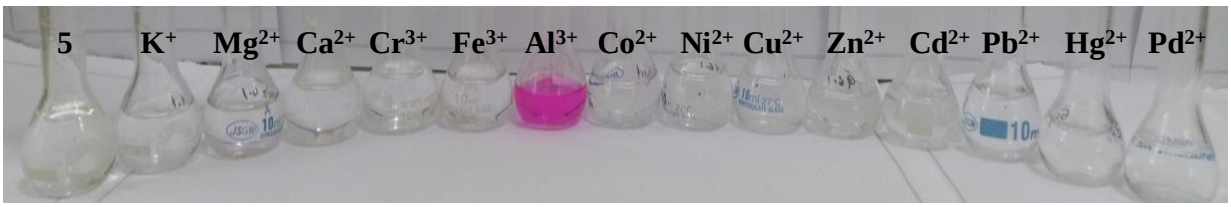

Figure 58: Colorimetric changes of probe **5** (20 μM, CH_3OH) in presence of different metal ions.

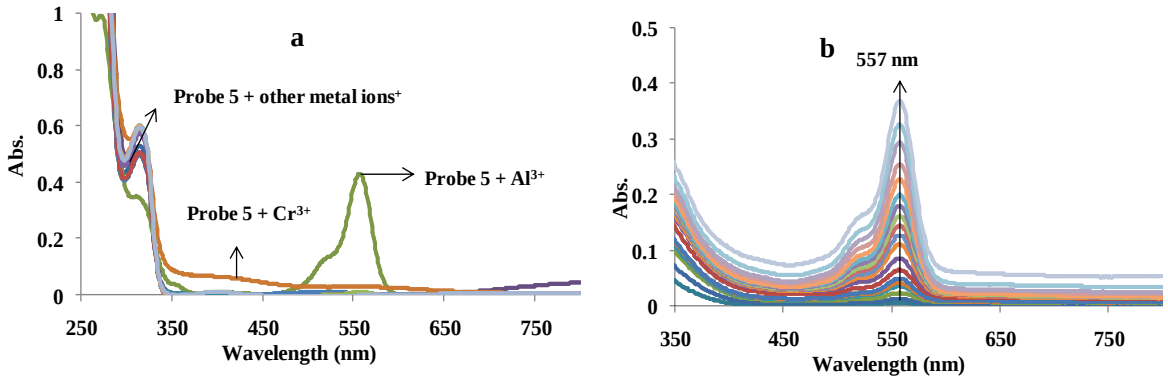

Figure 59: a) Absorption spectra of probe **5** (20 μM, CH_3OH) in presence of different metal ions; b) Absorption spectra of probe **5** (20 μM, CH_3OH) on addition of 0-240 μM of Al^{3+}.

Upon gradual addition of Al^{3+} ions from 0-240 μM in probe **5** (20 μM, CH_3OH), it was observed that the intensity of the absorption band of probe **5** (20 μM, CH_3OH) at 313 nm started decreasing and intensity of the band at 557 nm eventually increased (**Figure 59b**). The binding stoichiometry of metal chelated was determined by performing Job's plot experiment. The plot between absorbance and varying molar concentration of Al^{3+} ($[Al^{3+}]/([Al^{3+}]+[\text{Probe } \mathbf{5}])$) from 0.1 to 1 gave an inclination point at 0.5 which revealed 1:1 stoichiometry between probe **5** and Al^{3+}(**Figure 60**).

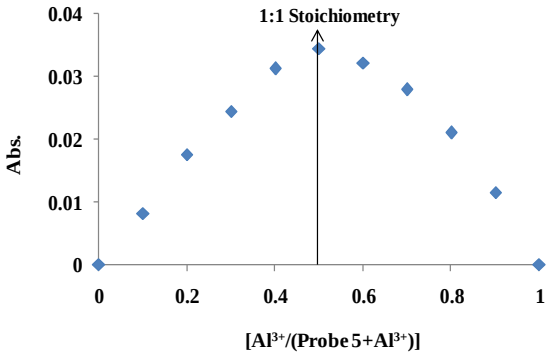

Figure 60: Job's plot depicting 1:1 stoichiometry for binding of Al^{3+} with probe **5**

4.1.3.2. Fluorescence studies of probes 5

The effect of different metal ions on probe **5** (20μM, CH_3OH) was studied by preparing 20μM solution in addition to 50 equiv. of different metal ions in CH_3OH. All these solutions were observed under UV lamp. No visible emission was observed in the solutions of the probes as well as in solutions having K^+, Mg^{2+}, Ca^{2+}, Pb^{2+}, Cr^{3+}, Fe^{2+}, Co^{2+}, Ni^{2+}, Cu^{2+}, Zn^{2+}, Cd^{2+}, Hg^{2+} and Pd^{2+}ions but the solution having Al^{3+} ions showed strong pink fluorescence (**Figure 61**).

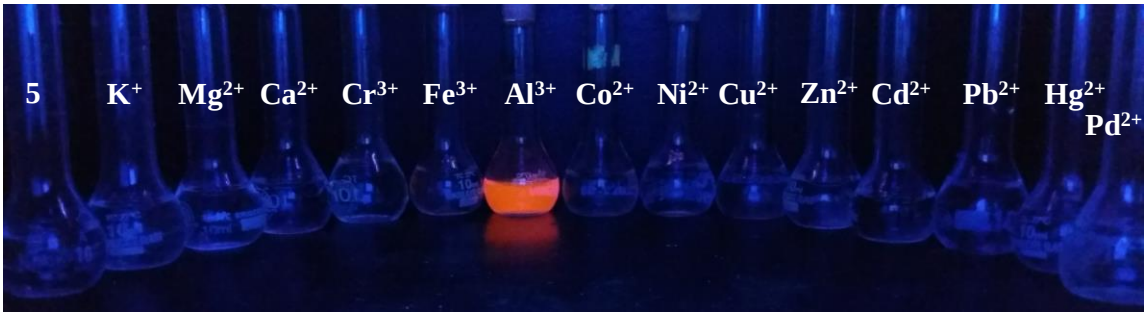

Figure 61: Probe **5** (20 μM, CH_3OH) in presence of different metal ions under UV-lamp

To further test the fluorescence response of probe **5** (20 μM, CH_3OH) towards different metal ions, emission spectra of all the solutions were recorded. Probe **5** (20 μM, CH_3OH) did not show any characteristic emission band whereas in the presence of Al^{3+} ions a significant enhancement at 584 nm was attained. Whereas, no change in the magnitude of emission band was observed in presence of rest of the metal ions (**Figure 62a**). Similarly, the incubation of Cr^{3+} in probe **5** gave a low intensity emission band at 584 nm.

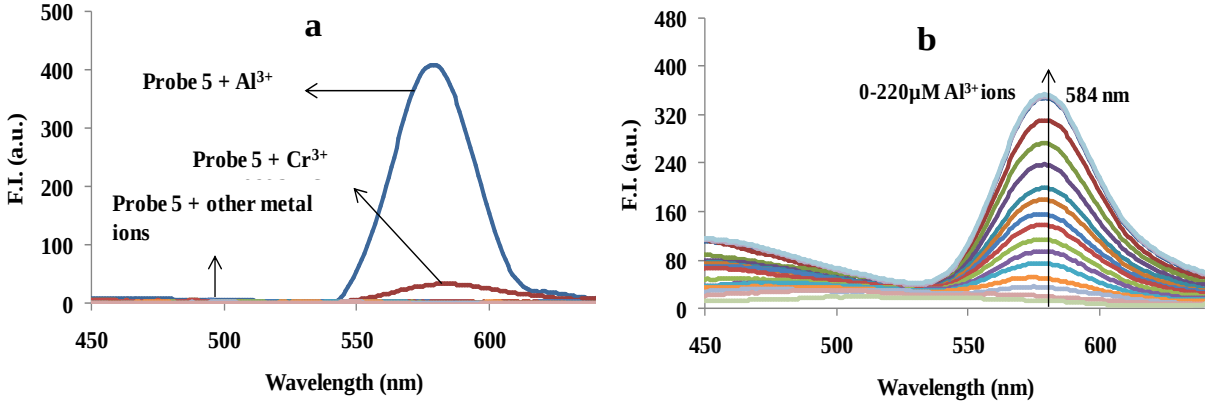

Figure 62: a) Emission response of probe **5** (20 μM, CH_3OH) in presence of different metal ions; b) Fluorescence spectra of probe **5** (20 μM, CH_3OH) on addition of 0-220 μM of Al^{3+}.

For determining the sensitivity of probe **5** (20μM, CH_3OH) towards Al^{3+} incremental addition of Al^{3+} ions was done in 20 µM solution of probe **5**. On complexation of probe **5** (20μM, CH_3OH) with Al^{3+} the fluorescence enhancement was observed due to spirolactam ring opening of rhodamine on binding with metal ion (**Figure 62b**). With addition of 0-220μM of Al^{3+} ions in solution of probe **5** the emission changes achieved a plateau and a simultaneous color change from colorless to pink was acquired. During the gradual addition of Al^{3+} in probe **5** (20 μM, CH_3OH) a low intensity band at 440 nm was also observed which can be due to the presence of number of interacting sites in probe **5** where Al^{3+} showed interactions at lower concentrations before forming the stable complex.

4.1.3.3. Detection Limit and Association Constant of probe 5:

The detection limit and binding constants were calculated from the fluorescence titrations profile. For calculating detection limit, a linear plot of fluorescence intensity versus varying concentration of Al^{3+} was plotted which revealed that probe **5** (20 μM, CH_3OH) was able to detect Al^{3+} at the lowest detection limit of 2.9×10^{-7} M and the association constants were calculated by using Benesi-Hildebrand equation and was found out to be 9.3×10^4 M^{-1}.

4.1.3.4. Kinetic Studies of Probe 5

For determining the response time of sensor as recognition system for Al^{3+} ions, the kinetic studies of probe **5** were investigated (**Figure 63**). On addition of 5 equiv. of Al^{3+}, the absorbance band at 557 nm increased with varying time. After 14 min. the intensity remained almost constant which indicated the completion of metal complexation between probe**5** (20 μM, CH_3OH) and Al^{3+}ions. The complexation of probe **5** with Al^{3+} followed first order kinetics and the linear plot between $In(C/C_0)$ and time having regression coefficient R^2=0.969 was used to calculate the rate constant $K_{\mathbf{probe5}} = 1.4\times 10^{-1}$ min^{-1}, by using equation: $K_{\mathbf{probe5}}$ = slope/2.303

Where, slope is the value attained from linear fit between $In(C/C_0)$ (where C is absorption intensity at time "t" and C_0 is the absorption intensity at "t_0") *vs*. time, and "$K_{\mathbf{probe5}}$" is the rate constant.

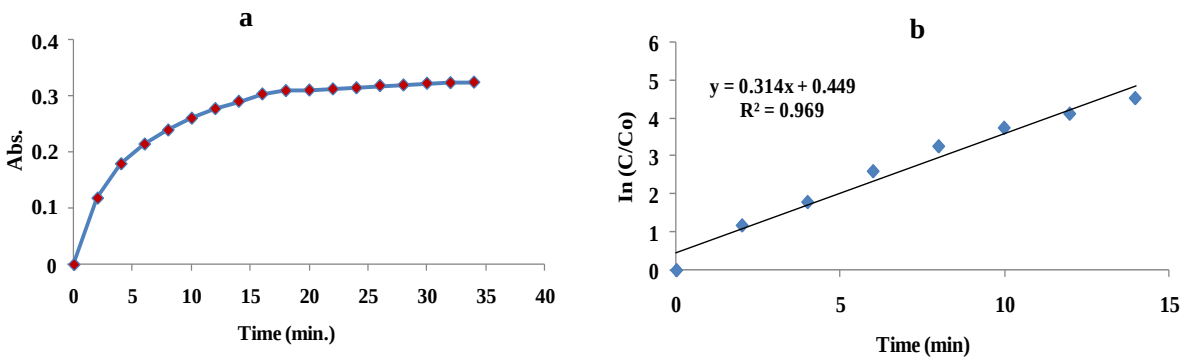

Figure 63: a) Time course of probe **5** (20μM, CH_3OH) responding towards 5 equiv. of Al^{3+}; b) Linear plot between *In*(C/C_0) *vs*. time (min)

4.1.3.5. Competitive binding studies:

The most important characteristic of probe **5** is to detect Al^{3+} even in the presence of other analytes. To confirm the selectivity of probe **5** towards Al^{3+} even in the presence of potentially competing background metal ions, absorption (**Figure 64a**) and emission spectra (**Figure 64b**) was recorded. Except for Cr^{3+} which shows slight interference, no other metal ion showed interference in probe **5** and Al^{3+} system.

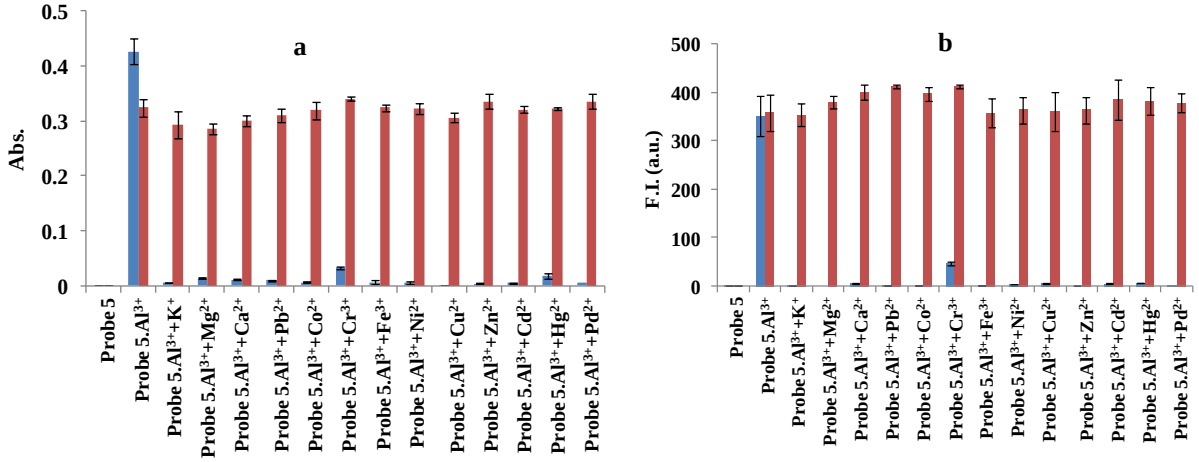

Figure 64: a) Absorption b) Emission selectivity profile of probe **5** (20 μM, CH_3OH), towards Al^{3+} ions in presence of 50 equiv. of different metal ions. The blue bars represent the intensity of probe **5** (20 μM, CH_3OH) in presence of 50 equiv. of different metal ions and red bars represent the intensity of probe **5** (20 μM, CH_3OH) in presence of 50 equiv. of Al^{3+} and 50 equiv. of other metal ions.

4.1.3.6. Life time measurements and quantum yield studies:

To attain an insight into the photophysics of probe **5** and its modulation in presence of Al^{3+} ions, fluorescence lifetimes of probe **5** as well as probe **5.Al^{3+}** were monitored. The fluorescence lifetime decay is shown in **figure 65** and its data is compiled in the table **3**. The average lifetime of probe **5** (20μM, CH_3OH) was found out to be 1.63 ns. Further, Al^{3+} was added into probe **5** (20μM, CH_3OH) and after 15 min its average lifetime decay was calculated to be 1.17 ns. The decrease in the lifetime decay of complex **5.Al^{3+}** was clearly due to Al^{3+} induced spirolactam ring opening and the formation of tightly bound complex which increases the non-radioactive decay process and hence the lifetime decreases[99,100]. The quantum yields of probe **5** and complex **5.Al^{3+}** were calculated by using equation (**4**) and the values given in **table 3**. Further, the K_r (radioactive) = Φ/τ_{avg} and K_{nr} (non-radioactive) = $(1- \Phi)/ \tau_{avg}$ were calculated and the values are listed in the **table 3**.

	τ_1(ns)	τ_2(ns)	χ^2	Average LifeTime (τ_{avg})(ns)	Φ	$K_{r(s^{-1})}\times10^9$	$K_{nr(s^{-1})}\times10^9$
Probe 5	1.48374	3.90113	1.11	1.63182	0.09	0.055	0.55
Probe 5+Al^{3+}	0.901553	1.72266	1.14	1.17839	0.22	0.188	0.67

Table 3: Time-resolve fluorescence data showing average lifetime decay of probe **5** and probe **5** in presence of Al^{3+} after 15 min.

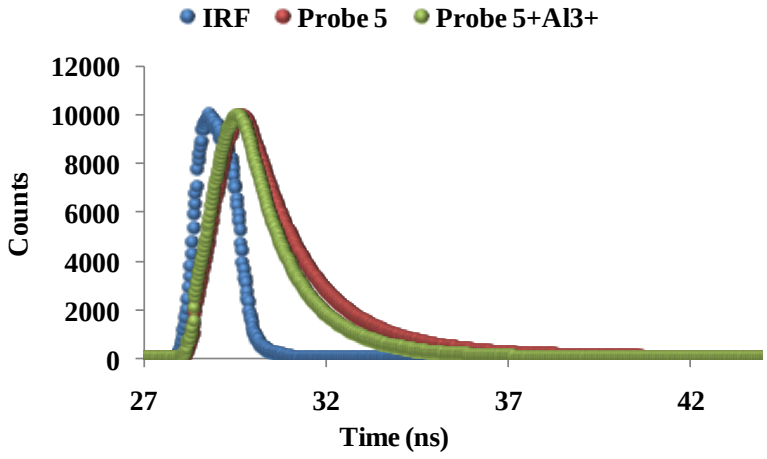

Figure 65: Time-resolved fluorescence decay of probe **5** and probe **5+Al^{3+}**.

4.1.3.7. Binding Mechanism:

To further investigate the binding mechanism of Al^{3+} to probe **5**, ^{1}H-NMR and mass titration was performed. Probe **5** showed characteristic triplet of $–CH_3$ (represented by H_a) of N,N-diethyleamine part attached to xanthene rings of rhodamine units at δ 1.03 ppm and multiplet for $–CH_2$ represented by H_b at δ 3.33 ppm. On adding 1equiv. of Al^{3+} into 5 mM solution of probe **5** (DMSO-d_6/CD_3OD-d_4) new peaks were formed at δ 1.32 ppm (H_{a1}) and δ 3.61 ppm (H_{b1}). The splitting and shifting in the aromatic protons was also observed from δ 6.0-9.0 region. Due to formation of metal-chelate the proton H_c (ortho to the spirolactam ring) and H_d showed slight downfield shift furthermore, due to charge delocalization on xanthenes part of rhodamine units protons H_e and H_f also gave downfield shift and merged with proton H_c and H_d respectively. The splitting in the signal at δ 6.2 ppm which represented proton H_g, H_h and H_i was also observed (**Figure 66**). This shift in the signals of protons attached to the spirocyclic rings of both the rhodamine units suggest the binding of Al^{3+} to the O of spirolactam ring and N of the ethylenediamine. Hence, the plausible mechanism for binding of Al^{3+} with probe **5** is shown in **scheme 29**. The mass titration also supported the binding mechanism deduced from ^{1}H-NMR titration. It gave a peak at m/z = 1107.11 a.m.u. which corresponds to probe **5**+$\mathbf{H^+}$+$\mathbf{Al^{3+}}$.

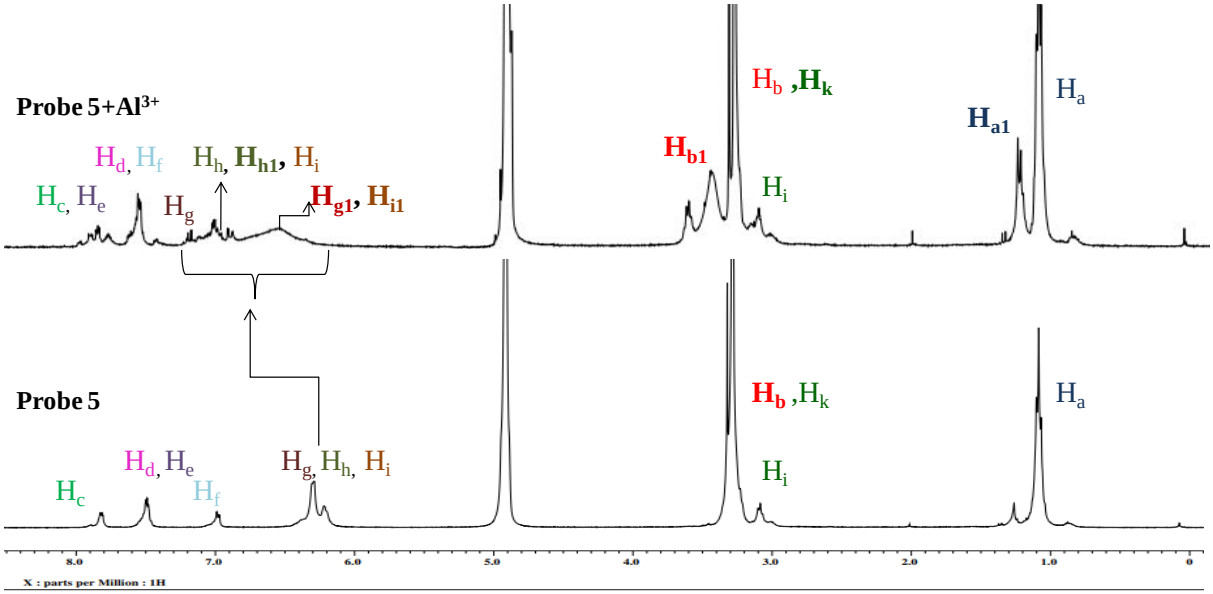

Figure 66: ^{1}H-NMR spectrum of probe **5** and probe **5**.Al^{3+} complex in DMSO-d_6/CD_3OD-d_4.

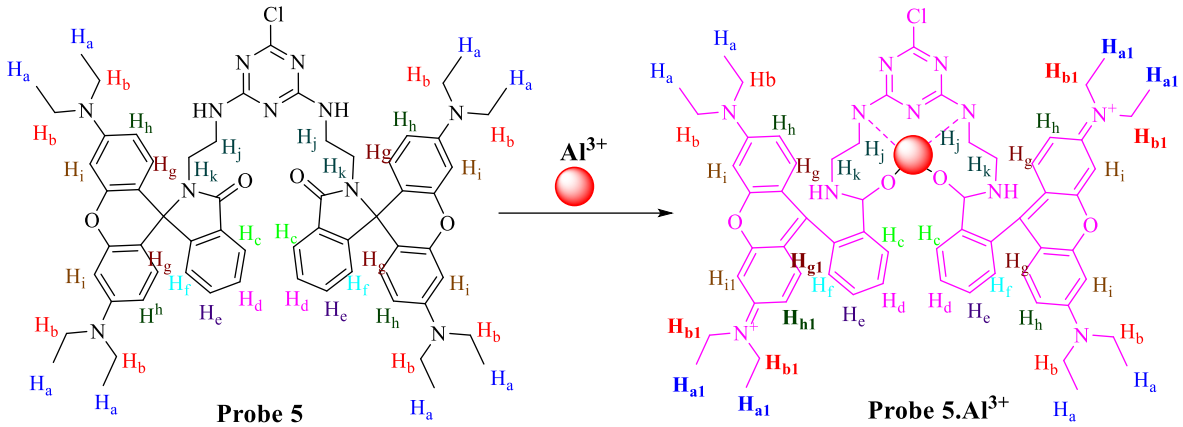

Scheme 29: Plausible binding mechanism of probe **5** with Al^{3+}.

4.1.4. Elaboration of inputs for construction of memory device:

4.1.4.1. Reversibility/ *On-Off* sensing properties of probe 5:

The reversible '*on-off*' fluorescence property of probe **5** (20μM, CH_3OH) with addition of Al^{3+} and other anions*viz.*, F^-, Cl^-, Br^-, I^-, OAc^-, CN^-,HSO_4^-, $H_2PO_4^-$ and NO_3^- have also been studied (**Figure 67a**). The enhancement observed due to probe **5.**Al^{3+}complex at 584 nm was quenched with the addition of $CN^-$and disappearance of pink color of the complex **5.Al^{3+}**. No change in the emission of the complex **5.Al^{3+}** was observed in presence of rest of the anions. The spirolactam ring opening of rhodamine and thus formed emission band at 577 nm of probe **5**.Al^{3+} complex was reversed with the addition of CN^-ions due to the abstraction of metal ion resulting in ring closure and quenching in fluorescence. This suggests the reversibility and reusability of probe **5**.

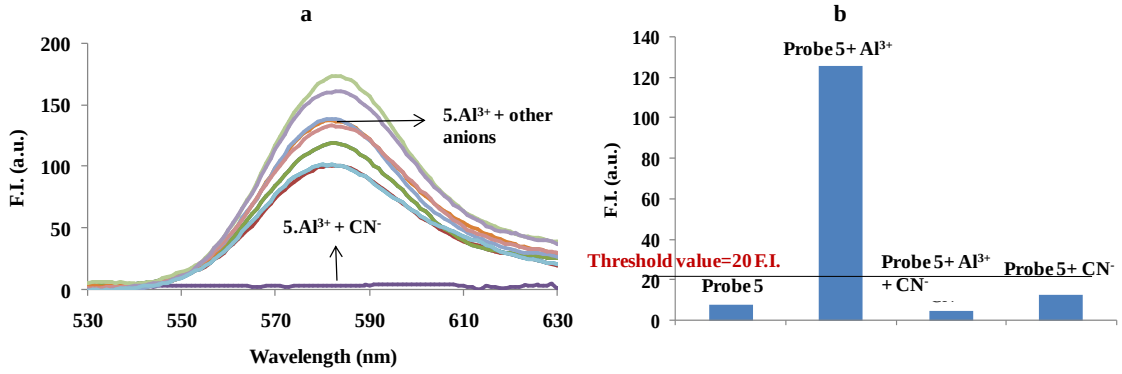

Figure 67: a) Emission response of **5.Al^{3+}**complex towards various anions; b) Bar graph showing the fluorescence intensities of probe **5** in absence and presence of Al^{3+}, CN^- and in presence of both the ions.

Hence, the changes in emission intensity of probe **5** is due to two ions: Al^{3+} which turns the emission "*on*" and CN^- turns the emission to '*off*' state. Further, a reversible and reproducible fluorescence switch was attained by alternately adding Al^{3+} and CN^- as shown in **figure 68**. This type of reproducible switch proves out to be of significant importance in IT (information and technology) field for processing information at molecular level. Most of the earlier reported logic devices/systems [101-102] are based on irreversible changes but, to perform calculations the process should be reversible. Thus, probe **5** based logic system has advantage over previously reported devices as it has reversible and reproducible switching process.

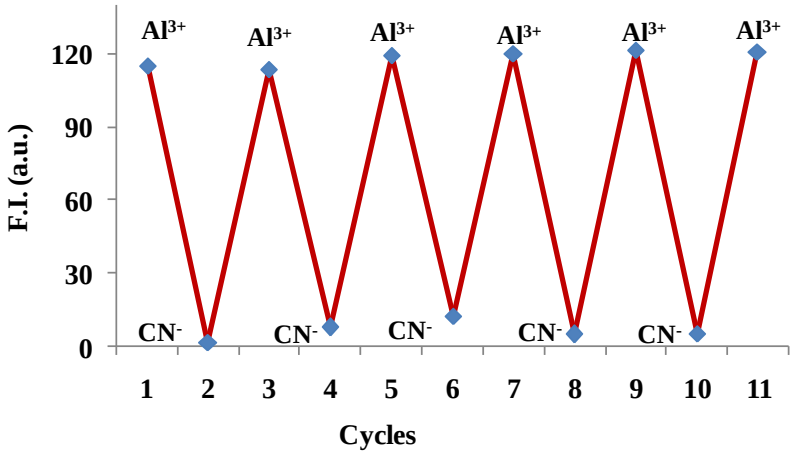

Figure 68: Fluorescence switching process by alternatively adding Al^{3+} and CN^- into probe **5** (20μM, CH_3OH).

4.1.4.2. Logic Operation:

The photophysical properties of probe **5** inspired us to investigate its application in logic gates by addition of Al^{3+} and CN^- and then monitoring of emission at 584 nm as the output. The INHIBIT logic gate is combination of AND and NOT gates. INHIBIT gate shows the inhibition of output signal by one type of input. To prove the INHIBIT function we chose In_1 as Al^{3+} and In_2 as CN^- and the output was measured at 584 nm. The emission intensity more than 15 at 584 nm (**Figure 67b**) was assigned value 1 ('*on*') and lower that it was assigned value 0 ('o*ff*'). In the absence of both the inputs the fluorescence intensity was low representing the '*off*' state. When only $In_1$was present the emission intensity was more than 15 at 584 nm and hence the state of the system was considered to be '*on*' represented by value 1. When only In_2 was present no enhancement in the emission was observed and hence lower value pointed towards the 'o*ff*' state of the system with

value 0. In the presence of both the inputs again, no emission band at 584 nm was observed and the value of the system was stated to be 0 i.e. '*off*' state. Hence, with In_2 it is necessary to apply NOT gate. Probe **5** displays its output signal in a way that it understands the requirement of AND function. Therefore, by sequential addition of the two inputs, the INHIBIT logic gate can be achieved (**Figure 69**) and its truth table represents the combination of inputs and the resulting outputs.

Truth table for INHIBIT logic circuit:

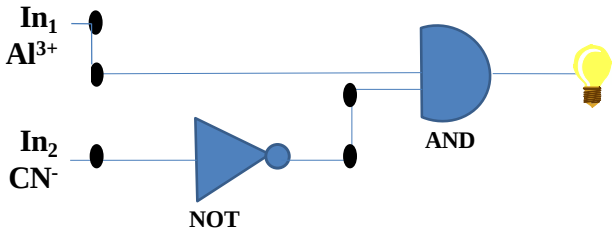

In_1 Al^{3+}	In_2 CN^-	OUT at 584nm (F.I.(a.u.))
0	0	0
1	0	1
0	1	0
1	1	0

Figure 69: Construction of molecular logic device having In_1=Al^{3+} and In_2=CN^-; truth table showing all the possible input combinations and their outputs at λ_{em}=584nm.

4.1.4.3. Construction of memory device

Molecular memory devices can be developed by sequential logic gates and have the capability of storing information. A feedback loop can be performed by these circuits. One of the outputs is memorized and acts as the input for the memory device. So, we have designed a sequential logic using binary function which displays "Write-Read-Erase-Read" property (**Figure 70a**). For our system we have chosen strong emission and weak emission output at 584 nm as the "*on"* i.e. value 1 and "*off"* state i.e. value 0 respectively. For the construction of the memory device we have chosen two inputs (i.e. $In_1$is Al^{3+} and In_2 is CN^-) as SET and RESET process (**Figure 70b**) and **figure 70c** displays the corresponding truth table for the memory device. When the system is given In_1 then the system given high emission at 584 nm and is considered to be "*on"* state with value 1 whereas, In_2, erases the data and the binary function is 0. This type of sequential logic gate circuits show similar behavior as that of semiconductors based logic. Most importantly these write-erase-write cycles can be repeated number of times without any change in intensity or concentration. In future, such type of systems can be used for developing microprocessors of integrated circuits.

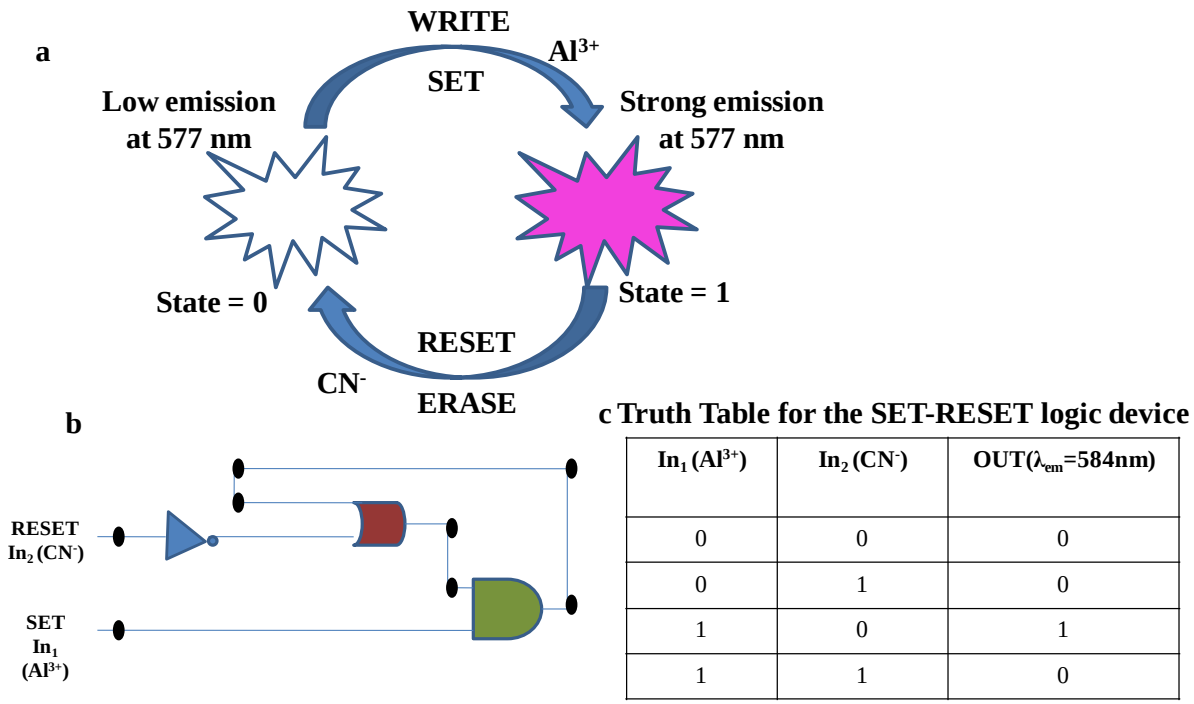

Figure 70: a) Demonstration of set-reset logic operation; b) Memory logic circuit with two inputs i.e. In_1=Al^{3+} and In_2=CN^-; c) truth table for the memory circuit.

4.1.5. Conclusion:

A dipodal system on triazine appended with two rhodamine B ethylenediamine units probe **5** was designed, synthesized and characterized. The sensing behavior of probe **5** was explored and was found out to be highly selective towards Al^{3+} ion sensing. Probe **5** (20 μM, CH_3OH) upon chelation with Al^{3+} gave colorimetric change from colorless to pink and it gave bright pink emission under UV lamp. The spectral studies revealed a large red shift in absorption band with formation of new band centered at 557 nm whereas; in fluorescence spectra a new band emerged at 584 nm, in the presence of Al^{3+}. The detection limit (2.9×10^{-7} M) and association constants (9.3×10^4 M^{-1}) were calculated from fluorescence titration profile which inferred that probe **5** formed a strong complex withAl^{3+} ions. The fluorescence switch of probe **5** was further found to be reversible and reproducible and was used for constructing a set-reset memory device.

4.1.6. Experimental sections

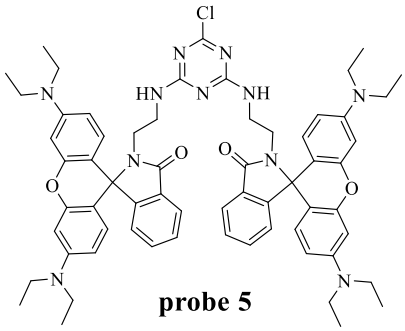

probe 5

For synthesizing probe **5**, Cyanuric chloride (0.1 g, 0.54 mmol) and Rhodamine B ethylenediamine (0.52 g, 1.1mmol) were dissolved in 30 mL ethanol in 100 mL flask. 10 equiv. of TEA (triethyleamine) was added as a base. The contents were stirred for 24 hours at room temperature. The colour of the reaction mixture turned from light brown to light pink. The reaction Was monitored through TLC in $CHCl_3$: CH_3OH (9:1). On completion of the reaction the reaction mixture was filtered and the filterate was concentrated to get light pink colour solid in 70% (0.41 g) yield. M.pt.= > 300°C **^{1}H NMR** (400 MHz, $CDCl_3$) δ 7.89 (m, 2H, ArH), δ 7.46 (m, 4H, ArH), δ 7.09 (m, 2H, ArH), δ 6.45 (m, 12H, ArH), δ 5.46 (t, 1H, -NH), δ 3.34 (m, 4H, $-CH_2$), δ 3.11 (m, 20H, $-CH_2$), δ 1.15 (m, 24H, $-CH_3$); ^{13}C NMR (100 MHz $CDCl_3$) δ 1.69.9 (-C=O), δ 168.1 (-C-Cl), δ 165.2 (-C=N),δ 153.7 (C-O-C), δ 153.4, 148.5, 137.8, 132.8,131.2, 129.1, 128.7, δ 123.7, 123.1, 108.0, 105.6, 97.8, 65.0 (spirocyclic C), 46.4, 44.2, 41.1, 12.5. **MS (ESI):** m/z at 1080.19 (M^++1)

4.2. Rhodamine-triazine based tripodal system for sensing of Al^{3+} and Cr^{3+} and its application as 3-input molecular logic device

4.2.1. Abstract

In this chapter we have discussed the synthesis of tripodal system wherein the chloride (Cl) of probe **5** was also replaced with rhodamine B ethylenediamine unit. Furthermore, the changes in the photophysical and sensing properties have also been discussed. A cooperative action due to numerous binding sites of tripodal system and the generation of amide ion due to spirolactam ring opening favors the formation of Al^{3+}-chelate. Probe **6** gave dual change (colorimetric and fluorimetric) in presence of Al^{3+} and Cr^{3+}. The interference studies proved that probe **6** was highly selective towards Al^{3+} having lowest detection limit of nM level. For its biological applicability its antibacterial activity was explored and compared to commercial drug. The ability of probe **6** to mimic logic devices was also explored and a 2-input INHIBIT logic function and 3-input OR-INHIBIT logic functions were designed.

4.2.2. Synthesis: Probe **6** was synthesized by taking cyanuric chloride (0.1g, 0.54 mmol) and rhodamine B ethylenediamine (0.78 g, 1.6 mmol) in ethanol in a round bottom flask and TEA (triethyleamine) was added as base. The reaction mixture was refluxed for 24 hrs. The reaction was monitored through TLC. On reaction completion, the contents were filtered and solid obtained was washed with water. Light brown solid was separated out and dried. Percentage yield = 75 (0.60 g), M. pt. = 310-330°C. ^{1}H NMR showed a multiplet of three aromatic protons at δ 7.89-7.84ppm, a multiplet of six aromatic protons at δ 7.43-7.40 ppm, multiplet of two aromatic protons at δ7.07-7.01ppm, multiplet of nineteen aromatic protons at δ 6.45-6.13 ppm, multiplet of 30H of $-CH_2$ of *N, N* diethylamine attached to xanthene core that merged with 6H of the ethylenediamine linker at δ 3.27 ppm, six aliphatic protons ($-CH_2$) of ethylenediamine linker at δ 3.16 and a triplet for 36H of $-CH_3$ of *N, N* diethylamine attached to xanthene core at δ 1.09 ppm.^{13}C-NMR showed signals at δ 1.67.9 (-C=O), δ 163.2 (-C=N),δ 154.1 (C-O-C), (δ): 153.8, 148.3, 138.1, 132.8,131.3, 129.2, 128.5, δ 123.7, 123.1, 108.0, 105.6, 97.8, 65.0 (spirocyclic C), 59.7 (-CH_2 of the ethylenediamine linker attached directly to the N of spirolactam ring), 44.2 (-CH_2 of *N, N* diethylamine attached to xanthene), 41.1 (-CH_2 of the ethylenediamine linker attached to cyanuric chloride) and 12.5 (-CH_3 of the *N, N* diethylamine

attached to xanthene).. The mass spectrum of probe **6** showed MS (ESI): m/z at 1529.83 (M^++1). Hence, from the ^{1}H NMR, ^{13}C NMR and mass spectrum, we corroborated the structure of probe **6** as shown in **Scheme 30.**

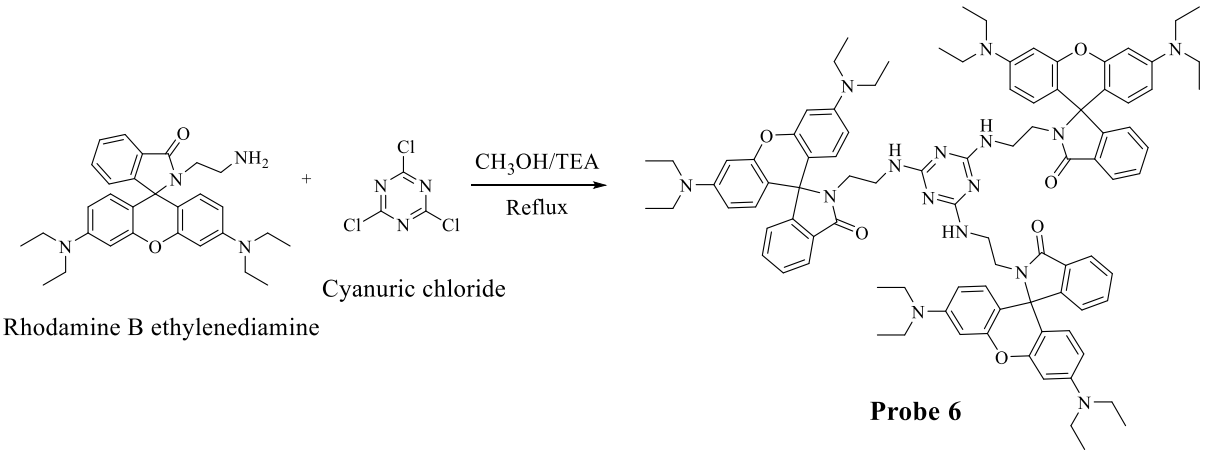

Scheme 30: Synthesis of probe **6**.

4.2.3. Results and Discussion:

4.2.3.1. Absorption response of probe 6 towards different metal ions

The selective metal ion binding capability of rhodamine based probes is generally due to metal-induced spirolactam ring opening of rhodamine and formation of xanthenes which generates electronic, colorimetric and spectral changes. Henceforth, we explored the binding capability of probe **6** (20μM, CH_3OH) with a series of alkali, alkaline and transition metal ions such as, Na^+, Ca^{2+}, Mg^{2+}, Al^{3+}, Cr^{3+}, Fe^{3+}, Co^{2+}, Ni^{2+}, Cu^{2+}, Zn^{2+}, Pb^{2+}, Hg^{2+} and Pd^{2+}.

The colorimetric changes hold a great importance in the field of sensing. Hence, probe **6** was tested for its colorimetric change in the presence of different metal ions. originally probe **6** was colorless and remained the same in the presence of 1000 μM of Na^+, Ca^{2+}, Mg^{2+}, Fe^{3+}, Co^{2+}, Ni^{2+}, Cu^{2+}, Zn^{2+}, Pb^{2+}, Hg^{2+} and Pd^{2+} ions but in the presence of same amount of Al^{3+} an intense pink color was achieved whereas, in presence of Cr^{3+} the solution turned faintly pink (**Figure 71**).

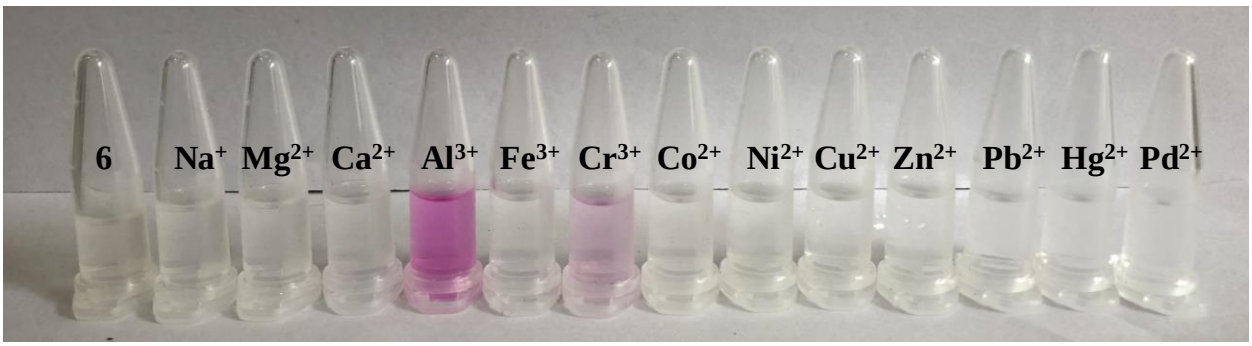

Figure 71: Visual **c**olorimetric changes of probe **6** (20 μM, CH_3OH) in presence of different metal ions.

Probe **6** gave its absorption band in the UV region i.e. below 350 nm due to its n-π* and π- π* transitions. On incubating probe **6** with different metal ions such as Na^+, Ca^{2+}, Mg^{2+}, Fe^{3+}, Co^{2+}, Ni^{2+}, Cu^{2+}, Zn^{2+}, Pb^{2+}, Hg^{2+} and Pd^{2+}, no spectral change was noticed. But on addition of Al^{3+} the absorption maxima showed a major red shift with the formation of a new intense absorption band centered at 557 nm with a shoulder at ~520 nm (**Figure 72a**). A slight spectral change in presence of Cr^{3+} was also attained at the same wavelength.

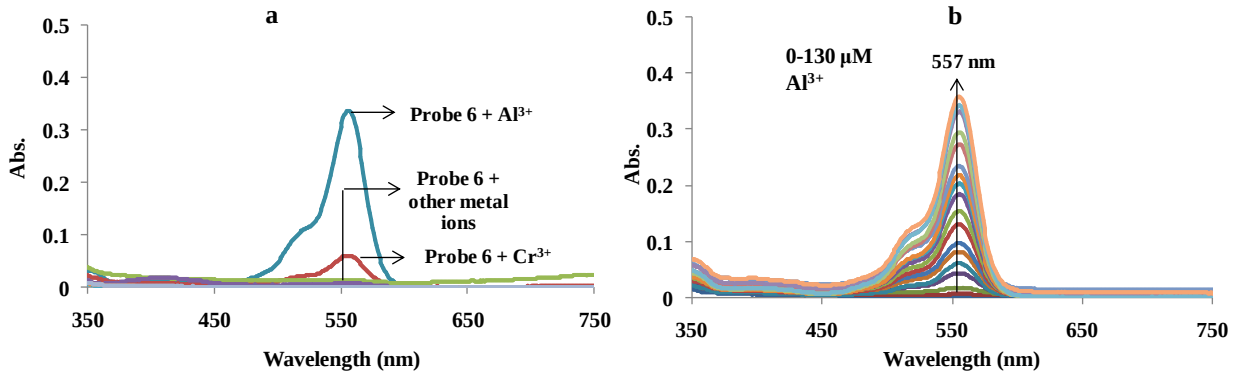

Figure 72: a) Absorption response of probe **6** (20 μM, CH_3OH) in presence of different metal ions; b) Absorption spectra of probe **6** (20 μM, CH_3OH) on addition of 0-130μM of Al^{3+}

Further, the absorption spectral change upon gradual addition of Al^{3+} and Cr^{3+} were recorded. With each incremental addition of the respective ions, the band at 557 nm intensified and reached its plateau with addition of 130 μM of Al^{3+} ions (**Figure 72b**) and 110 μM of Cr^{3+} ions. The formation of this band at 557 nm with a shoulder at 520 nm clearly manifests the spirolactam ring opening of rhodamine due to formation of metal-chelates with each ion. For determining the binding stoichiometries of both the trivalent metal ions with probe **6** absorption

titrations were performed. A non linear plot between absorbance intensity and [M^{3+}/(Probe **6**+M^{3+})] revealed the 1:1 binding stoichiometries of metal-complexes (**Figure 73**).

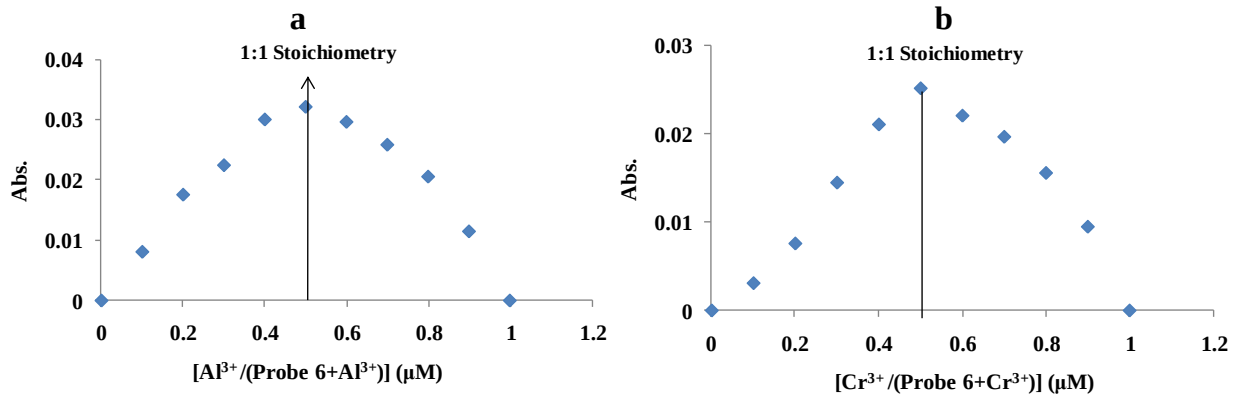

Figure 73: Job's plot depicting 1:1 stoichiometry for binding of probe **6** with a) Al^{3+}b) Cr^{3+}

4.2.3.2. Emission response of probe 6 towards various metal ions

The effect of metal ions on probe **6** was also observed under UV lamp. Probe **6** gave a bright pink emission in the presence of Al^{3+} ions and faint pink emission in presence of Cr^{3+} whereas, the presence of all the other metal ions did not show any emission when exposed to UV light (**Figure 74**).

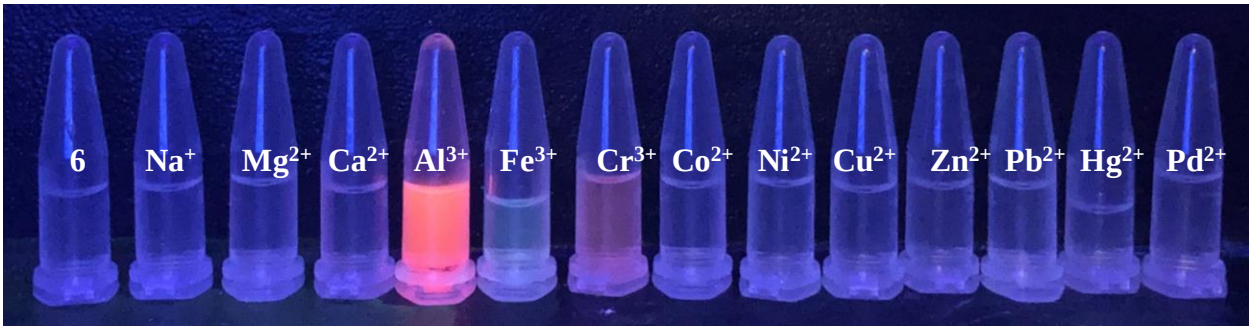

Figure 74: Probe **6** (20 μM, CH_3OH) in presence of different metal ions under UV-lamp

The fluorescence spectra of probe **6** gave a low intensity band at 505 nm. The emission spectra remain unaltered in the presence of all the other ions except for Al^{3+} and Cr^{3+}. The presence of Al^{3+} gave an intense emission band at 587 nm and much weaker response was observed in the presence of Cr^{3+} ions (**Figure 75a**). The spectra clearly showed that the magnitude of

enhancement of fluorescence intensity was achieved in the presence of Al^{3+} ions whereas presence of Cr^{3+} could not give an appreciable increase in fluorescence intensity.

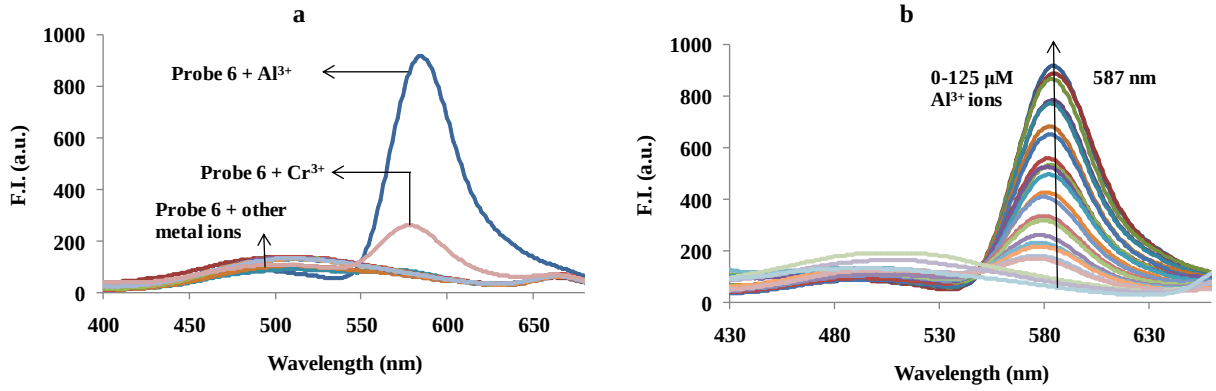

Figure 75: a) Emission response of probe **6** (20 μM, CH_3OH) in presence of different metal ions; b) Fluorescence spectra of probe **6** (20 μM, CH_3OH) on addition of 0-125μM of Al^{3+}

The fluorescence titrations were performed to explore the binding constants and detection limits for probe **6** with respective ions. The increasing addition of metal ion led to subsequent increase in the intensity of emission band at 587 nm and with the addition of 125 μM of Al^{3+} the titration reached its plateau (**Figure 75b**). Whereas, the incremental addition of Cr^{3+} into probe **6** did not give any significant change till addition of 65 μM and further addition to 105 μM, gave a low intensity band at 587 nm. For the titration profiles the detection limit and binding constants were calculated and are listed in **Table 4**. The detection limits was calculated from the linear plot ($R^2 \approx 1$) between fluorescence intensity *vs.* varying metal ions concentration (**Figure76**) whereas, the binding constants were calculated by using Benesi-Hildebrand equation. According to the tabulated data probe **6** is highly sensitive towards sensing of Al^{3+} ions as it could sense it to 43×10^{-9}Mlevel and moreover, it has high binding affinity towards Al^{3+} ions than Cr^{3+} ions which is ascribed to the small ionic radii of Al^{3+}.

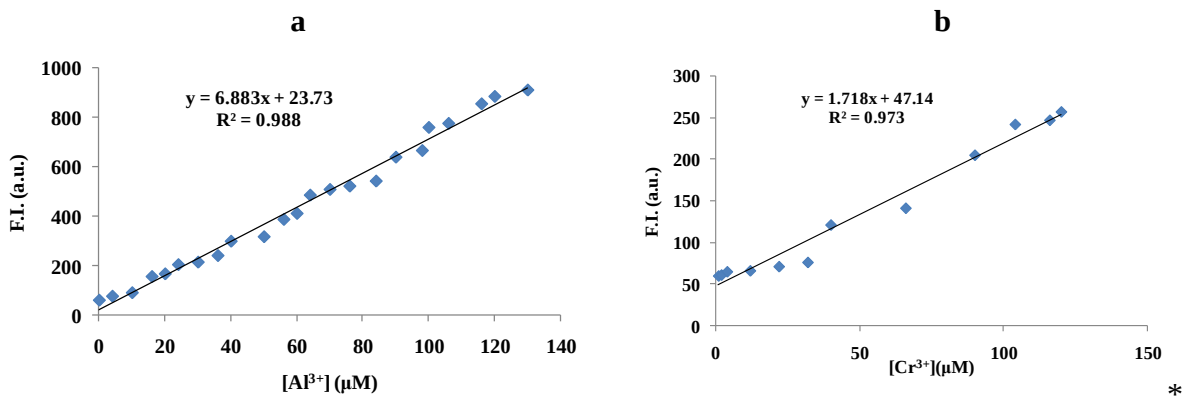

Figure 76: Linear plot between fluorescence intensity vs. increasing concentration of a) Al^{3+}b) Cr^{3+}into probe **6**(20µM)

	Detection Limits (M)	**Binding Constants (M^{-1})**
Probe 6 + Al^{3+}	43×10^{-9}	3.8×10^{5}
Probe 6 + Cr^{3+}	1.75×10^{-7}	1.2×10^{3}

Table 4: Detection limits and binding constants of probe **6** for sensing different ions

4.2.3.3. Kinetic study of probe 6:

For determining the time taken for probe **6** to complete the binding process with Al^{3+} ions, the kinetic studies were performed. Upon adding 5 equiv. of Al^{3+} into probe **6**, the absorbance intensity increased with time and after 10 min it remained almost constant (**Figure 77**). This indicated that the complexation process between probe **6** and Al^{3+} ions was completed in 10 mins. The complexation reaction between probe **6** and Al^{3+} followed first order kinetics which was achieved by a linear plot between $In(C/C_0)$ and time (min), having regression coefficient: R^2= 0.971. The rate constant for the first order reaction was calculated to be K_{probe6} = 1.1 min^{-1}, by using equation: K_{probe6} = slope/2.303,

Where, slope is the value attained from linear fit between $In(C/C_0)$ (where C is absorption intensity at time "t" and C_0 is the absorption intensity at "t_0") *vs*. time, and "K_{probe6}" is the rate constant for probe **6.**

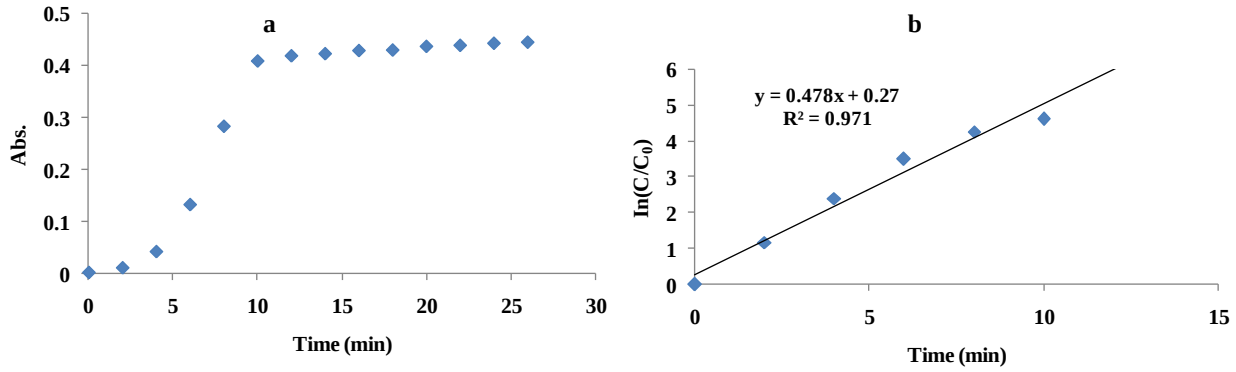

Figure 77: a) Time course of probe **6** (20μM, CH_3OH) responding towards 5 equiv. of Al^{3+}.b) linear plot between *In*(C/C_0) *vs.* time

4.2.3.4. Quantum yields and life time measurements:

In order to attain insight into the photophysics and modulations undergone by probe **6** on binding with Al^{3+} ions we performed the time-resolve fluorescence experiment to find out the life times of probe **6** as well as complex **6.Al^{3+}**. The lifetime of probe **6** was 1.74 ns and for complex **6.Al^{3+}** was 0.91 ns (**Table 5**), whereas the quantum yield of complex **6.Al^{3+}**was higher than that of probe **6**. The decrease in the lifetime on complexation was due to structural rigidity attained by rhodamine spirolactam ring open form due to complexation with metal ion which increases the non-radioactive decay pathway (**Figure 78**). Hence, due to high quantum yield the enhancement was observed on complexation but due to increased non-radioactive decay process the life time decreases.

	τ_1(ns)	**τ_2(ns)**	**χ^2**	**Average LifeTime(τ_{avg}) (ns)**	**Φ**	**$K_{r(s^{-1})}\times10^9$**	**$K_{nr(s^{-1})}\times10^9$**
Probe 6	1.48374	3.90113	1.13	1.74966	0.092	0.053	0.52
Probe 6+Al^{3+}	0.689493	1.52098	1.04	0.919491	0.37	0.41	0.70

Table 5: Time-resolve fluorescence data showing average lifetime decay of probe **6** and probe**6** in presence of Al^{3+} after 10 min.

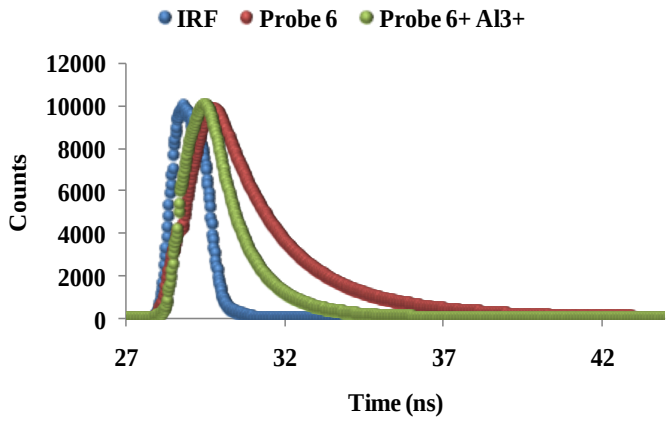

Figure 78: Time-resolve fluorescence decay of probe **6** and probe **6+Al^{3+}**.

4.2.3.5. Competitive binding studies:

To test the selectivity of probe **6** towards sensing of Al^{3+} ions over other metal ions including Cr^{3+}, competitive experiments were performed. Herein, 1000 μM of Al^{3+} ions were added into 20 μM of probe **6** and then the absorbance (**Figure 79a**) and fluorescence intensities (**Figure 79b**) were recorded in presence of 1000 μM of different ions. These patterns were further compared with the absorbance and fluorescence data of solutions where probe **6** (20 μM, CH_3OH) was incubated with 1000 μM of each ion. Figure **79** clearly shows that absorbance intensity (at 557 nm) and emission intensity (at 587 nm) of probe **6** (20 μM, CH_3OH) in presence of Al^{3+} was not affected by presence of other metal ions. Hence, from **figure 79** it can be justified that detection of Al^{3+} was selective with slight interference from Cr^{3+}.

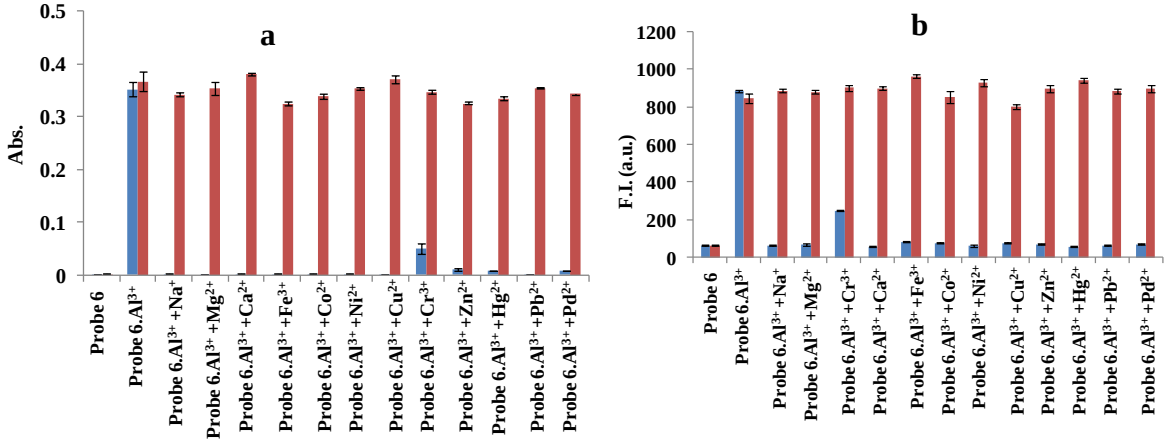

Figure 79: Selectivity profile of probe **6** (20 μM, CH_3OH), towards Al^{3+} ions in presence of 50 equiv. of different metal ions. The blue bars represent the intensity of probe **6** (20 μM, CH_3OH) in presence of 50 equiv. of different

metal ions and red bars represent the intensity of probe **6**(20 μM, CH_3OH) in presence of 50 equiv. of Al^{3+} and 50 equiv. of other metal ions a) absorption b) emission.

4.2.3.6. Binding Mechanism:

For finding out the binding mechanism and to justify the ring-opening mechanism on binding of Al^{3+} with probe **6**, ^{1}H-NMR titrations were performed. For carrying out the titration, 1 equiv. of Al^{3+} ions were added into 5 mM solution of probe **6** in DMSO-d_6/CD_3OD-d_4. Probe **6** gave a multiplet for 30H of $–CH_2$ (of *N*, *N* diethyleamine attached to xanthenes part of rhodamine B unit and of diethyleamine of linker) at δ 3.27 ppm (**H_b**) and a multiplet for $–CH_3$ (of *N*, *N* dithyleamine attached to xanthenes part of rhodamine B) at δ 1.09 ppm (**H_a**). Upon binding with Al^{3+} ions these protons split new signals adjacent to the respective signals of $–CH_2$ and $–CH_3$ were formed at δ 3.44 ppm (**H_{b1}**) and δ 1.12 ppm (**H_{a1}**) (**Figure 80**) clearly showing delocalization of charge due to spirolactam ring opening of rhodamine. Whereas, a slight downfield shift in the aromatic protons along with splitting of signals was also observed which strengthen our hypothesis of metal-induced ring opening of rhodamine. To further support our proposed mechanism, mass titration was performed to find out the binding mechanism of probe **6** with Al^{3+} ions. It gave a peak at m/z = 1556.24 a.m.u. which corresponds to probe **6**+$\mathbf{H^+}$+$\mathbf{Al^{3+}}$. The three rhodamine units form a cavity where Al^{3+} having smaller radii fit in easily and bind with N and O of rhodamine units. This justifies the 1:1 stoichiometry attained by job's plot experiment. The plausible mechanism is shown in **scheme 31**.

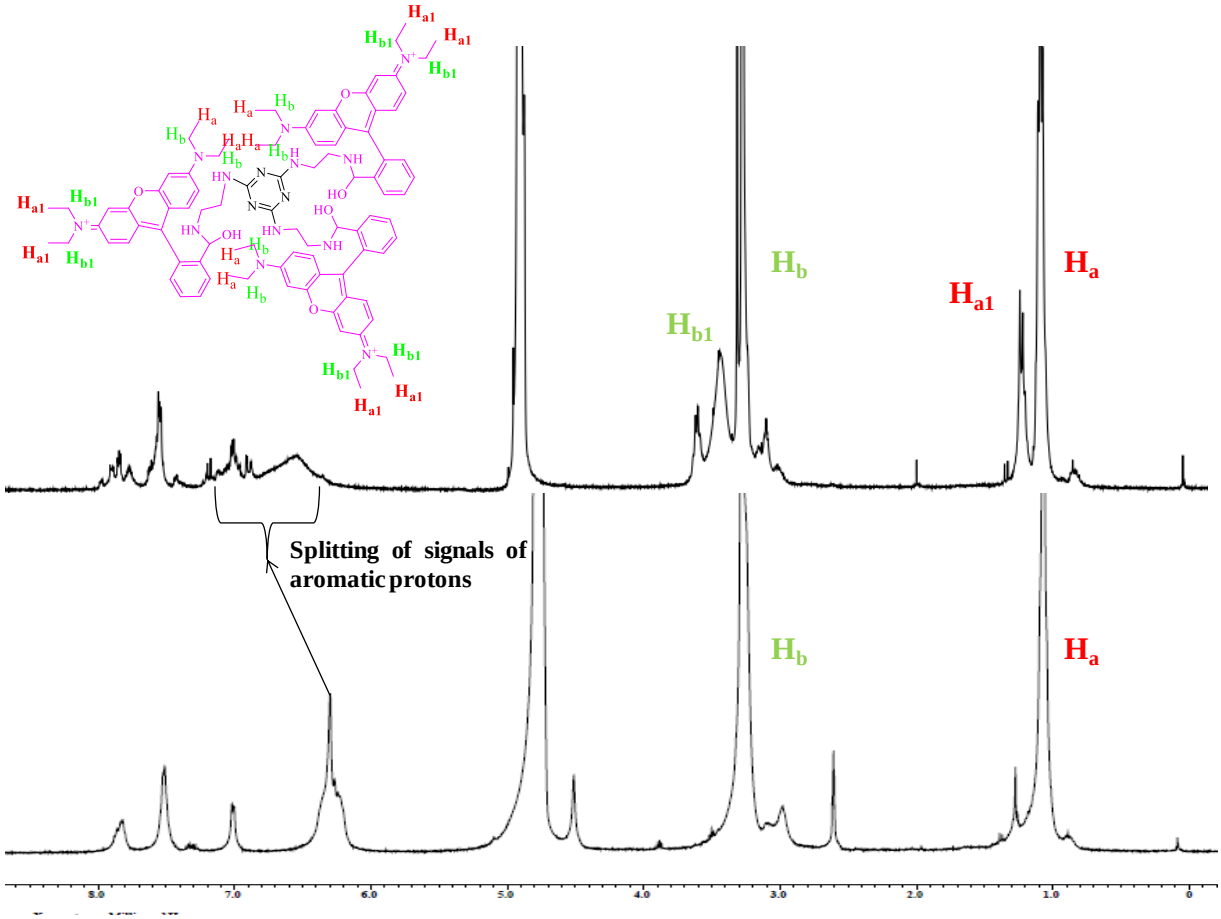

Figure 80: ^{1}H-NMR titration of probe **6** in presence of 1 equiv. of Al^{3+} in DMSO-d_6/CD_3OD-$d_4$and structures showing the proton labeling.

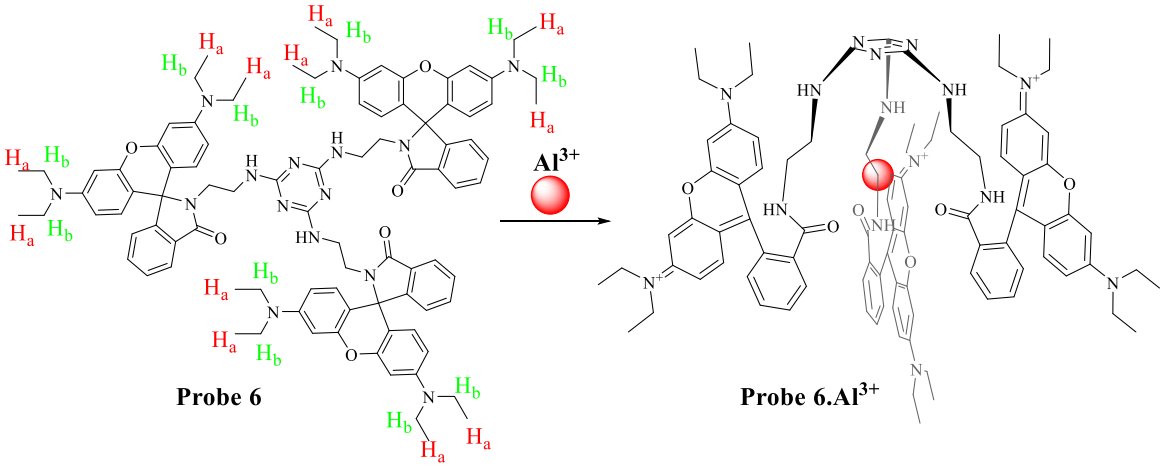

Scheme 31: Plausible binding mechanism of probe **6** with Al^{3+}

4.2.3.7. Practical applicability

4.2.3.7.1. Anti-bacterial activity:

Cyanuric chloride and various other triazine have been known to possess various therapeutic activities like antimicrobial, antifungal, antiviral, anticancer, antimalarial, antiulcer, anesthetic, analgesic, antiarthritic, sedative, antibacterial etc. [**103-106**]. Considering these facts we tested probe **6** for its antibacterial activity against four gram positive (*Enterococcus faecalis*, *Bacillus subtilis*, *Listeria sp.*, *Staphylococcus aureus*) and four gram negative bacteria (*Escheria coli*, *Salmonella enteric*, *Acinetobacter calcoacetius*, *Serratia marcescens*). The antibacterial activity was carried out by dilution method and commercially available tetracyclin was used as the reference drug. The MIC values of probe **6** and tetracyclin against different bacteria are given in **Table 5**. Probe **6** was found to inhibit the growth of some bacteria but its activity against *Bacillus subtilis* and *Acinetobacter calcoacetius*, having MIC values of 1.56 μg/ml which were comparable to the commercially available drug; tetracycline. Hence, it can be concluded that probe **6** can act as inhibitor for growth of *Bacillus subtilis* and *Acinetobacter calcoacetius* bacteria.

Antibacterial Activity (expressed as MIC in μg/ml)								
	Gram Positive Bacterial Strains				**Gram Negative Bacterial Strains**			
	Enterococcus faecalis MTCC No. 6845	**Bacillus Subtilis MTCC No. 441**	**Listeria sp. MTCC No. 4214**	**Staphylococcus aureus MTCC No. 902**	**Escheria Coli MTCC No. 448**	**Salmonella enteric MTCC No. 1165**	**Acinetobacter calcoacetius MTCC No. 1948**	**Serratia marcescens MTCC No. 2645**
Probe 6	200	**1.56**	200	125	125	200	**1.56**	50
Tetracyclin (reference drug)	1.56	1.56	6.25	1.56	1.56	100	1.56	1.56

Table 5: Antibacterial activity profile of probe**6**.

4.2.3.7.2. "*On-Off*" fluorescence switch of probe 6.Al^{3+}:

Probe **6.Al^{3+}** was further tested for its on-off fluorescence switching behavior in presence of different anions. It was observed that except for CN^- whereas no other anion *viz*. F^-, Cl^-, Br^-, I^-, SCN^-, $H_2PO_4^-$, HSO_4^- etc. could give the significant and reversible emission change (**Figure 81a,**

81b). Presence of CN^- gave quenching of the emission band at 587 nm along with colorimetric reversal i.e. the solution turned pink to colorless. This dual (colorimetric as well as fluorimetric) change was attained due to abstraction of Al^{3+} ions by CN^- which leads to spirolactam ring closure. The similar change was observed for Cr^{3+} ions (**Figure 81c**). This reversibility experiment proved the reusability of probe **6**.

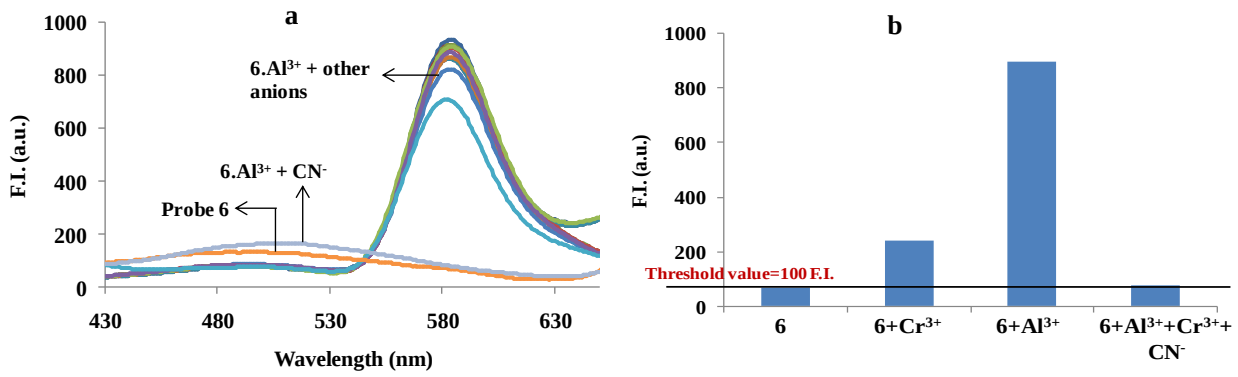

Figure 81: a) Emission response of complex **6.Al^{3+}** towards different anions; b) bar graph representation of emission intensity in presence of different ions in probe **6**.

4.2.4. Mimicking logic gates:

The fluorescence switching pattern of probe **6** inspired us to explore the applicability of probe **6** in designing logic devices/ operations by adding inputs *viz.* Al^{3+}, Cr^{3+} and CN^- and then recording the emission output at 587 nm. Herein, we have discussed the designing of different input systems.

4.2.4.1. Formation of 2-input INHIBIT logic gate:

The formation of INHIBIT gate, two logic functions are required i.e. AND and NOT. For demonstrating INHIBIT function, we chose Al^{3+} (In_1) and CN^- (In_2) as the two inputs and the output (OUT_1) was considered at 587 nm. If the intensity at 587 nm is more than threshold value (100 F.I.) then the output is assigned 1 ("*On*") and if it is below 100 then it is assigned 0 ("*Off*"). It was observed that in presence of In_1 (Al^{3+}) and absence of In_2 (CN^-) the intensity at 587 nm is higher than 100 and hence the output is 1 i.e. "*On*" state. In the absence of In_1 (Al^{3+}) and presence of In_2 (CN^-) the intensity was below the threshold value and hence the OUT was assigned 0 ("*Off*" state). Even in the presence of both the inputs the intensity was lower than the

threshold value and hence the OUT was considered to be in "*Off*" state. The combinations of the inputs is listed in truth table alongwith the design of the INHIBIT logic gate (**Figure 82**).

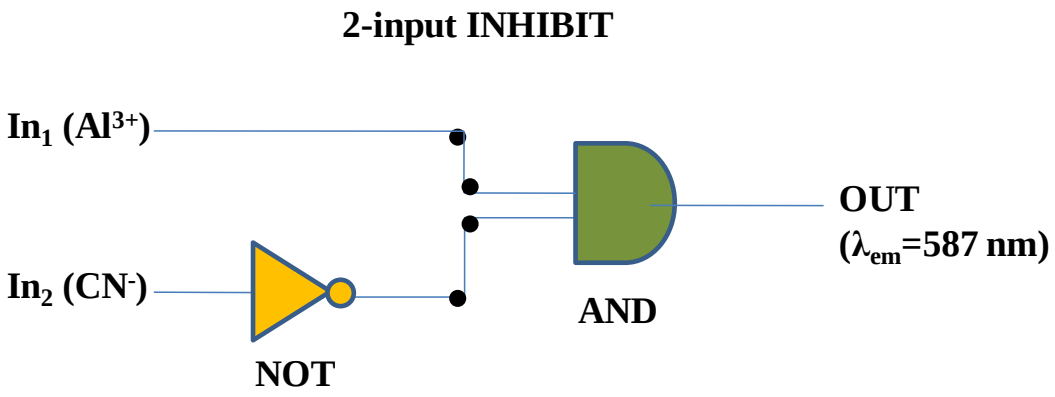

Truth Table: for 2-input INHIBIT logic gate

$In_1(Al^{3+})$	$In_2(CN^-)$	OUT (λ_{em}=587 nm)
0	0	0
1	0	1
0	1	0
1	1	0

Figure 82: Formation of 2-input INHIBIT logic function having output at 587 nm alongwith truth table showing combination of different inputs and their subsequent outputs.

4.2.4.2. Formation of Advanced 3-input OR-INHIBIT logic gate:

To mimic an OR-INHIBIT logic gate the three inputs i.e. In_1 (Al^{3+}) In_2 (Cr^{3+}) and In_3 (CN^-) and the output (OUT) at 587 nm were considered. In the absence of In_1 (Al^{3+}) and In_2 (Cr^{3+}) the output response at 587 nm was below 100 and hence indicated an "*Off*" state. In the presence of either of the two inputs i.e. In_1 (Al^{3+}) and In_2 (Cr^{3+}) and absence of In_3 (CN^-) the emission instensity was more than the threshold value and hence the output was in "*On*" state. In the presence of In_3 (CN^-) and either/both of the two inputs (In_1 and In_3) the output response was low and hence represented "*Off*" state. Thus, from the truth table and OR-INHIBIT logic function the 3-input logic circuit could be understood (**Figure 83**).

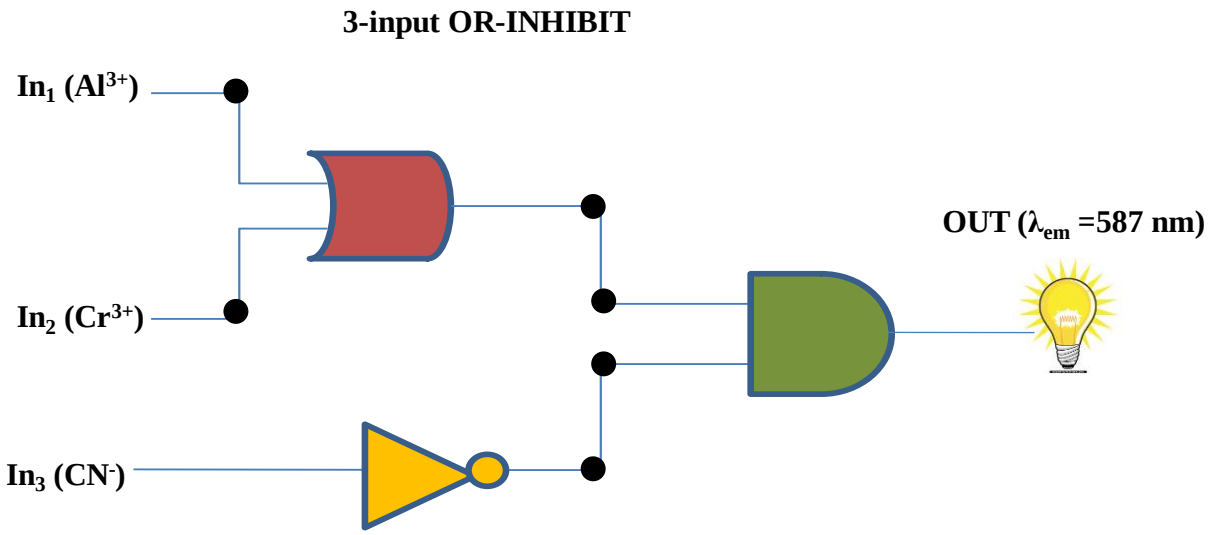

Truth Table: for 3-input OR-INHIBIT logic circuit

In_1 (Al^{3+})	In_2(Cr^{3+})	In_3 (CN^-)	OUT_2 (λ_{em}=587 nm)
0	0	0	0
1	0	0	1
1	1	0	1
1	0	1	0
0	1	0	1
0	1	1	0
0	0	1	0
1	1	1	0

Figure 83: Formation of 3-input OR-INHIBIT logic function having output at 587 nm alongwith truth table showing combination of different inputs and their subsequent outputs.

4.2.5. Conclusion:

A cyanuric chloride attached to three rhodamine B ethylenediamine units was synthesized and its photophysical properties were evaluated. It displayed a dual change i.e. colorimetric as well as the fluorescence turn-on in presence of Al^{3+} and Cr^{3+} ions. Probe **6** was found to be highly selective towards binding with Al^{3+} ions in 1:1 stoichiometry having binding constant of 3.8×10^5 M^{-1}. The increase in the quantum efficiency from 0.092 (probe **6**) to 0.37 (complex **6.Al^{3+}**) was in accordance with the enhancement obtained in emission studies on complexation. Further, the antibacterial activity of probe **6** revealed that it had the capability of inhibiting bacterial growth of *Bacillus subtilis* and *Acinetobacter calcoacetius* bacteria. The reversible switch of complex **6.Al^{3+}** was also considered for construction of molecular logic functions considering emission response at 587 nm.

4.2.6. Experimental section:

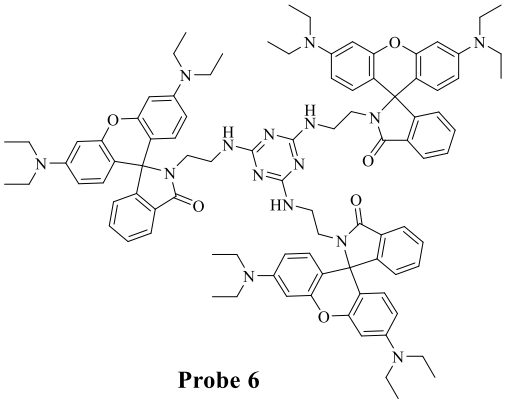

Probe 6

Synthesis of probe **6:** Cyanuric chloride (0.1 g, 0.53 mmol) and Rhodamine B ethylenediamine (0.7 g, 1.4 mmol) were dissolved in 30 mL ethanol in 100 mL flask using 10 equiv. of TEA as base. The contents were refluxed for 24 hours at 70°C. The reaction was monitored through TLC in $CHCl_3$: CH_3OH (9:1). On completion of the reaction the reaction mixture was filtered and the filterate was concentrated to get light brown colour solid. Percentage yield = 75 (0.60 g) M.pt = >300°C,**^{1}H NMR** (400 MHz, $CDCl_3$) δ 7.89 (m, 3H, ArH), δ 7.43 (m, 6H, ArH), δ 7.07 (m, 2H, ArH), δ 6.45-6.13 (m, 19H, ArH), δ 3.27 (m, 30H, -CH_2), δ 3.16 (m, 6H, -CH_2), δ 1.09 (m, 36H, -CH_3); **^{13}C NMR** (400 MHz, $CDCl_3$) δ 1.67.9 (-C=O), δ 163.2 (-C=N), δ 154.1 (C-O-C), (δ): 153.8, 148.3, 138.1, 132.8, 131.3, 129.2, 128.5, δ 123.7, 123.1, 108.0, 105.6, 97.8, 65.0 (spirocyclic C), 59.7, 44.2, 41.1, 12.5. **MS (ESI):** m/z at 1529.83 (M^++1).

Chapter 4: Conclusion

In this chapter we have studied the effect of presence different number of rhodamine units, on the ion sensing ability of probes. Hence, we have synthesized and characterized the colorimetric and fluorescence "*off-on*"rhodamine based dipodal and tripodal systems. The presence of multiple chelating sites as we go from probe **5** to probe **6** increased which further increased the binding strength and gave lower detection limits. The reversible fluorescence switch of both the probes formed the basis for construction of molecular logic functions. The biological applicability of probe **6** was also studied and it was found to have anti bacterial activity.

Probe	**Sensing of ion**	**Medium**	**Association constant**	**Detection limit**
Probe**5**	Al^{3+}	CH_3OH	$9.3 \times 10^4\ M^{-1}$	2.9×10^{-7} M
Probe**6**	Al^{3+}	CH_3OH	$3.8 \times 10^5\ M^{-1}$	43×10^{-9}M

Conclusion of thesis:

We have developed several chromo-fluorescent probes for sensing of specific ions. All the probes possessed the capability of visual eye sensing and gave fluorescence "*off-on*" switch for particular ion. Phenalenedicarbonitrile and their derivative have been explored less for their sensing capabilities hence, we have synthesized and explored the unique sensing behavior of two phenalene based probes with different chromophoric units attached, in mixed aqueous media. Rhodamine B derivative when attached to highly electron deficient precursor i.e. Phenalenedicarbonitrile led to unique fluorescence and colorimetric "*on-off*" phenomenon. Further, we have synthesized rhodamine based probes (varying in the number of rhodamine units present) and explored their sensing behavior in aqueous/ mixed aqueous mediums. The presence of more rhodamine units provided multiple interaction sites for the ion to bind which led to improvement in the limit of detection of the probes. For the practical application of the probes we explored the capability of the probes to detect ions in industrial waste water and tap water. In addition to real-time sampling we used our probe for intracellular sensing of ions by using A549 cervical cancer line cells as well as we explored the anti-bacterial activity of probe. Furthermore, we even used our probes for construction of various molecular circuits and devices such as encoders, decoder, memory devices and keypad lock.

Future Prospective:

- Sensors having even high sensitivities can be synthesized for water quality assessments and could be efficient used in sensing of ions in biological systems as well.
- Development of additional novel ion sensors based on small rigid π-conjugated systems like phenalenedicarbonitriles.
- Multipodal systems having easy synthetic construction, high selectivity and sensitivity for particular ions in aqueous medium can be developed.

References:

1. A. T. Wright and E. V. Anslyn, *Chem. Soc. Rev*., 2006, **35**, 14-38.
2. V. Amendola and L. Fabbrizzi, *Chem. Commun*., 2009, 513-531.
3. L. Prodi, *New J. Chem*., 2005, **29**, 20-31.
4. J. Yoon, S. K. Kim, N. J. Singh and K. S. Kim, *Chem. Soc. Rev*., 2006, **35**, 355-360.
5. A. W. Czarnik, Fluorescent Chemosensors for Ion and Molecule Recognition, 1994, **22**, 405-406.
6. H. Kobayashi, M. Ogawa, R. Alford, P. L. Choyke and Y. Urano, *Chem. Rev*., 2010, **110**, 2620-2640.
7. E. J. New, *ACS Sensors*, 2016, **1**, 328–333.
8. S. M. Ng, M. Koneswaran and R. Narayanaswamy, *RSC Adv*., 2016, **6**, 21624–21661.
9. C. J. Chang, T. Gunnlaugsson and T. D. James, *Chem. Soc. Rev*., 2015, **44**, 4484–4486.
10. S. Chowdhury, B. Rooj, A. Dutta and U. Mandal, *J. Fluoresc*., 2018, **28**, 999-1021.
11. H.Zhu, J. Fan, B. Wang and X. Peng, *Chem. Soc. Rev.*, 2014, **44**, 4337-4366.
12. B. Valeur, Molecular Fluorescence, Digital Encyclopedia of Applied Physics, 2003, 477-531.
13. B. X. Shen and Y. Qian, *Sens. Actuators B: Chem*., 2017, **239**, 226-234.
14. D. Cheng, W. Zhao, H. Yang, Z. Huang, X. Liu and A. Han, *Tetrahedron Lett*., 2016, **57**, 2655- 2659.
15. S. Saha, P. Mahato, M. Baidya, S. K. Ghosh and A. Das, *Chem. Commun*., 2012, **48**, 9293-9295.
16. Y. J. Gong, X. B. Zhang, C. C. Zhang, A. L. Luo, T. Fu, W. Tan, G. L. Shen and R. Q. Yu, *Anal. Chem*., 2012, **84**, 10777-10784.
17. M. Sulka, A. N. Kursunlu, B. Girgin, O. O. Karakus and E. Guler, *J.Photochem. Photobiol. A: Chem.*, 2017, **349**, 129-137.
18. H. C. Xia, X. H. Xu, and Q. H. Song, *Anal. Chem*., 2017, **89**, 4192-4197.
19. L. Tong and Y. Qian, *J. Photochem. Photobiol. A: Chem.*, 2019, **368**, 62-69.
20. H. Sharma, J. M. White, J. Lin, E. J. New and F. M. Pfeffer, *Sens. Actuators B: Chem*., 2019, **300**, 126825-126833.

21. N. Wanichacheva, O. Hanmeng, S. Kraithong and K. Sukrat, *J. Photochem. Photobiol*. *A: Chem.*, 2014, **278**, 75-81.
22. H. N. Kim, M. H. Lee, H. J. Kim, J. S. Kim and J. Yoon, *Chem. Soc. Rev*., 2008, **37**, 1453-1744.
23. Y. Xiao, F. Liu, X. Qian and J. Cui, *Chem. Commun*., 2005, 239-241.
24. Y. Xiao, F. Liu, Z. Chen, W. Zhu, Y. Xu and X. Qian, *Chem. Commun*., 2015, **51**, 6480-6488
25. E. Noelting and K. Dziewonsky, *Ber. Dtsch. Chem. Ges*., 1905, **38**, 3516.
26. V. Dujols, F. Ford and A. W. Czarnik, *J. Am. Chem. Soc*., 1997, **119**, 7386-7387.
27. Y. Wang, H.Q. Chang, W.N. Wu, X.J. Mao, X.L. Zhao, Y. Yang, Z.Q. Xu, Z.H. Xu andL. Jia, *J. Photochem. Photobiol*. *A: Chem.*, 2017, **335**, 10–16.
28. R. Arumugaperumal, V. Srinivasadesikan, M.C. Lin, M. Shellaiah, T. Shuklaa and H.C. Lin, *RSC Adv*., 2016, **6**, 106631–106640.
29. Y. Yang, C.Y. Gao, T. Li and J. Chen, *ChemistrySelect*, 2016, **15**, 4577–4581.
30. A. K. Mahapatra, S. Mondal, S. K. Manna, K. Maiti, R. Maji, Md. R. Uddin, S. Mandal, D. Sarkar, T. K. Mondal and D. K. Maiti, *Dalton Trans*., 2015, **44**, 6490–6501.
31. J. C. Qin, J. Yan, B. D. Wang and Z. Y. Yang, *Tetrahedron Lett*., 2016, **57**, 1935–1939.
32. H. Zheng, X. Q. Zhan, Q. N. Bian and X. J. Zhang, *Chem. Commun*., 2013, **49**, 429–447.
33. F. Abebe, P. Perkins, R.Shaw and S. Tadesse, *J. Mol. Struct*., 2020, **1205**, 127595-127601.
34. A. Rai, A.K. Singh, A.K. Sonkar, A. Prakash, J. K. Roy, R. Nagarajan and L. Mishra, *Dalton Trans*., 2016, **45**, 8272–8277.
35. J. Hu, Z. Hu, Z. Chen, H.W. Gao and K. Uvdal, *Anal. Chim. Acta*, 2016, **919**, 85–93.
36. A. Ghosh, A. Sengupta, A. Chattopadhyay and D. Das, *RSC Adv*., 2015, **5**, 24194–24199.
37. A. Kumar, C. Kumari, D. Sain, S. K. Hira, P. P. Manna and S. Dey, *ChemistrySelect*, 2017, **10**, 2969–2974.
38. X. Q. Chen, T. Pradhan, F. Wang, J. S. Kim and J. Yoon, *Chem. Rev*., 2012, **112**, 1910–1956.
39. R. Lenk, A. Tessier, P. Lefranc, V. Silvestre, A. Planchat, V. Blot, D. Dubreuil and J. Lebreton, *J. Org. Chem*., 2014, **20**, 9754-61
40. Y. Xiang and A. Tong, *Org. Lett*., 2006, **8**, 1549-1552.

41. S. Sahana, G. Mishra, S. Sivakumar and P. K. Bharadwaj, *J. Photochem. Photobiol. A:Chem*., 2018, **351**, 42-49.
42. V. Bhalla, N. Sharma, N. Kumar and M. Kumar, *Sens. Actuators B: Chem*., 2013, **178**, 228–232.
43. C. Y. Li, C. X. Zou, Y. F. Li, J. L. Tang and C. Weng, *Dyes Pigm*., 2014, **104**, 110–115.
44. N. R. Chereddy, K. Suman, P. S. Korrapati, S. Thennarasu and A. B. Mandal, *Dyes Pigm*., 2012, **95**, 606–613.
45. Z. Zhou, M. Yu, H. Yang, K. Huang, F. Li, T. Yi and C. Huang, *Chem Commun*., 2008, 3387-3389.
46. K. Huang, H. Yang, Z. Zhou, M. Yu, F. Li, X. Gao, T. Yi and C. Huang, *Org Lett*., 2008, **10**, 2557–2560.
47. A. J. Weerasinghe, A. N. Oyeamalu, F. A. Abebe, A. R. Venter and E. Sinn, *J. Fluoresc*., 2016, **26**, 891-898.
48. N. R. Chereddy, S. Thennarasu and A. B. Mandal, *Dalton Trans*., 2012, **41**, 11753–11759.
49. L. Huang, F. Hou, J. Cheng, P. Xi, F. Chen, D. Bai and Z. Zeng, *Org. Biomol. Chem*., 2012, **10**, 9634-9638.
50. Z. Zhang, C. Deng and H. Song, Inorg. *Chem. Commun*., 2018, **95**, 56-60.
51. S. Saha, P. Mahato, G. U. Reddy, E. Suresh, A. Chakrabarty, M. Baidya, S. K. Ghosh and A. Das, *Inorg. Chem*., 2011, **51**, 336–345.
52. J. Huang, Y. Xu and X. Qian, *Dalton Trans*., 2014, **43**, 5983–5989.
53. D. Xue, C. Zheng, C. Fan, G. Liu and S. Pu, *J. Photochem. Photobiol.A: Chem.*, 2015, **303-304**, 59-66.
54. S. Adhikari, S. Ta, A. Ghosh, S. Guria, A. Pal, M. Ahir, A. Adhikary, S. K. Hira, P. P. Manna and D. Das, *J. Photochem. Photobiol. A: Chem*., 2019, **372**, 49-58.
55. P. Mahato, S. Saha, E. Suresh, R. D. Liddo, P. P. Parnigotto, M. T. Conconi, M. K. Kesharwani, B. Ganguly and A. Das, *Inorg. Chem*., 2012, **51**, 1769–1777.
56. A. J. Weerasinghe, C. Schmiesing and E. Sinn, *Tetrahedron Lett*., 2009, **50**, 6407-6410.
57. L. Tang, Y. Li and J. Qian, *J. Chem. Res.*, 2010, 216-218.
58. P. Xie, F. Guo, Y. Xiao, Q. Jin, D. Yao and Z. Huang, *J. Lumin*., 2013, **140**, 45-50.
59. V. K. Gupta, N. Mergu and A. K. Singh, *Sens. Actuators B: Chem.*, 2015, **220**, 420-432.

60. Y. Lei, Y. Su and J. Huo, *Spectrochim. Acta. A*, 2011, **83**, 149-154.
61. O. P. Sunnapu, N. G. Kotla, B. Maddiboyina, G. S. Asthana, J. Shanmugapriya, K. Sekar, S. Singaravadivel and G. Sivaraman, *Sens. Actuators B: Chem.*, 2017, **246**, 761-768.
62. H. Liu, X. Wan, T. Liu, Y. Li and Y. Yao, *Sens. Actuators B: Chem.*, 2014, **200**, 191-197.
63. Y. Yang, K. Yu, L. Yang, J. Liu, K. Li and S. Luo, *Sensors*, 2015, **15**, 49-58.
64. Z. Yang, M. She, B. Yin, J. Cui, Y. Zhang, W. Sun, J. Li and Z. Shi, *J. Org. Chem*., 2011, **77**, 1143–1147.
65. Y. Hu, J. Wang, L. Long and X. Xiao, *Luminescence*, 2015, **31**, 16-21.
66. J. C. Qin, Z. Y. Yang, G. Q. Wang and C. R. Li, *Tetrahedron Lett*., 2015, **35**, 5024-5029.
67. L. He, V. L. So and J. H. Xin, *Sens. Actuators B: Chem*., 2014, **192**, 496-502.
68. C. R. Lohani, J. M. Kim, S. Y. Chung, J. Yoon and K. H. Lee, *Analyst*, 2010, **135**, 2079-2084.
69. S. Goswami, S. Paul and A. Manna, *RSC Adv*., 2013, **3**, 10639-10643.
70. M. Yu, R. Yuan, C. Shi, W. Zhou, L. Wei and Z. Li, *Dyes Pigm*., 2013, **99**, 887-894.
71. F. Yan, M. Wang, D. Cao, N. Yang, Y. Fu, L. Chen and L. Chen, *Dyes Pigm*., 2013, **98**, 42-50.
72. Z. Li, Q. Hu, C. Li, J. Dou, J. Cao, W. Chen and Q. Zhu, *Tetrahedron Lett*., 2014, **55**, 1258-1262.
73. A. Dhara, A. Jana, S. K. Mandal, A. R. Khuda-Bukhsh, N. Guchhait and S. K. Kar, *Inorg. Chimica. Acta*, 2014, **423**, 454-461.
74. A. Sahana, A. Banerjee, S. Lohar, B. Sarkar, S. K. Mukhopadhyay and D. Das, *Inorg. Chem*., 2013, **52**, 3627-3633.
75. N. R. Chereddy, P. Nagaraju, M. V. N. Raju, V. R. Krishnaswamy, K. P. Sai, P. Bangal and J. R. Vaidya, *Biosens. Bioelec*., 2015, **68**, 749-756.
76. S. Samanta, T. Ray, F. Haque and G. Das, *J. Lumin*., 2016, **171**, 13-18.
77. N. R. Chereddy, M. V. N. Raju, B. M. Reddy, V. R. Krishnaswamy, P. S. Korrapati, B. J. M. Reddy and V. J. Rao, *Sens. Actuators B: Chem.*, 2016, **237**, 605-612.
78. H. Kilic and E. Bozkurt, *J. Photochem. Photobiol. A: Chem.*, 2018, **363**, 23-30
79. R. Alam, R. Bhowmick, A. S. M. Islam, A. Katarkar, K. Chaudhuri and M. Ali, *New J. Chem*., 2017, **41**, 8359-8369
80. S. Dey, S. Sarkar, D. Maity and P. Roy, *Sens. Actuators B*: *Chem.*, 2017, **246**, 518-534.

81. A. Roy, S. Das, S. Sacher, S. K. Mandal and P. Roy, *Dalton Trans*., 2019, **48**, 17594-17604.
82. V. K. Gupta, N. Mergu, L. K. Kumawat and A. K. Singh, *Talanta*, 2015, **144**, 80-89.
83. J. W. Jeong, B. A. Rao and Y. A. Son, *Sens. Actuators B: Chem.*, 2015, **208**, 75-84.
84. Tang, G. L. Zhang and W. S. Liu, *Sens. Actuators B: Chem.*, 2017, **253**, 1055-1062.
85. S. Mondal, C. Bandyopadhyay and K. Ghosh, *Supramol. Chem*., 2019, **31**, 1-8.
86. A. Roy, U. Shee, A. Mukherjee, S. K. Mandal and P. Roy, *ACS Omega*, 2019, **4**, 6864-6875.
87. S. Mabhai, M. Dolai, S. K. Dey, A. Dhara, S. M. Choudhary, B. Das and A. Jana, *Spectrochim. Acta A*, 2019, **219**, 319-332.
88. F. Liu, X. Qian, J. Cui, Y. Xiao, R. Zhang and G. Li, *Bioorg. Med. Chem*., 2006, **14**, 4639-4644.
89. M. Zhang, M. Yu, F. Li, M. Zhu, M. Li, Y. Gao, L. Li, Z. Liu, J. Zhang, D. Zhang, T. Yi and C. Huang, *J. Am. Chem. Soc*., 2007, **129**, 10322-10323.
90. S. Wang, S. Xu, G. Hu, X. Bai, T. D. James and L. Wang, *Anal. Chem*., 2016, **88**, 1434-1439.
91. A. Coskun, M. D. Yilmaz and E. U. Akkaya, *Tetrahedron Lett*., 2006, **47**, 3689-3691.
92. L. Q. Xiong, M. X. Yu, M. J. Cheng, M. Zhang, X. Y. Zhang, C. J. Xu and F. Y. Li, *Mol. BioSyst*., 2009, **5**, 241-243.
93. (a) Z. Zhang, Y. Liu, T. Song, Z. Xue, X. Shen, F. Liang, Y. Zhao, Z. Li and H. Sheng, *Br. J. Cancer*, 2013, **108**, 1870-1878; b) Z. Zhang, H. Yang, G. Wu, Z. Li, T. Song and X. Li, *Eur. J. Med. Chem*.,2011, **46**, 3909-3916; c) T. Song, Q. Chen, X. Li, G. Chai and Z. Zhang,*J. Med. Chem*., 2013, **56**, 9366-9367.
94. (a) S. Derinkuyu, K. Ertekin, O. Oter, S. Denizalti and E. Cetinkaya, *Anal. Chim. Acta*,2007, **588**, 42–49; (b) J. L. Tan, M. X. Zhang, F. Zhang, T. T. Yang, Y. Liu, Z. B. Li and H. Zuo, *Spectrochim. Acta A*, 2015, **140**, 489-494.
95. (a) R. F. Kubin and A. N. Fletcher, *J. Lumin*., 1952, **27**, 455-462; (b) S. Dey, S. Sarkar, D. Maity and P. Roy, *Sens. Actuators B: Chem*., 2017, **246**, 518-534; (c) J. V. Herraez and R. Belda, *J. Sol. Chem*., 2006, **35**, 1315-1328.
96. R. R. Dash, A. Gaur and C. Balomajumder, *J. Haz. Mat*., 2009, **163**, 1-11

97. A. B. Othman, J. W. Lee, J. S. Wu, J. S. Kim, R. Abidi, P. Thuery, J. M. Strub, A. V. Dorsselaer and J. Vicens, *J. Org. Chem*., 2007, **72**, 7634-7640.
98. S. B. Maity and P. K. Bharadwaj, *Inorg. Chem*., 2013, **52**, 1161-1163.
99. S. Hazra, C. Bodhak, S. Chowdhury, D. Sanyal, S. Mandal. K. Chattopadhyay and A. Pramanik, *Anal. Bioanal. Chem*., 2019, **41**, 1143-1157.
100. A. Dhara, A. Jana, N. Guchhait, P. Ghosh and S. K. Kar, *New J. Chem*., 2014, **38**, 1627.
101. D. Tong, H. Duan, J. Wang, Z. Yang and Y. Lin, *Sens. Actuators B: Chem*., 2014, **195**, 80-84
102. Y. He, Y. Chen, C. Li and H. Cui, *Chem. Commun*., 2014, **50**, 7994-7997.
103. S. R. Dighade, S. D. Patil, M. M. Chincholkar and N. R. Dighade, *Asian J. Chem*., 2003, **15**, 1184-1186.
104. A. Solankee and I. Thakor, *Indian J. Chem*., 2006, **45B**, 517-522.
105. A. Solanki and J. Patel, *Indian J. Chem*., 2004, **43B**, 1580-1584.
106. B.B. Baldaniya and P.K. Patel, *E. J. Chem*., 2009, **6**, 673-680

List of Publications:

1. Ruhi Mehta and Vijay Luxami*, "Rhodamine-anthraquinone based dyad for rapid and selective sensing of Al^{3+} with potential application for real-time sampling and molecular logic circuits." *Inorg. Chem. Commun*., 2020, **115**, 107863

2. Ruhi Mehta, Pawandeep Kaur, Diptiman Choudhary, Kamaldeep Paul and Vijay Luxami*, "Al^{3+} induced hydrolysis of rhodamine-based Schiff-base: Applications in cell imaging and ensemble as CN^- sensor in 100 % aqueous medium" *J. Photochem. Photobiol. A: Chem*., 2019, **380**, 111851

3. Ruhi Mehta, Vijay Luxami*, "A novel '*on-off*' rhodamine derivative for colorimetric and sensitive detection of CN^- and its application as encoder, decoder and molecular keypad lock" *ChemistrySelect*, 2020, **5**, 13429-13438

4. Ruhi Mehta, Vijay Luxami*, "A Phenalenedicarbonitrile Based Sensor for Selective Estimation of CN^- ions in Industrial Waste" *J. Mol. Struct*., 2021, **1234**, 130077

Conferences Attended:

• Presented poster on "Rhodamine-based Schiff-base for selective and sequential detection of Al^{3+} and CN^- ions" in 10^{th} National conference on Chemical and Environmental Sciences: Innovations and Advances-2018, Punjabi University, Patiala.

• Presented poster on "Rhodamine-anthraquinone dyad for selective detection of Al^{3+} ions at7.04" in National Conference on Futuristic Aspects in Chemical Science and Technology, Punjab University, Chandigarh (2018).

SUMMARY

Since past few decades, the development of ion selective chromo-fluorescent molecules has attracted attention due to their potential and wide practical applications. These molecules have applicability in designing molecular switches and logic devices, optical data storing systems, use in medicinal and biological sciences[1-4] as well as for formulation of chemosensors[5-9]. In addition to fluorescence changes, the colorimetric changes allow on-site and inexpensive ways to detect presence of ions in real-time samples. Numerous ion sensing chromo-fluorescent compounds have been fabricated by using small molecules like BODIPY, coumarin, naphthalimide, fluorescein, rhodamine etc.[10-17] All these molecules have worked as excellent fluorophore for the preparation of fluorescent chemosensors because of π-conjugated skeletons and rigid structure. Rhodamine has always provided an ideal framework for formulating ion sensors due to its high quantum yields, large extinction coefficients and unique photophysical properties.[18] Another precursor having excellent spectral properties, structural rigidity and easy synthetic pathways for their preparation isis1-oxo-1*H*-phenalene-2,3-dicarbonitrile (phenalenedicarbonitrile).[19,20] In present research work we have developed few chromo-fluorescent probes for sensing of specific ions. All the probes possessed the capability of visual eye sensing and gave fluorescence "*off-on*" switch for particular ion. Phenalenedicarbonitrile and their derivative have been explored less for their sensing capabilities hence, we have synthesized and explored the unique sensing behavior of two phenalene based probes attached with different chromophoric units, in mixed aqueous mediums. Rhodamine B derivative when attached to highly electron deficient precursor i.e. Phenalenedicarbonitrile led to unique fluorescence and colorimetric "*on-off*" phenomenon. Further, we have synthesized rhodamine based probes (varying in the number of rhodamine units present) and explored their sensing behavior in aqueous/ mixed aqueous mediums. The presence of more number of rhodamine units provided multiple interaction sites for the ion to bind which led to improvement in the limit of detection of the probes. For the practical application of the probes we explored the capability of the probes to detect ions in industrial waste water and tap water. In addition to real-time sampling we used our probe for intracellular sensing of ions by using A549 cervical cancer line cells as well as we explored the anti-bacterial activity of probe. Furthermore, we even used our probes for

construction of various molecular circuits and devices such as encoders, decoder, memory devices and keypad lock.

CHAPTER 2: Synthesis and evaluation of photophysical properties of phenalene-dicarbonitrile derivatives for CN^- sensing

General introduction: In this chapter we have discussed the synthesis and photophysical properties of two phenaledicarbonitrile based moieties prepared by introduction of different amine derivatives, by following oxidative nucleophilic substitution reaction of aromatic hydrogen i.e. S_NAr^H. Phenalenedicarbonitrile has a planar and rigid π-conjugated structure having fluorescence emission at longer wavelength. Its derivatives have been widely explored for their anti-cancer and other biological activities, still they have been explored less in the field of ion sensing. So, in order to find out the sensing behavior and to explore the photophysical properties of phenalenedicarbonitrile due to the presence of different substituents, we have categorized this chapter into two parts:

2.1. Phenalenedicarbonitrile based colorimetric and fluorescent probe for detection of CN^- in industrial effluent

Probe **1** has been synthesized by linking 4-aminothiophenol to electron deficient phenalenedicarbonitrile unit by following S_NAr^H reaction which is also classified under green chemistry as the aromatic proton and not any other leaving group has been replaced by the aminothiophenol unit. The synthesized probe **1** was further characterized by ^{1}H-NMR, ^{13}C-NMR and mass spectroscopy. The effect of various anions was further studied in CH_3CN-H_2O (9:1 v/v). Probe **1 (**20 μM, CH_3CN-H_2O (9:1 v/v)) originally showed a pink color and was non-emissive when observed under UV-lamp. Upon addition of various anions *viz.* F^-, Cl^-, Br^-, I^-, SCN^-, $H_2PO_4^-$, HSO_4^-, NO_3^- and AcO^- it did not show any colorimetric change but on addition of CN^- the pink color bleached out and it gave a yellow emission under UV light. Henceforth, we further investigated its spectral behavior in presence of various anions. Probe **1** gave its absorption maxima centered at 527 nm and weak emission at 567 nm but, the presence of CN^-led to decrease in the intensity of absorption band at 527 nm and a new band of low intensity at 454 nm was formed. Whereas, the emission intensity increased in the presence of CN^- at 567 nm along with glowing yellow emission under UV light. Binding mechanism of CN^- with probe

1was analyzed through ^{1}H-NMR titration and IR spectroscopy. The ^{1}H-NMR spectra of probe **1** in presence of 1 equiv. of CN^- gave the formation of a new singlet peak at δ 4.75 ppm and on adding D_2O this peak diminished which clearly suggest the formation of cyanohydrins due to attack of CN^- on –C=O of phenalenedicarbonitrile. This proposed mechanism was further supported by IR spectroscopy as on adding CN^- the –C=O peak at 1737 cm^{-1} diminished and an intense peak at 1640.6cm^{-1} corresponding to –C-O stretching was attained along with formation of –OH peak at 3454-3558 cm^{-1} which asserted that CN^- ions attack chemodosimetrically on the -C=O of probe **1** to form cyanohydrins compound. Probe **1** was also used for detection of CN^- in industrial waste. The fluorescence switch '*off-on*' behavior of probe **1** in presence of a specific ion, was used to design a 1-to-2 decoder.

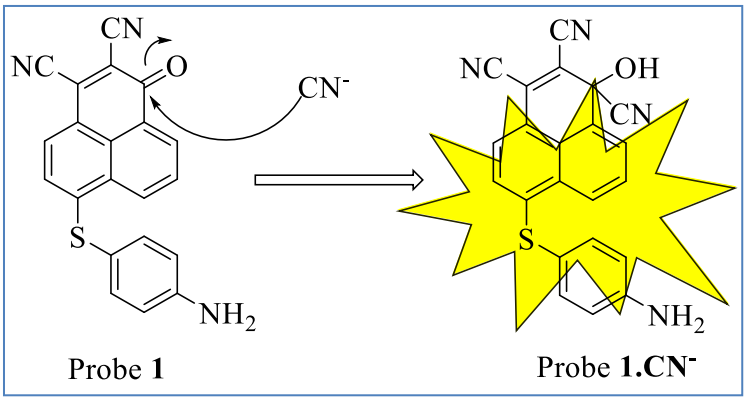

Figure 1: Binding mechanism of probe **1** with CN^- and its application as 1-to-2 decoder.

2.2. A novel '*on-off*' rhodamine based sensor for colorimetric detection of CN^- and its application as encoder-decoder and molecular keypad lock

In this section we have discussed the synthesis, characterization and ion sensing behavior of another phenalenedicarbonitrile based probe **2**developed by substituting the aromatic proton of phenalenedicarbonitrile precursor by rhodamine B ethylenediamine unit. Probe **2** was originally purple in color and gave a bright pink emission under UV light. Various metal ions such as Na^+, K^+, Mg^{2+}, Ca^{2+}, Al^{3+}, Pb^{2+}, Cr^{3+}, Fe^{2+}, Co^{2+}, Ni^{2+}, Cu^{2+}, Zn^{2+}, Hg^{2+} and $Pd^{2+}$and anions such as F^-, Cl^-, Br^-, I^-, SCN^-, $H_2PO_4^-$, HSO_4^-, NO_3^-, OAc^- and CN^- were added into probe **2** (20 µM, CH_3OH-H_2O (4:1 v/v) *pH* 7.04) to find out any visual changes. It was observed that probe **2** gave colorimetric change i.e. bleaching out of purple color, in presence of only CN^- ions and when observed under UV lamp it was found to be non-emissive. Following this observation we studied

its UV-Vis and fluorescence response towards various ions. Probe **2** (20 µM, CH_3OH-H_2O (4:1 v/v) *pH* 7.04) displayed an absorption band at 577 nm with shoulder at 520 nm and fluorescence band at 593 nm, which are the characteristic spectral behavior of rhodamine in spirolactam ring open form. This observation was ascribed to the intramolecular charge transfer (ICT) from rhodamine B unit to electron deficient phenalenedicarbonitrile unit. Amongst all the ions only CN^- ions caused significant spectral change by giving a ratiometric absorption spectral response. The presence of CN^- ions hindered the ICT process of probe **2** and showed a blue shift in absorption band of probe **2** with formation of new band at 488 nm and decrease in emission intensity was also observed. From the spectral changes it could be inferred that the ring closure phenomenon occurred in presence of CN^-. Phenalenedicarbonitrile being an electron deficient precursor gets charge/energy transfer from rhodamine B moiety. Whereas, upon exposing probe **2** to CN^-, the nucleophilic addition at –C=O of phenalenedicarbonitrile unit satisfies the charge deficiency of the phenalenedicarbonitrile unit and the charge/energy transfer from rhodamine unit comes to a halt and thus closes the spirolactam ring. The absorption reversible switch due to opening and closing of spirolactam ring of rhodamine and fluorescence reversibility of **2.CN**$^-$ complex has been achieved with Fe^{3+} ions. This '*off-on*' fluorescence switch formed the basis for the construction of multiple molecular logic circuits like encoder, decoder and a molecular logic circuit. The sequential addition of ions (CN^- and Fe^{3+}) into probe **2** and their fluorescence behavior was further used to construct a molecular keypad lock.

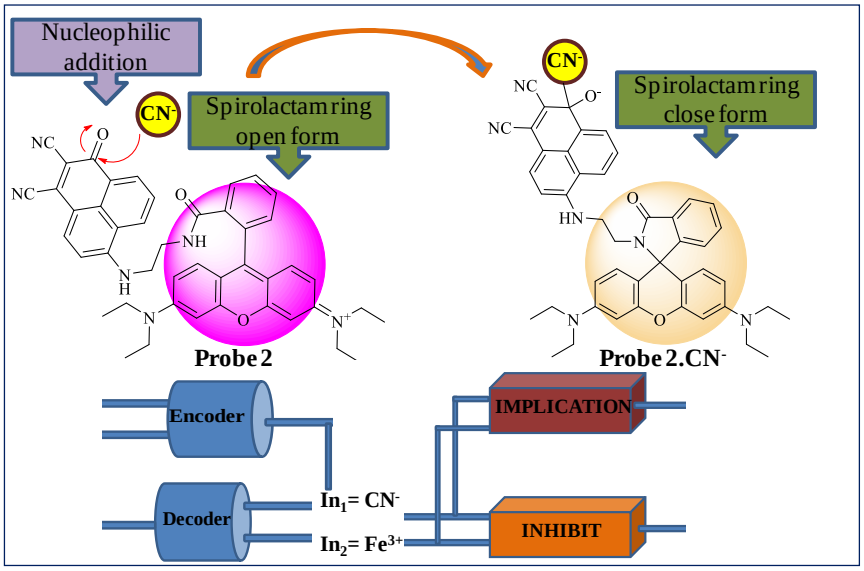

Figure 2: Binding mechanism of probe **2** with CN^- and its application as decoder, encoder and IMP-INH logic circuit.

CHAPTER 3: Rhodamine based hybrids and their sensing behavior: application for sensing of Al^{3+} in real-time samples

General introduction: In this chapter we have synthesized two rhodamine based sensors and studied their sensing behavior by changing the number of rhodamine units attached to different units. Numerous rhodamine based sensors have been developed for sensing of various transition and heavy metal ions but, sensing of Al^{3+} in aqueous/mixed aqueous mediums has always faced problems due to its strong hydration ability and poor coordination. Considering all these facts we have synthesized, characterized and studied the behavior of two rhodamine based sensors which selectively formed chelate with Al^{3+} ions in mixed aqueous and 100% aqueous medium.

3.1. Rhodamine-anthraquinone based dyad for sensing of Al^{3+} in real time sample and its application in generation of molecular logic device

A new rhodamine-anthraquinone based '*off-on-off*' colorimetric and fluorimetric sensor was designed, synthesized and characterized by ^{1}H, ^{13}C NMR and Mass spectrometric techniques. It was found out to be sensitive and selective towards Al^{3+} without any interference from other competitive metal ions. A visual color change from faint red to pink was also observed in the presence of only Al^{3+}. Probe **3** did not display any emission but on treating with Al^{3+}it gave a fluorescence turn-*on* response along with fluorescence enhancement at 587 nm. The chromo-fluorescent response of probe **3** towards Al^{3+} asserted the metal induced spirolactam ring opening mechanism of rhodamine. Probe **3** could detect Al^{3+} in wide *pH* range of 7-11. The complex **3.Al^{3+}** was further tested for its reversibility by treating it with different anions. The emission of **3.Al^{3+}** was quenched only in the presence of CN^{-} ions. Based on this result, molecular logical circuits were constructed with a combination of AND, OR, NOT, NOR gates. The capability of probe **3** to detect Al^{3+} in real time sample was also achieved.

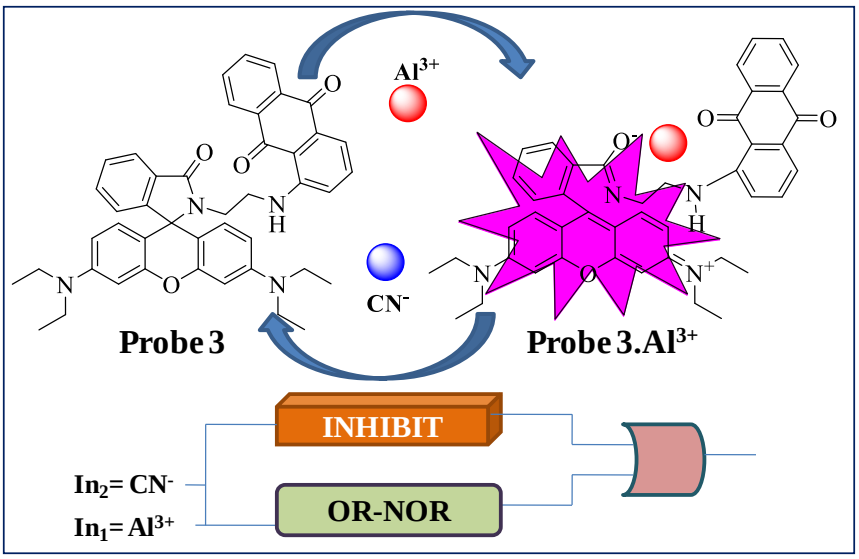

Figure 3: Binding mechanism of probe **3** with $Al^{3+}$and its use in construction molecular logic circuits.

3.2. Rhodamine-terephthaldehyde based Schiff base Al^{3+} sensor and its ensemble for sensing of CN^- in 100% aqueous medium: Application in live cell imaging

A novel Schiff base having terephthaldehyde appended with two rhodamine units has been synthesized, which exhibited fluorogenic and chromogenic response on binding with Al^{3+} ions in 100% aqueous system at *pH* 7.04. The binding of probe **4** with Al^{3+} ions was not hindered by the presence of background metal ions. Probe **4** was found to be capable of sensing Al^{3+} in *pH* range of 6-10. The binding of probe **4** with Al^{3+} led to hydrolysis on one side resulting in formation of free –CHO group which was further tested for its sensing ability. The ensemble **4.Al^{3+}** and proved out to be CN^- sensor accompanied by colorimetric as well as fluorimetric changes.

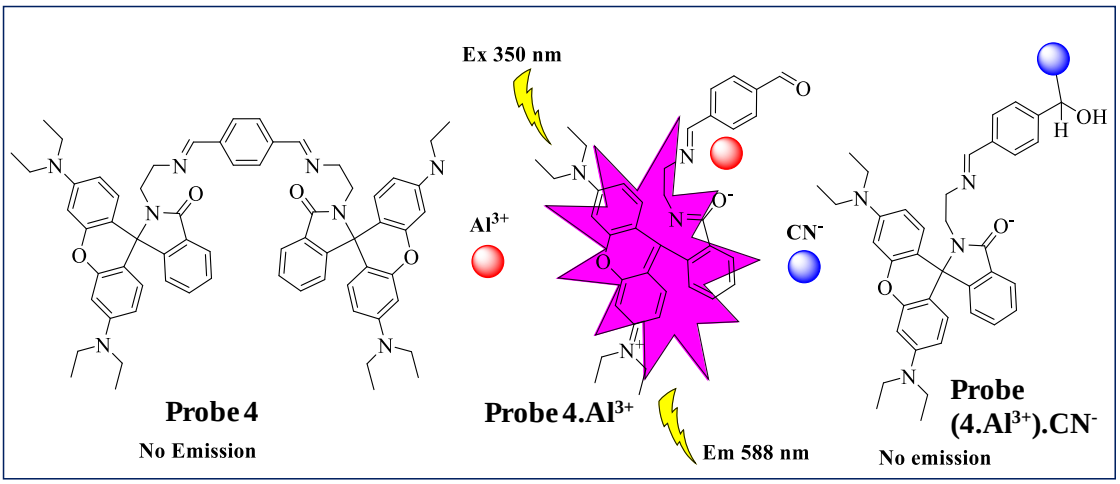

Figure 4: Binding mechanism of probe **4** with Al^{3+} and of probe (**4.Al^{3+}**) ensemble with CN^-

CHAPTER 4 Synthesis of rhodamine based hybrid molecules and the quantification of optical signals for construction of logic gates

General introduction: The synthesis of probe **4** prompted us to synthesize dipodal and tripodal systems as these systems have multiple chelating sites. In chapter we have discussed the synthesis evaluation of two probes having more than on rhodamine unit. The dipodal and tripodal systems have numerous binding sites due to which they have the capability of forming strong complexes with metal ions. Hence, we designed probe **5** and **6** keeping in mind few consideration 1) rhodamine has suitable binding groups which bind with specific ions 2) presence of more than one rhodamine unit will provide number of chelating sites and the sensor will have high binding affinity towards metal ion 3) the formation of a cavity will ensure selective binding as it will strongly bind to metal ions having smaller ionic radii 4) the rhodamine ring opening and closing process can generate '*on-off*' colorimetric and fluorimetric switch which can form the basis of constructing molecular logic operations 5)presence of cyanuric chloride can give the probe some therapeutic benefits.

4.1. Rhodamine-triazine based dipodal system for sensing of Al^{3+} and its application for construction of a read-write-erase molecular memory device

A novel rhodamine B based colorimetric and fluorescence '*off-on*' probe was designed and fabricated by joining two rhodamine units to cyanuric chloride *via*. ethylenediamine linkers. This

dipodal probe was further characterized by NMR and mass spectroscopic techniques. The effect of various ions on probe **5** were investigated which revealed its colorimetric and spectral sensitivity towards of Al^{3+} ions over other metal ions in CH_3OH. Probe **5** was originally colorless and non-emissive due to existence of rhodamine B in its spirolactam ring close form. Upon adding Al^{3+} ions the solution of probe **5** (CH_3OH) turned pink and gave bright pink emission under UV lamp. In presence of Al^{3+}, the spectral studies gave the formation of absorption band at 557 nm with a shoulder at 520 nm and fluorescence band at 587 nm. The presence of Al^{3+}causedspirolactam ring opening of rhodamine unit of probe **5**which induced colorimetric, absorption and fluorescence '*off-on*' changes. Probe **5** formed a 1:1 complex on binding with Al^{3+} ions. The presence of two rhodamine units gave multiple chelating sites for Al^{3+} to bind tightly having binding constant $K_a = 9.3 \times 10^4\ M^{-1}$. The detection limit was calculated from the fluorescence titration profile and was found out to be 29×10^{-8} M. The fluorescence switch of probe **5** was further found to be reversible and reproducible in presence of CN^- ions and was used for constructing a set-reset memory device.

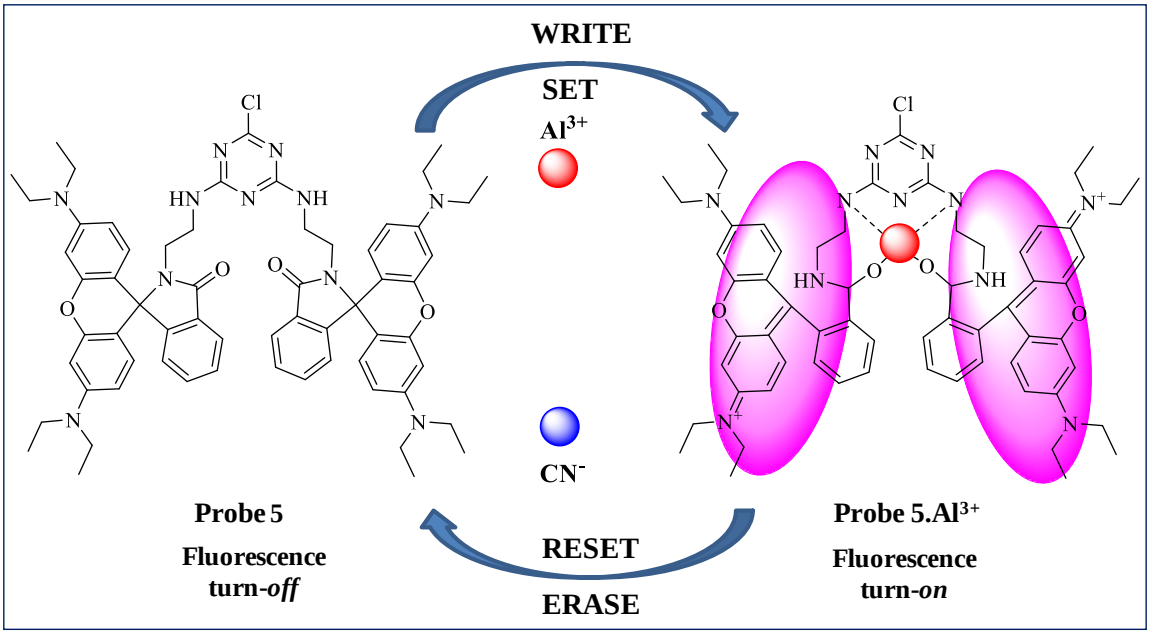

Figure 5: Binding mechanism of probe **5** with $Al^{3+}$and its use in construction of *set-reset* or *write-erase* based memory device.

4.2. Rhodamine-triazine based tripodal system for sensing of Al^{3+} and Cr^{3+} and its application as 3-input molecular logic device

In this chapter we have discussed the synthesis of tripodal system wherein the chloride (Cl) of probe **5** was also replaced with rhodamine B ethylenediamine unit. Furthermore, the changes in the photophysical and sensing properties have also been discussed. A cooperative action due to numerous binding sites of tripodal system and the generation of amide ion due to spirolactam ring opening favors the formation of Al^{3+}-chelate. Probe **6** gave dual change (colorimetric and fluorimetric) in presence of Al^{3+} and Cr^{3+}. The interference studies proved out that probe **6** was highly selective towards Al^{3+} having lowest detection limit of nM level. For its biological applicability its antibacterial activity was explored and compared to commercial drug. The ability of probe 6 to mimic logic devices was also explored and a 2-input INHIBIT logic function and 3-input OR-INHIBIT logic functions were designed.

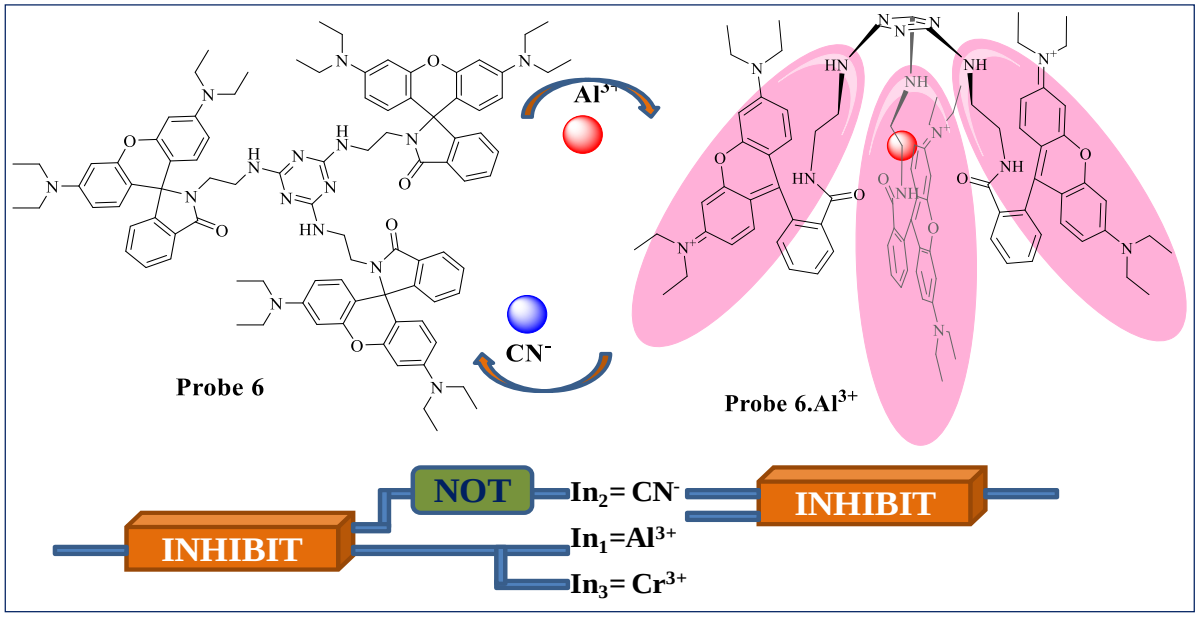

Figure 6: Binding mechanism of probe **6** with $Al^{3+}$and its use in construction molecular logic circuits having different number of inputs.

Conclusion of thesis:

We have developed few chromo-fluorescent probes for sensing of specific ions. All the probes possessed the capability of visual eye sensing and gave fluorescence '*off-on*' switch for particular ion. Phenalenedicarbonitrile and their derivative have been explored less for their sensing capabilities hence, we have synthesized and explored the unique sensing behavior of two phenalene based probes attached with different chromophoric units, in mixed aqueous mediums. Rhodamine B derivative when attached to highly electron deficient precursor i.e. Phenalenedicarbonitrile led to unique fluorescence and colorimetric '*on-off*' phenomenon. Further, we have synthesized rhodamine based probes (varying in the number of rhodamine units present) and explored their sensing behavior in aqueous/ mixed aqueous mediums. The presence of more number of rhodamine units provided multiple interaction sites for the ion to bind which led to improvement in the limit of detection of the probes. For the practical application of the probes we explored the capability of the probes to detect ions in industrial waste water and tap water. In addition to real-time sampling we used our probe for intracellular sensing of ions by using A549 cervical cancer line cells as well as we explored the anti-bacterial activity of probe. Furthermore, we even used our probes for construction of various molecular circuits and devices such as encoders, decoder, memory devices and keypad lock.

Future Prospective:

- Sensors having even high sensitivities can be synthesized for water quality assessments and could be efficient used in sensing of ions in biological systems as well.
- Development of more novel ion sensors based on small rigid π-conjugated systems like phenalenedicarbonitriles.
- Multipodal systems having easy synthetic pathway, high selectivity and sensitivity for particular ions in aqueous medium can be developed.

References:

1. A. T. Wright and E. V. Anslyn, *Chem. Soc. Rev*., 2006, **35**, 14-28.
2. V. Amendola and L. Fabbrizzi, *Chem. Commun*., 2009, 513-531.
3. L. Prodi, *New J. Chem*., 2005, **29**, 20-31.
4. J. Yoon, S. K. Kim, N. J. Singh and K. S. Kim, *Chem. Soc. Rev*., 2006, **35**, 355-360.
5. H. Kobayashi, M. Ogawa, R. Alford, P. L. Choyke and Y. Urano, *Chem. Rev*., 2010, **110**, 2620-2640.
6. E. J. New, *ACS Sensors*, 2016, **1**, 328–333
7. S. M. Ng, M. Koneswaran and R. Narayanaswamy, *RSC Adv*., 2016, **6**, 21624–21661
8. C. J. Chang, T. Gunnlaugsson and T. D. James, *Chem. Soc. Rev*., 2015, **44**, 4484–4486
9. S. Chowdhury, B. Rooj, A. Dutta and U. Mandal, *J. Fluoresc*., 2018, **28**, 999-1021
10. B. X. Shen and Y. Qian, *Sen. Actuators B: Chem*., 2017, **239**, 226-234.
11. D. Cheng, W. Zhao, H. Yang, Z. Huang, X. Liu and A. Han, *Tetrahedron Lett*., 2016, **57**, 2655- 2659
12. S. Saha, P. Mahato, M. Baidya, S. K. Ghosh and A. Das, *Chem. Commun*., 2012, **48**, 9293-9295.
13. Y. J. Gong, X. B. Zhang, C. C. Zhang, A. L. Luo, T. Fu, W. Tan, G. L. Shen and R. Q. Yu, *Anal. Chem*., 2012, **84**, 10777-10784.
14. M. Sulka, A. N. Kursunlu, B. Girgin, O. O. Karakus and E. Guler, *J. Photochem. Photobiol. A: Chem*., 2017, **349**, 129-137.
15. H. C. Xia, X. H. Xu, and Q. H. Song, *Anal. Chem*., 2017, **89**, 4192-4197
16. L. Tong and Y. Qian, *J. Photochem. Photobiol.A: Chem.*, 2019, **368**, 62-69
17. H. Sharma, J. M. White, J. Lin, E. J. New and F. M. Pfeffer, *Sens. Actuators B: Chem*., 2019, **300**, 126825-126833
18. N. Wanichacheva, O. Hanmeng, S. Kraithong and K. Sukrat, *J. Photochem. Photobiol. A: Chem*., 2014, **278**, 75-81.
19. H. N. Kim, M. H. Lee, H. J. Kim, J. S. Kim and J. Yoon, *Chem. Soc. Rev*., 2008, **37**, 1453-1744
20. Y. Xiao, F. Liu, X. Qian and J. Cui, *Chem. Commun*., 2005, 239-241

List of Publications:

1. Ruhi Mehta and Vijay Luxami*, "Rhodamine-anthraquinone based dyad for rapid and selective sensing of Al^{3+} with potential application for real-time sampling and molecular logic circuits." *Inorg. Chem. Commun*., 2020, **115**, 107863
2. Ruhi Mehta, Pawandeep Kaur, Diptiman Choudhary, Kamaldeep Paul and Vijay Luxami*, "Al^{3+} induced hydrolysis of rhodamine-based Schiff-base: Applications in cell imaging and ensemble as CN^- sensor in 100 % aqueous medium" *J. Photochem. Photobiol. A: Chem*., 2019, **380**, 111851
3. Ruhi Mehta, Vijay Luxami*, "A novel '*on-off*' rhodamine derivative for colorimetric and sensitive detection of CN^- and its application as encoder, decoder and molecular keypad lock" *ChemistrySelect*, 2020, **5**, 13429-13438
4. Ruhi Mehta, Vijay Luxami*, "A Phenalenedicarbonitrile Based Sensor for Selective Estimation of CN^- ions in Industrial Waste" *J. Mol. Struct*., 2021, **1234**, 130077

Conferences Attended:

- Presented poster on "Rhodamine-based Schiff-base for selective and sequential detection of Al^{3+} and CN^- ions" in 10^{th} National conference on Chemical and Environmental Sciences: Innovations and Advances-2018, Punjabi University, Patiala.

- Presented poster on "Rhodamine-anthraquinone dyad for selective detection of Al^{3+} ions at7.04" in National Conference on Futuristic Aspects in Chemical Science and Technology, Punjab University, Chandigarh (2018).